Geological Survey of Canada
Commission géologique du Canada

RADIOGENIC AGE AND ISOTOPIC STUDIES: REPORT 2

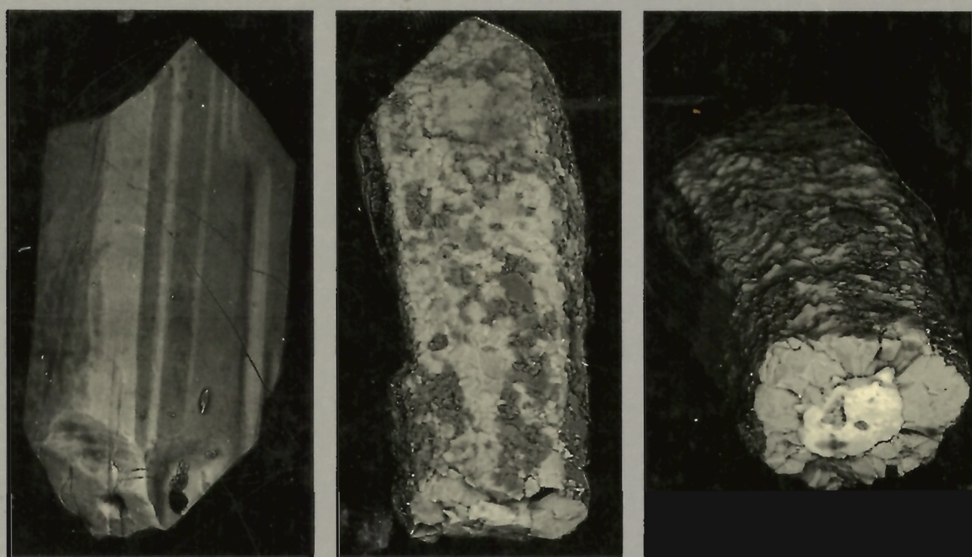

Canada

STAFF, GEOCHRONOLOGY SECTION: GEOLOGICAL SURVEY OF CANADA

Research Scientists:	Otto van Breemen J. Chris Roddick Randall R. Parrish James K. Mortensen
Post-Doctoral Fellows:	Mary Lou Bevier Francis Ö. Dudás Ernst Hegner
Professional Scientists:	W. Dale Loveridge Robert W. Sullivan Patricia A. Hunt Reginald J. Theriault
Technical Staff:	Jack L. Macrae Klaus Santowski Jean-Claude Bisson Diane Bellerive Fred B. Quigg Rejean J.G. Seguin

Sample crushing and preliminary mineral separation are done by the Mineralogy Section

GEOLOGICAL SURVEY OF CANADA

PAPER 88-2

RADIOGENIC AGE AND ISOTOPIC STUDIES: REPORT 2

1988

Energy, Mines and Resources Canada

Énergie, Mines et Ressources Canada

Available in Canada through

authorized bookstore agents and other bookstores

or by mail from

Canadian Government Publishing Centre
Supply and Services Canada
Ottawa, Canada K1A 0S9

and from

Geological Survey of Canada offices:

601 Booth Street
Ottawa, Canada K1A 0E8

3303-33rd Street N.W.,
Calgary, Alberta T2L 2A7

100 West Pender Street,
Vancouver, B.C. V6B 1R8

A deposit copy of this publication is also available for reference
in public libraries across Canada

Cat. No. M44-88/2E
ISBN 0-660-13084-X

Prices subjects to change without notice

Cover

SEM photographs of baddeleyite and zircon-rimmed baddeleyite from coronotic olivine metadiabase, Ontario Grenville Province.

Top Left: single baddeleyite crystal (200μ long) with typical polysynthetic twinning.

Top centre and right: two views of the same grain (400μ long) of baddeleyite (light grey core) partly replaced by polycrystalline zircon and retaining baddeleyite crystal habit.

Bottom: Stereophoto pair of baddeleyite care (light grey) from which zircon rim (medium grey) has partly peeled away; faceted projections on surface of baddeleyite, which is a single crystal, are negative zircon crystals formed at the bases of individual columns or replacing zircon (aggregate grain is 290μ long). U-Pb isotope analyses suggest an age difference of 120 Ma between the two Zr phases.

Original manuscript received: 08 08 1988
Final version approved for publication: 20 10 1988

CONTENTS

ERRATA

Paper 87-2, Radiogenic Age and Isotopic Studies: Report 1

Page 53, Table 1
Change $^{206}Pb = 100$ to $^{206}Pb = 1000$

Page 53, Table 1
Change $^{207}Pb/^{207}Pb$ to $^{207}Pb/^{206}Pb$

Page 82, Figure 1
Sample 12 on map should be plotted on NE side of Gordon Bay.

Page 116, column 1, line 21-22
Should read: "upper and lower intercept ages are 2664 $\pm$3 Ma and ca. 160 Ma."

Pages147 and 159
The figures on pages 147 and 159 have been transposed. The captions are correct.

INTRODUCTION

''Radiogenic Age and Isotopic Studies'' is an annual collection of reports presenting data from the Geochronology Section of the Lithosphere and Canadian Shield Division. The main purpose of this collection is to make geochronological and other radiogenic isotope data produced by the Section available promptly to the geological community. Reports make full presentation of the data, relate these to field settings, and make comparatively short interpretations. Readers are cautioned that some data reported here are part of work in progress, and more extensive publications may follow at a later date. Other geochronological and isotope data produced in the laboratory but published in outside journals or separate GSC publications are summarized at the end of this report.

The first two reports cover advances and/or reviews of analytical techniques. The past year has seen the establishment of the $^{40}Ar/^{39}Ar$ and Nd/Sm techniques at the Geochronology Section as routine procedures. Analytical papers presented here include a discussion of error propagation analysis as applied to $^{40}Ar/^{39}Ar$ data, and a report of a high performance liquid chromatography (HPLC) technique for the extraction and purification of Nd, Sm, and other trace elements. Conventional chemical separation techiques are also employed for Nd isotope tracer studies. Results of research now in progress using these techniques will appear in forthcoming volumes.

Geochronological support of geological mapping programs at the GSC can be of immediate economic significance, for example by delineating the eastern margin of the gold-bearing Slave Province (van Breemen and Henderson, this volume and preceding volume). In addition, the Section is playing an increasingly important role in regional metallogenic and specific mineral deposit studies. Examples of research now in progress include placing constraints on the age of formation of stratiform base metal and iron-formation hosted gold mineralization in the Slave and Superior provinces (see for example Mortensen et al., this volume) and on the age of epigenetic gold mineralization in the Superior Province (e.g. Anglin et al., this volume). Much of the K-Ar dating carried out by the Section is done as part of mineral deposit research. Direct dating of epigenetic mineralization

La publication annuelle « Âge radiométrique et études isotopiques » est une série de rapports présentant les données produites par la Section de la géochronologie de la Division de la lithosphère et du bouclier canadien. Cette série a pour principal objectif de permettre aux géologues d'avoir accès rapidement aux données géochronologiques et aux données sur les isotopes formés par décomposition radioactive. Les rapports présentent les données dans leur intégralité ainsi qu'une description de la géologie des lieux et de courtes interprétations des données. Il est à signaler que certaines de ces données proviennent de travaux en cours de sorte que des données plus exhaustives seront publiées à une date ultérieure. D'autres données géochronologiques et isotopiques produites dans le laboratoire mais publiées dans des revues scientifiques extérieures ou dans d'autres publications de la CGG sont résumées à la fin du présent rapport.

Les deux premiers rapports traitent des progrès accomplis ou présentent une analyse des techniques analytiques, ou les deux. Depuis l'an dernier, les techniques de datation par les méthodes $^{40}Ar/^{39}Ar$ et Nd/Sm sont couramment utilisées dans la Section de la géochronologie. L'un des documents analytiques traite de l'analyse de propagation des erreurs sur les rapports $^{40}Ar/^{39}Ar$ et un autre fait état de la technique de chromatographie en phase liquide à haut rendement pour l'extraction et la purification de Nd, de Sm et d'autres éléments en traces. On utilise également des techniques classiques de séparation chimique pour l'étude d'indicateurs isotopiques Nd. Les résultats des travaux de recherche en cours dans lesquels ces techniques sont utilisées seront présentés dans des volumes ultérieurs.

L'apport de la géochronologie aux programmes de cartographie géologique à la CGC peut revêtir une importance économique immédiate, notamment pour délimiter la bordure est de la provice aurifère des Esclaves (van Breemen et Henderson, le présent volume). De plus, la section joue un rôle grandissant dans la réalisation d'études métallogéniques régionales et d'analyses de certains gisements minéraux. Parmi les travaux de recherche en cours, on remarque celui sur la limitation de l'âge de mise en place d'une minéralisation aurifère dans une formation stratiforme de métaux de base et de fer dans using a variety of techniques (e.g. U-Pb on rutile and $^{40}Ar/^{39}Ar$ on muscovite) is underway on samples from Newfoundland and Yukon Territory. Pb isotope analysis of sulphides using conventional mass spectrometer techniques is also undertaken as part of many mineral deposit studies. Procedures now being developed (in conjunction with Canada Centre for Mineral and Energy Technology research personnel) using ion microprobe (SIMS) techniques to perform in situ Pb and S isotope analyses of sulphides will expand this capability.

les provinces des Esclaves et du lac Supérieur (voir par exemple Mortensen et coll., le présent volume) et l'âge d'une minéralisation aurifère épigénétique dans la province du lac Supérieur (par exemple, Anglin et coll., le présent volume). La plupart des datations au K-Ar réalisées par la section ont été faites dans le cadre de recherches sur les gisements minéraux. La datation par diverses techniques d'une minéralisation épigénétique (par ex., par les méthodes U-Pb effectuée sur le rutile et $^{40}Ar/^{39}Ar$ effectuée sur la muscovite porte actuellement sur des échantillons provenant de Terre-Neuve et du Yukon. Une analyse isotopique du plomb dans des sulfures par des techniques de spectrométrie de masse classiques a aussi été entreprise dans le cadre de nombreuses études de gisements minéraux. Les méthodes actuellement mises au point (en collaboration avec le personnel de recherche du Centre canadien de la technologie des minéraux et de l'énergie) et faisant appel à des techniques par sonde ionique (SIMS) pour réaliser in situ des analyses isotopiques de Pb et de S de sulfures accroîtront cette capacité.

J.K. Mortensen

The assessment of errors in $^{40}Ar/^{39}Ar$ Dating

J.C. Roddick[1]

Roddick, J.C., The assessment of errors in $^{40}Ar/^{39}Ar$ dating; in Radiogenic Age and Isotopic Studies: Report 2, Geological Survey of Canada, Paper 88-2, p. 3-8, 1988.

Abstract

Numerical error analysis is applied to typical $^{40}Ar/^{39}Ar$ data. It extends previous error treatments to all possible variables used in the calculation of ages of samples and shows that in some cases minor corrections may contribute significantly to age uncertainties. Isochron plots using ^{36}Ar as a reference isotope are not suitable for data analysis - the correlation plot with ^{40}Ar as a reference is preferred. The irradiation parameter, J, is the primary limitation on the precision of age determinations. Close control of this parameter permits age precision of 0.1 % (1σ) but 0.5 % is typical.

Résumé

L'analyse numérique des erreurs porte sur des données types de $^{40}Ar/^{39}Ar$. Elle permet d'étendre les traitements d'erreurs antérieurs à toutes les variables possibles utilisées dans la datation d'échantillons et elle montre que, dans certains cas, des corrections mineures peuvent augmenter considérablement les incertitudes de datation. Les isochrones utilisant ^{36}Ar comme isotope de référence ne conviennent pas à l'analyse des données: il est préférable d'utiliser la courbe de corrélation avec ^{40}Ar comme isotope de référence. Le paramètre d'irradiation J constitue la principale limite à la précision des datations. Le contrôle étroit de ce paramètre permet des précisions de datation de 0,1 % (1σ), mais il est plus courant d'obtenir une précision de 0,5 %.

INTRODUCTION

The $^{40}Ar/^{39}Ar$ technique is now recognized as a precise method of dating geological samples. It has a number of advantages over the conventional K-Ar method, one of which is the ability to obtain an age by the measurement of argon isotopic ratios, rather than the less precise procedure of separately measuring isotopic quantities of argon and potassium. Currently, precision in ratio measurements of 0.05 to 0.2 % (one standard error or 1σ) are routine in most laboratories. The determination of the final age involves a number of calculations and corrections of varying significance which, when combined, propagate into the error estimate of the ages of samples. Despite the propagation of these uncertainties, precision on ages of 0.1 % has been demonstrated on replicate standard samples under closely controlled conditions (Roddick, 1983). Others have indicated that ages can be determined routinely to ±2 Ma on 3000 Ma old samples (Lopez-Martinez et al., 1984) - a precision (0.07 %) comparable to high quality U-Pb zircon dating (Krogh, 1982). With claims of such high precision, it is critical that the uncertainties in the ages are shown to be derived by considering all significant sources of error and that these errors are appropriately propagated into the final ages.

Procedures for calculating the errors in $^{40}Ar/^{39}Ar$ ages were developed and published at an early stage in the application of the technique (Berger and York, 1970; Dalrymple and Lanphere, 1971). These procedures, however, involved a number of simplifications and approximations, because the calculations for error propagation are often very tedious, with partial derivatives required for each measured variable in a functional relationship. Recently, Roddick (1987) has shown that the application of a general numerical error propagation procedure permits consideration of all possible sources of error in quite complex analytical problems. It can also handle correlated errors and calculate correlation among the final results. Correlation is important in isochron or isotope ratio diagrams, which are often used in determining the ages of samples that may contain excess argon. In this article numerical error propagation is applied to a typical $^{40}Ar/^{39}Ar$ sample. Coupled with this is a discussion of the general significance of uncertainties in the measured variables, with regard to analytical errors in isotope ratio (isochron) diagrams and final ages.

[1] *Geological Survey of Canada, 601 Booth Street, Ottawa, Ontario K1A 0E8*

NUMERICAL ERROR PROPAGATION

In many radioactive dating schemes the ratio of daughter to parent isotopes (D/P) determines the age of a sample using the relation:

$$\text{Age} = \frac{1}{\lambda}\ln[1 + D/P] \quad (1)$$

where λ is the decay constant. The age is thus dependent on the D/P value and uncertainty or error in this value determines the error in the age. In $^{40}Ar/^{39}Ar$ dating the age of an unknown, t_u is given by:

$$t_u = \frac{1}{\lambda}\ln[1+R_uJ] \quad (2)$$

where: R_u = $*40/39_k$ for the unknown (*40 is the radiogenic daughter ^{40}Ar generated from decay of parent ^{40}K in the unknown and 39_k is the ^{39}Ar produced from ^{39}K in the same sample by irradiation with fast neutrons); J = a conversion factor for the production of ^{39}Ar from ^{39}K for the unknown, and which is determined from a standard sample irradiated with the unknown; λ = the total decay constant of ^{40}K. The product R_uJ is equivalent to the D/P ratio in the decay system.

In the procedure adopted here, the value $*40/39_k$ and its error are calculated first and then the value is substituted in equation 2 to calculate the age. This permits separate evaluations of the error in the age both with and without an error determined for J, since an error need not be assigned to J when comparing different gas fractions from a single sample. An analytical solution is used to calculate the error propagation in the age in equation 2 because of the simple form of this equation while numerical error propagation is used to determine the error in the more complex derivation of $*40/39_k$ values.

The numerical approach to error analysis incorporates the actual calculation of the values of interest in the error propagation procedure (Roddick, 1987). Calculation of R_u, the ratio $*40/39_k$ is subject to corrections because of ^{39}Ar produced from Ca and ^{40}Ar produced from K by irradiation of the sample, and also because of atmospheric Ar (^{40}Ar, ^{36}Ar) in the sample and the gas extraction system. In addition, ^{36}Ar and ^{37}Ar are produced by irradiation of Ca, necessitating a correction to the atmospheric Ar (^{36}Ar), and providing a reference (^{37}Ar) for the Ca corrections. Mak et al. (1976) have developed a formalism of this calculation which separates these factors into 3 terms which emphasize their significance. Abbreviating the argon isotopes to their masses, the equation of Mak et al. is:

$$*40/39_k = (40/39)_m(1\text{-}f_1) - 295.5(36/39)_m(1\text{-}f_2) - (40/39)_k \quad (3)$$

where 295.5 = $^{40}Ar/^{36}Ar$ in atmospheric argon; m and k refer to measured isotope ratios in a sample and a pure K salt respectively; f_1 and f_2 are functions of the argon ratios 36/39 and 37/39 measured in the sample and an irradiated Ca salt (subscript ca):

$$f_1 = 1/[1\text{-}[1\text{-}(37/39)_{ca}/(37/39)_m]] \quad (4)$$

$$f_2 = f_1[1\text{-}(36/39)_{ca}/(36/39)_m] \quad (5)$$

To assess the error propagation, equation (3) can be differentiated and an analytical solution determined for the most significant variables. Dalrymple and Lanphere(1971) and Dalrymple et al. (1981) have done this for an equation similar to equation 3 and present an error equation using error estimates for only the three isotope ratios measured in the sample. With the numerical approach, errors in all the variables in equations 3,4, and 5 may be evaluated and propagated into the final $*40/39_k$. An example is given in Table 1 of such an error analysis for this ratio and other ratios used in isotope ratio plots. The derivation of the parameters for ratio plots is given before a detailed discussion of the error table.

ERROR PROPAGATION APPLIED TO ISOTOPE RATIO DIAGRAMS

A mineral sample is usually heated in a series of increasing temperature steps and the ages of the resulting gas fractions are compared to determine whether the sample has lost some of its Ar during its geological history. Similar ages from most fractions indicate an undisturbed sample. Results from these gas fractions may also be examined on isotope ratio diagrams using the ^{40}Ar isotope as reference (39/40 - 36/40; a correlation plot) or the ^{36}Ar isotope as reference (39/36 - 40/36; an isochron plot). In these plots the 40 and 36, after correction for extraction line blank, are the total ^{40}Ar and ^{36}Ar extracted in the individual steps; 39 represents 39_k, following corrections as in equation 3. No assumptions are made about the composition of $^{40}Ar/^{36}Ar$ trapped in the sample at the time of crystallization or closure of the argon system, rather this quantity is determined as the intersection of linear gas fraction data arrays with one axis of the plots. The $*40/39_k$ and thus the age of the sample is determined from the intersection of the linear array with the other axis (in correlation plots) or from the slope of the array (in isochron plots). Additional details of these plots are given by Roddick et al. (1980) and Gillespie et al. (1983). Roddick et al. (1980) compared the two forms of ratio plotting and concluded that the isochron plots are often misleading and that the correlation plot is a much superior form of data display and processing. While the correlation plot has generally been adopted (McDougall, 1981; Lopez-Martinez et al., 1984) some still feel it necessary to compare the two forms of display (Chopin and Monié, 1984) while others still use the isochron plot (Foland, 1983). Here the significant differences of the two plots, as related to analytical error, will be discussed.

One important feature of both diagrams is that the plotted parameters have correlated errors, mainly because of uncertainty in atmospheric Ar blank corrections. Thus, for assessing errors in these parameters, uncertainty in blanks must also be considered. The equations used to correct the measured ratios for Ar blank are similar to equation 3 but term 2 is replaced with a correction for the blank and is expressed as a ratio of blank ^{40}Ar (40_{bl}), to 39_k in the analysis; i.e. for 39/40 and 39/36:

$$39/40 = 1/[(40/39)_m(1\text{-}f_1) - 40_{bl}/39_k - (40/39)_k] \quad (6)$$

$$39/36 = 1/[(36/39)_m(1\text{-}f_2) - (40_{bl}/39_k)/295.5] \quad (7)$$

and

$$40/36 = (39/36)/(39/40); \quad 36/40 = 1/(40/36) \quad (8)$$

(where f_1 and f_2 are as in equations 4 and 5.)

While the above equations and equation 3 can be used to calculate the required parameters, errors in the measurement of the intensity of a specific isotope can introduce correlations between the errors in the measured ratios involving that isotope. These correlations should be accounted for in the error analysis. For example, the uncertainty in common 39 affects both $(36/39)_m$ and $(40/39)_m$. These potential correlations may be avoided by using measured quantities of the four Ar isotopes, together with their associated errors, as the primary variables for error analysis and subsequently forming the ratios to insert in the above equations. Table 1 details a numerical error analysis of the isotope ratio plot parameters and $^*40/39_k$ (errors on 40/36 and 36/40 are the same) showing the contributions of errors in the measured Ar isotope intensities and a number of other variables. These others include the blank ^{40}Ar, the 40/36 measured for air (≈290), which is used for mass discrimination corrections, and the ratios of neutron produced Ar from K and Ca as discussed above. The data are from the 950°C step of a 100 Ma hornblende with 0.74 % K which released 14 % of its total ^{39}Ar in the heating step.

Table 1 shows that the Ar blank with an error of ±25 % produces the dominant variance in the plotting parameters and the correlation coefficient of 36/40 vs. 39/40 but provides no contribution to $^*40/39_k$ which determines the age of the gas fraction. The second most significant variable is the 36_m and its error component dominates the variance of $^*40/39_k$. These high errors have given rise to significant non-linearity in the error propagation calculation for 39/36, one parameter used in an isochron plot. This is indicated by the + and - superscripts indicating that the error magnification (EMAG) values[1] for this parameter differ by more than 5 % when evaluated using the positive and negative error limits on 36_m and the blank. In detail (not shown) for the 39/36 parameter the EMAG factor of 36_m is large (3.2) and varies from 3.0 to 3.4 while the EMAG factor of the Ar blank (0.5), ranges from 0.56 to 0.45. The + and − superscripts on these two variables indicate that the magnitude of the EMAG factors vary in opposite directions (+ = increase, - = decrease) when the uncertainties in the variables are deviated in a particular direction, so when combined with the other errors and summed to provide the variances on the parameter, they tend to cancel out. Therefore the final error in the 39/36 ratio has an apparently smaller uncertainty of +6.3 % to -3.9 % as listed in the lower part of Table 1 (cf. a range of 13.5 to 12.2 % rather than a single value of 12.7 %). Roddick (1987) has suggested that if these uncertainties are large then the errors are only approximations. Here the EMAG factors and errors on two variables are large enough to violate the assumption of linearity in the error propagation calculation of the 39/36. This suggests that the error in this parameter is not

Table 1. Numerical error analysis of ^{40}Ar-^{39}Ar ratios

	Parameter:		36/40	39/40	39/36	$^*40/39_k$	Cor. Coef.†
	Value		.000116	1137	980.	8.494	−.7786
	% Error		12.4	.374	12.7^+	.28	
	Variable					(Age = 98.0±.25 Ma)	
Name	**Value**$^\beta$	**% Error**$^\alpha$	%^{2} Variance contributions				
40_m cc	56.711	.016	.0005	.0003	.0000	.0003	.0004
39_m cc	6.363	.099	.0000	.0099	.0099	.0099	.0000
36_m cc	.019	2.4	47.8451	Z	47.8176^-	.0603	Z
37_m cc	36.578	.1	.0213	.0000	.0212	.0000	.0000
40 Blank cc	.800	25.	102.1242	.1287	109.5117^+	Z	-3.6250
Atm. $40/36_m$	291.5	.1	.0316	.0006	.0234	.0010	.0044
$40/39_k$	.016	10	.0003	.0003	Z	.0004	.0003
$36/39_{ca}$	.400	1	2.1245	Z	2.1251	.0027	Z
$37/39_{ca}$	1552.	1	2.1213	.0000	2.1127	.0030	.0040
Total variance:			154.2689	.1398	161.6216^+	.0775	-3.6158

% UNCERTAINTY IN PARAMETER ERRORS FOR +/- INPUT ERRORS

	36/40	39/40	39/36	$^*40/39_k$
+ Error	.22	.33	6.32	−.05
− Error	−.22	−.33	−3.89	.05

† = Correlation coefficient for first two parameters
%^{2} = Percentage squared
cc = x10^{-9} cm^3 STP
Z = Parameter not dependent on this variable
β = Measured gas quantities corrected for mass discrimination and decay
α = Errors at 1 standard error
+, − = Error subject to > 5 % variation in calculation for +/- input errors
Error increase (+) or decrease (−) for input error increase

[1] EMAG factors are the numerical equivalents of partial derivatives and representent a ratio of resultant fractional change in a parameter to a small fractional change in the component variable (Roddick, 1987).

well determined and should be treated with caution. Alternatively, if the errors on the variables could be reduced, the effects of the non-linearity would not be as significant. In contrast, the uncertainties in the other parameter errors are much less (±.05 to ±.33%) and indicate that the error propagation calculation is approximately linear for these parameters and this data set. Therefore the parameters used in a correlation plot and age calculation have well determined errors while one parameter in the isochron plot has a potentially unreliable error estimate. This is a general feature of $^{40}Ar/^{39}Ar$ data where small gas fractions often require large blank corrections to small ^{36}Ar abundances, and not a feature specific to this data set.

The correlation coefficient for parameters 1 and 2 (used in the correlation plot) is -0.7786 and shows a moderate negative correlation derived predominantly from the blank uncertainty[2]. In contrast, the correlation coefficient for the isochron parameters (calculated but not shown in Table 1) is +.9998. They are nearly perfectly positively correlated because both parameters (40/36; 39/36) are dominated by blank uncertainty in ^{36}Ar as reflected in the similar and high values of their errors. This high correlation coefficient is one of the main reasons for the suggestion that the isochron plot is not suitable for examining $^{40}Ar/^{39}Ar$ data (Roddick et al., 1980). Ludwig (1980) also discussed the difficulties of using very high correlation coefficients but as applied to regressions of U-Pb data.

The variance components from the K and Ca ratios result from the interference corrections and vary from insignificant for $(40/39)_k$ to minor for the Ca ratios. An error of 1% has been assigned to the two Ca ratios based on the data tabulated in Roddick (1983). Despite the low magnitude of errors, they contribute about 7% to the variance in $*40/39_k$, the parameter used to calculate the age of the gas fraction. The effects of these Ca corrections cannot be considered systematic and thus the uncertainty of the corrections cannot be ignored on the basis that they affect all analyses to a similar degree. For example, if the ages of cogenetic hornblende and biotite in a sample were compared, the hornblende would have Ca corrections similar to those in Table 1, while biotite, with no Ca, would be free of uncertainty from this source. While uncertainties in the Ca corrections have a very minor effect in this example, in other samples with high Ca and low K significant differences may arise. Therefore uncertainty in the Ca derived Ar should be included in the error analysis.

ERROR IN A $^{40}Ar/^{39}Ar$ AGE AND SIGNIFICANCE OF ERROR IN J

While the flexibility of the numerical approach is an advantage in complex calculations, as outlined above, because of the relative simplicity of the age equation (Equation 2), the uncertainty in the age of an unknown can be derived by analytical partial differentiation of this equation and incorporation in the error propagation formula (Berger and York, 1970; Dalrymple and Lanphere, 1971; Dalrymple et al., 1981). Following this procedure the % error in the age (Dalrymple et al., 1981) is:

$$\sigma_{t_u} = \frac{JR_u(\sigma_{R_u}^2 + \sigma_J^2)^{1/2}}{t_u \lambda (1+R_uJ)} \quad (9)$$

where σ_{R_u} and σ_J are the % standard errors of R_u and J, respectively, for the unknown.

This equation considers errors in both the measured $*40/39_k$ (R_u) and the irradiation parameter J and is suitable for inter-comparison of samples. However, for the assessment of the concordancy of a number of gas fractions in a single sample the uncertainty in J should be omitted, as all fractions have been subjected to exactly the same irradiation. The uncertainty of J, in this case, is systematic and changes in J will shift all ages of the gas fractions by similar amounts. If the ages of these fractions are considered identical within their error limits, they may be combined to provide a precise plateau age[3]. At this stage, the uncertainty in J should be quadratically combined with the error on the integrated $*40/39_k$ (using Equation 9) to provide an error suitable for comparison of the age with other samples. Similarly, in a correlation plot the $*40/39_k$, determined from the regression intercept of a number of gas fractions, may be used to calculate the sample age using Equation 2 and the error on the age using Equation 9.

The value of J is usually derived from the relation:

$$J = \frac{\epsilon^{\lambda t_s} - 1}{R_s} \quad (10)$$

where t_s and R_s are the age and measured $*40/39_k$ of the standard in the irradiation.

Berger (1975) pointed out that a more fundamental relation for J is:

$$J = \frac{\lambda}{\lambda_e} \frac{(D/P)}{R_s} \quad (11)$$

where $D/P = {}^{40}Ar^*/{}^{40}K$, the daughter/parent ratio for the standard; λ_e = decay constant of ^{40}K to ^{40}Ar.

[2] Previously an algebraic solution was given for this correlation coefficient using errors in the three measured sample Ar ratios and the blank (Roddick et al., 1980). Numerical propagation using the same errors is in good agreement with this algebraic solution.

[3] Berger and York (1981) noted that an error contraction occurs when number of gas fractions are integrated (combined), thus improving the precision on the measured $*40/39_k$. Fleck et al. (1977) suggested tests for the concordancy of gas fractions.

This expression for J emphasizes the dependency on a precisely and accurately known D/P value for the standard and that the calculated age of the standard has no significance. The error in J is thus dependant on the precision of the ratios D/P and R_s for the standard. It is common practice to not include uncertainty in D/P in the error calculation on the basis that all samples are referenced to the same standard mineral. Thus only the measured ratio R_s contributes to uncertainty in J. This is true for a standard, but in practice there is usually a neutron flux gradient over an irradiated container, and the J value for an unknown sample is calculated or interpolated at the position of the unknown. The uncertainty involved in this calculation of sample J must also be included in its error. In ideal circumstances a precision on sample J of 0.1 % (1σ) may be attained, though typically the precision is 0.5 % (Roddick, 1983). This J uncertainty is often the primary limitation on the precision of the age of samples. Thus for young (100 Ma) samples, 2σ uncertainties of ± 1 Ma may be typical. For very old samples (3000 Ma) uncertainties of ± 15 Ma (2σ) may be expected (including an error contraction from the logarithmic calculation of the age equation, Equation 2). Precision of ± 2 Ma (1σ) in 3000 Ma, as suggested by Lopez-Martinez et al. (1984), is unlikely unless a J precision of 0.15 % (1σ) is demonstrated.

The J factor is analogous to a mixed isotopic spike in U-Pb dating which is used to measure the ratio of elemental abundances. In contrast to that technique, where the isotopic spike can be precisely calibrated by repeated measurements with known standard U-Pb solutions, the J factor must be determined in each irradiation and, with a flux gradient, for each sample in the irradiation container. Thus, precise argon isotopic ratios may be measured and further improved by integrating plateaux gas fractions, but the final precision on the age of a sample is limited by the uncertainty in the irradiation J factor.

DISCUSSION AND CONCLUSIONS

The error analysis presented in Table 1 incorporates all variables used in equations 3 to 7 plus the mass discrimination correction. There are additional variables which, for clarity have not been included but which can be readily handled by the numerical error propagation routine. Additional factors could include: mass spectrometer corrections such as amplifier non-linearity and tail corrections; radioactive decay of ^{37}Ar and ^{39}Ar since the time of irradiation; corrections for chlorine derived ^{36}Ar (Roddick, 1983). In most cases these corrections will not be significant relative to the ones already discussed. Another factor to consider is correlation of the errors in the variables. The most likely possibility for correlation is in the two Ca corrections $(36/39)_{ca}$ and $(37/39)_{ca}$ where the common error in 39 might produce some correlation in these variables. Finally the uncertainties in the decay constants could be propagated into the final age. For comparison of K-Ar ages this is unnecessary but for rigorous comparison with ages from other decay schemes this source of error should be incorporated. Burghele (1987) presented a suitable formula for this error calculation.

Error analysis of typical *40/39 data shows how all possible sources of error may be easily propagated into the final age of a single sample. Previous error treatments (Dalrymple et al., 1981) have adequately dealt with the most significant sources of error. The approach advocated here shows that in some cases the minor corrections can be significant in adding uncertainty to a ^{40}Ar/^{39}Ar age. The difficulties of using isochron plots have been re-affirmed; if these are to be used, the possibility of both large and uncertain errors in 39/36 and very high correlation coefficients (+0.9998) due to blank corrections must be explicitly considered. Correlation plots with ^{40}Ar as a reference isotope are largely free of these problems. The irradiation parameter J is the primary limitation on high precision age determinations. This arises because of neutron flux gradients in an irradiation. Careful monitoring of these gradients using closely spaced standards can produce ages to 0.1 % precision.

ACKNOWLEDGMENTS

W. D. Loveridge is thanked for a careful review with numerous improvements to this article.

REFERENCES

Berger, G.W.
1975: ^{40}Ar/^{39}Ar step heating of thermally overprinted biotite, hornblende and potassium feldspar from Eldora, Colorado; Earth and Planetary Science Letters, v. 26, p. 387-408.

Berger, G.W. and York, D.
1970: Precision of the ^{40}Ar/^{39}Ar dating technique; Earth and Planetary Science Letters, v. 9, p. 39-44.

1981: Geothermometry from ^{40}AR/^{39}Ar dating experiments; Geochimica et Cosmochimica Acta, v. 45, p. 795-811.

Burghele, A.
1987: Propagation of error and choice of standard in the ^{40}Ar-^{39}Ar technique; Chemical Geology (Isotope Geoscience Section), v. 66, p. 17-19.

Chopin, C. and Monié P.
1984: A unique magnesiochloritoid-bearing high-pressure assemblage from the Monte Rosa, Western Alps: petrologic and ^{40}Ar/^{39}Ar radiometric study; Contributions to Mineralogy and Petrology, v. 87, p. 388-398.

Dalrymple, G.B. and Lanphere, M.A.
1971: ^{40}Ar/^{39}Ar technique of K-Ar dating: a comparison with the conventional technique; Earth and Planetary Science Letters, v. 12, p. 300-308.

Dalrymple, G.B., Alexander, E.C.Jr., Lanphere, M.A. and Kraker G.P.
1981: Irradiation of samples for ^{40}Ar/^{39}Ar dating using the Geological Survey TRIGA reactor; U.S. Geological Survey Professional Paper 1176.

Fleck, R.J., Sutter, J.F., and Elliot, D.H.
1977: Interpretation of discordant ^{40}Ar/^{39}Ar age-spectra of Megozoic tholeiites from Antarctica; Geochimica et Cosmochimica Acta, v. 41, p. 15-32.

Foland, K.A.
1983: ^{40}Ar/^{39}Ar incremental heating plateaus for biotites with excess argon; Isotope Geoscience, v. 1, p. 3-21.

Gillespie, A.R., Huneke, J.C., and Wasserburg, G.J.
1983: Eruption age of a Pleistocene basalt from ^{40}Ar-^{39}Ar analysis of partially degassed xenoliths; Journal of Geophysical Research, v. 88, B6, p. 4997-5008.

Krogh, T.E.
1982: Improved accuracy of U-Pb ages by the creation of more concordant systems using an air abrasion technique; Geochimica et Cosmochimica Acta v. 46, p. 637-649.

Lopez-Martinez, M., York, D., Hall, C.M., and Hanes, J.A.
1984: Oldest reliable $^{40}Ar/^{39}Ar$ ages for terrestrial rocks: Barberton Mountain komatiites; Nature, v. 307, p. 352-354.

Ludwig, K.R.
1980: Calculation of uncertainties of U-Pb isotope data; Earth and Planetary Science Letters, v. 46, p. 212-220.

Mak, E.K., York, D., Greive, R.A.F., and Dence, M.R.
1976: The age of the Mistastin Lake crater, Labrador, Canada; Earth and Planetary Science Letters, v. 31, p. 345-357.

McDougall, I.
1981: $^{40}Ar/^{39}Ar$ age spectra from the KBS Tuff, Koobi Fora Formation; Nature v. 294, p. 120-124.

Roddick, J.C.
1983: High precision intercalibration of ^{40}Ar-^{39}Ar standards; Geochimica et Cosmochimica Acta v. 47, p. 887-898.
1987: Generalized numerical error analysis with applications to geochronology and thermodynamics; Geochimica et Cosmochimica Acta v. 51, p. 2129-2135.

Roddick, J.C., Cliff, R.A., and Rex, D.C.
1980: The evolution of excess argon in Alpine biotites - a ^{40}Ar-^{39}Ar analysis; Earth and Planetary Science Letters, v. 48, p. 185-208.

Samarium-neodymium and rare-earth element liquid chromatography (HPLC) techniques at the geochronology laboratory, Geological Survey of Canada

R.W. Sullivan[1]

Sullivan, R.W., Samarium-neodymium and rare-earth element liquid chromatography (HPLC) techniques at the geochronology laboratory, Geological Survey of Canada; in Radiogenic Age and Isotopic Studies: Report 2, Geological Survey of Canada, Paper 88-2, p. 9-20, 1988.

Abstract

Procedures for high performance liquid chromatography (HPLC) separation of Sm and Nd for mass spectrometric isotope dilution analysis are described in detail. Whole-rock samples are spiked with a mixed ^{148}Nd-^{149}Sm tracer and dissolved either by lithium metaborate ($LiBO_2$) fusion or steel jacketed Teflon^{TM} pressure vessels. Using oxalic acid to complex Fe, REE are separated as a group using 3 ml cation exchange resin columns with HNO_3 acid. HPLC is used for the separation of Sm and Nd for mass analysis and for REE determination by visual spectrophotometry. Isotopic analyses of Sm and Nd are carried out using a Finnigan MAT 261 variable multicollector mass spectrometer. Blanks are currently about 500 pg Nd and 100 pg Sm. Advantages and disadvantages of HPLC for Sm-Nd studies are discussed.

Résumé

Des méthodes de séparation de Sm et Nd par chromatographie en phase liquide à haut rendement pour l'analyse de la dilution isotopique par spectrométrie de masse sont décrites en détail. Des échantillons de roches totales sont dopés à l'aide d'un traceur constitué d'un mélange de ^{148}Nd-^{149}Sm et dissous soit par fusion au métaborate de lithium ($LiBO_2$) ou dans des récipients sous pression en Teflon^{MC} chemisés d'acier. En utilisant de l'acide oxalique pour complexer le Fe, les terres rares sont séparées en utilisant des colonnes de résine cationique de 3 ml avec de l'acide HNO_3. La chromatographie en phase liquide à haut rendement est utilisée pour la séparation de Sm et Nd à des fins d'analyse de masse et pour la détermination des éléments des terres rares par spectrophotométrie visuelle. Des analyses isotopiques de Sm et Nd sont réalisées avec un spectromètre de masse à multicollecteur variable de modèle Finnigan MAT 261. Les blancs sont généralement d'environ 500 pg en Nd et de 100 pg en Sm. Les avantages et les inconvénients d'utiliser la chromatographie en phase liquide à haut rendement dans des études de Sm-Nd sont traités.

INTRODUCTION

Rare-earth element geochemistry and distribution patterns in rocks and minerals are of great interest to geoscientists. The determination of rare-earth elements (REE) in geological samples is difficult, however, because of their very similar chemical properties. Several analytical techniques are used: *see* Kantipuly and Westland (1988) for a review. Liquid chromatography has traditionally been used in organic chemistry and anionic species determination, but in recent years HPLC has rapidly developed as an analytical tool for many cationic species, including metals of interest to geoscientists.

The paper by Elchuk and Cassidy (1979) describing liquid chromatography (HPLC) for the separation of the lanthanides (REE), and subsequent collaborative work with the Geological Survey of Canada (Cassidy et al., 1986) demonstrated the applicability of HPLC as a separation and purification technique for Sm-Nd isotopic studies. Subsequently, Cassidy (1988) demonstrated the use of HPLC and discussed its advantages over other methods for REE determination in rocks. Inductively coupled plasma-mass spectrometry (ICP-MS) is also now being used for REE determinations: *see* Riddle et al. (1988) for a review.

[1] Geological Survey of Canada, 601 Booth Street, Ottawa, Ontario K1A 0E8

Conventional chemical separation methods for Sm-Nd isotopic studies are well established: *see* for example, Hegner et al. (in press); modified after Richard et al. (1976), and Nakamura et al. (1976) (Lugmair et al., 1975). A unique feature of the HPLC method described in this paper, however, is that it not only provides Sm and Nd separates free of all other REE for mass analysis but also can provide REE determinations as a bonus. This method should be of interest to geoscientists, particularly geochronologists.

The procedures reported in this paper are based on the work of Cassidy, but have been modified and developed further to reflect the requirements of Sm-Nd mass analysis for isotopic studies.

The entire procedure used for Sm-Nd mass analysis and REE determinations from whole-rocks is described in detail. Associated problems and future work are also discussed.

SAMPLE DISSOLUTION AND SPIKING

Samples are processed in clean chemistry facilities as described by Parrish et al. (1987). Preparation of reagents is described in their respective sections.

The spike used for isotope dilution analysis is a mixed ^{148}Nd-^{149}Sm tracer doped with a very small amount of ^{145}Nd and ^{152}Sm to facilitate more precise calibration using the critical mixture technique (Hofmann, 1971). The concentration of the spike is 6.9564 microgram ^{148}Nd and 14.069 microgram ^{149}Sm per gram previously calibrated against Ames metal reference standards. It is dispensed by weight from teflon dropping bottles. A typical dose of spike for a 250 mg sample containing 25 ppm Nd and 7 ppm Sm is 0.05 - 0.10 gm. This yields a solution which is usually sufficient for HPLC chromatography and mass analysis. A ^{145}Nd-^{152}Sm spike is used for reagent blank determinations.

Two methods of dissolution are in use: (i) an HF-HNO_3-HCl hot plate/steel jacketed Teflon™ pressure vessel "bomb" dissolution. This procedure works well, has lower dissolution blanks than the second method (typically 200 pg Nd, 20 pg Sm) but is time consuming and rather tedious; and (ii) a graphite crucible, lithium metaborate ($LiBO_2$) fusion technique. This procedure is simpler and very rapid but currently suffers from higher dissolution blanks (e.g. 3500 pg Nd, 150 pg Sm) originating mainly from the flux (Table 1). Purification procedures for $LiBO_2$ are discussed later. Each method produces quite different solution matrices but both are easily handled by the ion-exchange (IONEX) column procedures described in the next section. The dissolution procedures are described in detail in the Appendix.

[1] The use of specific commercial products does not imply endorsement by the Geological Survey of Canada.

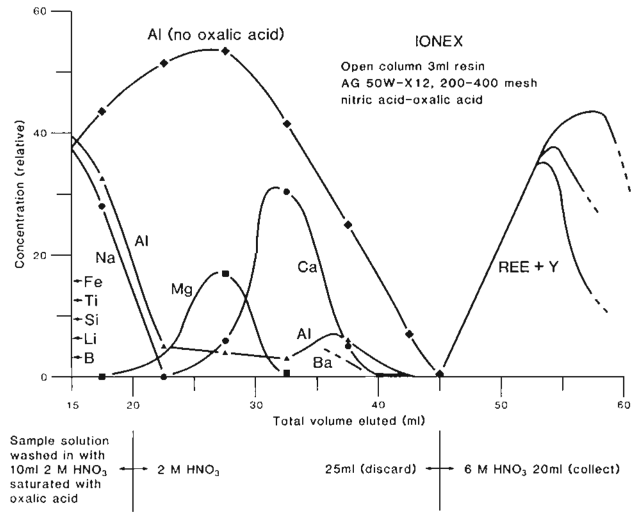

Figure 1: Sketch of typical ion-exchange elution curves for the group separation of REE + Y from major rock elements. Open columns with 3 ml AG 50W-X12 cation resin are used with HNO_3 acid as the eluent. The Si, Li and B (from fusion method only) elute in the sample wash. Fe, Ti and Al are initially complexed with oxalic acid and elute quickly. REE + Y are strongly held in 2 M HNO_3 but elute sharply and quantitatively with 6 M HNO_3. Behaviour of Al is of particular interest (see text). Column performance was characterized by ICP-ES, ICP-MS and HPLC methods.

IONEX: GROUP SEPARATION of REE + Y

Quantitative bulk separation and pre-concentration of the rare-earth elements (REE, atomic numbers 57-71) plus Yttrium (Y, atomic number 39) is performed using small open columns containing 3 ml of AG 50W-X12, 200-400 mesh, H+ form cation exchange resin[1] (Bio.Rad, Richmond, CA). HNO_3 is the primary eluting acid, but an oxalic-nitric acid mixture is used initially to complex the Fe, Ti and the Al (*see* Fig. 1). Yttrium, with similar chemical properties (group IIIB), elutes with the REE. Nitric acid is the preferred acid for ion-exchange separation of REE from rock solutions because the resin in this medium is more tolerant to column overloading and provides much better separation from the major rock elements, with the exception of Fe (Crock et al., 1984). The Fe problem is resolved, however, by the use of oxalic acid. A strong anionic Fe-oxalate complex forms which immediately elutes from the cationic column. In our experience, Al can be a problem because it can interfere with REE determination by HPLC if not completely separated. Aluminum is also effectively handled, however, with oxalic acid, provided enough is available. Figure 1 presents a typical separation of elements with the elution of Al both with and without oxalic acid in the sample wash. Gast et al. (1970) showed that Al together with Fe, Ti, Zr and U elute immediately using 0.5 M oxalic acid alone. It seems that the complexing of Al is inhibited by HNO_3 causing it to elute somewhat later. Aluminum is of additional interest because it apparently can exist as two species (possibly as Al^{+3} as well as an oxalate complex) (Fig. 1). This dual species behaviour of Al is possibly analogous to that reported by Ahrens et al. (1963) and by Aulis et al. (1985).

The REE+Y are held very strongly on the column at lower concentrations of HNO_3, thus permitting complete removal of the majors. For example, up to 45 ml (20 ml more than required to elute the major elements) of 2 M HNO_3 have been eluted through the column without breakthrough of the REE (Fig. 1). The large amounts of Li and B from the flux, and the Si from the rock (fusion procedure only) pass rapidly through the column without problem. The REE+Y elute sharply as a group in 6 M HNO_3. The 20 ml solution is dried down in preparation for the HPLC separation.

The IONEX column chemistry procedures are outlined in Figure 1 and described in detail in the Appendix.

HPLC: REE+Y DETERMINATION AND COLLECTION OF Sm and Nd

Apparatus and process

The HPLC equipment used in this laboratory is pictured in Figure 2 and major components are shown schematically in Figure 3. Following the schematic, the ternary solvent delivery system (Spectra Physics, model SP 8700, Santa Clara, CA) provides reagent solution (mobile phase) under program control of composition (%A, B, C), and flow rate under either isocratic or gradient elution conditions. The system is easy to program and is very flexible. Reagents are delivered to the sample injector which is a syringe loading rotary valve (model 7125, Rheodyne, Berkeley, CA). The sample solution is introduced into the mobile stream by first filling a sample loop (100 microlitre) via the port (valve in LOAD position) using a needle-syringe. Partial loop fillings can also be done. When all is ready the solvent delivery system is initialized and the valve is turned to the INJECT position which causes the mobile phase to pick up the sample from the loop and deliver it to the separation column. This action also starts a timer and the integrator. The column, a 4.6 mm by 15 cm bonded reverse-phase (5 micron Supelcosil LC-18, Supelco, Bellefonte, PA) separates the REE from each other and delivers them to the collection valve (model 7030, Rheodyne, Berkeley,CA). This valve diverts the sample either for chromatographic analysis or for collection of Sm and Nd for mass analysis (*see* Fig. 3, mode 1 and 2). For REE+Y analysis a post column colour reaction is performed by introducing a solution of Arsenazo III (Ar III) into the analyte stream via a zero dead volume Tee mixer, fabricated in house, based on a design of Elchuk and Cassidy (1979). The Ar III is delivered at a uniform flow (low baseline noise) by a syringe pump (model 314, Isco, Lincoln, NE). A colour reaction occurs between the Ar III and the analytes which is sensed by a variable wavelength UV-Vis detector (model SF773, Kratos, Westwood, NJ) set at 658 nm. The detector produces an analogue signal proportional to the amount of analyte.The signal is analyzed by a computing integrator (model 4270, Specta Physics, Santa Clara, CA). This integrator is a powerful analytical tool capable of sophisticated analyses of complex signals. The integrator produces an analytical report containing a chromatogram with retention times (RT) for each peak (*see* Fig. 7). Parameters required for regular analyses or calibration runs are entered into the integrator via a dialogue routine and stored in memory.

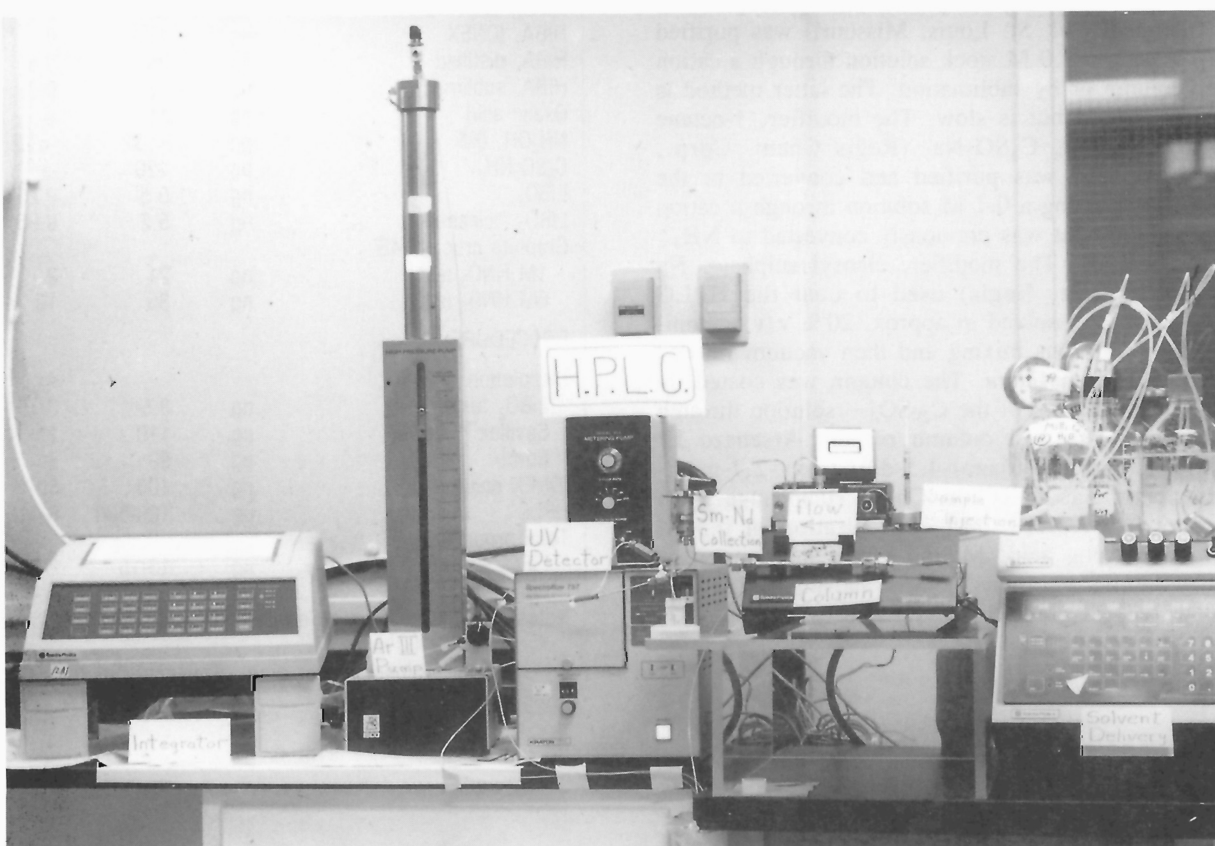

Figure 2: The HPLC equipment in use in the Geochronology Laboratory, GSC. Sample flow is from right to left.

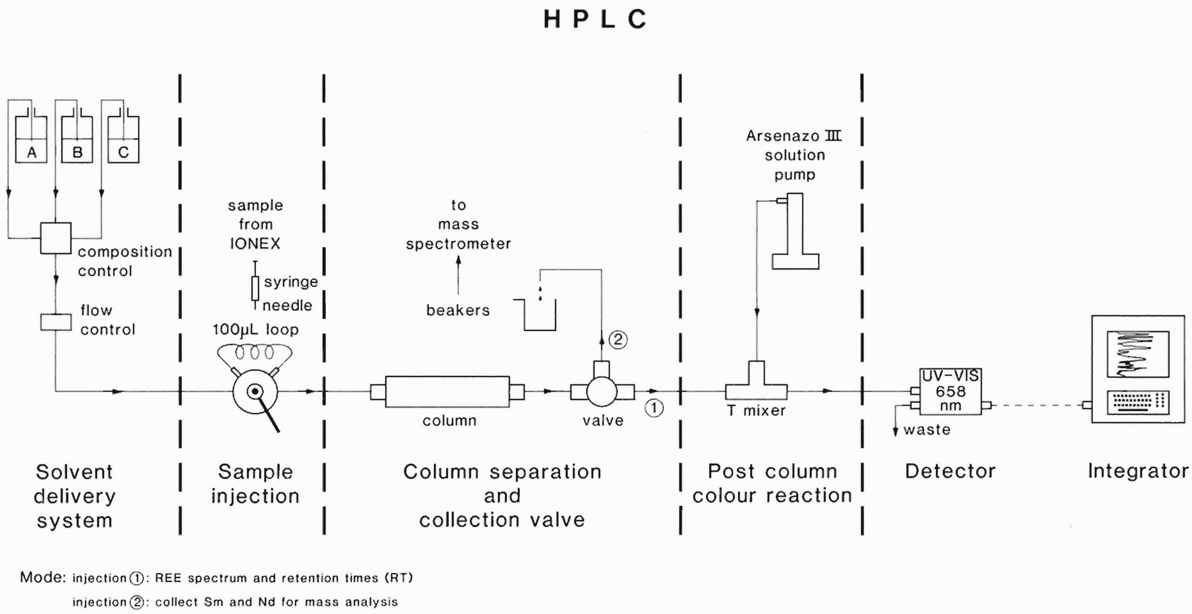

Figure 3: Schematic drawing showing the major components of the HPLC system. Currently two sample injections are performed, the first to obtain a REE chromatogram and the second to collect Sm and Nd cuts for mass analysis. This is done by turning the collector valve at the correct moment to divert the eluent. Sample flow is from left to right.

HPLC reagents and materials

Water is purified with an integrated 2 part system, reverse osmosis (Milli-RO) and a finishing unit (Milli-Q, Millipore, Bedford, MA). All aqueous solutions are vacuum filtered (0.45 micron). The α-hydroxyisobutyric acid (HIBA), (Sigma Chemical Co., St. Louis, Missouri) was purified either by passing a 2.0 M stock solution through a cation exchange column or by sublimation. The latter method is preferred (Table 1) but is slow. The modifier, 1-octane sulphonate, Na salt, C_8SO_3Na, (Regis Chem. Corp., Morton Grove, IL) was purified and converted to the NH_4^+ form by passing a 0.1 M solution through a cation exchange column that was previously converted to NH_4^+ form with NH_4OH. The modifier, eicosyl sulphate, Na salt, ($C_{20}H_{41}SO_4Na$, Regis) used to coat the HPLC columns was first dissolved in approx. 20% v/v acetonitrile/water by vigorous mixing and then vacuum filtered through 0.45 micron filters. The column was coated by pumping about 1200 ml of the $C_{20}SO_4-$ solution through it at 1ml/min. The post column reagent Arsenazo III (3,6-bis((o-arsenophenyl)azo)-4,5-dihydroxy-2,7-naphthalenedisulphonic acid), (Fluka Chem.,Hauppauge, NY) was prepared at $1.2X10^{-4}$ M concentration in 0.5 M reagent grade acetic acid. Mobile phase solutions were prepared at the concentrations required and adjusted to a pH of 4.6 with reagent grade 5 M NH_4OH.

Table 1. Current Sm and Nd reagent, and procedure blanks[1]

REAGENT[2]	ng/pg	Nd	Sm
H_2O	pg	0.05	0.09
HNO_3, 6M	pg	2.6	0.5
HIBA, IONEX	pg	130	6
HIBA, distilled	pg	35	0.5
HIBA, sublimed	pg	15	0.2
Oxalic acid	pg	11	—
NH_4OH, 5M	pg	<32	<22
$C_8SO_3NH_4$	pg	120	—
$LiBO_2$	ng	5.5	0.25
$LiBO_2$ "cleaned"	ng	5.2	0.95
Graphite cruc. UF4S			
1M HNO_3 leach	ng	21	2
6M HNO_3 leach	ng	85	10
PROCEDURE			
Dissolution			
$LiBO_2$ fusion	ng	3.5	0.15
Savillex™ beaker	pg	110	11
Bomb	pg	89	8
IONEX column	pg	100	50
HPLC	pg	100-500	6-110
Total procedure			
$LiBO_2$ fusion	ng	10-15	2-3
Bomb	pg	500	100

Notes: [1]All blanks were determined by IDMS, uncertainties are 20-100%.
[2]Blank values are per gram of reagent

HPLC column separation mechanisms

Separation occurs by interaction between analytes and reagents in the mobile phase (e.g. HIBA is a complexing reagent for REE), and the stationary solid phase (e.g. the modified surface of the column packing).

(i) Separation

The HPLC separation can be considered an ion-exchange mechanism similar to the more conventional resin type ion-exchange column separation. In contrast to resin beads which are porous, the HPLC column packing consists of solid rigid silica gel spheres onto which a charged surface character is developed. This layer provides charged sites where ion-exchange occurs. A description follows for the specific columns used in our laboratory (*see* Fig. 4). The reader is directed to Snyder and Kirkland (1979), and Tarter (1987) for a thorough treatment of the theory and application of HPLC.

A nonpolar, hydrocarbon functional group (R) is chemically bonded (by the manufacturer) to the silica gel, namely a C_{18} alkane called octadecylsilane (ODS). This is a widely used bonding group. A surface ion-exchange character is provided by introducing a modifier, either dynamically in the mobile phase (Type A, Fig. 4) or by permanently coating the column (Type B). In both types the nonpolar end of the modifier adsorbs to the nonpolar R group on the column, while the polar (ionic) end of the modifier provides the ion-exchange site. There is a rapid mass transfer of reagents and analytes between this charged surface and the mobile phase. In Type A columns, where the modifier is added dynamically as part of the mobile phase, the ion-exchange capacity of the column can be easily and rapidly changed. For metal ion separations good peak resolution and high column efficiencies are also valuable characteristics of these types of columns (Cassidy et al., 1987).

The two modifiers used in our laboratory are 1-octanesulphonate, NH_4 form ($C_8SO_3^-$) which is introduced dynamically into the column in the mobile phase at constant concentration (0.01 M), and eicosylsulphate, Na form ($C_{20}SO_4^-$) which is permanently coated onto the HPLC column.

The former technique is more flexible and gives somewhat better separations, but because the $C_8SO_3^-$ is in the mobile phase (HIBA also), it remains in the Sm and Nd fractions collected from the column, and is loaded on the mass spectrometer filament. In contrast to the HIBA which sublimes, a persistent residue from the $C_8SO_3^-$ remains on the filament. Provided there is sufficient Nd (approx. 100 ng) available on the filament, the presence ofthe $C_8SO_3^-$, although tricky and somewhat messy to load, does not interfere with mass analysis. It was felt, however, that the presence of the $C_8SO_3^-$ would probably seriously jeopardize future analyses of small amounts of Nd(e.g. from minerals). Another problem was the pervasive presence of barium in the $C_8SO_3^-$ (and other HPLC reagents, discussed later). For these reasons, the technique of permanently coating the column with the $C_{20}SO_4^-$ modifier was initiated.

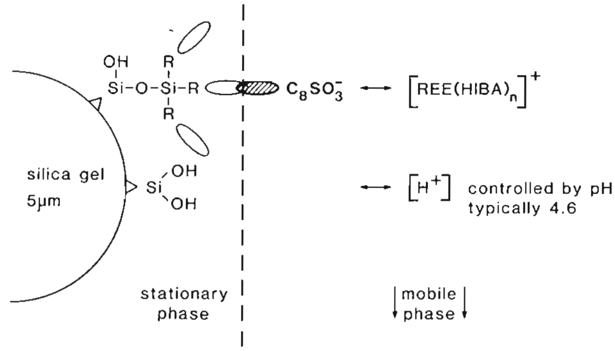

Type A: Ion exchange character provided dynamically by $C_8SO_3^-$

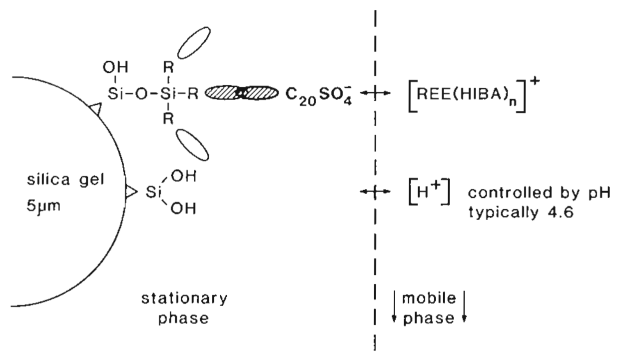

Type B: Ion exchange character provided by permanently coated $C_{20}SO_4^-$

Figure 4: Sketch illustrating separation mechanisms on octadecylsilane (C_{18}, R above) bonded reverse phase HPLC columns. The mechanism is basically a "high performance" cation-exchange between REE-HIBA complexes in the mobile (eluent) phase and ion-exchange sites on the surface of the solid stationary phase. Rapid mass transfer occurs giving sharp separations. Ion-exchange sites are developed dynamically with the modifier in the mobile phase, Type A, or by a modifier permanently coated on the solid phase, Type B. Separation is easily controlled by changing the HIBA concentration in the mobile phase (*see* text and Fig. 6).

This technique, although somewhat less flexible, also produces good Sm and Nd separations and, because there is no modifier added to the mobile phase, has the desirable advantage of providing very clean filament loads.

(ii) REE-HIBA complexes

The HPLC column separation of the REE is facilitated by the use of a complexing reagent, α-hydroxyisobutyric acid (HIBA; also called methyl lactic acid, MLA), which is known to be an excellent complexing agent for the lanthanides (Campbell, 1973). The distribution of the REE cations between the solid phase (ion-exchange sites) and the mobile phase is determined primarily by the affinity of the REE for the HIBA, while the relative strength of the HIBA complexes is determined by the ionic radii of the REE (Korkisch, 1969, p.197-202). Since the heavy REE have smaller radii and the highest affinity for the HIBA (Fig. 5), they begin to elute first. Another factor affecting separation is the decrease in the positive charge density of the REE-HIBA complexes. REE in aqueous solutions are usually trivalent cations but the complexes are less positively charged. The net decrease depends on the degree of complexation (Dionex, 1987). Thus the HIBA-Lu complex being the least positively charged (Fig. 5), would begin to elute first while the HIBA-La complex being the most positively charged would be the last. Thus the distribution of the REE between the ion-exchange layer and the mobile phase can be controlled by increasing the concentration of the HIBA in the mobile phase. At low concentrations (e.g. 0.05 M) the REE are weakly complexed and dwell longer on the column. As the HIBA concentration is increased (e.g. to 0.40 M) more complexation occurs and the REE shift more into the mobile phase. They elute faster and selectively in order of decreasing atomic number (i.e. Lu to La). Changing the HIBA concentration is easily accomplished by programming the solvent delivery system, i.e. using gradient elution. The pH of the mobile phase is also important because the H^+ competes with the REE for ion-exchange sites. The mobile phase is prepared at a constant pH of 4.6.

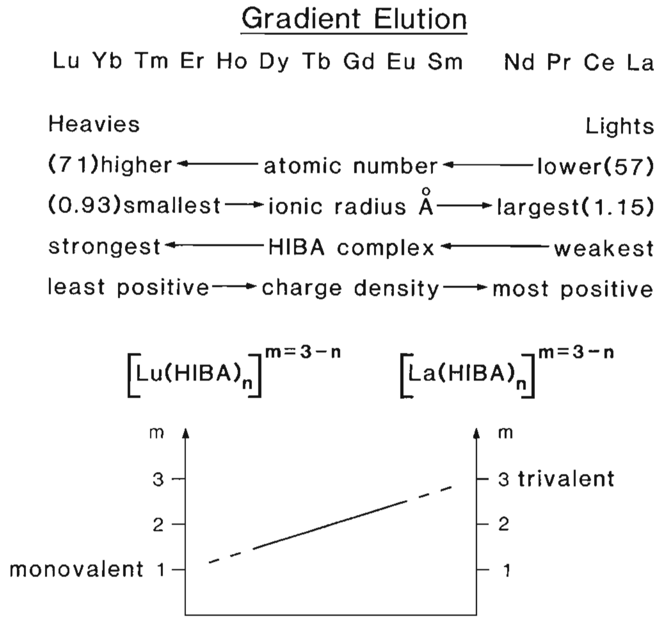

Figure 5: The relationship between ionic radius (approx.), HIBA complexation and positive charge density of the REE. Gradient elution is used to precisely increase the HIBA concentration and thereby selectively elute the REE. At lower HIBA concentrations the heavy REE are more strongly complexed and elute first while the light REE are more strongly held on the column (*see* text).

HPLC separation and collection of Sm and Nd

As the separation of REE is easily controlled by changing the concentration of the HIBA, the separation can be optimized with three things in mind: (i) most importantly, a good separation of Nd from Sm (i.e. no overlap of these elements); (ii) good overall peak resolution for accurate REE determination; and (iii) a runtime as short as possible, which is usually a compromise between (i) and (ii).

The separation of Sm and Nd at different concentrations of HIBA is illustrated in Figure 6 and an example of a chromatogram from a REE+Y standard solution is shown in Figure 7.

The current technique is to perform two 100 microlitre injections of the same rock sample. The first is to obtain a chromatogram with retention times (RT), (Fig. 8a). This gives an immediate and reliable indication of the REE distribution in the sample. Any problems with prior chemistry also now become apparent. In addition, a REE determination (analysis) report is generated at this time. This first injection also serves to precondition all the HPLC components with sample solution to minimize any possible cross contamination.

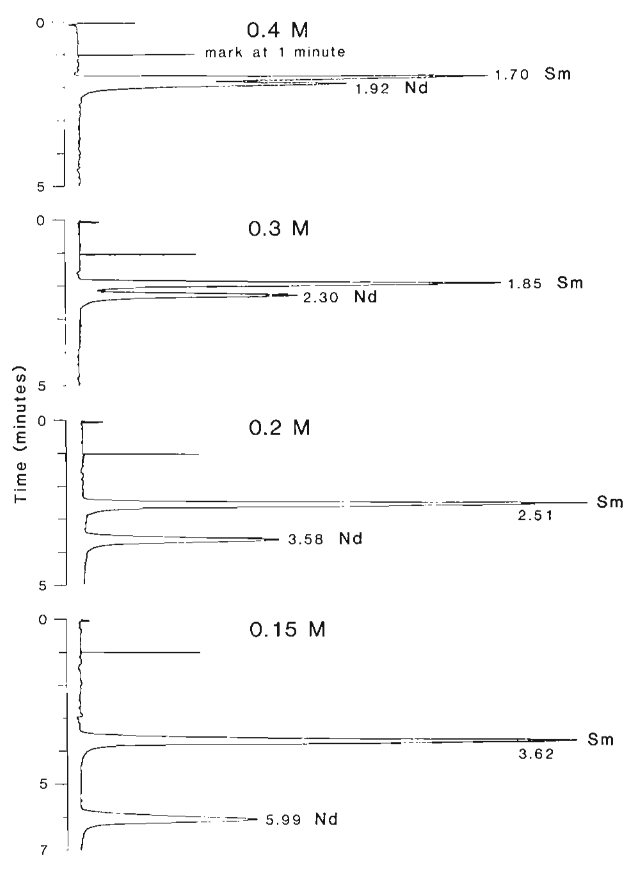

Figure 6: HPLC isocratic separations of Sm and Nd at different concentrations of HIBA. At 0.4 and 0.3 M the separation is poor, but at 0.15 M it is excellent (over 2 minutes), but the separation time is longer. In these examples the column was dynamically modified with $C_8SO_3^-$(0.01 M) in the mobile phase. Note the sharp well resolved peaks. The power of HPLC is the ability to easily change conditions to optimize results.

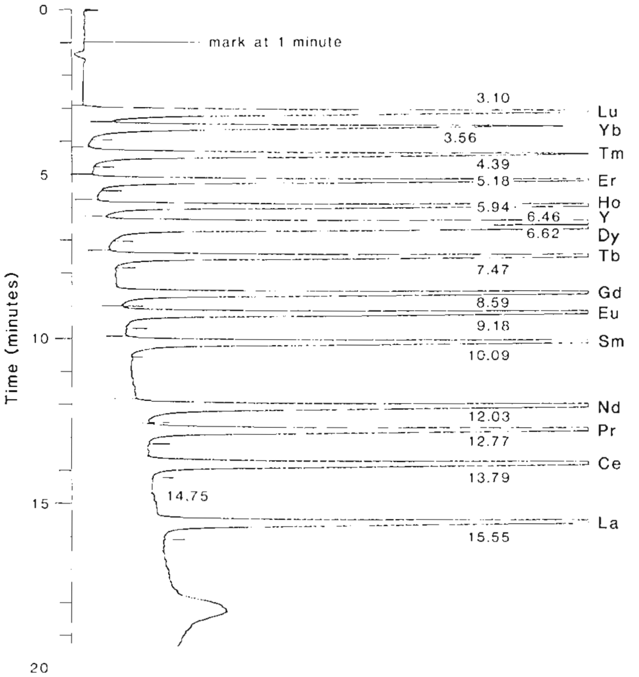

Figure 7: HPLC chromatogram of a 100 microlitre injection of a REE + Y standard (1 microgram each/ml). A gradient elution ranging from 0.05 to 0.40 M HIBA was used with $C_8SO_3^-$ (0.01 M) in the mobile phase to dynamically modify the column. Note the sharp well resolved peaks except for Y which interferes with Dy. The rising baseline is due to the increasing concentration of HIBA.

The second injection is to collect the Sm and Nd cuts for mass analysis by turning the collection valve at the appropriate moment (Fig. 8b). The correct times to collect the cuts are easily obtained by scaling the peak widths on the chromatogram with a centimetre ruler (chart speed is 1 cm/min.). The RTs are also a guide. Repeat injections are remarkably reproducible (RTs ±2 sec.) so that very complete Sm and Nd cuts are possible. An external timer is used for this purpose (a modified MICRONTA clock/timer, Radio Shack 63-734, wired with a magnetic reed switch to the injector valve).

The REE+Y sample from the IONEX column separation is taken up in 500 microlitres of 0.05 M HIBA and filtered through a 0.45 micron disposable cartridge (Millex-HV4, SJHV004NS, Millipore, Bedford, MA.) using disposable plastic syringes. Filtration is necessary to protect the HPLC components from particles. Sometimes there is a residual from the IONEX column separation which will not dissolve in 0.05 M HIBA. This is ignored because the REE dissolve totally in the HIBA. The sample solution is introduced into the HPLC system via the sample injector valve with disposable plastic syringes, and reusable stainless steel needles. The 100 microlitre sample loop is filled and, when all is ready the valve is turned to the INJECT position to begin the analysis. Currently each run takes about 25 minutes which includes the time needed to re-establish equilibrium in the column and to bring the system back to a state of readiness between injections. Between samples the injection valve is cleaned thoroughly with 1 M HNO_3, water and mobile phase. The collection valve is cleaned by rotating it repeatedly to waste.

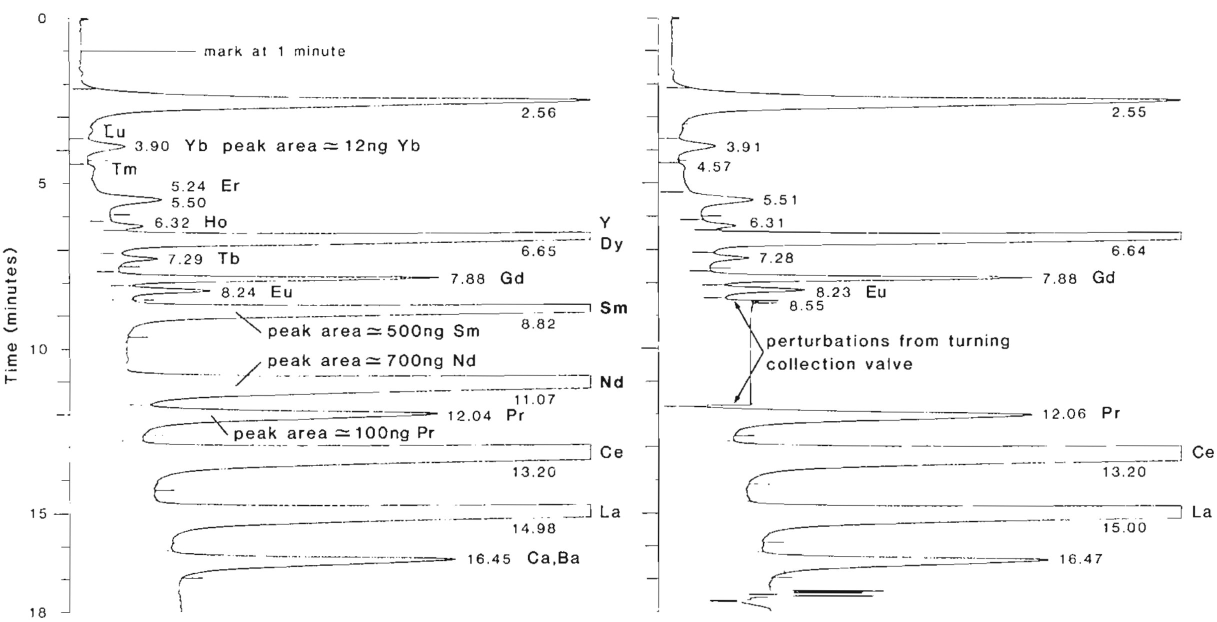

a b

Figure 8: Examples of chromatograms (annotated) of REE from a gneiss containing 15.12 ppm Nd and 2.51 ppm Sm (isotope dilution). A gradient elution was used with a permanently coated column. Currently two injections are performed for each sample. The first (a) to obtain a chromatogram with retention times (RT) and for REE determination. The second (b) to collect Sm and Nd for mass analysis by turning the collection valve at the correct time which is determined by scaling the chromatogram (a). Nd is separated from Sm by over 2 minutes. This rock was relatively enriched in light REE compared to the heavy REE. The sensitivity of HPLC is about 0.5 ng. Traces of non REE + Y elements from the rock were detected at RT 2.56 and 16.45 min. but these do not interfere with the REE. HPLC chromatograms are remarkably reproducible, RT ± 2 seconds.

Currently samples are injected and separated using a permanently coated column with a gradient elution from 0.05 to 0.40 M HIBA at a flow of 1 ml/min.; from 0.05 to 0.12 M over 2 min., held at 0.12 M for 3 min., then from 0.12 to 0.2 M over 5 min., and from 0.20 to 0.40 M over 5 min., and then down to 0.05 M over 5 min. The eluted metal ions are monitored with the UV-Vis detector set at 658 nm, after a postcolumn reaction with Arsenazo III delivered at a flow of 1 ml/min. For the collection of Sm and Nd, which are separated by about 2 minutes (Fig. 8), the collector valve is turned at the appropriate time diverting the Sm and Nd cuts into 7 ml Savillex™ vials. Each is collected for 30 seconds (0.5 ml). During the time between the Sm and Nd collection the mobile phase is sent to waste, thus flushing the collector parts of any Sm tail. The cuts are then evaporated (HIBA sublimes) on a hot plate at 100 to 135°C. When dry, 1 to 2 drops of 6 M HCl are added and taken to dryness to remove any remaining HIBA and to convert samples to chlorides, ready for mass analysis.

REE determinations

Quantitative analysis is performed using the computing integrator (SP4270) which resolves the signals to produce analyses by peak area integration. Several commonly used chromatographic methods are available but the most appropriate for this application is "external standardization" whereby sample concentrations are calculated based on stored peak area "calibration curves" for each analyte. Calibration for each peak is necessary because detector response is different for each analyte. Typically, calibration is performed by injecting 2 standards, which contain all the analytes of interest, at different but known concentrations. The standards are selected to bracket the estimated concentrations in the sample solutions. "Calibration curves" are generated for each analyte using a slope-intercept form of linear equation based on response factors (RF=area/conc.). Concentrations of unknown sample analytes are then calculated from the calibration curve using the measured peak area of each unknown. Typically, a calibration can be done once in the morning and be good for the rest of the working day.

This method requires a reliable chromatographic system and good analytical technique. Since the RF values are determined by peak area per unit of concentration, the accuracy of HPLC analyses depends on injection volumes being identical for sample and calibration.

The HPLC system has been primarily used to separate Sm-Nd for mass analysis which can proceed independently of REE quantification. Considerable developmental work has been done, however, to perform REE determinations on a routine basis. Duplicate analyses (injections) of standards indicate reproducibility to be about 1%. An evaluation of preliminary results indicate that REE can be routinely determined to better than 3% accuracy. Sensitivity is about 0.5 ng. Some quantification problems do exist, however. The most serious is the chromatographic interference of Y with Dy (e.g. Figs. 7, 8). Scandium will also interfere with Lu if present, but this has not been a problem so far.

MASS ANALYSIS

Mass spectrometry of Sm and Nd is performed on a Finnigan-MAT 261variable multicollector mass spectrometer using double Re filament loads, and analyzed as metals in static multicollection mode. Metal oxides have not been detected during runs.

Sm and Nd samples are loaded in clean (HEPA filtered) air onto 0.03″ zone refined filaments that have been degassed at > 2000 °C for at least 5 minutes. The samples are taken up with 1-2 microlitres of 0.3 M H_3PO_4 acid , dried on the evaporation filament and "glowed" 30-40 seconds at 2.2-2.4 amps. This loading provides steady growing signals, typically lasting more than 2 hours at 1 volt ^{144}Nd from 20 ng Nd load. Loadings with water and 0.3 M HCl were tried but generally gave unstable, dying signals.

Evaporation filaments for Nd run at 1.7 amps. (1.6-2.2), and at 4.8 amps. (4.6-5.2) for the ionization filament current. The currents are slightly lower for Sm.

Mass analysis for Nd consists of statically measuring masses 143, 144, 145, 146 and 148 while monitoring 147 for possible Sm interference, with a ^{144}Nd beam at 0.5 to 3 volts. Nd analyses are normalized to $^{146}Nd/^{144}Nd$ of 0.7219. An analysis consisting of at least 200 ratios (12 per block) is usually obtained (over 60 min.) with uncertainties on $^{143}Nd/^{144}Nd$ ratio of $\pm$ 0.00001 to $\pm$ 0.00003 (2 sigma of the mean). Analyses are generally free of interferences from other REE (e.g. no Ce) and with $^{144}Sm/^{144}Nd$ < 0.01%. Analysis of BCR-1 produces a $^{143}Nd/^{144}Nd$ ratio of 0.512594 $\pm$ 15 and $^{147}Sm/^{144}Nd$ of 0.13781.

Mass analysis for Sm proceeds on a weaker signal, of 0.3 to 1.0 volts of ^{152}Sm, and consists of 5 to 7 blocks of static measurement of masses 147, 149 and 152. A $^{152}Sm/^{147}Sm$ of 1.78308 is used to correct for mass fractionation.

Nd and Sm are analyzed separately in batches using different cup configurations.

For reagent blanks spiked with ^{145}Nd-^{152}Sm, Nd and Sm are analyzed simultaneously and calculated from $^{145}Nd/^{146}Nd$ and $^{147}Sm/^{152}Sm$ or $^{149}Sm/^{152}Sm$.

DISCUSSION

Procedures for the extraction and purification of Sm and Nd from whole-rocks have been described in detail with particular emphasis on HPLC. Some problems associated with these procedures remain and are now discussed.

The fusion method of dissolution ensures rapid total sample dissolution but currently the Sm and Nd blanks, primarily from the $LiBO_2$ flux are high (Table 1). Methods to purify the flux are being pursued. Initial attempts to purify the $LiBO_2$ using procedures similar to Vocke et al. (1987), involving fractional crystallization, dehydration and grinding were unsuccessful. Preliminary tests using a chelating ion-exchange resin, Chelex 100 (Bio Rad, Richmond, CA) are encouraging (*see* De Barr et al., 1988).

The IONEX column separation of the REE+Y appears to be problem free, although traces of other elements originating from the rock solution are sometimes detected in the HPLC chromatograms (e.g. Fig. 8). Currently these do not interfere with the Sm, Nd separations nor the other REE. During development of the ion-exchange column separation, traces of Al, Cr and Ti were detected and interfered with the heavy REE. This was attributed to overloading of the IONEX column.

Currently the most serious problem associated with the HPLC method is the pervasive presence of traces of Ba, primarily from the HIBA. Barium lowers the ionization efficiency of Nd during mass analysis and has to be burned away. Barium oxide is also a potential problem due to isobaric interferences.

This problem has been greatly reduced by purifying reagents but still persists. Ion-exchange column purification procedures do not seem adequate to remove Ba to the level required. Sometimes in fact, the resin seems to add Ba. Recent tests using a solution of disodium ethylenediamineteta-acetate (EDTA) to pre-treat ion-exchange columns has been effective in removing traces of strongly held cations from the resin and is being investigated as a method of producing resin clean enough to remove traces of Ba from HIBA solutions, (D.J. Barkley, pers. comm., 1988). Sublimation of the HIBA was only partially successful in removing Ba and is slow. A more rapid method is by vacuum distillation (Cassidy, 1988). These methods are effective, however in reducing Sm, Nd blanks (Table 1). Purification methods to remove traces of Ba from the reagents are being pursued.

A minor but disconcerting problem can occur in HPLC systems, namely that of "mystery peaks". These are real in that they are detected, but they do not originate from the rock samples. They appear to come from bacteria or high molecular weight organics that build up in the HPLC column and eventually elute (Cassidy, 1987). These peaks can interfere with REE determination and require careful reagent preparation and close monitoring of the HPLC system.

HPLC: advantages and disadvantages for Sm-Nd studies

The use of HPLC as a separation method for Sm and Nd is new. One of the reasons for writing this paper is to introduce the method to scientists in other geochronology laboratories. For these reasons some advantages and disadvantages are presented based on the experience of the author to date.

Inductively coupled plasma spectrometry (ICP) and HPLC have, in recent years, become very important tools in inorganic analytical chemistry. HPLC equipment, reagents and techniques are fully researched and have matured to the point where complete analytical systems are now commercially available for elements and ions of interest to geoscientists. HPLC systems are flexible and quite reliable.

As a Sm-Nd separation method, however, HPLC is very equipment dependent and any failure in one of the major components would shut down the method until repaired. The total capital cost was about $35K when purchased in 1984/85. HPLC requires competent operation. All eluents have to be filtered.

The "high performance" in HPLC is a result of rapid mass transfer between the fine (0.5 micron) solid silica gel spheres and the analytes in the mobile phase. The HPLC column is basically a "high performance" ion-exchange column which can resolve peaks sharply and cleanly (e.g. Nd is separated cleanly from Sm and Ce). With the type of HPLC column described here, however, the Nd elutes after the Sm so that the column must be working efficiently to prevent Sm tailing. A powerful feature of HPLC is that separations can be optimized easily by changing the composition or flow rate of the eluent. Another useful feature is the chromatogram, which allows one to "see" the separation in real time. One can follow and monitor the quality of the separation which allows a measure of confidence that all is going well. HPLC is remarkably reproducible with RT $\pm$ 2 seconds for repeat injections and $\pm$ 10 seconds from day to day.

A big bonus of HPLC is the ability to rapidly determine all the REE with accuracy estimated at $\pm$ 3%. Quantification of the REE requires extra work, however, in preparing standards, performing calibrations etc., and in developing quantitative aliquoting and dilution techniques throughout the entire procedure from dissolution to analysis.

HPLC systems are stable and reproducible, and their performance is easily monitored. The efficiency and flexibility of HPLC columns are attractive features in providing optimized separation of Sm and Nd for isotopic studies. HPLC together with the IONEX column separation provide a rapid method for REE determination.

ACKNOWLEDGMENTS

I thank colleagues, Otto van Breemen, for his patient advice, Chris Roddick for providing leadership throughout, and Frank Dudás, who has been using the HPLC system for Sm-Nd, for his many helpful suggestions in the laboratory and for providing some data for this paper. A great debt is owed to R.M. Cassidy whose knowledge and experience was drawn upon many times. Co-workers at the GSC, G. Lachance, C. Grégroire and A. Martineau are thanked for assistance. Last but not least, I must thank my friend and colleague Dwight Barkley of CANMET who has generously provided advice and materiel on many occasions. C. Roddick and D. Barkley also provided useful comments upon reviewing the paper.

REFERENCES

Ahrens, L.H., Edge, R.A., and Brooks, R.R.
1963: Investigations on the development of a scheme of silicate analysis based principally on spectrographic and ion exchange techniques; Analytica Chimica Acta, v. 28, p. 551-573.

Aulis, R., Bolton, A., Doherty, W., Vander Voet, A., and Wong, P.
1985: Determination of yttrium and selected rare earth elements in geological materials using high performance liquid chromatographic separation and ICP spectrometric detection; Spectrochemica Acta, v. 40B, no. 1 2, p. 377-387.

Campbell, D.O.
1973: Rapid lanthanide and actinide separations with pressurized ion exchange chromatography; Proceedings of 10th Rare Earth Research Conference, Carefree, Arizona, p. 1098-1107.

Cassidy, R.M.
1988: Determination of rare-earth elements in rocks by liquid chromatography; Chemical Geology, v.67, p. 185-195.

Cassidy, R.M., Elchuck, S., and Joe, K.S.
1987: Experimental considerations in the practice of metal ion separations by dynamic exchange techniques; *in* Recent Developments in Ion Exchange, ed. P.A. Williams and M.J. Hudson; Elsevier Applied Science, London, p. 40-48.

Cassidy, R.M., Miller, F.C., Knight, C.H., Roddick, J.C., and Sullivan, R.W.
1986: Evaluation of dynamic ion exchange for the isolation of metal ions for characterization by mass and ∞ spectrometry; Analytical Chemistry, v.58, p. 1389-1394.

Crock, J.G., Lichte, F.E., and Wildeman, T.R.
1984: The group separation of the rare-earth elements and yttrium from geological materials by cation-exchange chromatography; Chemical Geology, v.45, p.149-163.

De Baar, H.J.W., German, C.R., Elderfield, H., and van Gaans, P.
1988: Rare earth element distributions in anoxic waters of the Cairaco Trench; Geochimica et Cosmochimica Acta, v.52, p. 1203-1219.

Dionex
1987: Determination of lanthanide metals; Technical Note TN23, Dionex Corporation, Sunnyvale, CA.

Elchuk, S. and Cassidy, R.M.
1979: Separation of lanthanides on high-efficiency bonded phases and conventional ion-exchange resins; Analytical Chemistry, v.51, p. 1434-1438.

Gast, P.W., Hubbard, N.J., and Wiesmann, H.
1970: Chemical composition and petrogenesis of basalts from Tranquility Base; Proceedings of the Apollo 11 Lunar Science Conference, v. 2, p. 1143-1163.

Hegner, E., Kyser, T.K., and Hulbert, L.
Nd, Sr and O isotopic contraints on the petrogenesis of mafic intrusions in the Proterozoic Trans-Hudson Orogen of central Canada; Canadian Journal of Earth Sciences, (in press).

Hofmann, A.
1971: Fractionation corrections for mixed-isotpoe spikes of Sr, K and Pb; Earth and Planetary Science Letters, v. 10, p. 397-402.

Kantipuly, C.J. and Westland, A.D.,
1988: Review of methods for the determination of lanthanides in geological samples; Talanta, v. 35, no. 1, p. 1-13.

Korkisch, J.
1969: Modern Methods for the Separation of Rarer Metal Ions; Pergamon Press, NY.

Lugmair, G.W., Scheinin, N.B., and Marti, K.
1975: Sm-Nd age and history of Apollo 17 basalt 75075. Evidence for early differentiation of the lunar exterior; Geochimica et Cosmochimica Acta, Supplement 6, p. 1419-1429.

Nakamura, N., Tatsumoto, M., Nunes, P.D., Unruh, D.M., Schwab, A.P., and Wildeman, T.R.
1976: 4.4 b.y.-old clast in Boulder 7, Apollo 17: a comprehensive chronological study of U-Pb, Rb-Sr and Sm-Nd methods; Proceedings of the Lunar and Planetary Science Conferences, 7 th, p. 2309-2333.

Parrish, R.R., Roddick, J.C., Loveridge, W.D., and Sullivan, R.W.
1987: Uranium-lead analytical techniques at the Geological Survey of Canada: *in* Radiogenic Age and Isotopic Studies: Report 1; Geological Survey of Canada, Paper 87-2, p. 3-7.

Richard, P., Shimizu, N., and Allegre, C.J.
1976: ^{143}Nd/^{146}Nd, a natural tracer, an application to oceanic basalts; Earth and Planetary Science Letters, v. 31, p. 269-278.

Riddle, C., Vander Voet, A., and Doherty, W.
1988: Rock analysis using inductively coupled plasma mass spectrometry; review; Geostandards Newsletter, v. 12, p. 203-234.

Shirey, S.B.
1984: The origin of Archean crust in the Rainy Lake area, Ontario; unpublished Ph. D. thesis, State University of New York at Stony Brook, Stony Brook, N.Y.

Synder, L.R. and Kirkland J.J.
1979: Introduction to Modern Liquid Chromatography; John Wiley and Sons, Inc., N.Y.

Tarter, J. (editor)
1987: Ion Chromatography; Marcel Dekker Inc., N.Y.

Vocke, Jr., R.D., Hanson, G.N., and Grünenfelder, M.
1987: Rare earth mobility in the Roffna Gneiss, Switzerland; Contributions to Mineralogy and Petrology, v. 95, p. 145-154.

APPENDIX

DISSOLUTION PROCEDURES

For siliceous samples (more than about 60 % wt. SiO_2) in which refractory accessory phases (e.g. zircon) are potentially important REE reservoirs, conventional hot plate dissolutions are inadequate.

Two dissolution procedures are currently in use:

(i) HF-HNO_3-HCl hot plate/bomb:

A 200 mg aliquot of well mixed rock powder (minus 100 mesh) is weighed into a 15 ml Savillex™ screw-cap vessel, 0.05 to 0.15 g spike added, and charged with 2 ml conc. HNO_3 and 4 ml HF (48 %). With caps tightly closed the samples are refluxed overnight (minimum of 12 hours) on a hot plate (surface temp. about 135°C). After evaporation to dryness, the sample is taken up with 3 to 4 ml of 6 M HCl, recapped and refluxed on a hot plate (80 to 100°C) overnight. The above steps remove the bulk of the silica and facilitate the use of small volume (5 ml) bombs. The HCl solution is transferred into the Teflon™ crucibles for the bomb dissolution and evaporated to dryness. This HCl step seems necessary to dissolve sample precipitates. The bombs are similar to those used for zircon dissolution (Parrish et al.,1987) but are an older individual unit type. After adding 1 to 2 ml HF and 0.5 to 1 ml HNO_3, the bombs are sealed and heated in an oven at 200 to 230°C for 5 to 7 days. After evaporation, the sample is again taken up in 3 to 4 ml of 6 M HCl and placed on a hot plate overnight. Finally, after evaporation, the sample is taken up in 3 to 5 ml of 2 M HNO_3 saturated with oxalic acid, ready for IONEX column separation.

For more basic rocks (less than about 60 wt. % SiO_2) the bomb dissolution may be omitted, in which case the first 6 M HCl solution is evaporated and immediately taken up in 2 M HNO_3 saturated with oxalic acid.

(ii) $LiBO_2$ fusion:

Typically 250 mg of sample are intimately mixed with about 750 mg $LiBO_2$ flux (1:3) in a high-purity (UF4S) graphite crucible ready for fusion in a preheated muffle furnace at 1050°C. Just prior to fusion, 40 ml of 1 M HNO_3 acid, spiked with 0.05-0.10 g tracer, is prepared in a 100 ml Savillex™ screw-capped vessel containing a magnetic stir bar. A batch of 8 samples including a blank, are fused 4 at a time. The graphite crucibles sit on a flat optical grade quartz plate and are covered with quartz bell-jars. The quartz apparatus minimizes oxidation of the graphite which can be a source of blank (Shirey, 1984). In practice, however, the quartz covers are cumbersome to handle and because of the extra time required to uncover the crucibles the melt can partially cool and consequently hinder total transfer of the sample melt out of the crucible. The covers prevent contamination from the furnace itself and prevent cross contamination between samples although this is not known to be a problem. The samples are heated for 15 minutes at 1050°C and transferred quantitatively, as quickly as possible into their respective previously prepared 1 M HNO_3 solutions and magnetically stir-mixed. Minor sputtering occurs when the hot sample melt hits the acid solution but the quantitative loss of spiked solution is negligible. The samples are stirred for 1 hour or until dissolved, resulting in a clear (except for fine graphite from the crucibles) 100 % dissolved sample solution. This solution is stable for at least several days but should be processed fairly quickly because an insoluble gel eventually forms.

REAGENTS AND MATERIALS: DISSOLUTION AND IONEX

All chemicals unless otherwise stated are high purity reagent grade. Mineral acids HF, HNO_3 and HCl used for dissolution were further purified as per Parrish et al. (1987).

Lithium metaborate ($LiBO_2$), puratronic grade (Johnson Matthey Chemicals, England) was used without further purification and found to have high Sm and Nd blanks (Table 1). New graphite crucibles, UF4S (Ultra Carbon Corp., Bay City, Michigan) were preheated to about 1050°C before use. This sinters the crucibles which helps in transferring the fusion melt without loss. Used crucibles have to be very thoroughly cleaned before reuse to prevent cross contamination.

IONEX COLUMN CHEMISTRY PROCEDURE

Columns and resin cleaning

Commercially available 20 cm by 0.7 cm I.D. borosilicate glass ion-exchange columns are used (Bio.Rad, Richmond, CA). These have permanent 35 micron polyethylene bed supports and polypropylene end fittings which accommodate Luer type bottom caps to maintain liquid in the column. Matching funnels are used to filter the sample solutions and as eluent reservoirs.

The resin is initially soaked in a beaker with 6 M HNO_3, and alternately swirled with water and 6 M HNO_3 several times to expand and contract the resin, decanting off any fines. The resin is stored in 1 M HNO_3. The columns are charged with 3 ml resin (in 1 M HNO_3) and cleaned sequentially with 15 ml of 2, 6 and 8 M HNO_3, then back down to 1 M HNO_3 in which the resin is kept when the columns are not in use. Once used for samples and after eluting the REE+Y with 6 M HNO_3, the column is flushed with 2 × 10 ml 8 M HNO_3, then filled to the brim with 8 M HNO_3 and left overnight. After draining, the resin is backwashed directly with 1 M HNO_3 using a syringe and tubing with Luer fittings.

Column chemistry

For samples from the fusion dissolution procedure (ii), a 10 ml aliquot from the 40 ml sample solution is mixed with about 1 gm of oxalic acid crystals (pre-weighed in polymethylpentene (PMP) disposable beakers), covered with parafilm and heated gently with swirling until the oxalic has dissolved. This oxalic-nitric acid sample mixture is introduced into the resin column via a funnel through a Whatman no. 40 filter paper and allowed to drain. The sample is washed into the resin with a total of 10 ml of 2 M HNO_3 saturated with oxalic acid from a squirt bottle, using volume marks on the outside of the columns. Filtering is necessary to prevent graphite particles from the fusion process from fouling the resin. The funnel is removed, rinsed with water (discarding filter paper) and replaced on top of the column. The separation is continued by adding a total of 25 ml 2M HNO_3 (no oxalic) which is discarded. Finally the REE+Y are eluted with 20 ml 6 M HNO_3, collected in PMP beaker and evaporated to near dryness, ready for next step (HPLC).

The column chemistry for samples from the other hot plate/bomb dissolution procedure (i) is similar to the above except that the sample solution may be centrifuged instead of filtering before introducing it into the column, and a smaller volume of solution is loaded.

The age of the Mount Copeland Syenite Gneiss and its metamorphic zircons, Monashee Complex, southeastern British Columbia

R.R. Parrish[1] and R.J. Scammell[2]

Parrish, R.R., and Scammell, R.J., The age of the Mount Copeland Syenite in Gneiss and its metamorphic zircons, Monashee Complex, southeastern British Columbia; in Radiogenic Age and Isotopic Studies: Report 2, Geological Survey of Canada, Paper 88-2, p. 21-28, 1988.

Abstract

The Mount Copeland syenite gneiss is a subconcordant alkaline igneous intrusion within metasedimentary rocks that overlie Early Proterozoic crystalline basement in the Monashee Complex, southeastern British Columbia. The gneiss contains zircons of two ages: 740 ± 36 Ma relict grains and cores, interpreted as original igneous phenocrysts, and 59 ± 1 Ma metamorphic grains and overgrowths which form the bulk of the zircons in the rock. The Precambrian age of the syenite implies that its immediate country rocks are at least 740 Ma old. Although the U-Pb systematics resemble those of a ca. 60 Ma intrusion with inheritance, we tentatively reject a Tertiary age for the rock on the basis of its state of deformation and metamorphism. Instead, the widespread growth of metamorphic zircon at about 60 Ma ago is suggested to coincide with the final stages of Late Cretaceous-Paleocene metamorphism of the Omineca Belt and probable incursion of fluids related to intrusion of Eocene (?) leucogranitic rocks within the hanging wall of the Monashee décollement about 1 km structurally above the syenite gneiss. This event was followed very closely by Early Eocene normal faulting and tectonic denudation.

Résumé

Le gneiss à syénite du mont Copeland est une intrusion de roches ignées alcalines quasi concordantes au sein de roches métasédimentaires qui reposent sur un socle cristallin du début du Protérozoïque dans le complexe de Monashee, dans le sud-est de la Colombie-Britannique. Ce gneiss contient des zircons d'âges différents: des grains et des noyaux résiduels de 740 ± 36 Ma, que l'on considère comme les phénocristaux ignés d'origine, et des grains et surcroissances métamorphiques de 59 ± 1 Ma qui forment la grande partie des zircons contenus dans la roche. Comme la syénite date du Précambrien, les roches encaissantes immédiates ont au moins 740 Ma. Bien que les résultats systématiques U-Pb correspondent à une intrusion d'environ 60 Ma avec héritage, on rejeté temporairement un âge tertiaire pour cette roche compte tenu de sa déformation et de son métamorphisme. La croissance considérable de zircon métamorphique il y a environ 60 Ma coïnciderait plutôt avec les derniers stades du métamorphisme de la zone d'Omineca à la fin du Crétacé et au cours du Paléocène et avec une incursion probable de fluides liée à l'intrusion de roches leucogranitiques de l'Éocène (?) au sein du toit du décollement de Monashee, à environ 1 km structurellement au-dessus du gneiss à syénite. Cet événement a été suivi de très près par une formation de failles normales au début de l'Éocène et d'une dénudation tectonique.

INTRODUCTION

This contribution refines a preliminary U-Pb zircon age (Okulitch et al., 1981) for igneous crystallization of alkaline rocks in the vicinity of Mount Copeland, about 21 km northwest of Revelstoke, British Columbia (Fig. 1). The U-Pb systematics of zircons from this unit are unusual because of extensive growth of apparently metamorphic zircon very late in the history of the rock. This metamorphic zircon growth renders an estimation of the original age of the syenite difficult, because all crystals with original zircon are now mixtures of young and old material. More refined analytical methods are applied in this paper which were not available in the previous preliminary study. Igneous and metamorphic crystallization ages of zircon from the syenite gneiss and the relationship of the gneiss to enclosing metasedimentary gneiss have regional implications for the geology of the Monashee Complex of the southeastern Canadian Cordillera.

[1] Geological Survey of Canada, 601 Booth Street, Ottawa, Ontario, K1A 0E8
[2] Dept. of Geological Sciences, Queen's University, Kingston, Ontario, K7L 3N6

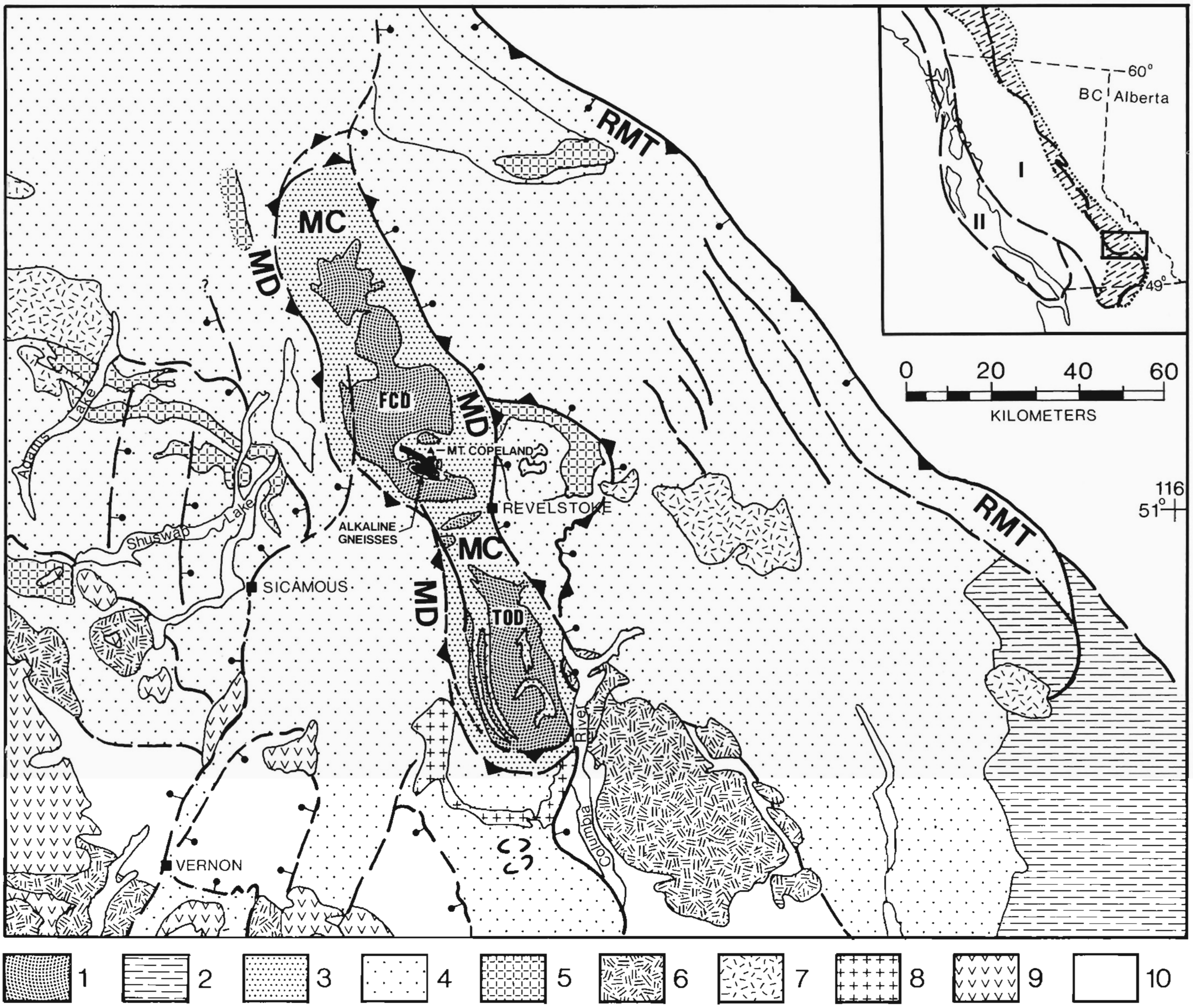

Figure 1. Tectonic map of southeastern British Columbia, modified after Hoy and Brown (1980), Journeay and Brown (1986), and Parrish et al. (1988). Faults marked in heavy lines are thrust faults (barbs), and normal faults (dots) with notation on the hangingwalls, and include the Monashee décollement (MD) and the Rocky Mountain Trench (RMT). On the eastern side of the Monashee Complex, the Monashee décollement is coincident with the Columbia River normal fault (identified by normal fault symbols). Map units are (1) Aphebian core gneiss of the Monashee Complex, (2) Mid-Late Proterozoic Belt-Purcell Supergroup, (3) Mantling gneiss of the Monashee Complex, (4) Late Proterozoic Windermere Supergroup, Paleozoic metasedimentary rocks of North American affinity and minor orthogneiss of uncertain age (Selkirk allochthon of Brown and Read, 1983), (5) Paleozoic granitic rocks, (6) Middle Jurassic granitic rocks, (7) Mid-Late Cretaceous granitic rocks, (8) Early-Middle Eocene Ladybird granitic rocks, (9) Miocene-Pliocene basalt, Middle Eocene volcanic and sedimentary rocks, (10) Late Paleozoic-Early Mesozoic allochthonous terrane, and Paleozoic allochthonous ultramafic rocks. FCD, Frenchman Cap dome; TOD, Thor-Odin dome. Inset map outlines the region's location in British Columbia with respect to the Omineca Belt (dashed), and allochthonous terranes I and II (outlined in heavy dashes) of Monger et al. (1982).

GENERAL GEOLOGY

The Monashee Complex is one of several metamorphic core complexes (Crittenden et al., 1980) that lie within the Omineca Belt, a major structural and metamorphic culmination which straddles the paleocontinental margin of North America and allochthonous terranes that where accreted during early Jurassic to mid-Cretaceous time (Monger et al., 1982). The complex is exposed through a window in the Selkirk Allochthon, and intervening Monashee décollement, a westerly rooted, mylonitic roof thrust (Brown et al., 1986). Mylonitic rocks of the Monashee décollement along the eastern boundary of the complex are overprinted by part of the Columbia River fault, a major east-dipping Eocene normal fault (Read and Brown, 1981; Journeay and Brown, 1986; Parrish et al., 1988).

Wheeler (1965) first recognized broad mappable lithostratigraphic units in the vicinity of Frenchman Cap dome. Subsequent detailed investigations have corroborated, refined and extended these subdivisions south to Thor-Odin dome (Hoy and Brown, 1980; McMillan, 1970; Reesor and Moore, 1971; Hoy and McMillan, 1979; Read, 1979a, 1980; Read and Klepaki, 1981; Duncan, 1984; Journeay, 1986; Scammell, 1986; Hoy, 1987). Lithological assemblages within the complex comprise Early Proterozoic core paragneiss and granitic orthogneiss, and an unconformably overlying, stratified mantling gneiss sequence.

Rocks in the Monashee Complex experienced at least three deformation events, and two high temperature prograde metamorphic episodes (Brown et al., 1986; Journeay, 1986; Scammell, 1986). Despite this intense penetrative strain and recrystallization, it is possible to make inferences regarding protoliths and stratigraphic order based on lithological compositions, geometry, contacts and, at some locations, preserved primary sedimentary structures indicating stratigraphic polarity (e.g. Scammell, 1986; Journeay, 1986). Structural thinning and thickening of mantling gneisses have been recognized. Preserved thickness of the succession ranges from about 750 m to greater than 2000 m (Scammell, 1986).

Mantling gneisses consist predominantly of siliciclastic and carbonate metasedimentary rocks. Most common are metamorphosed equivalents of quartz and quartz-feldspar arenites, pelites, and impure carbonate rocks, some of which occur as laterally extensive horizons. Less common metasedimentary units include a basal quartz-pebble conglomerate, stratabound lead-zinc deposits and impure scapolite-bearing marbles. Subordinate meta-igneous rocks include intrusive mafic, ultramafic, alkaline and carbonatitic rocks, and felsic and carbonatitic pyroclastic rocks (*see* Scammell, 1986; Hoy, 1987).

In the vicinity of Mount Copeland (Fig. 1), a suite of alkaline rocks makes up a 20 km long (unfolded length), 1 to 2 km thick body intimately folded with the host mantling gneisses (Fyles, 1970; Currie, 1976; Hoy and McMillan, 1979). Three composite suites have been delineated: (i) a core suite of nepheline syenite gneiss surrounded by (ii) a mafic suite dominated by alkaline amphibolite, in turn surrounded by (iii) a suite of grey syenite gneiss. These alkaline gneisses have experienced all recognized phases of deformation and metamorphism (Fyles, 1970; Currie, 1976), and currently parallel lithological layering in mantling gneiss with gradational contacts. Crosscutting relationships are suggested but not proven at a kilometre-scale (Currie 1976). Consequently it remains uncertain whether this alkaline body was originally concordant with or crosscutting the host mantling gneisses.

Okulitch et al. (1981) sampled a porphyritic syenite gneiss in the outermost suite of grey syenite gneiss (*see* Table 6.1 of Okulitch et al., 1981). Zircons extracted from this sample yielded a preliminary igneous crystallization age of 773 +280/-218 Ma. Most zircons were low in U and defined part of a chord connecting about 65 Ma with 773 Ma with the analyses falling close to the lower intercept. The explanation of Okulitch et al. (1981) involved resetting of the U-Pb system in the Early Tertiary, rather than growth of new zircon. In this study we present additional U-Pb data on zircon fractions from the same sample and from a separate sample of the same syenite gneiss phase collected nearby, which allow a more precise chord to be defined. We also present another explanation for the unusual pattern of discordance.

U-Pb ZIRCON GEOCHRONOLOGY

Within both samples of syenite gneiss (Fig. 1, exact loacations listed in Table 1), zircons range in size from about 40 to 150 microns in diameter. Their morphology is distinctive with most crystals being equant (maximum elongation 2:1) and multifaceted with complex, reasonably sharply defined faces. Most grains were very clear, but many had cloudy, well defined round cores with very clear overgrowths. We interpret the round shape of the cores to result from a resorption process. Sample WN-4-74, originally dated by Okulitch et al. (1981), had a greater proportion of cored and cloudy grains, relative to sample NEPHSY.

Analytical methods followed those outlined by Parrish et al. (1987a) and used microcapsules for mineral dissolution, a mixed ^{233}U-^{235}U-^{205}Pb tracer (Parrish and Krogh, 1987), multicollector mass spectrometry, and estimation of errors using numerical error propagation (Roddick, 1987). U and Pb blanks during this study were 50 and 20 pg, respectively.

Uranium contents in the zircons of the two samples of syenite gneiss were generally low to very low (12 to 280 ppm), with Pb contents in some clear fractions as low as 0.13 ppm (Table 1). Common Pb contents of very clear zircons were estimated as 30-40 ppb, the probable normal Pb content of gem quality zircons, but were much larger (2000 ppb) in the older, cloudier grains with significant amounts of core material. The common Pb correction for all analyses is significant, contributing to additional error.

Zircons were chosen to represent a wide range of proportions of clear to cloudy material (Table 1). The visible proportions of these components generally correlated with the U-Pb systematics (Fig. 2) and confirm that the zircons are mixtures of the two end members. Two fractions from sample WN-4-74 were abraded (Krogh, 1982), and all points remain essentially collinear.

Table 1. U-Pb zircon data Mount Copeland syenite gneiss

Analysis no. size[1]	*wt.* (mg)	U, ppm	Pb[2], ppm	$^{206}Pb/^{204}Pb$ [3]	Pb_c[4], (pg)	^{208}Pb[2] (%)	$^{206}Pb/^{238}U$ ± 1SEM %[5]	$^{207}Pb/^{235}U$ ± 1SEM %[5]	$^{207}Pb/^{206}Pb$ ± 1SEM %[5]	$^{207}Pb/^{206}Pb$ age, error (Ma)[6]
WN-4-747, Location: 50°07′30″N, 118°26′30″W (Okulitch et al., 1981) porphyritic syenite gneiss										
<20% cores, A	0.757	44.98	3.858	145	631	59.7	0.03769 (0.38)	0.3197 (1.3)	0.06152 (1.3)	657.5 (56.9)
>50% cores,A	0.182	76.63	7.268	138	395	47.3	0.05455 (0.48)	0.4681 (1.4)	0.06224 (1.4)	682.4 (60.0)
cloudy	1.291	279.6	20.20	144	8130	78.0	0.4547 (0.45)	0.3859 (1.4)	0.06155 (1.1)	658.4 (48.0)
NEPH SY7, Location: 50°07′08″N, 118°28′08″W, 6500′ elev. at head of Hiren Creek on old mining road 0.3km 060° from Mount Copeland mine; nepheline syenite gneiss										
>50% cores	0.190	158.6	1.827	469	43	19.1	0.01029 (0.29)	0.06837 (0.43)	0.04817 (0.35)	107.8 (16.4)
<50% cores	0.398	76.34	1.042	247	107	15.3	0.01280 (0.27)	0.09050 (0.65)	0.05129 (0.64)	253.9 (29.4)
clear	1.575	14.34	0.149	157	94	20.8	0.009151 (0.48)	0.05946 (1.4)	0.04713 (1.3)	55.7 (61.8)
clear	1.569	11.78	0.131	167	72	25.3	0.009222 (0.44)	0.05935 (1.1)	0.04667 (0.89)	32.5 (42.4)

Notes: [1]sizes of zircon fractions were about 100-150 microns, A=abraded; [2]radiogenic Pb; [3]measured ratio, corrected for spike and fractionation; [4]total common Pb in analysis corrected for fractionation and spike; [5]corrected for blank Pb and U, common Pb, errors quoted are 1 standard error of the mean in percent; [6]corrected for blank and common Pb, errors are 2 standard errors of the mean in Ma; [7]common Pb corrections use the Stacey-Kramers model with ages of 740 Ma for WN-4-74 and 60 Ma for NEPH SY, reflecting their core-rich and core-poor compositions, respectively.

A modified York (1969) regression (Parrish et al., 1987a) through the seven analyses yields an upper intercept of 740 ± 36 Ma, interpreted as the age of the cloudy core material, and lower intercept of 62.2 ± 1.2 Ma, with a MSWD of 1.08. The upper intercept is interpreted as the age of the cores.The two analyses of clear zircons with very low U content overlap concordia at 59.0 ± 0.7 Ma (Fig. 2), and more precisely date the clear zircon end member. The 62 Ma lower intercept of the regression line is very close to the age of the 59 Ma concordant zircons, but deviates from it probably because of slight rotation of the line due to small amounts of Pb loss in the cores prior to metamorphic zircon growth.

This study provides a clear example of a zircon population which is a physical mixture of zircons of two ages. The good fit of the points about the regression line argues but does not prove that the older zircons are of a homogeneous age and not a fortuitous mixture of various ages. This 740 Ma age differs greatly from the age of the underlying Precambrian crystalline basement (> 1.9 Ga, Evenchick et al., 1984; unpublished data of R.L. Armstrong and R.R. Parrish), and from the expected age of detrital zircons in adjacent metasediments presumably derived from such a crystalline source.

The equant, multifaceted nature of the clear zircons and their very low U content, suggests that they are metamorphic in origin. Metamorphic events of early Tertiary age have been demonstrated in southern Monashee Complex and Valhalla Complex to the south (Parrish et al., 1988; S. Carr, pers. comm., 1988), and render this a plausible explanation.

DISCUSSION

Age

On the basis of geochemistry and geometric relationships, Currie (1976) argued that the suite of alkaline rocks near Mount Copeland represented intrusive alkaline magmas. Based on geometric symmetry and gradational contacts with host mantling gneiss, Hoy (1987) suggested that the alkaline amphibolite suite and a large part of the grey syenite gneiss suite (dated in this study) were products of ultra-fenitization around an intrusive suite of nepheline syenite gneiss.

If the sample was igneous in origin, the U-Pb upper intercept date gives the time of intrusion. It is possible that the zircon cores were products of fenitization (which could explain the absense of igneous morphology of the cores); in this case the upper intercept age would probably still date the time of intrusion. Another possibility is that the zircon cores are an inherited component from the pre-fenitized rock. In this scenario the age would have little tectonic significance since the nature of the pre-fenitized rock would remain unknown. We believe it more likely that the older, about 740 Ma zircon cores are igneous in origin or related to fenitization, rather than being detrital or metamorphic, because detrital cores would generally have produced a wider scatter in data, and no 740 Ma metamorphism has been clearly documented in the Cordillera.

The origin of the abundant metamorphic zircons is not certain. Because the syenite gneiss has been involved in all of the deformational and metamorphic events, and because it is highly likely that at least some of these events predate the Paleocene (about 60 Ma; *see* Journeay, 1986; Journeay and Brown, 1986) we feel that the syenite gneiss cannot be Early Tertiary in age. This implies a metamorphic origin for the clear 60 Ma zircons in the rock, and it requires an explanation.

Few direct geochronological constraints on the age of deformation and metamorphism within the complex exist. A previous K-Ar hornblende age of 143 ± 6 Ma from this gneiss (Wanless et al., 1979) suggested some antiquity to the cooling of this region. To evaluate this scenario, this hornblende separate was re-analyzed at Queen's University with $^{40}Ar/^{39}Ar$ methods described in McBride et al. (1987). The table of data for this analysis is available from the authors, but is not reproduced here. The $^{40}Ar/^{39}Ar$ step heating age spectrum on this hornblende, illustrated in Figure 3, shows that large amounts of excess argon are to blame for the old total gas age. A saddle-shaped spectra is observed, and is explained by the degassing at increasing

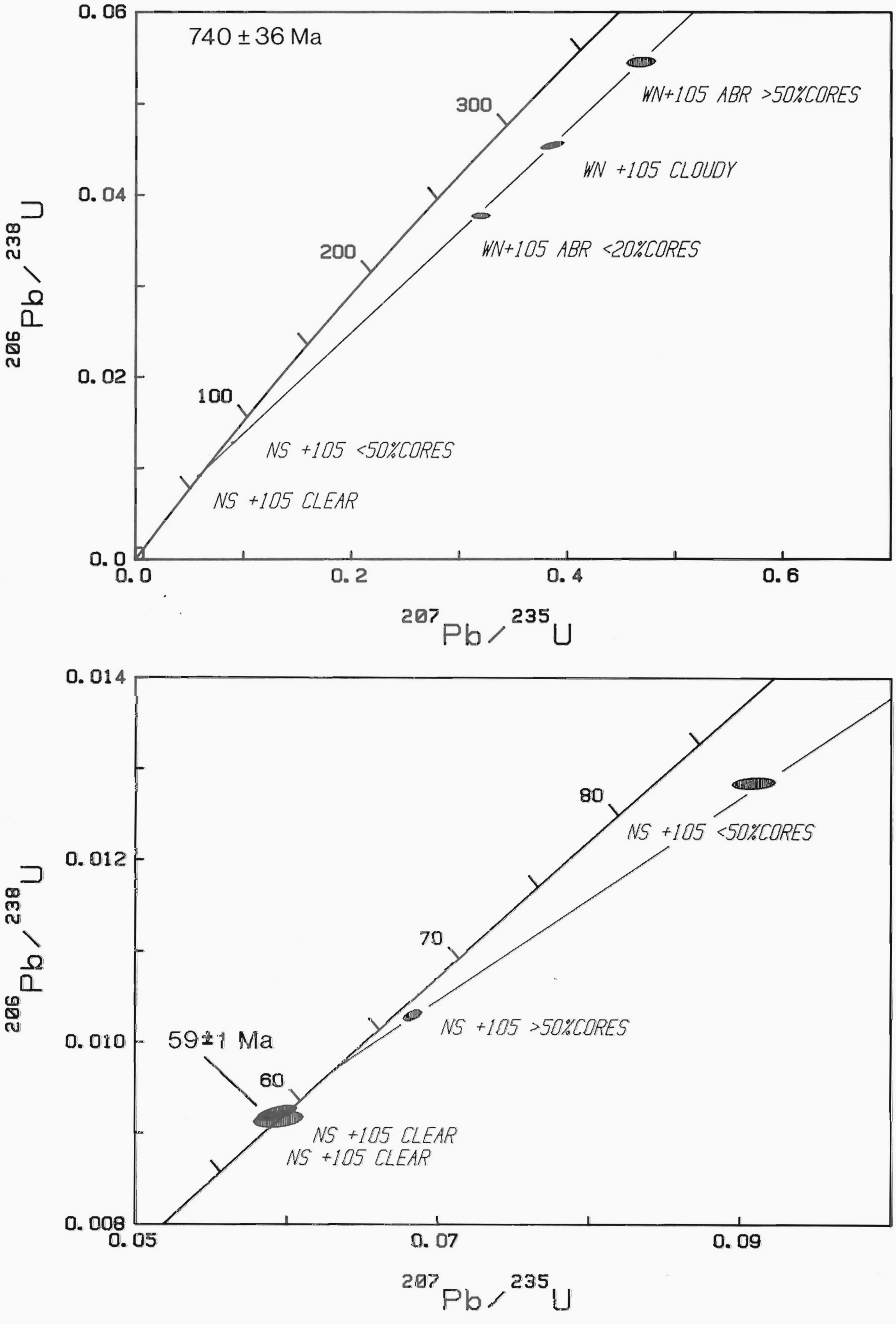

Figure 2. U-Pb concordia diagrams for the Mount Copeland syenite gneiss. Analyses are cross referenced to Table 1; NS refers to sample NEPH SY, whereas WN refers to sample WN-4-74. The bottom diagram is an inset showing the near concordant data from sample NEPH SY. Error ellipses are shown as two standard errors.

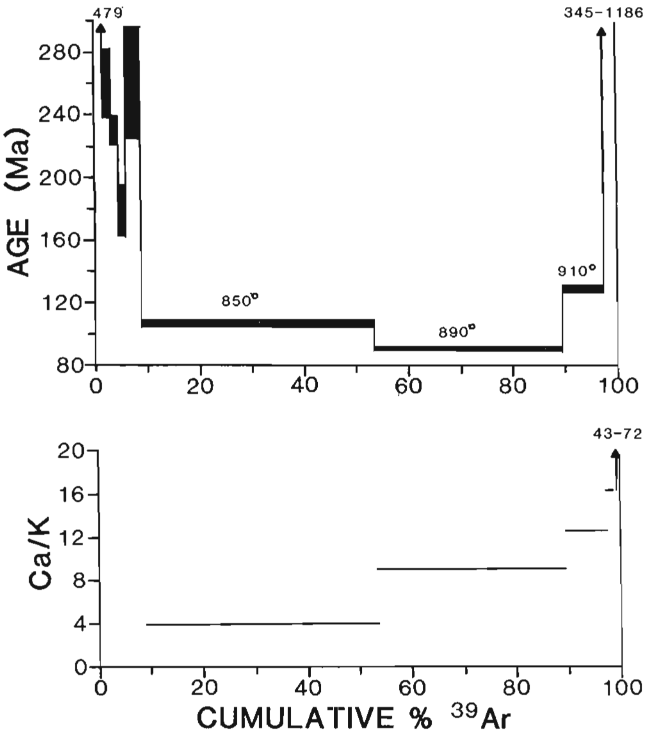

Figure 3. $^{40}Ar/^{39}Ar$ stepwise heating age spectra of hornblende from sample WN-4-74. The analytical data for this analysis are available from the authors. See text for discussion.

temperatures of two reservoirs which differed in their K/Ca ratios. These two reservoirs are probably hornblende (high K/Ca) and clinopyroxene (low K/Ca). Because clinopyroxene degases at higher temperature in a vacuum furnace and because both reservoirs contain excess Ar, a saddle shaped spectra is produced. Both phases contain significant excess argon which obscures the release spectra. Because the spectra fails to have any evidence of a plateau over a significant portion of the gas release, the data only imply that the hornblende closure age cannot be older than about 90 Ma, the bottom of the saddle. In support of this interpretation, biotite ages within the complex do not exceed 60 Ma, as recently summarized by Parrish et al. (1988).

We suggest that the about 60 Ma lower intercept age represents extensive growth of metamorphic zircon in the solid state. We present two speculative explanations.

The source of Zr and Si to produce the zircon may be the hydration of phases such as alkali clinopyroxene (which may contain substantial amounts of Zr) during the production of hornblende ± silica. This zircon-producing metamorphic reaction may have resulted from the influx of fluids and heat from possible late tectonic Paleocene-Eocene intrusions which we suggest may exist in the hangingwall of the Monashee décollement to the north and west. Alternatively, zirconium silicate may be relatively soluble in a hot fluid or solid alkali-carbonate phase. This might have allowed original igneous crystals to extensively dissolve during Early Tertiary high temperature metamorphic conditions and upon cooling, to grow in the metamorphic state. It is not clear why earlier metamorphism (middle and late Mesozoic, Journeay, 1986; Brown and Journeay, 1987) failed to result in growth of zircon regardless of the mechanism, but the absence of growth is implied by the data. Both speculative interpretations depend on high temperatures in Early Tertiary time; this is consistent with analogous tectonic and igneous events in southern Monashee Complex and Valhalla Complex to the south (Carr et al., 1987; Parrish et al., 1988) where latest Cretaceous to Eocene metamorphism, deformation, and plutonism have been documented. Also, to the north in northern Monashee Mountains, 63-100 Ma plutonism and metamorphism have recently been discovered (Sevigny et al., in press). These plutonic and metamorphic events were synchronous with, or immediatly preceded, Early Eocene normal faulting and tectonic denudation of the complex along the Columbia River fault system to the east (Fig. 1; Parrish et al., 1988) and possibly the Eagle River fault system to the west (Journeay and Brown, 1986; Brown and Journeay, 1987).

Geological Implications

The age of mantling gneiss protoliths has been a topic of some speculation (*see* Okulitch, 1984). Other isotopic studies provide broad constraints on their age. Core (basement) gneiss ranges in age from about 2.1 to 1.96 Ga, (2.0-2.1 Ga U-Pb zircon dates on orthogneisses intruding paragneisses, Parrish and Armstrong, 1983, and Wanless and Reesor, 1975). Pb-isotope analyses have recently been acquired from galena in stratiform lead-zinc deposits higher in the stratigraphic succession than the intrusive syenite (Hoy and Godwin, 1988). These data are interpreted to suggest that the deposit and some of the host mantling gneisses are Cambrian (about 500-550 Ma) in age (Hoy and Godwin, 1988).

An igneous crystallization age of 740 ± 36 Ma for the zircon cores implies that immediately enveloping and underlying mantling gneisses are older than 740 Ma. If gneisses higher in the sequence are Cambrian, the intervening 300 to 1000 m of mantling gneisses represent about 180 Ma of time. No obvious breaks occur in this part of the sequence. Either an unconformity existed and was subsequently obscured by deformation and metamorphism, or the intervening sequence was continuously deposited over about 200 Ma. The succession has the appearance of one depositional sequence with no major breaks. A similar situation exists in unmetamorphosed strata in northern Yukon where 750 Ma rhyolite is beneath strata with Early Cambrian trace fossils (Roots and Parrish 1988; Mustard et al., 1988), altough an unconformity may be present. It may be that the Pb-Zn deposits dated by Hoy and Godwin (1988) are epigenetic as opposed to syngenetic, allowing enveloping and underlying gneisses to be Precambrian in age. A solution to this problem is not yet clear.

Alkaline rocks occur within the Monashee Complex in several other forms (*see* e.g. Hoy, 1987; Journeay, 1986; Scammell, 1986). These include: (i) two lenticular concordant bodies (1.2 and 12 km long and several hundred metres thick at their widest) of syenite and nepheline syenite gneiss along the west flank of Frenchman Cap dome; one is intrusive into core gneiss and the other is intrusive into mantling gneiss 300m below the Pb-Zn deposits dated by Hoy and Godwin (1988), (ii) discordant intrusive carbonatite and associated fenites that also occur on the west flank of Frenchman Cap dome, (iii) an extensive (> 100 km length, metre-scale thickness) synsedimentary stratiform fragmental pyroclastic carbonatite mapped and described along the west and north flanks, and (iv) a lone concordant intrusive carbonatite body (> 3 km long, up to 300 m wide) also on the west flank of Frenchman Cap dome (''Ren'' carbonatite; *see* Hoy, 1987). The first three forms appear in the mantling gneiss sequence below the dated stratiform Pb-Zn sequence, while the ''Ren'' carbonatite occurs much higher. All occurrences of these alkaline rocks were affected by all preserved phases of deformation, and some are definitely synsedimentary. It may be that all alkaline magmatism in the complex is cogenetic, emplacement being during and/or just after mantling metasedimentary rocks were originally deposited.

A number of analyses have been attempted on some of these nearby carbonatitic rocks, but to date, almost all U-Pb zircon dates are latest Mesozoic to Paleocene-Eocene (R.R. Parrish unpublished data, 1987), and most zircons are concluded to be metamorphic in origin. However, a few analyses have older cores. The apparent lack of igneous grains in some raises the possibility that the cores in the Mount Copeland zircons could be in part xenocrysts; although a possible interpretation, we consider it less likely than that summarized above. There is still much to learn regarding the stability and growth of zircon in these types of alkaline rocks which have been strongly metamorphosed.

Alkaline rocks in the region outside the Monashee Complex are about 325 to 370 Ma old (Pell, 1986; Parrish et al., 1987b). The ages and genetic relationships, if any, between alkaline rocks in the Monashee Complex and those outside the complex remain indeterminate. No link is supported by the data now available.

CONCLUSIONS

Zircons from the Mount Copeland syenite gneiss are interpreted to consist of zircons 740 $\pm$ 36 Ma old of probable igneous parentage and metamorphic zircons 59 $\pm$ 1 Ma old. The 740 Ma age of the syenite places constraints on the age of the metasedimentary sequence which hosts the syenite gneiss, and the about 59 Ma growth of metamorphic zircon is probably related to latest Cretaceous to Paleocene (?) metamorphic and tectonic events within the Monashee Complex during, or immediately prior to, Early Eocene extensional tectonic denudation.

ACKNOWLEDGMENTS

This contribution greatly benefited from earlier U-Pb analytical work on sample NEPHSY by B.D. Ryan and R.L. Armstrong at the University of British Columbia, which was collected in 1979 by R.L. Armstrong. The earlier analyses had larger errors than those presented in this paper but retained overlapping uncertainties with recent data. These earlier data and their significance in terms of the tectonics and U-Pb zircon systematics were crucial in motivating us to repeat and refine the analyses on this interesting rock unit. We thank Klaus Santowski for expert mass spectrometry. R.L.Armstrong made many useful comments to the text.

REFERENCES

Brown, R. L., and P. B. Read
1983: Shuswap terrane of British Columbia: a Mesozoic ''core complex; Geology, v. 11, p. 164-168.

Brown, R. L., and J. M. Journeay
1987: Tectonic denudation of the Shuswap metamorphic terrane of southeastern British Columbia; Geology; v. 15, p. 142-146.

Brown, R. L., Journeay, J. M., Lane, L. S., Murphy, D. C., and Rees, C. J.
1986: Obduction, backfolding and piggyback thrusting in the metamorphic hinterland of the southeastern Canadian Cordillera; Journal of Structural Geology, v. 8, p. 255-268.

Carr, S. D., Parrish, R.R. Parrish and Brown, R.L.
1987: Eocene structural development of the Valhalla complex, southeastern British Columbia; Tectonics, v. 6, p. 175-196.

Crittenden, M. D., Coney, P. J., and Davis, G. H.
1980: Cordilleran Metamorphic Core Complexes; Geological Society of America, Memoir 153, 490p.

Currie, K. L.
1976: Notes and petrology of nepheline gneisses near Mount Copeland, British Columbia; Geological Survey of Canada, Bulletin 265, 28p.
1984: Structural evolution of the Thor-Odin gneiss dome; Tectonophysics, v. 101, p. 87-103.

Evenchick, C. A., Parrish, R.R. and Gabrielse, H.
1984: Precambrian gneiss and late Proterozoic sedimentation in north-central British Columbia; Geology, v. 12, p. 233-237.

Fyles, J.T.
1970: Jordan River area; British Columbia Department of Mines and Petroleum Resources, Bulletin 57, 64p.

Hoy, T.
1987: Geology of the Cottonbelt lead-zinc-magnetite layer, carbonatites and alkalic rocks in the Mount Grace area, Frenchman Cap dome, southeastern British Columbia; British Columbia Ministry of Energy, Mines and Petroleum Resources, Bulletin 80, 99p.

Hoy, T. and Brown, R. L.
1980: Geology of the eastern margin of Shuswap Complex, Frenchman Cap area; British Columbia Ministry of Energy, Mines and Petroleum Resources, Preliminary Map 43.

Hoy, T. and Godwin, C. I.
1988: (in press), Significance of a Cambrian date from galena lead isotope data for the stratiform Cottonbelt deposit in the Monashee Complex, southeastern British Columbia; Canadian Journal of Earth Sciences, v. 25, p. 1534-1541.

Hoy, T., and McMillan, W. J.
1979: Geology in the vicinity of Frenchman Cap gneiss dome; British Columbia Department of Energy, Mines and Petroleum Resources, Geological Fieldwork, 1979, Paper 1980-1, p. 17-22.

Journeay, J. M.
1986: Stratigraphy, internal strain and thermo-tectonic evolution of Northern Frenchman Cap dome: an exhumed duplex structure, Omineca hinterland, S.E. Canadian Cordillera; unpublished Ph. D.thesis, Queen's University, Kingston, Ontario, 399p.

Journeay, J. M. and Brown, R.L.
1986: Major tectonic boundaries of the Omineca belt in southern British Columbia: a progress report; *in* Current Research, Part A, Geological Survey of Canada, Paper 86-1A, p. 81-88.

Krogh, T. E.
1982: Improved accuracy of U-Pb ages by the creation of more concordant systems using an air abrasion technique; Geochimica et Cosmochimica Acta, v. 46, p. 637-649.

McBride, S. L., Clark, A. H., Farrar, E. and Archibald, D. A.
1987: Delimitation of a cryptic Eocene tectono-thermal domain in the Eastern Cordillera of the Bolivian Andes through K-Ar dating and 40Ar-39Ar step-heating; Geological Society of London, Journal, v. 144, p. 243-255.

McMillan, W. J.
1970: West flank, Frenchman's Cap gneiss dome, Shuswap terrane, British Columbia; *in*, Structure of the Southern Canadian Cordillera; J.O. Wheeler, ed. Geological Association of Canada, Special Paper 6, p. 99-122.

Monger, J. W. H., Price, R. A., and Templeman-Kluit, D. J.
1982: Tectonic accretion and the origin of two major metamorphic welts in the Canadian Cordillera; Geology, v. 10, p. 70-75.

Mustard, P. S., Donaldson, J. A. and Thompson, R.I.
1988: Trace fossils and stratigraphy of the Precambrian-Cambrian boundary sequence, upper Harper group, Ogilvie Mountains, Yukon; *in* Current Research, Part E, Geological Survey of Canada, Paper 88-1E, p. 197-203.

Okulitch, A.V.
1984: The role of the Shuswap metamorphic complex in Cordilleran tectonism: a review; Canadian Journal of Earth Sciences, v. 21, p. 1171-1193.

Okulitch, A. V., Loveridge, W. D., and Sullivan, R. W.
1981: Preliminary radiometric analyses of zircon from the Mount Copeland syenite gneiss, Shuswap metamorphic complex, British Columbia; *in* Current Research, Part A, Geological Survey of Canada, Paper 81-1A, p. 33-36.

Parrish, R.R. and Armstrong, R. L.
1983: U-Pb zircon age and tectonic significance of gneisses in structural culminations of the Omineca crystalline belt, British Columbia; Geological Society of America, Abstracts with Programs, v. 15, p. 324.

Parrish, R. R. and T. E. Krogh
1987: Synthesis and purification of 205Pb for U-Pb geochronology; Chemical Geology (Isotope Geoscience Section), v. 66, p. 103-110.

Parrish, R. R., Roddick, J.C., Loveridge, W.D. and Sullivan, R.W.
1987a: Uranium-lead analytical techniques at the geochronology laboratory, Geological Survey of Canada; *in* Radiogenic Age and Isotope studies; Report 1, Geological Survey of Canada, Paper 87-2, p. 3-7.

Parrish, R. R., Heinrich, S., and Archibald, D.
1987b: Age of the Ice River complex, southeastern British Columbia; *in* Radiogenic Age and Isotope Studies: Report 1; Geological Survey of Canada, Paper 87-2, p. 33-37.

Parrish, R. R., Carr, S.D. and Parkinson, D.W.
1988: Extensional tectonics and geochronology of the southern Omineca Belt, British Columbia and Washington; Tectonics, v. 7, p. 181-212.

Pell, J.
1986: Nepheline syenite gneiss complexes in British Columbia (82M,N; 83D; 93I); British Columbia Ministry of Energy, Mines and Petroleum Resources, Geological Fieldwork, 1985, Paper 1986-1, p. 255-260.

Read, P. B.
1979a: Relationship between the Shuswap Metamorphic Complex and the Kootenay Arc, Vernon east-half, southern British Columbia; *in* Current Research, Part A, Geological Survey of Canada, Paper 79-1A, p. 37-40.

Read, P. B.
1979b: Geology and mineral deposits, eastern part of Vernon east-half, British Columbia; Geological Survey of Canada, Open File 658 (map).

Read, P. B.
1980: Stratigraphy and structure: Thor-Odin to Frenchman Cap "domes", Vernon east-half map area, southern British Columbia; *in* Current Research, Part A, Geological Survey of Canada, Paper 80-1A, p. 19-25.

Read, P. B., and Brown, R.L.
1981: Columbia River fault zone: southeastern margin of the Shuswap and Monashee complexes, southern British Columbia; Canadian Journal of Earth Sciences, v. 12, p. 1127-1145.

Read, P. B. and Klepaclci, D. W.
1981: Stratigraphy and structure: northern half of Thor-Odin Nappe, Vernon east-half map area, southern British Columbia; *in* Current Research, Part A, Geological Survey of Canada, Paper 81-1A, p. 169-173.

Reesor, J. E. and Moore Jr., J. M.
1971: Petrology and structure of Thor-Odin gneiss dome, Shuswap Metamorphic Complex, British Columbia; Geological Survey of Canada, Bulletin 195, 149p.

Roddick, J.C.
1987: Generalized numerical error analysis with applications to geochronology and thermodynamics; Geochimica et Cosmochimica Acta, v. 51, p. 2129-2135.

Roots, C. F. and Parrish, R.R.
1988: Age of the Mount Harper volcanic complex, southern Ogilvie Mountains, Yukon; *in* Radiogenic Age and Isotopic Studies: Report 2, Geological Survey of Canada, Paper 88-2, p. 29-35.

Scammell, R. J.
1986: Stratigraphy, structure and metamorphism of the north flank of the Monashee Complex, southeastern British Columbia: a record of Proterozoic extension and Phanerozoic crustal thickening; unpublished M. Sc. thesis, Carleton University, Ottawa, 205p.

Sevigny, J. H., Parrish, R.R. and Ghent, E.D.
(in press) Petrogenesis of peraluminous granites, Monashee Mountains, southeastern Canadian Cordillera; Journal of Petrology.

Wanless, R. K. and Reesor, J. E.
1975: Precambrian zircon age of orthogneisses in the Shuswap Metamorphic Complex, British Columbia; Canadian Journal of Earth Sciences, v. 12, p. 326-332.

Wanless, R. K., Stevens, R.D., Lachance, G.R. and Delabio, R.N.
1979: Age determinations and geological studies, K-Ar Isotopic ages, Report 14; Geological Survey of Canada, Paper 79-2, 67p.

Wheeler, J. O.
1965: Big Bend map-area, British Columbia 82 M (east half); Geological Survey of Canada, Paper 64-32, 37p.

York, D.
1969: Least squares fitting of a straight line with correlated errors; Earth and Planetary Science Letters, .v 5, p. 320-324.

Age of the Mount Harper volcanic complex, southern Ogilvie Mountains, Yukon

C. F. Roots[1] and Randall R. Parrish[2]

Roots, C.F., and Parrish, Randall R., Age of the Mount Harper volcanic complex, southern Ogilvie Mountains, Yukon; in Radiogenic Age and Isotopic Studies: Report 2, Geological Survey of Canada, Paper 88-2, p. 29-35, 1988.

Abstract

Basaltic flows, overlain by subordinate rhyolite and andesite flows, occur within a clastic unit older than Cambrian dolostone and correlative with the Windermere Supergroup. This clastic-volcanic unit records a period of crustal extension which resulted in formation of the Paleozoic continental margin (Mackenzie Platform) of ancient northwestern North America.

A U-Pb zircon age determination from one of the rhyolites indicates it is 751 +26/-18 Ma old. Some of the zircons contain older visible inherited cores, which are reflected in at least some of the analyses. This age is similar to that of sills and diorite plugs in the Mackenzie Mountains (NWT-Yukon border), as well as the Huckleberry-Irene volcanics of northeastern Washington and southeast British Columbia. The age from Mount Harper can be linked with regional stratigraphy and provides additional evidence for a ca. 750 Ma magmatic pulse in the eastern Cordillera.

Résumé

Des coulées de basalte, recouvertes de coulées secondaires de rhyolite et d'andésite, se trouvent dans une unité de roches clastiques plus anciennes que la dolomie cambrienne et sont en corrélation avec le supergroupe de Windermere. Cette unité clastique et volcanique a connu une période de distension crustale qui a débouché sur la formation de la marge continentale paléozoïque (plate-forme du Mackenzie) de l'ancienne région correspondant au nord-ouest de l'Amérique du Nord.

Une datation par la méthode U-Pb appliquée aux zircons de l'un des rhyolites indique un âge de 751 +26/−18 Ma. Certains zircons contiennent des noyaux hérités visibles plus anciens, comme l'indiquent quelques analyses. Cet âge correspond à celui des filons-couches et des bouchons de diorite qui se trouvent dans les monts Mackenzie (frontière des T.N.-O. et du Yukon) ainsi que des roches volcaniques de Huckleberry et Irene dans le nord-ouest de l'État de Washington et le sud-ouest de la Colombie-Britannique. L'âge du complexe de Mount Harper peut être corrélé à la stratigraphie régionale et constituer un élément supplémentaire en faveur d'une impulsion magmatique survenue il y a environ 750 Ma dans la partie est de la Cordillère.

INTRODUCTION

The Mount Harper complex is a 105 km^2 area of basaltic and felsic extrusive rocks 40 km east of the Alaska-Yukon boundary (Fig. 1). It and the enclosing clastic rocks reveal a sequence of faulting, deposition, volcanism and subsidence in an extensional half-graben at the northwestern edge of ancient North America. Although telescoped northward during late Mesozoic thrusting, this part of the foreland thrust and fold belt is less deformed than time-equivalent rocks farther south, and original structures and stratigraphy remain intact. Among Cordilleran volcanics of this age, the Mount Harper occurrence is apparently unique in containing felsic volcanic rocks. An age of the Mount Harper complex would place better constraints on the age of extensional events in the Windermere Supergroup.

[1] Department of Earth Sciences, Ottawa-Carleton Geoscience Centre, Carleton University, Ottawa, Ontario (presently at: Geological Survey of Canada, 100 W. Pender St., Vancouver, British Columbia V6B 1R8.

[2] Geological Survey of Canada, 601 Booth Street, Ottawa, Ontario, K1A 0E8.

REGIONAL SETTING AND GEOLOGY OF VOLCANIC ROCKS

The southern Ogilvie Mountains comprise two Paleozoic tectonic elements, the Mackenzie Platform and Selwyn Basin (Fig. 1). Beneath the Mackenzie Platform, Middle and Upper Proterozoic shelf rocks have been telescoped (during the Late Jurassic and Cretaceous) and are presently exposed in an erosional window called the Coal Creek Dome (Green, 1972). The succession consists of thick, shallow-water carbonate units separated by clastic intervals, and is interpreted as the product of repeated extension events (Thompson et al., 1987). The volcanic rocks and conglomerate, silt and mudstone that form the upper and lower Harper group occur along the southern and western edge of the dome (Fig. 2). The Harper group (Fig. 3) overlies the Fifteenmile dolostone (correlated with Pinguicula Group of Eisbacher, 1981, and Mackenzie Mountains Supergroup of Aitken, 1981) and is succeeded by Cambrian dolostone (un-named CDb unit of Norris, 1982).

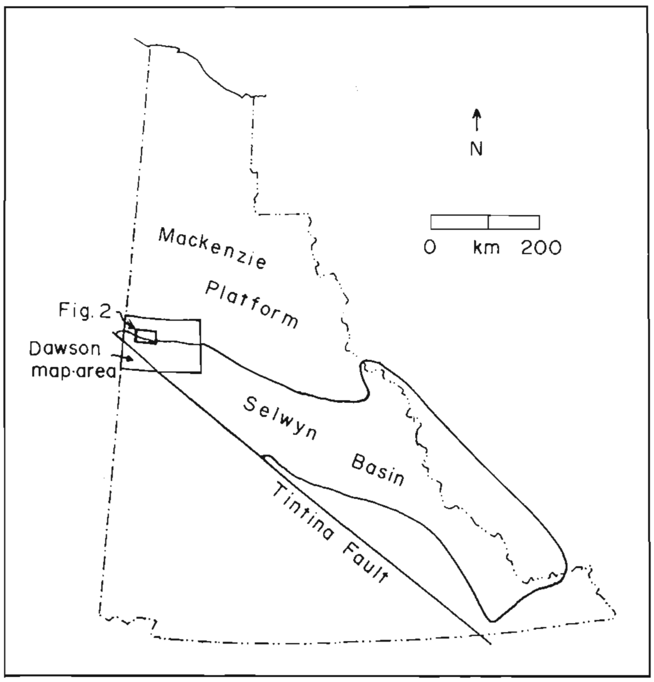

Figure 1. Yukon Territory showing the location of the Mount Harper area at the edge of Mackenzie Platform.

The long dimension of the Mount Harper volcanic complex coincides with the trend of the South Harper Fault (Fig. 2) whose Late Proterozoic north-side — down movement has been determined from stratigraphic changes across the fault. Its visible offset reflects post-Cambrian reactivation. The lower Harper group comprises a conglomerate wedge up to 1200 m thick along the north side of the fault, with sedimentary facies and features indicating derivation across the fault. The oldest basaltic flows of the complex overlie the conglomerate, and overstep the fault southward onto the older paleo-erosion surface (Fig. 4). Although cut by many later faults, the volcanic complex clearly post-dates the South Harper Fault and up to 4 km of erosion.

In the Mount Harper complex, a number of lithostratigraphic members are described (Roots, 1987). The first three are basaltic, and record the growth and partial destruction of a submarine edifice capped by subaerial cinder cones. Interdigitated rhyolite and andesite flows of a second igneous phase unconformably overlie basaltic rocks in the south part of the complex. The northern and western parts of the complex are covered by upper Harper group sedimentary rocks. Early Cambrian trace fossils near the top of the upper Harper group (Mustard et al., 1988) imply the existence of a major unconformity within this sedimentary sequence. The upper Harper group subaerial rocks are either unconformably (R. I. Thompson, pers. comm., 1988) or structurally (Roots, 1987) overlain by CDb dolostone. Whether the Harper group is ca. 550-600 Ma (when continental break-up occurred; e.g. Devlin and Bond, 1988) or older cannot be determined from the stratigraphy.

The rhyolite member (from which the zircons were extracted) comprises massive flows exposed over 6 km^2, with thin tuffs and dykes. Only rare outcrops of the columnar jointed flows remain, and the sample was collected from flow-banded massive rock on a conical ridge top that may have been an extrusive dome. Flows contain

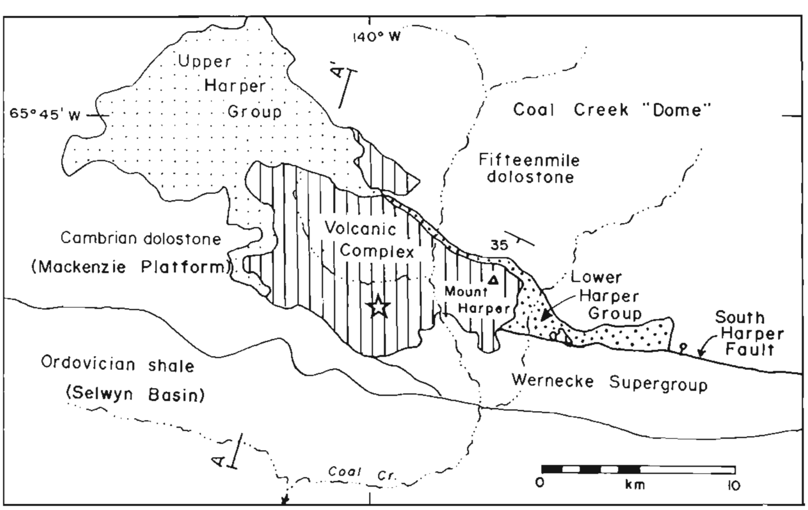

Figure 2. Geological units around the Mount Harper volcanic complex (striped). Star indicates location of the rhyolite sample used for dating; section A-A' is Figure 4.

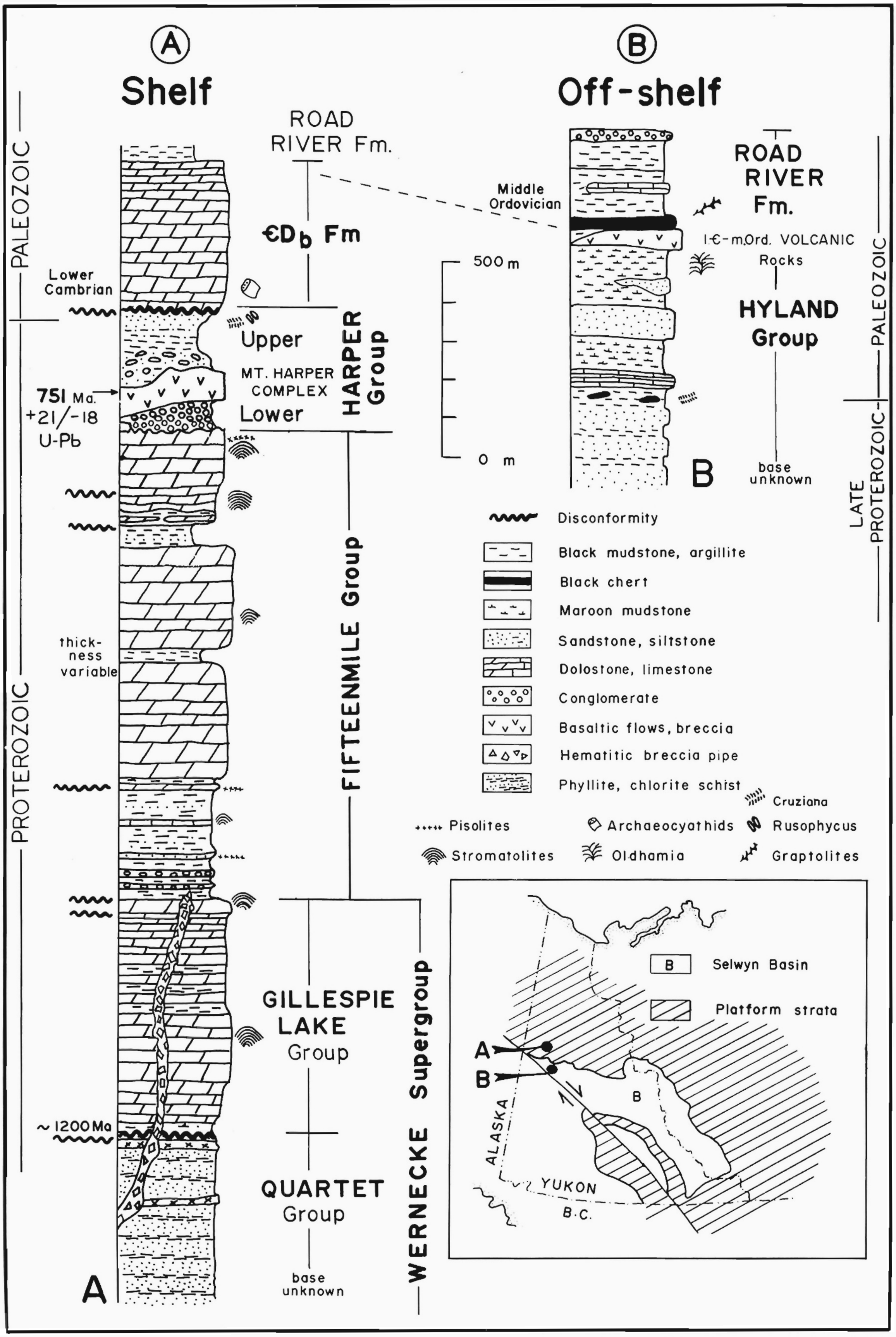

Figure 3. Schematic stratigraphic columns for the Mount Harper area of the western Yukon, modified from Thompson and Roots (1987).

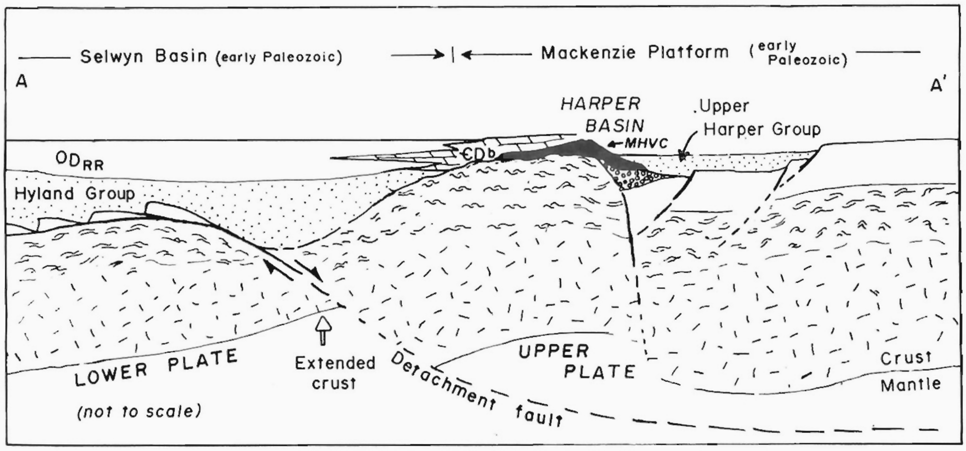

Figure 4. Schematic cross-section along line A-A' of Figure 2, before Mesozoic contraction. The Harper basin is a half-graben, with Mount Harper volcanic complex overstepping the South Harper Fault. The Hyland Group, to the south, overlies a speculative lower plate, consisting of continental crust thinned by extension.

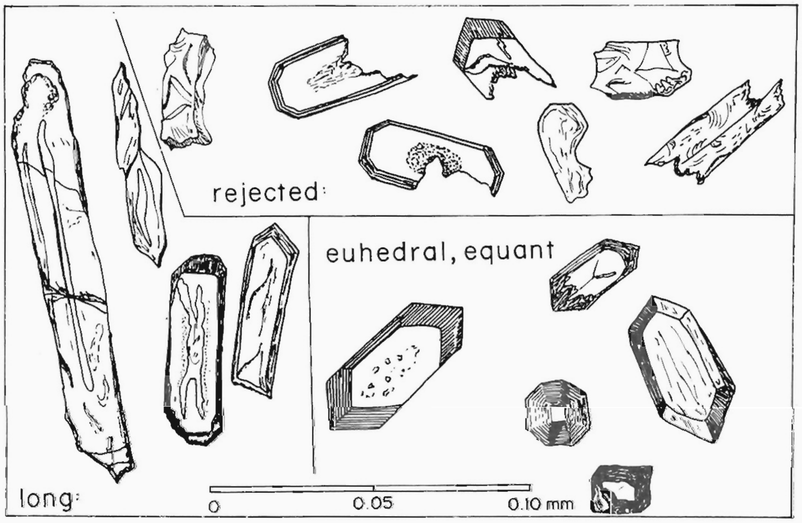

Figure 5. Sketches of zircon crystals from the Mount Harper rhyolite, drawn from photomicrographs. The different shapes are discussed in the text.

phenocrysts (sanadine 1-3 %, plagioclase 1-2 %, and quartz 0-2 %) and rare xenocrysts of garnet (probably andradite) in a sericitized holohyaline matrix.

Whole-rock analyses of 10 samples of the rhyolite member indicate 70-77 % SiO_2, 9-15 % Al_2O_3, Mg/(Mg+Fe) of 12-22 %, and secondary potassic enrichment. The rhyolite member contains the highest incompatible minor and trace element content in the complex (up to 453 ppm Zr).

U-Pb ZIRCON GEOCHRONOLOGY

A 50 kg sample of a quartz-phyric flow was collected in 1983 from the ridge 5 km southwest of Mount Harper (64°39'N, 140°00'W, Fig. 2). Preparation included standard crushing, Wilfley table, heavy liquid, and magnetic techniques (Parrish et al., 1987).

Zircon crystals in this sample displayed four distinctive shapes (Fig. 5): 1) long, narrow crystals with minute cavities along axes, 2) euhedral, doubly terminated crystals, commonly with concentric zoning and clear central regions, 3) less numerous, small equant crystals, many of which had cores with cloudy inclusions, and 4) a few grains with irregular shapes and rounded corners, which may have been xenocrystic. Whole crystals were hand-picked into additional fractions according to shape. Three of the fractions were air-abraded following the method of Krogh (1982).

Fractions were analyzed in 1984 and in 1986 using different techniques and drastically different minimum amounts of sample. The 1984 analyses were spiked with a ^{208}Pb-^{233}U-^{235}U tracer, whereas 1986 samples, selected from the small amount of remaining material, used a ^{205}Pb-^{233}U-^{235}U tracer (Parrish and Krogh, 1987). Pb blanks varied from 1-2ng in 1984 analyses to about 0.05 ng in 1986 analyses. Chemical and mass spectrometric procedures follow those of Parrish et al. (1987), except that 1984 analyses preceded the direct propagation of errors and simultaneous use of Faraday cups and electron multiplier.

Table 1. U-Pb Zircon Data, Mount Harper Complex

Analysis no.[1] size	Wt. (mg)	U, ppm	Pb^2, ppm	$^{206}Pb^3/^{204}Pb$	Pbc^4, (pg)	$^{208}Pb^2$ (%)	$^{206}Pb/^{238}U$ +/−1SEM%[5]	$^{207}Pb/^{235}U$ +/−1SEM%[5]	$^{207}Pb/^{206}Pb$ +/−1SEM%[5]	$^{207}Pb/^{206}Pb$ age, error (Ma)[6]
86-1 −62	0.101	220.8	27.18	553	304	13.6	0.1161 (0.21)	1.025 (0.36)	0.06400 (0.30)	741.7 (12.8)
86-2 +74,A	0.063	184.2	22.65	263	344	13.8	0.1158 (0.26)	1.021 (0.67)	0.06394 (0.65)	739.5 (27.6)
86-3 −62,A	0.023	180.0	22.98	449	73	13.4	0.1206 (0.29)	1.091 (0.41)	0.06559 (0.30)	793.4 (12.6)
84-1 −62	3.66	220.6	23.22	187	25400	15.1	0.09759 (0.35)	0.8724 (0.6)	0.06484 (0.6)	769.0 (25.2)
84-2 68,L	1.06	112.0	11.36	140	4806	16.5	0.09253 (0.35)	0.8193 (0.6)	0.06422 (0.6)	748.9 (25.1)
84-3 68,E,A	2.49	148.5	18.71	299	8721	14.1	0.1181 (0.35)	1.0583 (0.6)	0.06497 (0.6)	773.3 (25.2)
84-4 +74,E,L	1.13	115.4	12.55	195	4070	14.2	0.1018 (0.35)	0.8996 (0.6)	0.06407 (0.6)	744.1 (25.0)

Notes: [1]numbers refer to size of zircons in microns, A=abraded, L=elongate, E=equant; [2]radiogenic Pb; [3]measured ratio, corrected for spike and fractionation; [4]total common Pb in analysis corrected for fractionation and spike; [5]corrected for blank Pb and U, common Pb, errors quoted are 1 standard error of the mean in pecent; [6]corrected for blank and common Pb, errors are 2 standard errors of the mean in Ma; common Pb corrections use 740 Ma Stacey-Kramers model Pb.

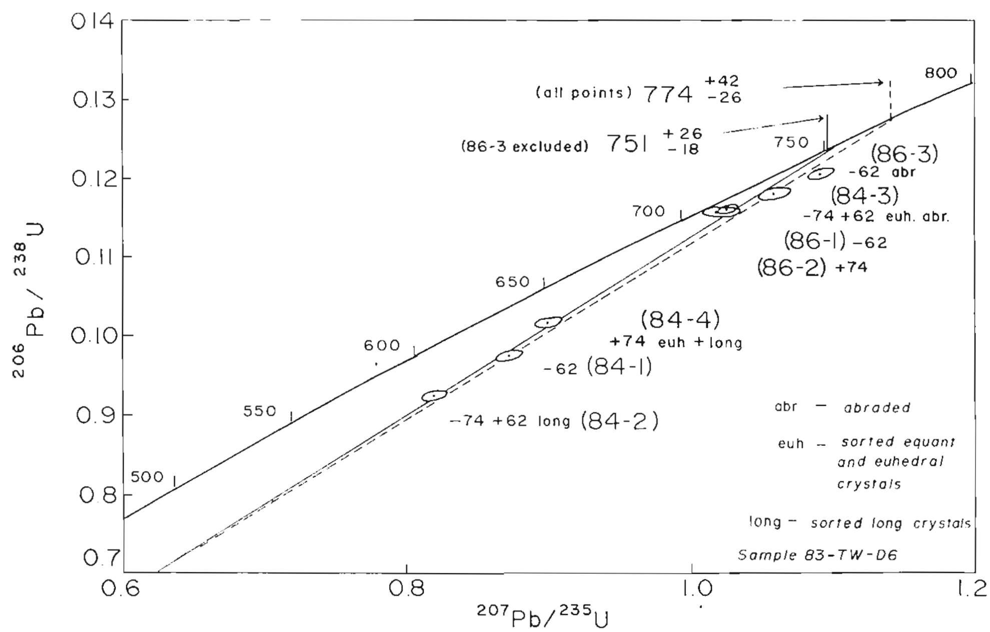

Figure 6. U-Pb concordia plot for zircons from the Mount Harper complex. The solid regression line is that favoured to most closely estimate the age of the rhyolite; the dashed regression line uses all data points. See text for discussion. Ellipses around data points represent two-standard errors.

U-PB ZIRCON RESULTS

Table 1 and Figure 6 show the analyses of seven fractions of zircon from the rhyolite. The three fractions prefixed 86 contained far fewer crystals than any of the four other fractions (prefixed 84-). Two things are evident from the data; first, there is scatter in the data about a regression line, and second, the most concordant analysis, which was composed of abraded equant grains, has a $^{207}Pb/^{206}Pb$ age significantly older than the other fractions.

It is reasonable to invoke higher degrees of surface-correlated Pb loss for the long crystals than the equant ones, while the abrasion technique has clearly helped reduce this alteration. The scatter is probably related to small degrees of inheritance of older source or xenocrystic zircon, giving rise to older Pb-Pb ages. Equant crystals are more likely to have cores, and this is borne out by sketches of crystals in Figure 5. It is quite likely that small amounts of this older core material are present in all of the fractions analyzed. The lack of sufficient high quality material precluded additional more concordant analyses, and the scatter in the data remains. We have chosen to regress six of the seven data points, leaving out analysis 86-3 which has a Pb-Pb age more than 20 Ma older than any other fraction (due to significantly more inheritance). The remaining six points have an MSWD of 3.13 with upper intercept of 751 +26/-18 Ma at the 2-standard error level. The lower intercept is essentially zero. We interpret this as the best age estimate of the Mount Harper rhyolite, although it may be biased towards being slighltly too old because of the small amounts of suspected inheritance. A regression of all seven points yields 774 +42/-26 Ma, but has an MSWD of 7.6; this line is also shown on Figure 6 for reference.

The source of the suspected inherited zircons, particularly evident in analysis 86-3 is uncertain, for the chemistry and petrography of the rhyolite provide seemingly conflicting evidence for crustal derivation. Both rhyolite and andesite at Mount Harper are strongly tholeiitic, and their similar proportions of incompatible elements (spidergram patterns) suggest that this second igneous phase differentiated from the mantle-derived basaltic pulse that produced the bulk of the complex (Roots, 1987). Andradite xenocrysts in the rhyolite, however, are indicative of assimilation at mid-crustal depth (cf. Pallister, 1987). Relict zircon may have survived from small amounts of felsic basement assimilated during ascent of the rhyolite magma.

Table 2. Igneous rocks associated with Windermere Supergroup

Rock Unit	Age (Ma)	Method	Source
Mt. Harper rhyolite, Yukon	751 +26/−18	U-Pb zircon	This study
Diabase sills, Mackenzie Mountains	766 +/− 24 769 +/− 27	Rb-Sr (WR) Rb-Sr (WR)	Armstrong et al. 1982
Quartz diorite plug, Coates Lake, Mackenzie Mountains	778 +3/−2	U-Pb, zircon	C.W. Jefferson and R.R. Parrish (in press)
Deserters granite, northern B.C.	728 +8/−7	U-Pb, zircon	Evenchick et al. (1984)
Mt. Blackman gneiss, part of Malton gneiss	741 +22/−20	U-Pb, zircon	Evenchick et al. (1984)
Mt. Copeland syenite gneiss, Monashee Cx	740 +/− 36	U-Pb, zircon	Parrish and Scammell (1988)
Slab isochron on layered paragneiss	750 +/− 60	Rb-Sr slab isocron	Duncan (1984)
Huckleberry volcanics, NE Washington	762 +/− 44	Sm-Nd mineral isochron	Devlin et al. (1988)

SIGNIFICANCE OF THE CA. 750 MOUNT HARPER VOLCANIC COMPLEX

Continental extension is demonstrated in the Mount Harper area by recognition of a Late Proterozoic fault that resulted in omission of units on one side and deposition of Upper Proterozoic clastic sediments, derived from across the fault, in a half-graben on the other (Thompson et al., 1987). After subsidence and deposition of the Harper group, stable carbonate shelf conditions resumed on the north side (the Mackenzie Platform). The area south of the Mount Harper complex, however, became a clastic basin, filled by Hyland Group (formerly the Grit Unit) and dark shales of the Selwyn Basin. Mount Harper volcanism indicates a miniumum age for the start of the extensional event which led to distinction of these two Paleozoic tectonic elements.

The zircon age falls in the range of several isotopic dates for igneous bodies ascribed to extensional tectonism in the eastern Cordillera, all within 25 Ma of 750 Ma (Table 2). Diabase sills (ca. 770 Ma) within the Tsezotene Formation, dated by Armstrong et al. (1982) which may have fed basalts within the Little Dal Group (Aitken, 1981) at the top of the Mackenzie Mountain Supergroup, provide the closest relative to the Mount Harper complex. The only dated extrusive rocks are the basaltic Huckleberry Formation of northeastern Washington (correlative with Irene Formation of British Columbia), which has yielded a ca. 760 Ma Nd-Sm mineral isochron (Devlin et al., 1988). Plutonic rocks from 730-780 Ma old occur throughout the Canadian Cordillera (Table 2). These roughly contemporaneous igneous rocks point toward a magmatic pulse about 750 Ma ago accompanying initial deposits of the Windermere Supergroup.

The Mount Harper volcanic complex is important to tectonic syntheses of the Windermere Supergroup in the northern Cordillera. Because the volcanic rocks are stratigraphically located within this regionally correlatable clastic sedimentary unit, the age of the Windermere Supergroup in this region can be tentatively assigned. In addition, the sequence of faulting, half-graben formation, volcanism and subsidence provides a rare exposure of initial Windermere conditions. It is the best preserved occurrence of its kind within the Windermere Supergroup.

ACKNOWLEDGMENTS

Fieldwork was conducted as part of the Ogilvie Mountains project under the direction of R. I. Thompson. C. Roots thanks John Moore, R. I. Thompson, and W. Goodfellow for discussions through the course of this work, which formed part of his Ph.D. thesis at Carleton University.

REFERENCES

Aitken, J. D.
1981: Stratigraphy and sedimentology of the upper Proterozoic Little Dal Group, Mackenzie Mountains, Northwest Territories; *in*: Proterozoic Basins of Canada, ed. F.H.A. Campbell; Geological Survey of Canada, Paper 81-10, p. 47-72.

Armstrong, R.L., Eisbacher, G. H., and Evans, P. D.
1982: Age and stratigraphic-tectonic significance of Proterozoic diabase sheets, Mackenzie Mountains, northwest Canada; Canadian Journal of Earth Sciences, v. 19, p. 316-323.

Devlin, W. J. and Bond, G. C.
1988: The initiation of the early Paleozoic Cordilleran miogeocline: evidence from the uppermost Proterozoic-Lower Cambrian Hamill Group of southeastern British Columbia; Canadian Journal of Earth Sciences, v. 25, p. 1-19.

Devlin, W. J., Brueckner, H. K., and Bond, G. C.
1988: New isotopic data and a preliminary age for volcanics near the base of the Windermere Supergroup, northeastern Washington, U.S.A.; Canadian Journal of Earth Sciences, (in press).

Duncan, I. J.
1984: Structural evolution of the Thor-Odin gneiss dome; Tectonophysics, v. 101, p. 87-130.

Eisbacher, G. H.
1981: Sedimentary tectonics and glacial record in the Windermere Supergroup, Mackenzie Mountains, north-western Canada; Geological Survey of Canada, Paper 80-27, 40p.

Evenchick, C. A., Parrish, R. R., and Gabrielse, H.
1984: Precambrian gneiss and late Proterozoic sedimentation in north-central British Columbia; Geology, v. 12, p. 233-237.

Green, L. H.
1972: Geology of Nash Creek, Larsen Creek and Dawson map-areas, Yukon Territory; Geological Survey of Canada, Memoir 364, 157p.

Jefferson, C. W. and Parrish, R. R.
in press: Late Proterozoic stratigraphy, U-Pb zircon ages, and extensional tectonics, Mackenzie Mountains, northwest Canada; Canadian Journal of Earth Sciences.

Krogh, T. E.
1982: Improved accuracy of U-Pb zircon ages by the creation of more concordant systems using an air abrasion technique; Geochimica et Cosmochimica Acta, v. 96, p. 637-649.

Mustard, P. S., Donaldson, J. A., and Thompson, R. I.
1988: Trace fossils and stratigraphy of the Precambrian-Cambrian boundary sequence, upper Harper group, Ogilvie Mountains, Yukon; *in* Current Research, Part E, Geological Survey of Canada, Paper 88-1E, p. 197-203.

Norris, D. K.
1982: Geology of Wind River map-area, Yukon Territory; Geological Survey of Canada, Map 1528A.

Pallister, J. S.
1987: Magmatic history of Red Sea rifting: perspective from the central Saudi Arabian coastal plain; Geological Society of America, Bulletin, v. 98, p. 400-417.

Parrish, R. R. and Krogh, T. E.
1987: Synthesis and purification of ^{205}Pb for U-Pb geochronology, Chemical Geology (Isotopic Geoscience Section), v. 66, p. 103-110.

Parrish, R. R., Roddick, J. C., Loveridge, W. D., and Sullivan, R. W.
1987: Uranium-lead analytical techniques at the geochronology laboratory, Geological Survey of Canana; *in* Radiogenic Age and Isotopic studies: Report 1; Paper 87-2, p. 3-7.

Parrish, R. R., and Scammell, R. J.
1988: The age of the Mount Copeland syenite gneiss and its metamorphic zircons, Monashee Complex, southeastern British Columbia; *in* Radiogenic Age and Isotopic Studies: Report 2; Geological Survey of Canada, Paper 88-2, (21-28).

Roots, C. F.
1987: Regional tectonic setting and evolution of the Late Proterozoic Mount Harper volcanic complex, Ogilvie Mountains, Yukon; unpublished Ph. D. thesis, Carleton University, Ottawa, 227p.

Thompson, R. I., Mercier, E., and Roots, C. F.
1987: Extension and its influence on Canadian Cordilleran passive margin evolution; Geological Society of London, Special Publication, 28, p. 409-420.

A U-Pb zircon age for the ophiolitic Deveraux Formation, Elmtree Terrane, northeastern New Brunswick[1]

C.R. van Staal[2], J.P. Langton[2] and R.W. Sullivan[2]

van Staal, C.R., Langton, J.P., and Sullivan, R.W., A U-Pb zircon age for the ophiolitic Deveraux Formation, Elmtree Terrane, northeastern New Brunswick; in Radiogenic Age and Isotopic Studies: Report 1, Geological Survey of Canada, Paper 88-2, p. 37-40, 1988.

Abstract

A U-Pb zircon age is reported for the ophiolitic Deveraux Formation in the Elmtree Terrane of northeastern New Brunswick. Zircons from a coarse gabbro preserved in a low strain pod in mylonitic gabbroic gneisses give an age of 461 ± 3 Ma. This age agrees within error with an earlier reported K-Ar hornblende age for the gabbroic gneisses. The data suggest that the Deveraux Formation is Middle Ordovician, coeval with or slightly younger than felsic and mafic magmatism in the neighbouring Miramichi Terrane. This interpretation is compatible with an earlier proposed back-arc marginal basin setting.

Résumé

On a daté par la méthode U-Pb appliquée aux zircons la formation l'ophiolitique de Deveraux dans le terrain d'Elmtree dans le nord-est du Nouveau-Brunswick. Des zircons provenant d'un gabbro grossier et conservés dans une masse peu déformée de gneiss à gabbro mylonitique ont donné un âge de 461 ± 3 Ma. Cet âge se situe dans les marges d'erreur d'un âge K-Ar du hornblende établi auparavant pour les gneiss gabbroïques. Les données semblent indiquer que la formation de Deveraux date de l'Ordovicien moyen, c'est-à-dire contemporain ou légèrement antérieur au magmatisme acidique et mafique du terrain avoisinant de Miramichi. Cette interprétation est compatible avec un environnement de bassin-arrière d'arc insulaire.

INTRODUCTION AND GEOLOGICAL SETTING

The Ordovician Elmtree Terrane (Fyffe, 1987; Fyffe and Fricker, 1987) in northeastern New Brunswick is a tectonic inlier to the north of the Ordovician Miramichi Terrane, from which it is separated by a narrow belt of Silurian sedimentary rocks of the Chaleur Group (Fig. 1). The relationships between these two terranes are of continuing interest since they are thought to represent the continuation of the Dunnage and Gander terranes of Newfoundland (Williams, 1978; Williams and Hatcher, 1982). A significant geological boundary, conveniently placed along the Rocky Brook-Millstream (RBM) fault system, was thought to separate these two terranes (Williams, 1978; Fyffe, 1982).

A substantial part of the Elmtree Terrane consists of the Fournier Group (Young, 1911) which includes a fragment of an ophiolite complex (Pajari et al., 1977; Rast and Stringer, 1980), thus supporting the correlation with the Dunnage Terrane. This fragment consists of gabbro that is intruded by plagiogranite, abundant, locally sheeted, diabase dykes, primitive tholeiitic basalt (Winchester and van Staal,1988) and minor sediment, which together comprise the Deveraux Formation (Pajari et al., 1977). The Fournier Group also includes the Pointe Verte Formation comprising alkali basalt (Winchester and van Staal, 1988 and unpubl. results), trachyte, feldspathic greywacke, slate and minor limestone. Graptolites and conodonts indicate a Llandeilian to early Caradocian age for the upper part of the Pointe Verte Formation (Nowlan, 1983; Fyffe, 1986). The boundary between the Deveraux and Pointe Verte Formations is, where exposed, characterized by a high strain zone (Langton and van Staal, unpubl. results). The original relationships between the two are therefore obscure.

Rather than interpreting the Elmtree and northern Miramichi as two separate terranes, van Staal (1987), van Staal and Langton (1988) and Winchester and van Staal (1988) argued that they once formed part of the same terrane, which was subsequently disassembled along the RBM fault system in post Lower Silurian times. Van Staal (1987) proposed that this entire terrane, including the ophiolitic Deveraux Formation, preserves the remnants of a telescoped marginal basin that opened due to back-arc extension

[1] Contribution to the Canada-New Brunswick Mineral Development Agreement, 1984-1989. Project carried by the Geological Survey of Canada, Lithosphere and Canadian Shield Division.
[2] Geological Survey of Canada, 601 Booth Street, Ottawa, Ontario K1A 0E8

in Middle Ordovician time. Accurate age determination of the ophiolitic Deveraux Formation provides a test of this hypothesis, since the back-arc model requires that this formation be coeval or younger than the Middle Ordovician (Fyffe, 1982) rift volcanics and sediments of the northern Miramichi Terrane (van Staal, 1987; Winchester and van Staal, 1988).

SAMPLE SELECTION AND DESCRIPTION

Two rock types were selected for U-Pb analysis in the course of this study: 1) coarse gabbro pods in amphibolite or mylonitic amphibolite and 2) plagiogranite dykes which intrude the gabbro. The plagiogranite intruded relatively late during the amphibolite facies deformation since it cuts through the foliation in the amphibolites but is itself also foliated, albeit weakly. The plagiogranite could therefore have formed in an off-axis environment and will not necessarily provide information concerning the formation time of the ophiolite if this high grade deformation is due to transform faulting as suggested by Flagler and Spray (1988).

The determined U-Pb zircon age of the coarse gabbro (461 ± 3 Ma) is interpreted as the formation age of the ophiolite. The dated gabbro occurs as a low strain pod in strongly deformed amphibolites which are exposed in a railway cut near Pointe Verte (Fig. 2; *see also* Fyffe and Noble, 1985, stop 7, or Fyffe, 1987, stop 5). This pod is interpreted as a segregation that acted as a competent body during the shearing, or as a relic of a heterogeneously deformed coarse gabbro layer. Nevertheless, an off-axis formation for this gabbro cannot be completely ruled out.

The U-Pb zircon age determination (in progress) of the plagiogranite, sampled at the same location, will be presented in an ensuing paper.

ANALYTICAL RESULTS

U-Pb analytical techniques follow those for zircon described in Parrish et al. (1987). Zircons were carefully selected by hand picking and were strongly abraded. Total blanks were about 2 and 10 picograms of U and Pb respectively. Analytical data are presented in Table 1 and displayed in Figure 3.

Zircons from the rock, ranging in size from +149 to -74 microns are clear, anhedral and pale pink or straw coloured. They generally appear equidimentional and blocky, but when turned on their sides often display a more typical prismatic zircon morphology.

Two fractions were successfully analyzed resulting in essentially concordant points in close agreement. Fraction C, however, plots slightly above concordia (Fig. 3). The best estimate of the age from this data is conservatively taken to be 461 ± 3 Ma.

The reason for fraction C plotting above concordia is uncertain, but it is probably due to an inappropriate composition used for the initial common lead correction and/or an incorrect mass fractionation correction for the lead. The results, shown in Table 1, were calculated using the Stacey-Kramers (1975) model for common lead. Re-calculations

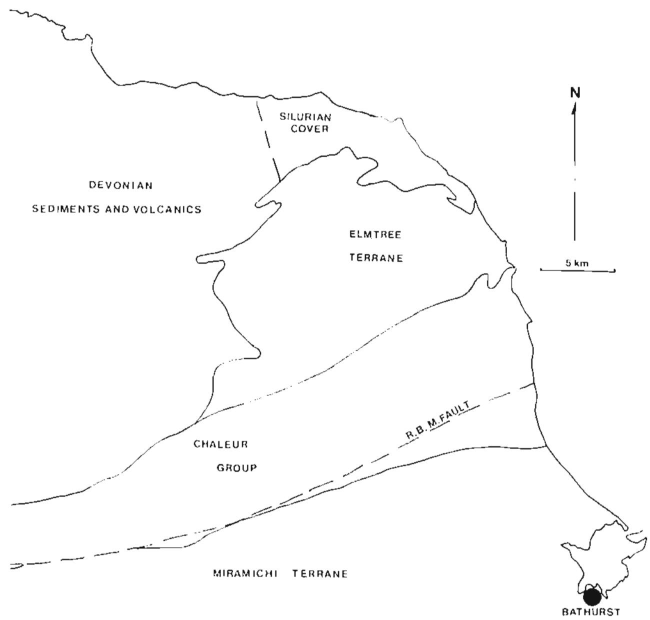

Figure 1. Simplified geological map of northern New Brunswick showing the positions of the Elmtree and Miramichi terranes.

using assumed but probably more appropriate "mantle type" initial common lead compositions, (Zartman and Doe, 1981), move the point slightly to the right and make it more concordant. The correction for mass fractionation in the Pb analysis may also have been underestimated. Due to the low quantity of Pb, the analysis was run at a higher filament temperature than normal. If the mass fractionation was higher than normal, the data point would have been shifted to the left of the concordia curve. These small uncertainties are well within the conservative error of ± 3 Ma. The results presented here are those generated by using normal data processing parameters.

DISCUSSION

The U-Pb zircon age reported here, i.e. 461 ± 3 Ma, falls in the early Llandeilian of the time scale of Snelling (1985) and in the middle to late Llandeilian of the DNAG time scale (Palmer, 1983), the time scale of Harland et al. (1982) and the new time scale of Haq and van Eysinga (1987). This age indicates that the Deveraux Formation is coeval or slightly older than the upper part of the underlying Pointe Verte Formation, which supports the structural evidence for a thrust between the two. The ophiolite fragment has the same age, or is younger than, the Middle Ordovician rift volcanics and associated plutons of the Miramichi Terrane (van Staal and Sullivan, unpubl. results; Bevier, 1988) which is consistent with the back-arc extension model proposed by van Staal (1987). It should also be noted that this age is significantly younger than the ages of the ophiolites in the Central Mobile Belt of the Newfoundland Appalachians reported by Dunning and Krogh (1985).

The U-Pb zircon age agrees within error with an earlier reported K-Ar hornblende cooling age of 462 ± 23 Ma (Davies et al., 1983) from an amphibolite sampled at the same location near Pointe Verte.

Table 1. U-Pb zircon analytical data: ophiolitic Deveraux Formation, New Brunswick

Sample and fraction[3]	Weight (mg)	U (ppm)	Pb* (ppm)	Measured[1] $^{206}Pb/^{204}Pb$	Isotopic abundances[2] ($^{206}Pb=100$) ^{204}Pb	^{207}Pb	^{208}Pb	Isotopic ratios $^{206}Pb/^{238}U$	$^{207}Pb/^{235}U$	$^{207}Pb/^{206}Pb$
Coarse Gabbro: JPG (47°50′36″N 65°46′00″W)										
A, +149,A	0.0192	71.1	5.75	436	0.0820	6.855	23.411	0.074405	0.580723	0.056606
C, +149,A	0.0678	31.8	2.54	676	0.0523	6.362	21.417	0.074126	0.572265	0.055992

NOTES: * Radiogenic Pb; [1]corrected for fractionation and spike; [2]corrected for Pb, U blank and common Pb; [3]size in microns; A abraded.

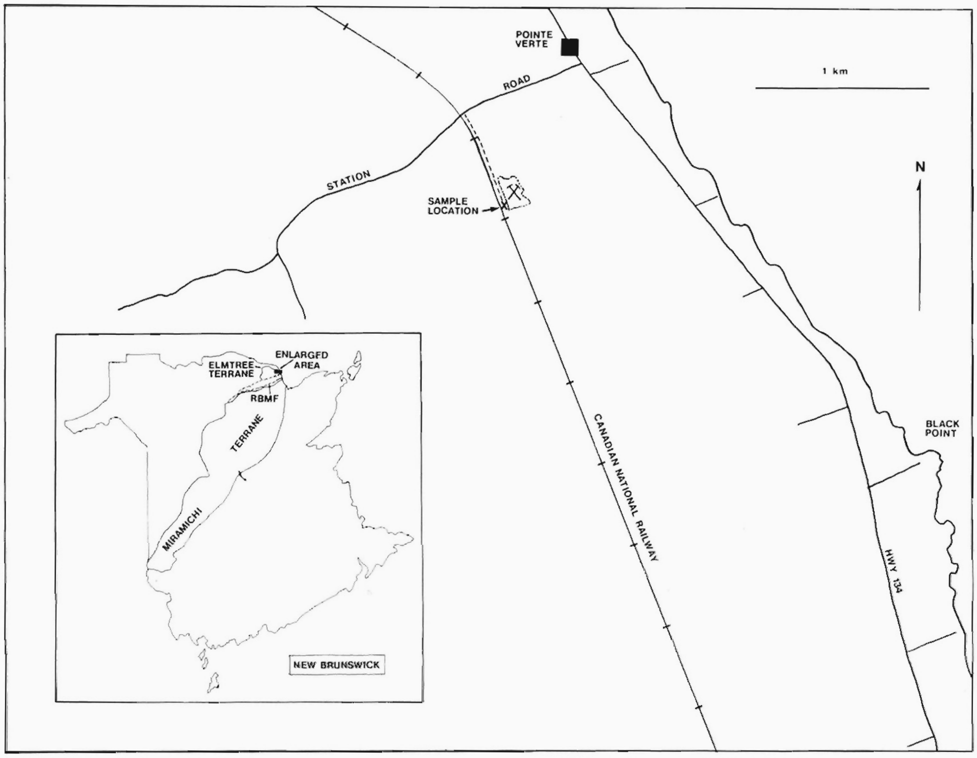

Figure 2. Sample location map.

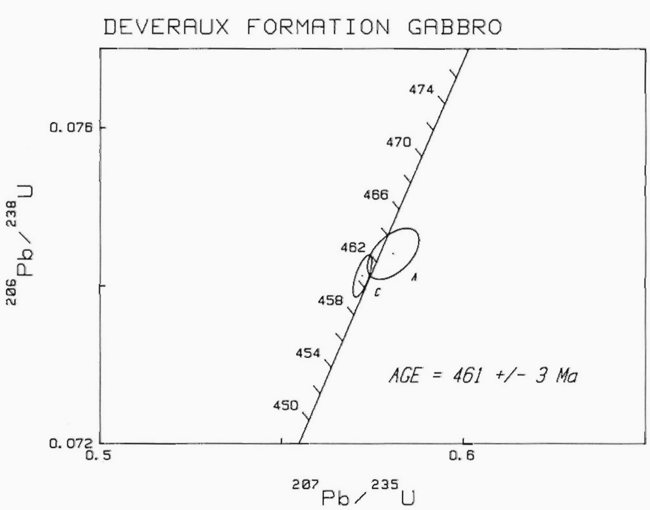

Figure 3. U-Pb concordia plot for zircon from a coarse gabbro in the ophiolitic Deveraux Formation. Errors are shown at the two sigma level.

The close agreement of these ages suggests that the amphibolite deformation took place during or very shortly after formation of the ophiolite complex and supports the interpretation of Flagler and Spray (1988) that the amphibolite facies deformation is associated with transform faulting. Microstructural studies show that the hornblende and plagioclase in the amphibolites generally have smoothly curved or straight interfaces and a tendency for low-energy polygonal grain boundary configurations. This differs from the mylonitic amphibolites which contain porphyroclasts of green hornblende and plagioclase in a matrix of fine, strongly elongated grains with serrated boundaries typical of dynamic recrystallization (Nicholas and Poirier, 1976, p. 169). Furthermore, low-energy grain boundary configurations appear to be rare and there is a marked alteration to chlorite, sphene and calcite.These retrograde minerals are generally also strongly deformed suggesting that mylonitization continued into sub-amphibolite facies conditions unlike the regular amphibolites. These mylonitic amphibolites occur near the base of the Deveraux Formation and along the contact with the underlying Pointe Verte Formation (Langton and van Staal, unpubl. results). Locally these mylonites are shallowly dipping and we therefore propose that some of the mylonitization is related to obduction of the ophiolite fragment.

ACKNOWLEDGMENTS

We are very grateful to Jim Mortensen for his enthusiastic help and his critical review of this paper. Dale Loveridge is thanked for his help in data reduction as is Herb Helmstaedt for his discussions and assistance in the field.

REFERENCES

Bevier, M.L.
1988: U-Pb geochronological studies of igneous rocks in New Brunswick (abstract); *in* Thirteenth Annual Review of Activities of the Department of Natural Resources and Energy of New Brunswick; Department of Natural Resources and Energy of New Brunswick.

Davies, J.L., Fyffe, L.R., and McAllister, A.L.
1983: Geology and massive sulphides of the Bathurst area, New Brunswick; *in*, Field trip guidebook to stratabound sulphide deposits, Bathurst area, New Brunswick, Canada and west-central New England, U.S.A., ed. D.F. Sangster; Geological Survey of Canada, Miscellaneous Report 36, p. 1-30.

Dunning, G.R. and Krogh, T.E.
1985: Geochronology of ophiolites of the Newfoundland Appalachians; Canadian Journal of Earth Sciences, v. 22, p. 1659-1670.

Flagler, P.A. and Spray, J.G.
1988: Metamorphism in shear zones within the Fournier oceanic fragment; *in* Geological Association of Canada/ Mineralogical Association of Canada/ Canadian Society of Petroleum Geologists, Joint Annual Meeting, St. John's, Newfoundland, Program with abstracts, v. 13, p. A39.

Fyffe, L.R.
1982: Taconian and Acadian structural trends in central and northern New Brunswick; *in* Major Structural Zones and Faults of the Northern Appalachians, ed. P. St-Julien and J. Belland: Geological Association of Canada, Special Paper 24, p. 117-129.
1986: A recent graptolite discovery from the Fournier Group of northern New Brunswick; *in* Eleventh Annual Review of Activities of the Department of Natural Resources and Energy of New Brunswick; Department of Natural Resources and Energy of New Brunswick, p.43-45.
1987: Stratigraphy and tectonics of the Miramichi and Elmtree terranes in the Bathurst area, northeastern New Brunswick; Geological Society of America, Centennial Field Guide - Northeastern section, p. 389-393.

Fyffe, L.R. and Fricker, A.
1987: Tectonostratigraphic terrane analysis of New Brunswick; Maritime Sediments and Atlantic Geology, v. 23, p. 113-122.

Fyffe, L.R. and Noble, J.P.A.
1985: Stratigraphy and structure of the Ordovician, Silurian and Devonian of northern New Brunswick; Geological Association of Canada/ Mineralogical Association of Canada; Fieldguide to Excursion 4.

Haq, B.U. and van Eysinga, W.B.
1987: Geological Time Table, 4th edition; Elsevier, Amsterdam.

Harland, W.B., Cox, A.V., Llewellyn, P.G., Pickton, C.A.G., Smith, A.G., and Walters, R.
1982: A geologic time scale; Cambridge University Press, Cambridge, U.K.

Nicholas, A. and Poirier, J.P.
1976: Crystalline Plasticity and Solid State Flow in Metamorphic Rocks; Wiley, New York, N.Y., 444 p.

Nowlan, G.S.
1983: Report on three samples from limestone in pillow basalts from the Pointe Verte Formation (northern New Brunswick); Geological Survey of Canada, Report 002.

Pajari, G.E., Rast, N., and Stringer, P.
1977: Paleozoic volcanicity along the Bathurst-Dalhousie geotraverse, New Brunswick and its relation to structure; *in* Volcanic Regimes in Canada, ed. W.R.A. Barager, L.C. Coleman and J.M. Hall; Geological Association of Canada, Special Paper 16, p. 114-124.

Palmer, A.R.
1983: The Decade of North American Geology, geologic time scale; Geology, v. 11, p. 503-508.

Parrish, R.R., Roddick, J.C., Loveridge, W.D., and Sullivan, R.W.,
1987: Uranium-lead analytical techniques at the Geological Survey of Canada; *in* Radiogenic Age and Isotopic Studies: Report 1; Geological Survey of Canada, Paper 87-2, p. 3-7.

Rast, N. and Stringer, P.
1980: A geotraverse across deformed Ordovician ophiolite and its Silurian cover, northern New Brunswick, Canada; Tectonophysics, v. 69, p. 221-245.

Snelling, N.J.
1985: An interim time scale; *in* The Chronology of the Geological Record, ed. N.J. Snelling; British Geological Survey, Memoir No. 10, p. 261-265.

Stacey, J.S. and Kramers, J.D.
1975: Approximation of terrestrial lead isotope evolution by a two-stage model; Earth and Planetary Science Letters, v. 26, p. 207-221.

van Staal, C.R.
1987: Tectonic setting of the Tetagouche Group in northern New Brunswick: implications for plate tectonic models of the nothern Appalachians; Canadian Journal of Earth Sciences, v. 24, p. 1329-1351.

van Staal, C.R. and Langton, J.P.
1988: Correlation between the Elmtree and Miramichi terranes: evidence for the Caledonian Orogeny in northeastern New Brunswick; *in* Geological Association of Canada/ Mineralogical Association of Canada/ Canadian Society of Petroleum Geologists, Joint Annual Meeting, St. John's, Newfoundland, Program with Abstracts, v. 13. p. A129.

Williams, H.
1978: Tectonic lithofacies map of the Appalachian orogen; Memorial University of Newfoundland, St. John's, Newfoundland, Map 1.

Williams, H. and Hatcher, R.D.
1982: Suspect terranes and accretionary history of the Appalachian Orogen; Geology, v. 10, p. 530-536.

Winchester, J.A. and van Staal, C.R.
1988: Middle Ordovician volcanicity in northern New Brunswick: geochemistry and probable tectonic setting; *in* Geological Association of Canada/ Mineralogical Association of Canada/ Canadian society of Petroleum Geologists, Joint Annual Meeting, St. John's, Newfoundland, Program with Abstracts, v. 13, p. A135.

Young, G.A.
1911: Bathurst district, New Brunswick, Canada; New Brunswick Department of Mines, Geological Survey Branch, Memoir No. 18-E, 92 p.

Zartman, R.E. and Doe, B,R.
1981: Plumbotectonics-the model; Tectonophysics, v. 75, p. 135-162.

K-Ar ages from the Minden area, Grenville Province, Ontario

R.M. Easton[1] and J.C. Roddick

Easton, R.M. and Roddick, J.C., K-Ar ages from the Minden area, Grenville Province, Ontario; in Radiogenic Age and Isotopic Studies: Report 2, Geological Survey of Canada, Paper 88-2, p. 41-44, 1988.

Abstract

An unmetamorphosed, undeformed trachyandesite dyke that intrudes Grenville gneisses near Minden, Ontario, has yielded K-Ar biotite and whole-rock ages of 898±17 and 902±12 Ma respectively. These ages date the time of emplacement of the dyke and are within in the range of an 850-900 Ma magmatic event in the Ottawa-Bonnechere graben system. If this dyke is related to this event, then it is the westernmost reported occurrence of this magnatism.

A nearby sample of micaceous marble from the Central Metasedimentary Belt Boundary Zone (CMBBZ) at Miners Bay just north of the dyke, has a K-Ar biotite age of 1061±14 Ma. This is similar to a U-Pb zircon age of 1060 Ma, related to deformation in the Boundary Zone, and indicates that excess argon occurs locally within the CMBBZ. The presence of excess argon in the CMBBZ has not been reported previously. A second sample from the Allsaw Anorthosite body, about 5 km east of Minden, has a K-Ar biotite age of 944±14 Ma, consistent with 915 to 950 Ma K-Ar biotite cooling ages in the area.

Résumé

Un dyke non métamorphisé et non déformé de trachyandésite recoupant des gneiss de Grenville près de Minden, en Ontario, a été daté par la méthode K-Ar effectuée sur la biotite et sur la roche totale à 898±17 et 902±12 Ma, respectivement. Selon les âges obtenus, l'intrusion du dyke a eu lieu pendant l'événement magmatique survenu il y a 850 à 900 Ma dans le système de grabens d'Ottawa et Bonnechère. Si l'intrusion de ce dyke est associée à cet événement, il s'agirait de la manifestation la plus à l'ouest de cet épisode de magmatisme.

Un échantillon voisin de marbre micacé provenant de la zone à la limite métasédimentaire Centrale à Miners Bay, juste au nord du dyke, donne un âge de 1061+14 Ma établi à l'aide de la méthode K-Ar appliquée à la biotite. Cet âge est semblable à celui de 1060 Ma, déterminé par la méthode U-Pb appliquée aux zircons, lié à la déformation observée dans la zone limite, et indique une teneur en argon non radiogénique à certains endroits de la zone. La présence d'argon non radiogénique dans la zone limite est signalée pour la première fois. Un autre échantillon provenant du massif d'anorthosite d'Allsaw, à environ 5 km à l'est de Minden, a été daté par la méthode K-Ar appliquée à la biotite à 944±14 Ma, ce qui correspond à une période de refroidissement de cette région de 915 à 950 Ma, également établie à l'aide de la méthode K-Ar appliquée à la biotite.

INTRODUCTION

During recent mapping of the Precambrian rocks of the Minden area of southern Ontario (Easton, 1986a, 1988) a post-Grenville trachyandesite dyke which intrudes the deformed gneisses of the Central Metasedimentary Belt Boundary Zone (CMBBZ) was found 15 km south of Minden. It is unusual for the area, as it is an undeformed, post-metamorphic intrusion with an alkaline character not previously noted in dykes of the Minden-Haliburton-Bancroft area. The closest compositional equivalent in southern Ontario is a trachybasalt to trachyandesite flow described by Lafleur and Hogarth (1981) from Buckingham, Quebec (Fig. 1), that has a K-Ar age of 573±32 Ma. As the Buckingham flow is associated with the development of the Ottawa-Bonnechere graben, the presence of a related dyke in the Minden area would possibly document the tectonic effects of graben development over a wider area than previously recognized. K-Ar dating has been carried out on the dyke, in order to test this hypothesis.

[1] *Ontario Geological Survey, 77 Grenville Street, Toronto, Ontario*
[2] *Geological Survey of Canada, 601 Booth Street, Ottawa, Ontario, K1A 0E8*

GEOLOGY AND SAMPLING

The trachyandesite dyke varies in width from 20 to 100 cm and locally engulfs large rafts of the gneissic country rock. The country rock consists of thinly layered mafic and granitic gneisses which are protomylonitic, and which are gradational between irregular layered gneiss and straight gneiss (to use the terminology of Hanmer and Ciesielski, 1984). The dyke rock is a leuco- to mesocratic, pinkish to purplish weathering, biotite-phyric, undeformed, unmetamorphosed, fine grained rock with a weak trachytic texture and a poorly-developed chill margin. The samples were collected from the core of the dyke, remote from any rafts of country rock. The rock has an alkaline chemical character, and is a trachyandesite or an alkaline diorite (Easton, 1986a).

The Grenville country rock was sampled at Miners Bay just north of the dyke, and on the margin of the Allsaw Anorthosite body (Fig. 1). Exact sample locations are given in Hunt and Roddick (1988).

RESULTS AND DISCUSSION

Four K-Ar ages were determined, two on the Minden trachyandesite dyke (3762, 3763, Table 1) and two on biotites from the surrounding Grenville-age rocks (3761, 3764) to check for possible anomalous Ar behaviour in the CMBBZ. The expected K-Ar biotite cooling ages of the country rock are 900 to 950 Ma, based on previous K-Ar ages in the area (Easton, 1986b).

The analytical results are given in Table 1 for all the samples. The interpretation of the ages of dyke are straightforward. The rock is unmetamorphosed, and the biotite age of 898 ± 17 Ma, although higher than expected, is consistent with the field relations indicating that this dyke is post-Grenvillian (i.e. post "Ottawan Orogeny"). The whole-rock age on the same sample (902 ± 12 Ma) is in good agreement with the biotite age. As discussed below, sample 3764 undoubtedly contains some excess Ar, but it is unlikely that the dyke is similarly affected. The whole-rock sample has a K content similar to the biotite, however, the K in the whole-rock is mainly in feldspar. Thus the two phases, biotite and feldspar, have concordant ages. It is unlikely that the two minerals would incorporate similar proportions of excess argon, consequently the age defines the time of intrusion of the dyke.

Magmatic activity along the Ottawa-Bonnechere graben has been protracted, and has occurred at 420, 450-480, 540-570, 700 and 850-900 Ma (Easton, 1986b). If this trachyandesite dyke is related to magmatic activity at 850-900 Ma, associated with rifting in central and eastern Ontario, it represents the westernmost manifestation of this activity in central Ontario. The unique chemistry supports its relation to the earliest rifting magmatism.

Sample 3761 is a coarse biotite sample from a pink calcite-biotite fracture filling in the Allsaw Anorthosite body, which is a large tectonic sheet surrounded by marble breccia that occurs about 10 km east of the main deformation zone in the CMBBZ (Fig. 1; Easton, 1988). This biotite probably formed near the peak of the Ottawan Orogeny in this area. The age of 944 ± 14 Ma is in reasonable agreement with ^{40}Ar-^{39}Ar total gas ages of 916 ± 15 and 898 ± 15 Ma obtained from biotite samples from the Bark Lake diorite located 15 km east-southeast of the Allsaw Anorthosite (Berger and York, 1981; Fig. 1).

Sample 3764 is a coarse biotite from a metamorphic reaction rim surrounding a calc-silicate clast in marble tectonic breccia at Miners Bay. The biotite probably formed during the peak of the Ottawan Orogeny in this area. The sample has a K-Ar age of 1061 ± 14 Ma. This age is in remarkable agreement with U-Pb ages from syntectonic pegmatites from Carnarvon and Hawk Lake which date the peak of deformation in the CMBBZ at 1065 ± 15 Ma (van Breemen and Hanmer, 1986). The K-Ar age of 1061 ± 14 Ma is considerably higher than other biotite ages in the area (e.g. sample 3761 and the Bark Lake data of Berger and York, 1981), and given its similarity to the U-Pb zircon age on deformation in the area, probably contains some excess Ar which is giving a higher than expected age. It is noteworthy that sample 3764 is from the zone of most intense deformation in the CMBBZ, and excess Ar is commonly found associated with major deformation zones. Workers planning K-Ar or Ar-Ar work in the vicinity of the CMBBZ should be aware of the potential presence of an excess Ar component, as indicated by sample 3764.

Table 1. K-Ar data for rocks near Minden, Ontario.

Field No.	Lab. no.	Material	K wt% ± 1σ%	Rad 40Ar cc/gm 10^{-7}	% Atmos. ^{40}Ar	Age ± 2σ Ma
85RME-956	3761	Biotite	7.84 ± 0.75	3776	1.52	944 ± 14
85RME-950	3762	Biotite	7.74 ± 1.0	3498	0.92	898 ± 17
85RME-950	3763	Whole rock	8.24 ± 0.5	3746	0.23	902 ± 12
85RME-952	3764	Biotite	7.76 ± 0.6	4356	0.94	1061 ± 14

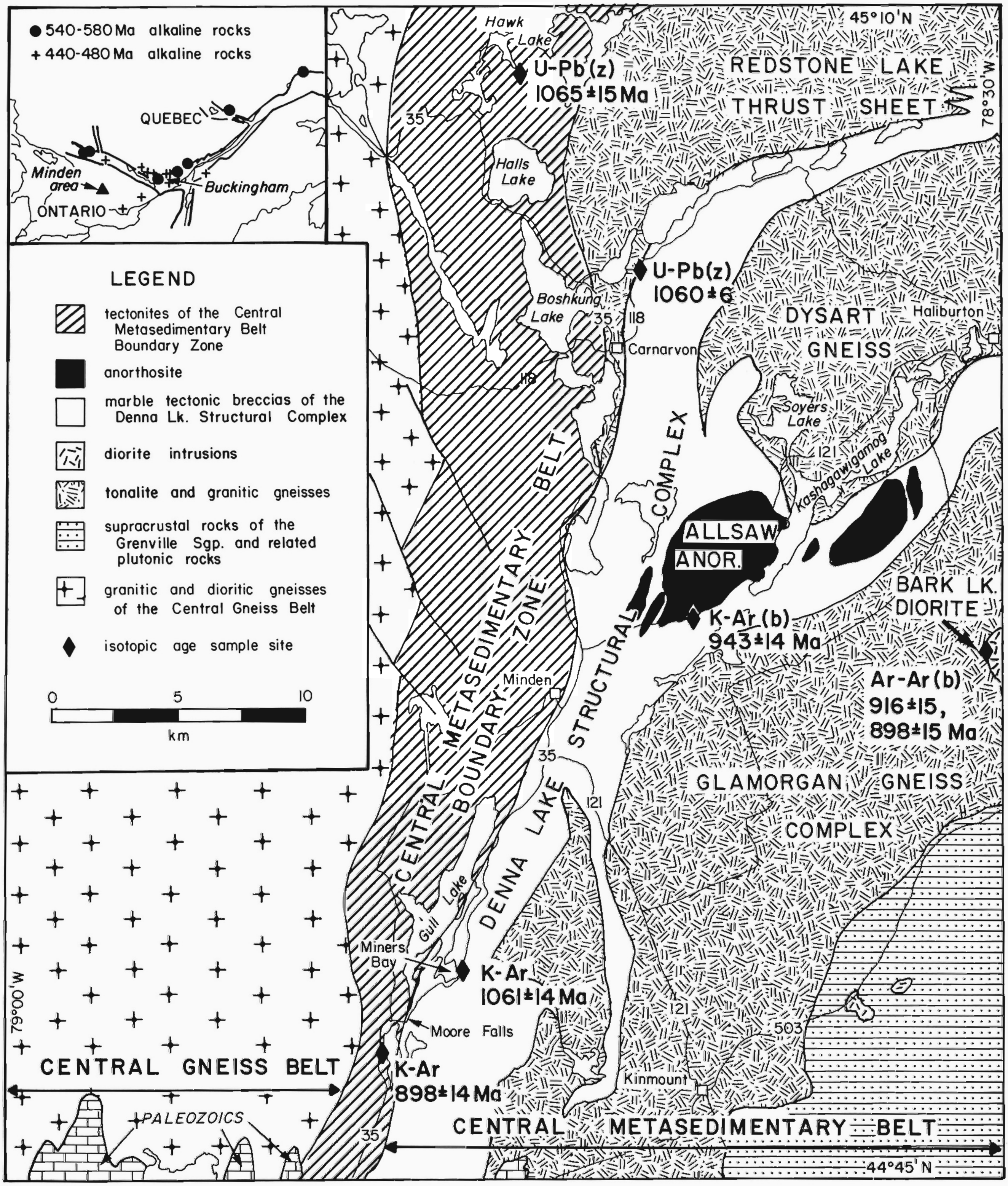

Figure 1: Location of K-Ar samples reported here and other geochronological data from the Minden area, Ontario, (geology from Easton, 1986a; U-Pb ages from van Breemen and Hanmer, 1986; Ar-Ar ages from Berger and York, 1981). Inset shows location of Minden area to Ottawa-Bonnechere graben system.

REFERENCES

Berger, G.W. and York, D.
1981: Geothermometry from $^{40}AR/^{39}$ AR dating experiments; Geochimica et Cosmochimica Acta, v. 45, p. 795-812.

Easton, R.M.
1986a: Precambrian Geology of the Digby-Lutterworth area, Haliburton, Peterborough and Victoria Counties; Ontario Geological Survey, Open File Report 5601, 270p.
1986b: Geochronology of Ontario; Ontario Geological Survey, Open File Report 5592, 179p.
1988: Geology of the Minden area; Ontario Geological Survey, Preliminary Map P.3106, scale 1:50 000.

Hanmer, S.K. and Ciesielski, A.
1984: A structural reconnaissance of the Central Metasedimentary Belt, Grenville Province, Ontario and Quebec; *in* Current Research, Part B, Geological Series of Canada, Paper 84-1B, p. 121-131.

Hunt, P.A. and Roddick, J.C.
1988: A compilation of K-Ar ages: Report 18; *in* Radiogenic Age and Isotopic Studies: Report 2; Geological Survey of Canada, Paper 88-2.

Lafleur, J. and Hogarth, D.D.
1981: Cambro-Proterozoic volcanism near Buckingham, Quebec; Canadian Journal of Earth Sciences, v. 18, p. 1817-1823.

van Breemen, O. and Hanmer, S.K.
1986: Zircon morphology and U-Pb geochronology in active shear zones: studies on syntectonic intrusions along the northwest boundary of the Central Metasedimentary Belt, Grenville Province, Ontario; *in* Current Research, Part B, Geological Survey of Canada, Paper 86-1B, p. 775-784.

U-Pb zircon ages of granites and syenites in the Central Metasedimentary Belt, Grenville Province, Ontario

O. van Breemen and A. Davidson

van Breemen, O., and Davidson, A., U-Pb zircon ages of granites and syenites in the Central Metasedimentary Belt, Grenville Province, Ontario; in Radiogenic Age and Isotopic Studies: Report 2, Geological Survey of Canada, Paper 88-2, p. 45-50, 1988.

Abstract

U-Pb zircon age determinations of granitoid rocks from Elzevir and Frontenac terranes within the Central Metasedimentary Belt suggest that major plutonism in these adjacent terranes was separated in time by at least 60 Ma. Ages from Elzevir terrane are: 1, Addington pluton, 1245 $^{+15}_{-10}$ Ma, and 2, Deloro granite, 1241 ± 2 Ma. Ages from Frontenac terrane are: 3, Rockport granite, 1173 ± 4 Ma, and 4, Gananoque syenite, 1162 ± 3 Ma.

Résumé

Des datations par la méthode U-Pb appliquée aux zircons de roches granitoïdes provenant des terrains d'Elzevir et de Frontenac dans la zone métasédimentaire Centrale semblent indiquer qu'un plutonisme important aurait affecté ces deux terrains adjacents mais à des périodes différentes, séparées par un intervalle d'au moins 60 Ma. Les âges obtenus pour le terrain d'Elzevir sont: 1) pluton d'Addington, 1245 $^{+15}_{-10}$ Ma et, 2) granite de Deloro, 1241 ± 2 Ma. Les âges obtenus pour le terrain de Frontenac sont: 3) granite de Rockport, 1173 ± 4 Ma et, 4) syénite de Gananoque, 1162 ± 3 Ma.

INTRODUCTION

This paper reports ages of plutonic rocks from two different terranes in the Central Metasedimentary Belt of the Grenville Province in Ontario. Two, the Addington granite and the peralkaline Deloro granite, are from the Elzevir terrane and two, the Rockport granite and the Gananoque syenite, are from the Frontenac terrane (Fig. 1). Plutonic rocks in the Elzevir terrane are varied in composition; they range from ultramafic and gabbroic through granodioritic to granitic, along with both saturated and undersaturated syenitic rocks. They intrude deformed sedimentary and volcanic rocks of the Grenville Supergroup in and around the Hastings metamorphic "low" (Carmichael et al., 1978), one of few areas in the Grenville Province where rocks in greenschist facies occur. Some plutons are overlain by the Flinton Group (Moore and Thompson, 1980), a folded and metamorphosed sedimentary succession preserved in narrow synclines but not known to have been intruded by plutonic rocks. In the Frontenac terrane, the plutonic rocks are mainly granite and saturated monzonite or syenite, locally associated with minor amounts of gabbro. They also intrude deformed rocks of the Grenville Supergroup which, however, are wholly sedimentary and include facies not present in the Elzevir terrane (*see* Davidson, 1986, Fig. 6). Metamorphic grade in the country rocks is granulite facies of low pressure type; the plutonic rocks do not appear to have been metamorphosed at this grade, though they are locally foliated and some are marginally mylonitized.

[1] Geological Survey Canada, 601 Booth Street, Ottawa, Ontario K1A 0E8

U-Pb zircon isotopic data (Table 1) was obtained using techniques described by Parrish et al. (1987). A modified form of York's (1969) least squares fitting is used to calculate regression lines (Fig. 2, 3).

CASE STUDIES

Addington pluton (Sample 1; 86DM1a)

The Addington granite pluton has the form of a folded sheet that wraps the southwest closure of the Clare River synform, a complex, major fold overturned to the northwest (Fig. 1). It is emplaced within volcanic and sedimentary rocks of the Grenville Supergroup, but may have been unroofed before deposition of the Flinton Group in which conglomerate carries clasts of Addington-like granite. The predominant granitoid rock is fine grained, equigranular, sugary, pink biotite leucogranite, locally with minor muscovite, and appears to be recrystallized. In the widest part of its exposure at the southwest closure, however, it retains a weakly preserved, medium grained igneous texture, despite having a well- developed foliation, and contains scattered microcline megacrysts and rare xenoliths of more mafic rock. It is from this part of the pluton that the dated sample was collected, on the north side of Old Troy Road 3.35 km northeast of the intersection with Ontario Highway 37.

Separated zircons are clear and colourless to pale yellow, forming short, euhedral to subhedral prisms (length to breadth ratio 1:1 to 2:1) dominated by simple (100) prism and (101) bipyramid faces. There is little evidence of rounding of crystal faces, either by resorption or by overgrowth.

Table 1. U-Pb isotopic data

Sample and zircon fraction In microns	Weight (mg)	U (ppm)	Pb* (ppm)	Measured $^{206}Pb/^{204}Pb$	Isotopic abundances (^{206}Pb=1000) ^{204}Pb	^{207}Pb	^{208}Pb	Isotopic ratios $^{206}Pb/^{238}U$	$^{207}Pb/^{235}U$	Age,Ma $^{207}Pb/^{206}Pb$
1. Addington pluton (86-DM-1a; 44 31.2 N, 77 17.6 W)										
a, +149,M2	0.020	125.1	26.95	555	0.706	90.79	118.9	2.20452	2.2792	1217.2
b, −149+105N2	0.070	202.6	42.82	5610	0.060	82.19	106.1	0.20729	2.3249	1229.8
c, −149+105M2	0.052	221.1	46.77	1164	0.604	89.29	116.2	0.20179	2.2473	1215.9
d, −105+74M1	0.049	125.4	28.37	558	1.337	99.99	145.4	0.20622	2.3066	1224.4
e, −105+62N1	0.037	221.1	46.30	615	1.420	101.06	148.1	0.20640	2.3049	1221.2
f, +105,M1M2	0.020	192.1	41.46	5692	0.059	82.52	109.5	0.21101	2.3765	1237.9
g, +105,M1M2	0.015	179.6	38.69	618	1.333	100.40	153.5	0.21065	2.3698	1235.7
2. Deloro pluton (86-DM-2a; 44 29.7 N, 77 33.6 N)										
a, −105+74,N1	0.046	322.2	70.14	4327	0.077	82.53	125.3	0.20915	2.3572	1239.3
b, −105+74,M1	0.059	322.3	71.02	5051	0.060	82.71	130.0	0.21100	2.3815	1242.1
c, −105+74,M2	0.046	310.7	69.86	1704	0.431	87.89	143.3	0.21067	2.3766	1241.2
d, −105+74,M2	0.018	271.9	59.64	989	0.715	91.84	147.4	0.21163	2.3857	1239.7
3. Rockport granite (86-DM-135; 44 22.5 N, 75 55.2 W)										
a, +149,M0	0.058	495.0	99.73	3543	0.149	80.81	151.6	0.18951	2.0565	1164.6
b, −149+105,M0	0.050	357.5	71.35	3063	0.107	80.27	127.2	0.19179	2.0825	1166.0
c, −149+74,M1	0.031	315.0	58.35	3460	0.094	79.73	105.7	0.18239	1.9717	1157.1
d, −105+74,M0	0.076	346.5	69.95	2675	0.228	81.94	146.5	0.19027	2.0650	1164.9
e, −74,M0	0.052	303.3	61.55	1734	0.340	85.05	139.0	0.19157	2.1194	1202.9
4. Gananoque syenite (86-DM-9b; 44 22.2 N, 76 11.9 W)										
a, +105,N0	0,094	86.98	18.84	1026	0.574	86.82	178.2	0.19693	2.1365	1164.2
b, −105+74,N0	0.089	91.31	20.88	592	1.305	97.07	213.9	0.19806	2.1467	1162.3
c, −74+62,N0	0.106	103.3	22.49	1024	0.680	88.24	178.3	0.19729	2.1385	1162.4
d, −62,N0	0.100	96.50	21.10	1074	0.592	86.97	183.7	0.19785	2.1431	1161.1

* Radiogenic lead
N,M Respectively non-magnetic or magnetic at given side slope angle on Frantz magnetic separator

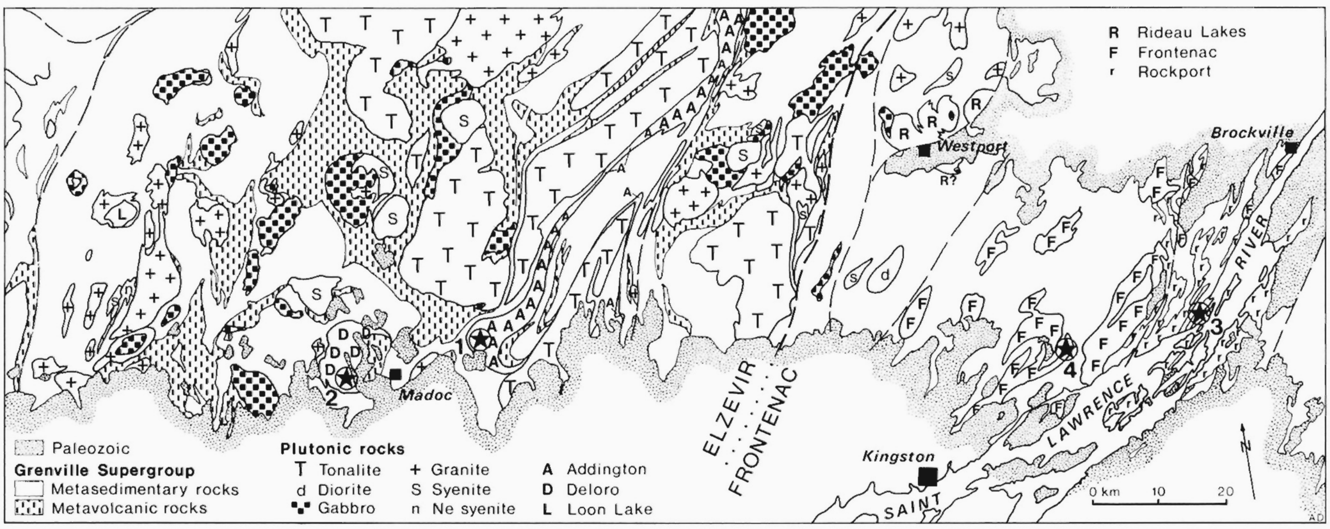

Figure 1. Generalized geology of parts of Elzivir and Frontenac terranes, Central Metasedimentary Belt; their boundary is placed at the easter limit of metavolvanic rocks and tonalitic plutons. Circles stars mark sample locations, numbered as in text and Figures 2 and 3.

Uranium concentrations range from 125 to 220 ppm. The first four analyzed fractions (1a, 1b, 1c, 1d) follow a curvilinear distribution which causes some uncertainty concerning the upper age intercept (Fig. 2). Fractions 1e, 1f and 1g were more strongly abraded, especially the coarsest of these, for which only rounded interiors of crystals remained after abrasion. A regression line through these three data points gives upper and lower intercept ages of 1245 $^{+40}_{-6}$ Ma and ca. 900 Ma respectively. The lower intercept age clearly indicates that more than one event may have affected the zircons before possible slight recent Pb loss. As a result of the latter effect, the lower intercept age may be significantly young. If the regression line is constrained to pass through 1050 Ma, assuming little or no recent Pb loss, the upper intercept age is 1253 $^{+9}_{-8}$Ma.

The possibility that the distribution of data points reflects a mixing of older cores within younger igneous zircons cannot be discounted. Such an hypothesis is supported by the unambiguous igneous morphology of the zircons but not by the absence of cores. The preferred interpretation, based on the regularity of data points and agreement of fractions

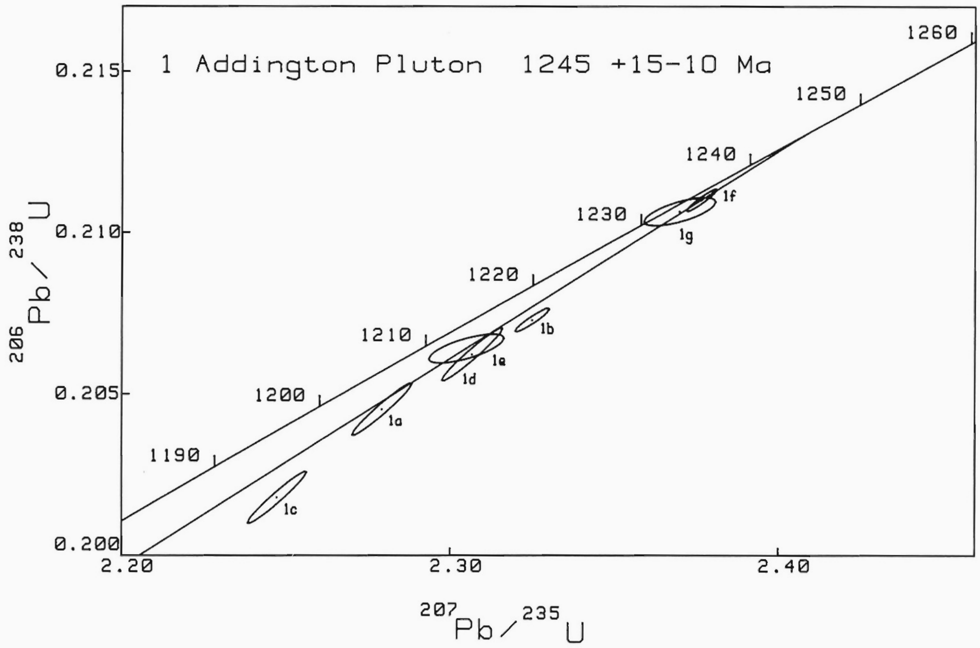

Figure 2. Isotope ratio plot for zircons from: 1, Addington pluton. Numbers and letters with data points correspond to those of Table 1.

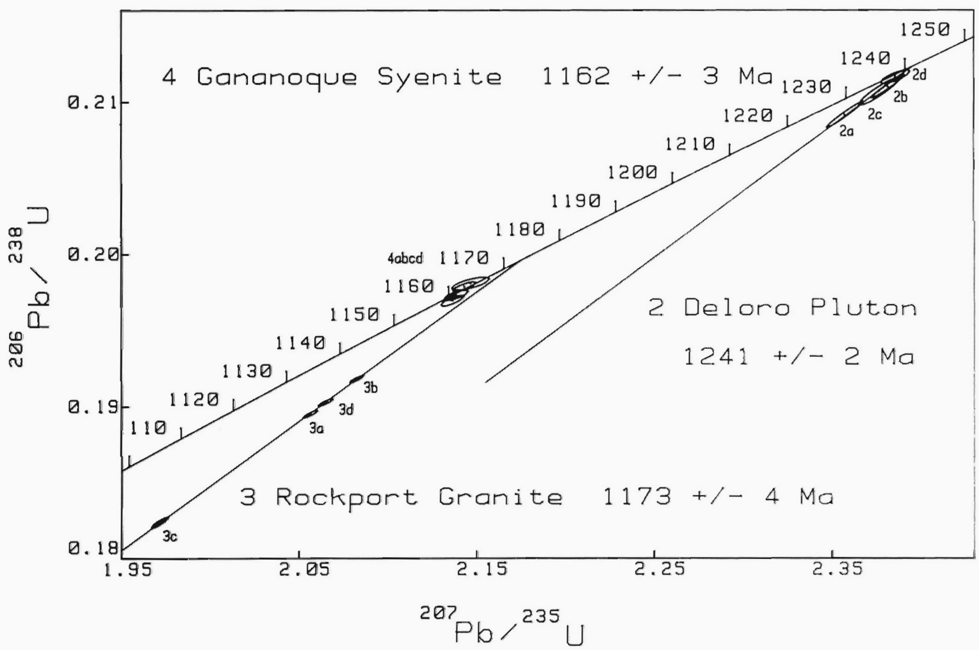

Figure 3. Isotope ratio plot for zircons from: 2, Addington granite; 3, Rockport granite and Ganenoque syenite. Numbers and letters with data points correspond to those of Table 1.

1f and 1g is that these zircons do not have a significant inherited component but were affected by a later Grenvillian metamorphic event. In view of the euhedral to subhedral crystal morphology, the mechanism for this U-Pb disturbance is not understood, although it could be related to slight radioactive lattice damage followed by annealing (Gebauer and Grünenfelder, 1976). Based on the regression of data points 1e, 1f and 1g and the $^{207}Pb/^{206}Pb$ model ages of the coarse, strongly abraded fractions, the age and uncertainties of the Addington granite are placed at 1245 $^{+15}_{-10}$ Ma.

Deloro pluton (sample 2; 86DM2a)

A large part of the Deloro pluton is a crescent-shaped mass of granite, concave to the southeast (Fig. 1). The arms of the crescent encompass a unit of bimodal volcanic rocks (basalt, rhyolite plus felsic pyroclastic rocks) which the granite intrudes, plus a younger mass of granophyric granite. Lenticular units of gabbro and syenite occur at its western margin, in contact with mafic metavolcanic rocks. Where exposed elsewhere, the country rock is marble of the Grenville Supergroup; parts of the contact of the pluton are unconformably overlain by Paleozoic sedimentary rocks.

The intrusion is of ring complex type and it is possible that the adjacent volcanic rocks are related to it (Abdel-Rahman and Martin, 1987). The plutonic rocks display little if any evidence of deformation in the field, although thin sections of the granite show strained and partly recrystallized quartz. Thin sections also show formation of secondary biotite, acicular amphibole and rare stilpnomelane in place of primary amphibole, and small mafic dykes that postdate the Deloro granite contain metamorphic epidote and chlorite. The non-deformed appearance of the plutonic rocks and of the spatially associated volcanic rocks on the east side contrasts with the deformed state of pelitic metasediments in the nearby Madoc syncline, equated with the Flinton Group (Moore and Thompson, 1980), in which a vertical, east-northeast-trending slaty cleavage is strongly developed.

The dated sample comes from the main unit of peralkaline and hypersolvus granite, collected from the easternmost outcrop exposed on the north side of Highway 7. The granite contains deep blue riebeckite and accessory fluorite and zircon. Separated zircons are clear and colourless to pale yellow, forming euhedral short prisms (length to breadth ratio 1:1 to 2:1) dominated by simple (100) and (101) prism and bipyramid faces typical of high level alkaline or peralkaline granites (Pupin, 1980). Cores are not evident and inclusions are rare. Fine fractures are common but were mostly avoided during hand picking.

Uranium concentrations are relatively high (270 to 320 ppm). On a concordia plot (Fig. 3) the data points are concordant (2d) to 1.4 % discordant (2a). Regression analysis yields a straight line fit (MSWD = 2) with an upper intercept age of 1241 ± 2 Ma and a lower intercept close to the origin. The upper intercept age is interpreted to reflect the time of intrusion and igneous crystallization.

Rockport granite and Gananoque syenite (sample 3, 86DM135; sample 4, 86DM9b)

Northwest of the St. Lawrence River (Fig. 1), Frontenac terrane is underlain in large part by a variety of layered siliceous and feldspathic gneiss and granulite, including minor amounts of quartzite, pelitic gneiss, amphibolite and pyroxene granulite. This assemblage displays complex fold patterns, trending mainly northeast, and occurs in large tracts within marble tectonite(Wynne-Edwards, 1967). Southeast toward the St. Lawrence the proportion of marble decreases and quartzite becomes a dominant lithology in quartzofeldspathic granulite and gneiss. Several granitoid plutons intrude these metasedimentary rocks; smaller masses of gabbro, diorite and quartz diorite are also present, some associated with the granitoid plutons, others separate.

The granitoid rocks were divided into two types by Wynne-Edwards (1963). Frontenac-type plutons range in composition from monzonite and syenite to quartz monzonite and granite, characterized by medium-to coarse-grain size. In contrast, bodies of Rockport type are composed exclusively of comparatively fine grained, leucocratic granite. Frontenac-type granitoids form several discrete stocks in the triangular region between Westport, Kingston and Brockville. Rockport-type granite, on the other hand, occurs only within the belt of steeply northwest-dipping quartzofeldspathic granulite and quartzite within a few kilometres of the St. Lawrence, where it forms interconnected, northeast-trending lenticular masses and sheets (Wynne-Edwards, 1962, 1963). Whereas Frontenac-type plutons generally have sharply defined contacts, Rockport-type granite forms numerous dykes and veins in its country rocks and is locally replete with both small and large metasedimentary xenoliths; it is also locally migmatitic, its leucosomes carrying abundant tourmaline. Wynne-Edwards (1963) reported that granite of Rockport type occurs both as xenoliths and as dykes in adjacent Frontenac-type plutons; he concluded that both types "...were mobile at the same stage, but that their relative mobility varied from time to time and from place to place, so that they alternately cut and include each other". All of the granitoid plutonic rocks south of Westport have been reported to have abnormally high ^{18}O ratios (Shieh, 1985).

The sample of Rockport granite was collected from a roadside outcrop of pink, fine grained, inclusion-free granite 1 km along the road to Escott north of its intersection with the 1000 Islands Parkway at the village of Rockport. Separated zircons are subhedral and prismatic with length to breadthratios between 2:1 and 3:1. Fractures are common and many grains are broken. Cores are also recognizable; an attempt was made to avoid cored grains during hand picking, but this may not have been achieved in the poor quality coarsest fraction nor in the finest fraction.

Uranium concentrations are high, ranging from 300 to 500 ppm. A straight line can be fitted through data points 3a, b, c and d (MSWD = 0.25) (Fig. 3), corresponding to an upper intercept age of 1173 ± 4 Ma and a lower intercept age of ca. 240 Ma. The upper intercept age is interpreted as the time of granite emplacement and crystallization. The finest fraction (3e, not plotted) shows evidence of an older component, having a $^{207}Pb/^{206}Pb$ model age of 1202.9 Ma (Table 1).

The sample of Gananoque "syenite" was collected from the South Lake pluton (Shieh, 1985), one of two similar quartz-poor granitoid plutons adjacent to the occurrences of Rockport granite to the southeast. The sample site is a roadside outcrop on the east side of Highway 32, 4.25 km north of its intersection with the north ramp of Highway 401. The rock is massive, homogeneous, fresh, purplish grey and coarse grained. It is in fact quartz monzonite, with approximately equal parts of K-feldspar and oligoclase and about 10 % quartz; it contains bright green augite, brownish hornblende and minor biotite, accessory apatite, titanite and zircon. The separated zircons are clear, euhedral to subhedral elongate prisms with length to breadth ratios between 3:1 and 4:1. Fluid inclusions are common; cores were not recognized.

Uranium concentrations are quite low (90 to 100 ppm) and the data points are concordant (4b, c, d) to slightly discordant (4a) (Fig. 3) with $^{207}Pb/^{206}Pb$ model ages ranging from 1161.1 to 1164.2 Ma (Table 1). The age of emplacement and crystallization of this unit is placed at 1162 ± 3 Ma.

COMMENTS

Modern U-Pb zircon techniques of age determination on the varied plutonic rocks in the Central Metasedimentary Belt are considered to reflect very closely the ages of intrusion and igneous crystallization, permitting penetration of the metamorphic "up-dating" imposed on other radio-isotopic systems. K-Ar and Ar-Ar mineral and whole-rocks ages in this region generally range between 1100 and 850 Ma with the majority between 1050 and 950 Ma (*see* Easton, 1986),although anomalously old ages are also known (e.g. Tudor gabbro; Hayatsu and Palmer, 1975). Rb-Sr whole-rock isochron ages are generally somewhat older (1100-1000 Ma), and some determined in the area of the Hastings "metamorphic low" are older, approaching the U-Pb zircon ages determined for the same plutons (e.g. Elzevir pluton: Rb-Sr 1240 ± 50 Ma, Bell and Blenkinsop, 1980; U-Pb ca. 1275 Ma, L.M. Heaman, pers. commun. 1988; Tallan Lake granodiorite: Rb-Sr 1244 ± 32 Ma, U-Pb 1254 Ma, Heaman et al., 1986). Three of the four plutons reported on here were previously dated by the Rb-Sr whole-rock isochron method: Addington, 1060 ± 30 Ma (Bell and Blenkinsop, 1980); Deloro, 1087 ± 37 Ma (Wanless and Loveridge, 1972); Gananoque, 1085 ± 44 Ma (Krogh and Hurley, 1968). These ages coincide with the time of widespread regional metamorphism in the Ontario Central Metasedimentary Belt (1085 Ma, Heaman et al., 1986; ca. 1050 Ma, Easton, 1986, Fig. 9). Similar U-Pb zircon ages have been determined for syntectonic granitoids in the Central Metasedimentary Belt Boundary Zone (van Breemen and Hanmer, 1986) and for pegmatites and metamorphic zircon in the adjacent Central Gneiss Belt (van Breemen et al., 1988).

It is becoming evident that major magmatism occurred in Elzevir terrane in the age range 1280 to 1240 Ma. This age range applies to most of the plutonic rock types so far dated by the U-Pb zircon method, regardless of their petrogenetic type and corresponding paleoenvironmental implications. For example, the tonalite- granodiorite suite (T in Fig. 1) and coeval, spatially related volcanic rocks (Heaman et al., 1987), interpreted as a subduction-related arc complex (Windley, 1986), are only a little older than the nearby Deloro granite, whose peralkaline character and ring complex form have prompted the interpretation that it is anorogenic (Abdel- Rahman and Martin, 1987).

The 1173 and 1162 Ma ages determined respectively for the Rockport and Gananoque plutons in Frontenac terrane are significantly younger than most plutonic rocks so far dated precisely in Elzevir terrane. These ages are corroborated by recently determined ages for four other Frontenac-type plutons (1177-1165 Ma; Marcantonio et al., 1988). Together these ages confirm Wynne-Edwards' (1973) field observation that the Rockport- and Frontenac-type granitoids are coeval. The age range for plutonism in Frontenac terrane compares closely to ages determined for syntectonic pegmatite (U-Pb zircon, 1161 Ma) that dates ductile shearing in the Parry Sound shear zone (van Breemen et al., 1986), and intrusion of gabbro in the Algonquin region (U-Pb baddeleyite, 1170 Ma; Davidson and van Breemen, in press). Interestingly, the Rideau Lakes plutons (R in Fig.1), petrologically similar to the Frontenac-type plutons, are somewhat younger (1076 ± 2 Ma; L.M. Heaman, pers. commun., 1988), and are similar in age to the syenitic core of the Loon Lake pluton in Elzevir terrane (1090 Ma; Heaman et al., 1982), the oldest carbonatite dykes near the Central Metasedimentary Belt Boundary Zone to the north (1090 Ma; Heaman et al., 1988) and the syenitic plutons in the Gatineau region of the Central Metasedimentary Belt in Quebec(1089- 1083 Ma; Corriveau et al., 1988).

In summary, precise dating continues to provide constraints (and surprises) that may require existing tectonic models to be modified or even abandoned. Although separated by nearly 200 km, the disparate paleotectonic environments seemingly implied by the nature of the rocks and events dated at ca. 1250 Ma, ca. 1170 Ma and ca. 1085 Ma must all be reconciled in any historical tectonic model applied either to individual terranes or to the southwestern-Grenville Province as a whole.

REFERENCES

Abdel-Rahman, A.M. and Martin, R.F.
1987: The Deloro anorogenic igneous complex, Madoc, Ontario. 1. Geochemistry and feldspar mineralogy of the felsic plutonic rocks; Canadian Mineralogist, v. 25, p. 321-336.

Bell, K. and Blenkinsop, J.
1980: Whole rock Rb-Sr studies in the Grenville Province of southeastern Ontario and western Quebec - a summary report; *in* Current Research, Part C, Geological Survey of Canada, Paper 80-1C, p. 152-154.

Carmichael, D.M., Moore, J.M., Jr., and Skippen, G.B.
1978: Isograds around the Hastings metamorphic "low", *in* Toronto '78, Field Trips Guidebook, ed. A.L. Currie, and W.O. Mackasey; Geological Association of Canada, p. 325-346.

Corriveau, L., Gorton, M., Heaman, L., and van Breemen, O.
1988: Late Precambrian potassic plutons in the CMB of theGrenville Province: a petrographic, geochemical and isotopic preview; Geological Association of Canada, Program with Abstracts, v. 13, p. A26.

Davidson, A.
1986: New interpretations in the southwestern Grenville Province; *in* The Grenville Province; ed. J.M. Moore, A. Davidson, and A.J. Baer; Geological Association of Canada, Special Paper 31, p. 61-74.

Davidson, A. and van Breemen, O.
— Baddeleyite-zircon relationships in coronitic metagabbro, Grenville Province, Ontario; implications for geochronology; Contributions to Mineralogy and Petrology (in press).

Easton, R.M.
1986: Geochronology of the Grenville Province; *in* The Grenville Province; ed. J.M. Moore, A. Davidson and A.J. Baer; Geological Association of Canada, Special Paper 31, p. 127-173.

Gebauer, D. and Grünenfelder, M.
1976: U-Pb zircon and Rb-Sr whole rock dating of low grade metasediments: Montagne Noire; Contributions to Mineralogy and Petrology, v. 59, p. 13-32.

Hayatsu, A. and Palmer, H.C.
1975: A K-Ar isochron study of the Tudor gabbro, Grenville Province, Ontario; Earth and Planetary Science Letters, v. 25, p. 208-212.

Heaman, L.M., Davis, D.W., Krogh, T.E., and Lumbers, S.B.
1987: Geological evolution of the Central Metasedimentary Belt (CMB), Ontario: a U-Pb perspective; Geological Association of Canada, Program with Abstracts, v. 12, p. 54.

Heaman, L.M., Lumbers, S.B., and Vertolli, V.
1988: The timing of carbonatite emplacement within the CMB, Ontario; Friends of the Grenville, Grenville Workshop 1988, Program with Abstracts, p. 11.

Heaman, L.M., McNutt, R.H., and Krogh, T.E.
1986: Geological significance of U-Pb and Rb-Sr ages for two pretectonic granites from the Central Metasedimentary Belt, Ontario; *in* The Grenville Province; ed. J.M. Moore, A. Davidson and A.J. Baer; Geological Association of Canada, Special Paper 31, p. 209-221.

Heaman, L.M., Shieh, Y.-N., McNutt, R.H., and Shaw, D.M.
1982: Isotopic and trace element study of the Loon Lake pluton, Grenville Province, Ontario; Canadian Journal of Earth Sciences, v. 19, p. 1045-1054.

Krogh, T.E. and Hurley, P.M.
1968: Strontium isotope variations and whole rock isochron studies in the Grenville Province of Ontario; Journal of Geophysical Research, v. 73, p. 7107-7125.

Marcantonio, F., Dickin, A.P., Heaman, L.M., and McNutt, R.H.
1988: The geochronology and isotope geochemistry of granites from the Westport - Gananoque area in the Grenville Province of Ontario; Friends of the Grenville, Grenville Workshop 1988, Program and Abstracts, p. 14.

Moore, J.M, Jr. and Thompson, P.H.
1980: The Flinton Group: a late Precambrian metasedimentary succession in the Grenville Province of eastern Ontario; Canadian Journal of Earth Sciences, v. 17, p. 1685-1707.

Parrish, R.R., Roddick, J.C., Loveridge, W.D., and Sullivan, R.W.
1987: Uranium-lead analytical techniques at the geochronology laboratory, Geological Survey of Canada; *in* Radiogenic Age and Isotopic Studies: Report 1; Geological Survey of Canada, Paper 87-2, p. 3-7.

Pupin J.P.
1980: Zircon and granite petrology; Contributions to Mineralogy and Petrology, v. 73, p. 207-220.

Shieh, Y.-N.
1985: High ^{18}O granitic plutons from the Frontenac Axis, Grenville Province of Ontario, Canada; Geochimica et Cosmochimica Acta, v. 49, p. 117-123.

van Breemen, O. and Hanmer, S.
1986: Zircon morphology and U-Pb geochronology in active shear zones: studies on syntectonic intrusions along the northwest boundary of the Central Metasedimentary Belt, Grenville Province, Ontario; *in* Current Research, Part B, Geological Survey of Canada, Paper 86-1B, p. 775-784.

van Breemen, O., Davidson, A., and Corriveau, L.
1988: Recent U-Pb dating, southwestern Grenville Province; Friends of the Grenville Workshop 1988, Program and Abstracts, p. 17.

van Breemen, O., Davidson, A., Loveridge, W.D., and Sullivan, R.W.
1986: U-Pb zircon geochronology of Grenville tectonites, granulites and igneous precursors, Parry Sound, Ontario; *in* The Grenville Province, ed. J.M. Moore, A. Davidson and A.J. Baer; Geological Association of Canada, Special Paper 31, p. 191-207.

Wanless, R.K. and Loveridge, W.D.
1972: Rubidium-strontium isochron age studies, report 1; Geological Survey of Canada, Paper 72-23, 77 p.

Windley, B.F.
1986: Comparative tectonics of the western Grenville and the western Himalaya; *in* The Grenville Province, ed. J.M. Moore, A. Davidson and A.J. Baer; Geological Association of Canada, Special Paper 31, p. 341-348.

Wynne-Edwards, H.R.
1962: Gananoque area, Ontario; Geological Survey of Canada, Map 27-1962.
1963: Brockville-Mallorytown area, Ontario; Geological Survey of Canada, Map 7-1963.
1967: Westport map-area, Ontario, with special emphasis on the Precambrian rocks; Geological Survey of Canada, Memoir 346, 142 p.

York, D.
1969: Least squares fitting of a straight line with correlated errors; Earth and Planetary Science Letters, v. 5, p. 320-324.

Two U-Pb zircon ages from eastern Glennie Lake Domain, Trans-Hudson Orogen, Saskatchewan

G. Delaney[1], S.D. Carr[2], and R.R. Parrish[3]

Delaney, G., Carr, S.D., and Parrish, R.R., Two U-Pb zircon ages from eastern Glennie Lake Domain, Trans-Hudson Orogen, Saskatchewan, in Radiogenic Age and Isotopic Studies: Report 2, Geological Survey of Canada, Paper 88-2, p. 51-58, 1988

Abstract

Within the eastern Glennie Lake Domain of the Trans Hudson Orogen of Saskatchewan, the Wood Lake batholith intrudes metavolcanic and meta-arkosic rocks of the Pine Lake and Ourom Lake sequences. The climax of deformation and metamorphism in the area postdates all of these units, but predates 1836+/-7 Ma.

Detrital zircon grains from the Ourom Lake meta-arkose are 1850 to 1863 Ma old, as demonstrated by nearly concordant analyses on single abraded grains. From zircon geochronology the Wood Lake batholith is constrained to be 1850 +1/-2 Ma old.

The synvolcanic arkosic rocks are thus 1850 Ma old, and together with metavolcanic rocks represent a younger cycle of volcanism and molasse type sedimentation than previously recognized. Deformation and metamorphism in the region followed closely at about 1840 Ma.

Résumé

Dans l'est du domaine de Glennie Lake de l'orogène Transhudsonnien en Saskatchewan, le batholithe de Wood Lake recoupe les roches métavolcaniques et méta-arkosiques des séquences de Pine Lake et d'Ourom Lake. Le point culminant de la déformation et du métamosphisme dans cette région est postérieur à la formation de ces unités mais antérieur à 1836+/−7 Ma.

L'âge des grains détritiques de zircon dans l'arkose métamorphisée d'Ourom Lake varie de 1850 à 1863 Ma, tel que révélé par des analyses presque concordantes de grains uniques usés par frottement. En se fondant sur la géochronologie des zircons, l'âge du batholithe de Wood Lake est fixé à 1850 +1/−2 Ma.

Les arkoses synvolcaniques ont par conséquent 1850 Ma et représentent, avec les roches métavolcaniques, un cycle de volcanisme et de sédimentation molassique plus récent que celui qui avait auparavant été établi. La déformation et le métamorphisme de cette région se sont succédés de près, il y a environ 1840 Ma.

INTRODUCTION

The Glennie Lake Domain (GLD) lies between the Kisseynew gneiss belt and the La Ronge Domain and Maclean Lake Belt of the Trans Hudson Orogen (Fig. 1). This enigmatic region (GLD) comprises predominantly granitoid rocks (uncoloured on Figure 1) with narrow belts of metavolcanic and metasedimentary rocks (*see* Fig. 1 for their terminology). The GLD has been interpreted as the remnant of one or more Lower Proterozoic arc terranes which, together with minor incorporated Archean gneiss, collided with the adjacent La Ronge Domain (Lewry, 1981; Lewry et al., 1987; Chiarenzelli et al., 1987; Chiarenzelli and Lewry 1988), and was in part overthrust by it.

This paper reports on U-Pb zircon age determinations from the Ourom Lake meta-arkose and the Wood Lake batholith in the eastern part of the Glennie Lake Domain (Locales 1 and 2, Fig. 2). The Wood Lake batholith intrudes part of the Pine Lake greenstone belt. It is deformed and metamorphosed and its age places constraints on at least part of the tectonic history within the GLD.

Relationships between belts of metasedimentary rocks in this part of the Trans-Hudson Orogen are uncertain. A general correlation has been made for a semi-continuous belt of meta-arkose that extends from the Bing Lake area of the La Ronge Belt (Padgham, 1960, 1963; Lewry, 1983; Macdonald and Broughton, 1980; Thomas, 1987) across the

[1] Saskatchewan Energy and Mines, 1914 Hamilton Street, Regina, Saskatchewan, S4P 4V4
[2] Department of Earth Sciences, Ottawa-Carleton Geoscience Centre, Carleton University, Ottawa, Ontario, K1S 5B6
[3] Geological Survey of Canada, 601 Booth Street, Ottawa, Ontario K1A 0E8

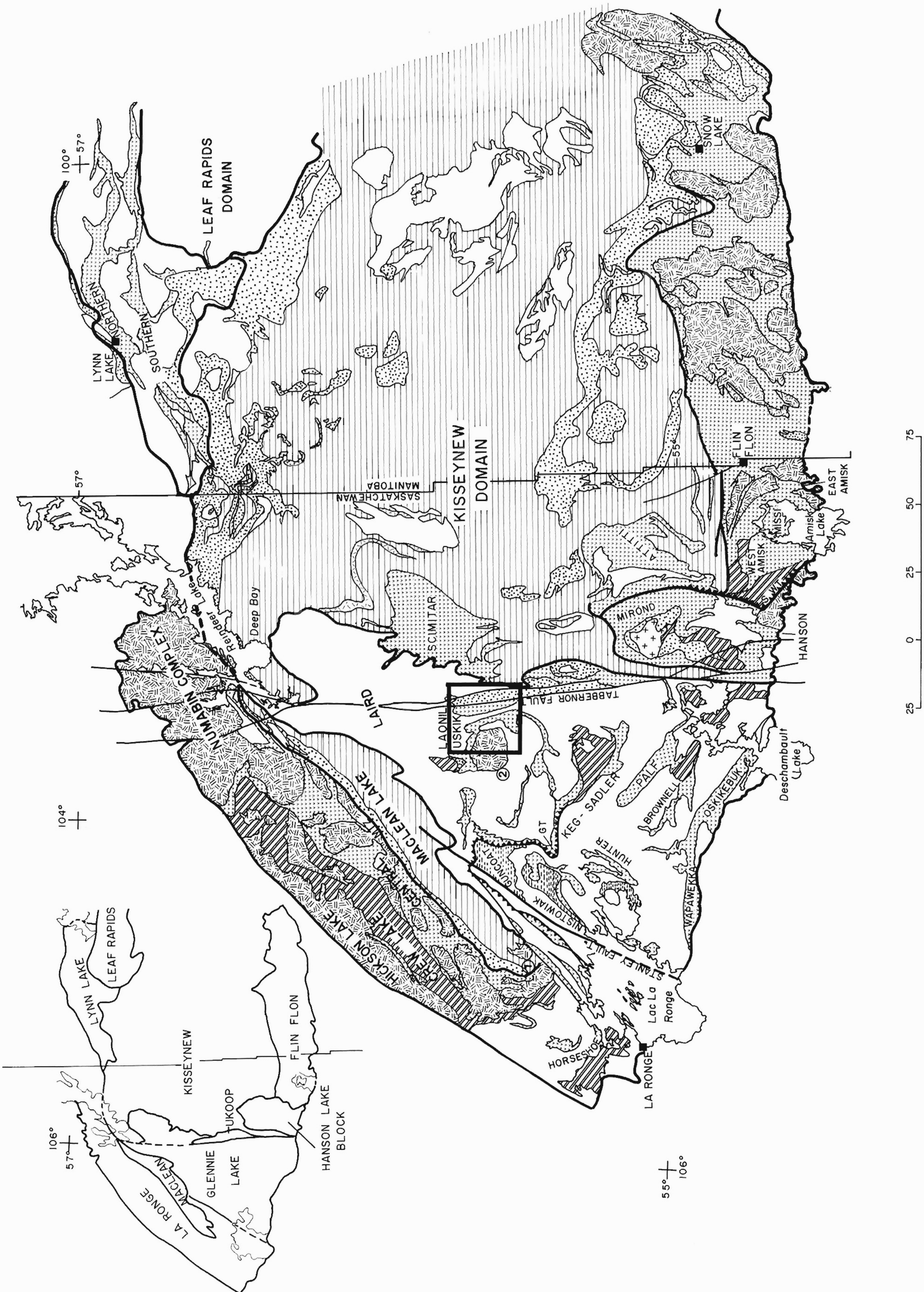
LEAF RAPIDS DOMAIN
LYNN LAKE
NORTHERN
SOUTHERN
KISSEYNEW DOMAIN
SASKATCHEWAN
MANITOBA
SNOW LAKE
FLIN FLON
EAST AMISK
WEST AMISK
MISSI
Amisk Lake
MIROND
HANSON
SCIMITAR
Deep Bay
Reindeer Lake
NUMABIN COMPLEX
LAIRD
LAONIL
USKIK
TABBERNOR FAULT
KEG - SADLER
PALF
BROWNELL
OSKIKEBUK
Deschambault Lake
WAPAWEKKA
HUNTER
NISTOWIAK
GUNCOAT
GT
STANLEY FAULT
Lac La Ronge
HORSESHOE
LA RONGE
MACLEAN LAKE
CENTRAL
CREW LAKE
HICKSON LAKE
100° 57°
57°
55°
104°
55° 106°
Kilometres
25 0 25 50 75
106° 57°
LA RONGE
MACLEAN
GLENNIE LAKE
TUKOOP
HANSON LAKE BLOCK
KISSEYNEW
FLIN FLON
LYNN LAKE
LEAF RAPIDS

Figure 1. Map of the Reindeer Lake Zone, Manitoba and Saskatchewan modified from Saskatchewan Geological Survey (1987), Manitoba Energy and Mines (1986), and Geological Survey of Canada and Manitoba Mineral Division (1987). Numbered locations: 1. Bing Lake 2. Eyahpaise Lake Pluton. Domains/subdomains: Kisseynew = Kisseynew Domain; MacLean Lake = Maclean Lake Belt; Glennie Lake = Glennie Lake Domain; Ukoop = Ukoop Lake Segment; LaRonge = LaRonge Domain; Crew Lake = Crew Lake Belt; Hickson Lake = Hickson Lake Pluton; Numabin Complex; Horseshoe = La Ronge Horseshoe terrane; Laird = Laird Lake Complex; Lynn Lake = Lynn Lake Domain; Leaf Rapids = Leaf Rapids Domain; Flin Flon = Flin Flon Domain; Greenstone belts: Central = Central Metavolcanic Belt; Guncoat; Hunter = Hunter Bay; Wapawekka-Oskikebuk; Brownell = Brownell Lake; Palf = Palf Lake; Keg-Sadler = Keg Sadler Lakes; Laonil-Uskik = Laonil-Uskik Lakes, Hanson = Hanson Lake Volcanics; Northern = Lynn Lake Northern Belt; Southern = Lynn Lake Southern Belt; Flin Flon greenstone regions: West Amisk; Missi (Island); East Amisk. Hornblendic gneiss complexes (volcanogenic): Scimitar = Scimitar Lake Complex; Attitti = Attitti Lake Complex; Sandy = Sandy Narrows; Mirond = Mirond Lake. Shear zones or thrusts: MTZ = McLennan Lake Tectonic Zone; S-WT = Sturgeon Weir Thrust; GT = Guncoat Thrust. Box shows location of Figure 2.

LOWER PROTEROZOIC

- Kisseynew-type metagreywacke/paragneiss including: quartzofeldspathic garnet-biotite gneiss, amphibolite, quartz-feldspar-rich gneiss, metaconglomerate, migmatite
- Metagreywacke (other domains): generally biotite gneiss, atypically garnetiferous
- Greenstone belts: hornblende gneiss, migmatite, metavolcanic rocks
- Meta-arkose, metaconglomerate, pelitic metasedimentary rocks
- Felsic granitoid pluton
- Felsic granitoid terrane (undivided)
- Enderbite sills (Harriot Lake area)
- Mylonitic gneiss (Guncoat and Nistoiak type)

ARCHEAN

- Charnockitic granite
- Domain boundary
- Major fault or shear zone
- Thrust zone

northern part of the Kisseynew Domain (Gilboy, 1980) to the Lynn Lake greenstone belt (Gilbert et al., 1980; Manitoba Energy and Mines, 1986; Zwanzig, 1976; 1977). This belt includes the McLennan Group of the La Ronge Domain and the Sickle Group of the Kisseynew Domain and Lynn Lake greenstone belt (Lewry, 1983). Discrete bodies of meta-arkose in the GLD (Fig. 2) are similar to the Sickle Group and the two groups of sediments are probably correlative. In the GLD, although most meta-arkosic rocks overlie greenstone assemblages,some are intercalated with greenstone. The Ourom Lake meta-arkose (Fig. 2) is intercalated with the Pine Lake metavolcanic rocks (Budding and Kirkland, 1956; Delaney, 1987), and the age of their detrital zircons places constraints on the age and source of the volcanic and sedimentary rocks.

GEOLOGY OF THE EASTERN GLENNIE LAKE DOMAIN

The east-central part of the Glennie Lake Domain is underlain by supracrustal and granitoid rocks (Fig. 2) and is cut by a segment of the major sinistral north-northwest-trending Tabbernor Lake Fault. West of the Tabbernor Lake Fault, two north-northwest-trending belts of the Pine Lake metavolcanic rocks flank paragneiss and subordinate migmatite. To the east of the fault and west of the Reindeer River is a narrow belt of metavolcanics. They are mostly fine grained volcaniclastic rocks with subordinate intermediate and mafic volcanics, and have been subjected to amphibolite facies metamorphism.

The Ourom Lake meta-arkose, a thick sequence that includes conglomerate and conglomeratic facies, is mostly on the east side of the Tabbernor Lake Fault. Near the fault, primary structures are preserved; farther east, metamorphic grade increases and gneiss, migmatite and granitoid rocks predominate. On the west side of the Tabbernor Lake Fault (Delaney, 1987) some relatively thin sequences of meta-arkose that are similar to, and are correlated with, the Ourom Lake meta-arkose are intercalated with volcaniclastic rocks. Farther to the south basic intrusive and metavolcanic rocks are intercalated within, and overlie, the arkoses (Kirkland, 1957, 1976). This association is distinct from the McLennan-Sickle arkoses which unconformably to rarely conformably overlie metavolcanic assemblages. These relationships are interpreted to indicate that deposition of the Ourom Lake meta-arkoses overlapped the waning stages of Pine Lake volcanism.

Structural relationships in the supracrustal rocks define at least three folding episodes. F1 folds form a series of large-scale north-northwest to north-trending asymmetrical to isoclinal antiforms and synforms. S1, a prominent bedding — parallel foliation and gneissosity, is well developed throughout much of the area. F2 folds are defined by a strong crenulation cleavage that is most common in the hinges of small-scale asymmetrical folds. These structures are most abundant in the area flanking the Tabbernor Lake Fault. Although predominantly northeast-trending, orientations are somewhat variable. Evidence of a third folding event was only observed east of the Tabbernor Lake Fault, near Ourom Lake, where an east-southeast-trending cleavage (S3) cuts both the bedding parallel S1 foliation and the S2 crenulation cleavage. In this area the Tabbernor Lake Fault does not appear to display significant lateral movement, although it is a major topographic lineament.

Granitoid rocks of the area vary in composition and geological setting (Fig. 2). Leucocratic granodiorite and granodiorite gneiss northeast of the Ourom Lake meta-arkose is interpreted to be derived from supracrustal rocks. Granitic rocks in the Eisler Lake area are cut by the gabbroic Eisler Lake intrusion. The late tonalitic Eyahpaise Lake pluton which underlies the region southeast of Eisler Lake is intruded by younger zoned granodiorite. The northern end of the granodioritic Wood Lake batholith intrudes the Pine Lake metavolcanics in the Uskik Lake area.

More discrete intrusive bodies underlie the southwest part of the eastern Glennie Lake Domain (Fig. 2). Early phases include quartz monzonite and granodiorite ("X" pattern, Fig. 2). These are intruded by granitic ("+" pattern, Fig. 2) and gabbroic rocks in the Eisler and Uskik Lake areas, and are interpreted to be post-volcanic but pre-tectonic. This suite includes the Wood Lake granodiorite. The youngest plutonic rocks are post-tectonic granodiorite west of Eisler Lake.

The second sample for U-Pb age determination reported in this paper is from the northern end of the Wood Lake batholith (Kirkland, 1976), a variably foliated hornblende-biotite granodiorite (Locale 2, Fig. 2). The batholith is a N-S elongate body about 58 km long and 13-16 km wide. Although the pluton has been deformed and metamorphosed, it is interpreted to be post- Pine Lake volcanism, but it probably pre-dates a number of other dated mafic to intermediate intrusions in the GLD. Its age should place constraints on the age of volcanism and plutonism in the area.

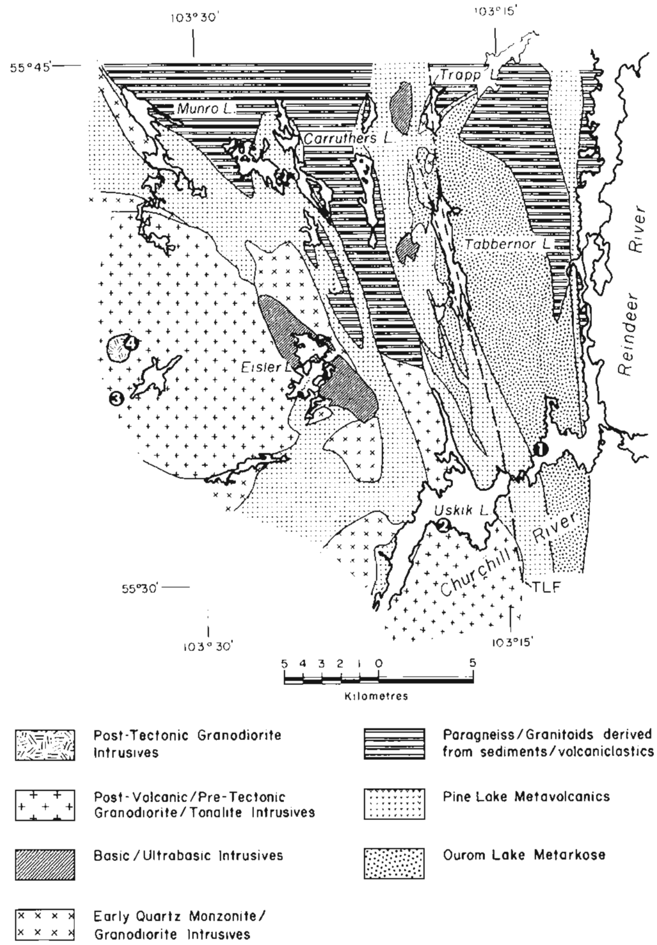

Figure 2. Map of the Carruthers — Uskik Lakes area, eastern Glennie Lake Domain. TLF = Tabbernor Lake Fault. Numbers correspond with sample locales as follows: 1. Ourom Lake meta-arkose, sample 8722-439; 2. Wood Lake granodiorite, sample 8722-438; 3. Eyahpaise Lake pluton, sample HUD83-13 (Bickford et al., 1986); 4. Late pluton that cuts HUD83-13, sample HUD83-14 (Bickford et al., 1986)

PREVIOUS GEOCHRONOLOGY

Seven samples from the Glennie Lake Domain were analyzed in a reconnaissance U-Pb dating program (Van Schmus and Bickford, 1984; Bickford and Van Schmus, 1985; Van Schmus et al., 1987), and the data, summarized in Table 1, include two units from the study area, the Eyahpaise Lake Pluton and a later phase which intrudes it (HUD83-13 and 14, locales 3 and 4 of Fig. 2). Within the limits of error, all of these data except the late pluton which cuts the Eyahpaise Lake pluton (locale 4, Figure 2) are at least 1845 Ma old, ranging from 1836±7 Ma to over 1880 Ma.

U-Pb ZIRCON GEOCHRONOLOGY

Analytical methods

U-Pb analytical methods follow those outlined in Parrish et al. (1987). Techniques utilized strong air abrasion on all zircon fractions and crystals (Krogh, 1982), dissolution in microcapsules (Parrish 1987), a mixed ^{205}Pb-^{233}U-^{235}U isotopic tracer (Parrish and Krogh, 1987), multicollector mass spectrometry (Roddick et al., 1987), and assessment of errors by numerical error propagation (Roddick, 1987). Individual zircon crystals were analyzed for the meta-arkose to ensure that each analysis represented a unique age and not a mixture of several ages. U and Pb blanks were 1 and 6 pg, respectively, except for analysis 6, which was assigned a larger blank (90 pg) as a result of handling problems. Errors on Figures 3 and 4 are shown as two standard errors. Common lead corrections were uniformly very low and compositions assumed were those given by 1850 Ma Stacey and Kramers (1975) model lead. The linear regression procedure is outlined in Parrish et al. (1987).

For the detrital zircon single grain analyses, the ages accepted as geologically meaningful are the $^{207}Pb/^{206}Pb$ ages, because all of the analyses except one are less than 1 % discordant. However, the $^{207}Pb/^{206}Pb$ age is a minimum for non-concordant analyses because the pattern of discordance cannot be determined.

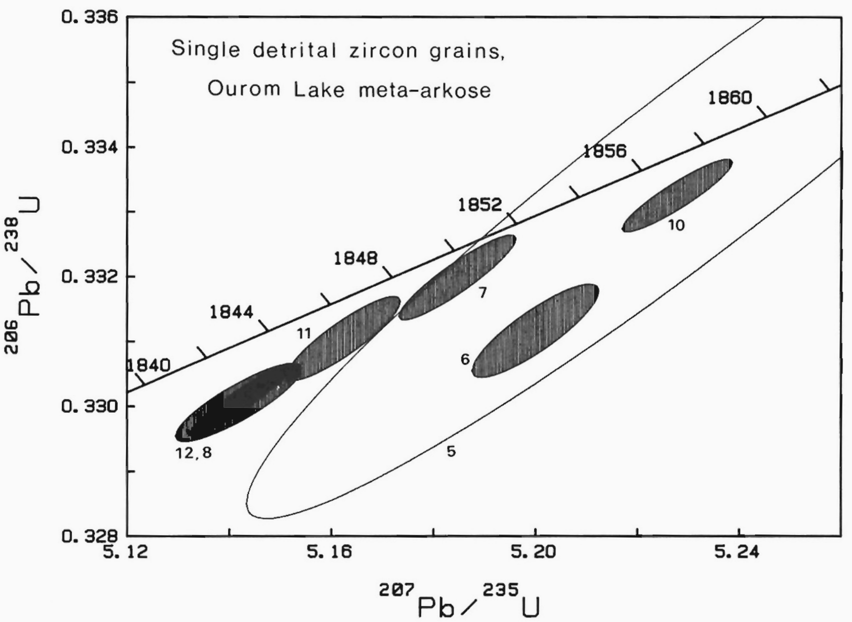

Figure 3. U-Pb concordia diagram for 7 out of 8 detrital zircons from Ourom Lake meta-arkose (sample 8722-439). Analysis 9 is significantly discordant and does not plot on the figure but is listed in Table 1. Analyses 6, 7, 8, 11, and 12 are also shown on Figure 4. The range in ages of the zircons is estimated as ca. 1850-1852 Ma for analyses 7, 8, 11, and 12 and 1858-1863 Ma for analyses 5, 6, and 10. Inspection of Figure 4 shows that it is likely that all detrital of zircons exceed the age of zircons from the Wood Lake batholith, but by as little as 1 Ma.

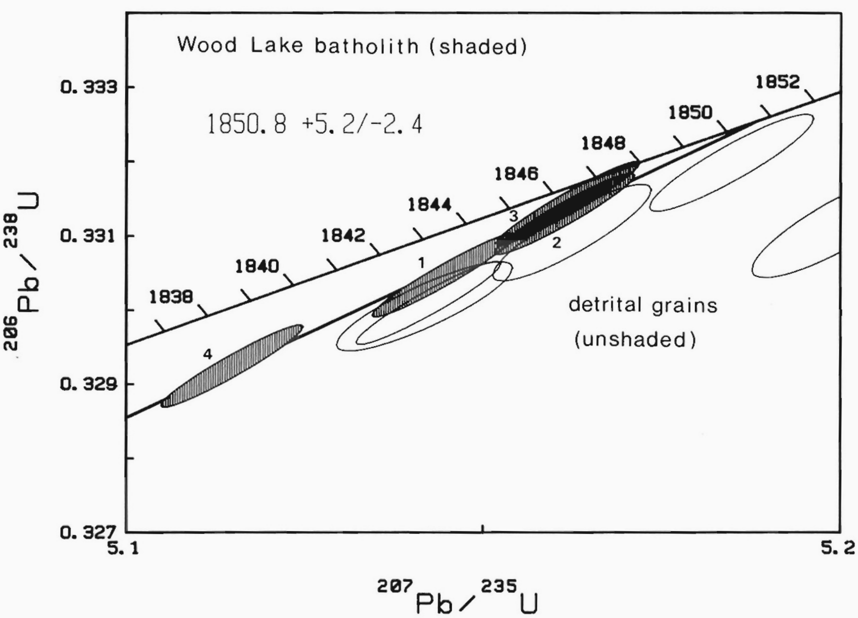

Figure 4. U-Pb concordia diagram for zircons of Wood Lake batholith (sample 8722-438). Shaded ellipses show data for Wood Lake batholith, while unshaded ones represent the youngest single detrital zircon analyses from the Ourom Lake meta-arkose. Errors are drawn to represent two standard errors. Numbers refer to fractions in Table 1.

Table 1. Summary of U-Pb age dates, Glennie Lake Domain.

Sample	Unit	Age (Ma)
HUD83-61	Carroll Lake gneiss	1893+/-35
HUD83-71	Palf Lake metarhyolite	1881+/- 6
HUD83-111	Deschambault Narrows tonalite	1850+/- 4
HUD83-121	Wykes Lake Pluton (gdr)	1850+/- 9
HUD83-131	Eyahpaise Lake Pluton	1859+/- 5
HUD83-141	Late Pluton; cuts HUD83-13	1836+/- 7
HUD83-161	"Older gneiss"; = Eyahpaise?	1852+/-12
8722-4383	Wood Lake batholith	1850+1/-2*
8722-4393	Ourom Lake meta-arkose, detrital zircons	1850-1863*
Sources: Van Schmus et al. (1987); this study*.		

Ourom Lake meta-arkose (sample 8722-439)

The sample chosen was a thin — to medium — bedded buff-weathering meta-arkose; it is described in detail in Appendix 1. Of the detrital zircons extraced from the meta-arkose sample, eight high quality crystals of various morphologies were selected and abraded. Neither overgrowths nor internal cores were observed, and the grains were homogeneous. Some had crystal faces with subrounded ends (fractions 6, 7 and 8) whereas the others were moderately rounded.

All analyses, excepting grain 10 which had high U content, are plotted on Figure 3 and in part on Figure 4. Pb-Pb ages of grains range from 1848 to 1862 Ma with individual errors of 1.2 to 2.3 Ma (except analysis 6). There

Table 2. U-Pb Analytical data

Analysis #, size[a]	wt[b] (mg)	U, ppm	Pb,[c] ppm	$^{206}Pb^{d}/^{204}Pb$	Pb[e] (pg)	$^{208}Pb^{c}$ %	$^{206}Pb/^{238}U$, ±1SEM[f]	$^{207}Pb/^{235}U$ ±1SEM %[f]	$^{207}Pb/^{206}Pb$ +1SEM %[f]	$^{207}Pb/^{206}Pb$, age,error Ma[g]
Granodiorite sample 8722-438, south shore of Uskik Lake										
1:cl,abr,+149	0.0282	152.1	52.22	12370	7	7.9	0.3305 (.09)	5.145 (.10)	0.1129 (.03)	1846.7 (1.0)
2:cl,abr,+149	0.0181	180.8	62.28	8774	8	7.9	0.3313 (.08)	5.161 (.10)	0.1130 (.03)	1848.1 (1.1)
3:cl,abr,+149	0.0264	234.4	80.38	13730	9	7.5	0.3314 (.09)	5.162 (.10)	0.1130 (.03)	1847.5 (1.0)
4:cl,abr,+105	0.0337	89.83	30.48	7671	8	7.1	0.3292 (.09)	5.115 (.10)	0.1127 (.03)	1842.9 (1.1)
Ourom Lake Meta-arkose sample 8722-439										
6:cl,abr,+149	0.0044	108.6	37.52	128	92	7.5	0.3336 (.80)	5.230 (.83)	0.1137 (.27)	1859.6 (8.9)
7:cl,abr,+149	0.0076	83.8	28.36	1875	7	6.3	0.3312 (.11)	5.200 (.12)	0.1139 (.06)	1862.3 (2.3)
8:cl,abr,+149	0.0029	210.2	73.54	1822	7	9.1	0.3320 (.10)	5.185 (.11)	0.1133 (.05)	1852.5 (1.6)
9:cl,abr,+149	0.0083	239.9	84.01	5295	8	9.7	0.3301 (.09)	5.142 (.10)	0.1130 (.03)	1847.9 (1.2)
10:cl,abr,+149	0.0079	571.1	170.50	5171	17	3.3	0.3031 (.09)	4.513 (.10)	0.1080 (.03)	1765.5 (1.2)
11:cl,abr,+149	0.0179	85.0	28.45	2443	13	4.7	0.3332 (.09)	5.228 (.10)	0.1138 (.04)	1860.6 (1.6)
14:cl,abr,+105	0.0067	122.2	42.74	2379	7	9.4	0.3310 (.10)	5.162 (.10)	0.1131 (.05)	1849.8 (1.8)
16:cl,abr,+105	0.0080	109.5	38.13	1366	14	9.3	0.3301 (.09)	5.142 (.12)	0.1130 (.06)	1848.0 (2.3)

[a]cl=clear, abr=abraded, sizes (i.e. +149, +105) refer to average size of zircons in microns.
[b]weighing error 0.002 mg.
[c]radiogenic Pb.
[d]measured ratio, corrected for spike and fractionation.
[e]total common Pb in analysis corrected for fractionation and spike.
[f]corrected for blank Pb and U, common Pb, errors quoted are 1 standard error of the mean in percent.
[g]corrected for blank and common Pb, errors quoted are 2 standard error of the mean in Ma.

is no apparent correlation between the crystal morphology and age. Analysis 10 is much more discordant, has higher U content, and is not used in the discussion of data. The zircons have a tightly defined age span (1.85-1.86 Ga) and were likely derived from a volcanic-plutonic source. The age of the arkose must be no older than about 1850 Ma since zircons of this age occur as detrital grains in the sediment.

Wood Lake granodiorite (sample 8722-438)

The Wood Lake granodiorite is a medium grained, buff- to light grey weathering, leucocratic granodiorite with rare amphibolitic xenoliths, aligned with the weak to moderate foliation of the granodiorite (*see* Appendix 1).

Zircons in the granodiorite are typical of igneous crystals; they are euhedral and range in shape from stubby to needle-shaped. There were no visible cores. The highest quality clear crystals were chosen and abraded to remove any possible overgrowths (none observed) and to minimize surface correlated Pb-loss.

Four fractions are nearly concordant and yield an upper intercept age of 1850.8 +5.2/-2.4 Ma (modified York II regression, Fig. 4). Considering the data from the meta-arkose previously presented and the pattern of analyses presented on Figure 4 which show that the detrital zircons are consistently older than the batholith, we interpret the age of the batholith as 1850 +1/-2 Ma.

DISCUSSION

The 1850 Ma Wood Lake granodiorite intrudes the Pine Lake metavolcanic rocks and by inference the related synchronous meta-arkose of the Ourom Lake sequence. Therefore the stratified rocks must be 1850 ±1 Ma old because they also contain detrital zircons of essentially the same (1850 Ma) age. It seems most reasonable to view the arkose as having been derived from relatively nearby 1.85-1.86 Ga volcanic-plutonic rocks in a synvolcanic setting. The only uncertainty in this assertion is the fact that the sample of arkose is separated from the Wood Lake batholith by the Tabbernor Lake fault, and it may not necessarily be exactly the same sequence as that intruded by the dated Wood Lake batholith.

Because the arkose is intercalated with the Pine Lake metavolcanic rocks, they must also be essentially the same (1.85 Ga) age, and are thus younger than other 1.87-1.89 Ga volcanic rocks of the region (Van Schmus and Bickford, 1987). These volcanic and sedimentary rocks thus represent a second cycle of volcanism and sedimentation prior to the climax of deformation and metamorphism which affected both of the rock units dated in this study.

Structural relationships when integrated with U-Pb dates presented in this study, indicate that folding events recognized in these rocks occurred after 1850 Ma but before post-kinematic plutonism at about 1836 ±7 Ma.

Field relationships were interpreted to indicate that the Wood Lake batholith, although younger than the Pine Lake metavolcanic rocks, represented an intrusive episode earlier than that which emplaced the 1859 ±5 Ma Eyahpaise Lake pluton (Table 1). The U-Pb zircon ages, however, contradict this conclusion. Instead, the data suggest that some sedimentary-volcanic sequences are younger than older plutons, and that contact relations may not all be intrusive. The 1850 Ma Wood Lake batholith would appear to represent a terminal phase in the major episode of plutonism which occurred in the Trans-Hudson Orogen between 1870-1850 Ma ago. Furthermore, this episode of plutonism appears to have been coeval with the waning stages of late volcanism and concomitant molasse-type sedimentation. Climactic deformation and metamorphism of this part of the Trans-Hudson Orogen is thus about 1.84 Ga old.

The Ourom Lake arkosic and related metavolcanic rocks represent a second cycle of depositional events following earlier volcanism and plutonism. If they are correlative with theMcLennon-Sickle arkoses to the northeast in the Lynn Lake area, then it can be inferred that the second cycle rocks young to the southeast, since the lithologically similar second cycle Missi Group in the Flin Flon belt are 1832 ±2 Ma old (Gordon et al., 1987). If these correlations are correct, it would appear that accretion and related deformation of arc terranes progressed from north to south toward the Superior craton.

ACKNOWLEDGMENTS

We particularly thank Klaus Santowski and Dale Loveridge for performing the mass spectrometry.

REFERENCES

Bickford, M.E. and Van Schmus, W.R.
1985: Preliminary U-Pb age data for the Trans-Hudson Orogen in northern Saskatchewan: new and revised results; *in* Summary of Investigations 1985, Saskatchewan Geological Survey; Saskatchewan Energy Mines, Miscellaneous Report 85-4, p. 63-66.

Bickford, M.E., Van Schmus, W.R., Macdonald, R., Lewry, J.F., and Pearson, J.G.
1986: U-Pb zircon geochronology project for the Trans-Hudson Orogen: current sampling and recent results; *in* Summary of Investigations 1986, Saskatchewan Geological Survey; Saskatchewan Energy Mines, Miscellaneous Report 86-4, p. 101-107.

Budding, A.J. and Kirkland, S.J.T.
1956: The geology of the Reindeer River area; Saskatchewan Department of Mines and Resources, Report 22, 42p (reprinted 1987).

Chiarenzelli, J.R., Lewry, J.F., and Landon, M.
1987: Bedrock geology, Iskwatikan Lake area: evidence for Hudsonian juxtaposition of Proterozoic and Archean rocks along a ductile detachment surface; *in* Summary of Investigations 1987, Saskatchewan Geological Survey; Saskatchewan Energy Mines, Miscellaneous Report 87-4, p. 46-51.

Chiarenzelli, J. R. and J. F. Lewry
1988: The Nistowiak gneisses: evidence of a collisional suture in the Trans-Hudson Orogen, northern Saskatchewan; Program with abstracts, Geological Association of Canada, v. 13, p. A20.

Delaney, G.D.
1987: Bedrock geological mapping, Carruthers — Uskik Lakes area (part of NTS 63M-11 and -12); *in* Summary of Investigations 1987, Saskatchewan Geological Survey; Saskatchewan Energy Mines, Miscellaneous Report 87-4, p. 8-17.

Geological Survey of Canada, and Manitoba Minerals Division
1987: Geological Highway Map of Manitoba, 1987; Mineral Development Agreement Special Publication No. 1.

Gilbert, H.P., Syme, E.C., and Zwanzig, H.V.
1980: Geology of the metavolcanic and volcaniclastic metasedimentary rocks in the Lynn Lake area; Manitoba Department of Energy and Mines, Mineral Resources Division, Geology Pap 80-1, 118p.

Gilboy, C.F.
1980: Geology of the Reindeer Lake South (southeast) area; Saskatchewan Mineral Resources, Report 198, 62p.

Gordon, T.M., Hunt, P. A., Loveridge, W. D., Bailes, A.H., and Syme E.C.
1987: U-Pb zircon ages from the Flin Flon and Kisseynew belts, Manitoba: Chronology of Early Proterozoic crust formation; Geological Association of Canada, Program with Abstracts, v. 12, p. 48.

Kirkland, S.J.T.
1957: The geology of the Manawan Lake area (north half), Saskatchewan; Saskatchewan Department of Mineral Resources, Report 27, 22p.

1976: The geology of the Manawan Lake area (south half), Saskatchewan; Saskatchewan Department Mineral Resources, Report 175, 24p.

Krogh, T. E.
1982: Improved accuracy of U-Pb ages by the creation of more concordant systems using an air abrasion technique; Geochimica et Cosmochimica Acta, v. 46, p. 637-649.

Lewry, J.F.
1981: Lower Proterozoic arc-microcontinent collisional tectonics in the western Churchill Province; Nature, v. 294, no.5836, p. 69-72.

1983: Character and structural relations of the 'McLennan Group' meta-arkoses, McLennan-Jaysmith Lakes area; *in* Summary of Investigations 1983, Saskatchewan Geological Survey; Saskatchewan Energy and Mines, Miscellaneous Report 83-4, p. 49-55.

Lewry, J.F., Thomas, D.J., Macdonald, R., and Chiarenzelli, J.
1987: Structural relations in accreted terranes of the Trans-Hudson Orogen, Saskatchewan: telescoping in a collisional regime; Geological Association of Canada/Mineralogical Association Canada, Joint Annual Meeting, Saskatoon, May 1987, Program of with Abstracts, v. 12, p. 67, (abstract).

Macdonald, R. and Broughton, P.
1980: Geological map of Saskatchewan (provisional edition); Saskatchewan Mineral Resources, scale 1:1 000 000.

Manitoba Energy and Mines
1986: Bedrock geology compilation map series, Granville Lake, Manitoba Energy and Mines, Map NTS 64C, scale 1:250,000

Padgham, W.A.
1960: The geology of the Otter lake area (west half), Saskatchewan; Saskatchewan Department Mineral, Resources, Report 41, 34p.

1963: The geology of the Otter Lake area (east half), Saskatchewan; Saskatchewan Department of Mineral Resources, Report 56, 51p.

Parrish, R. R.
1987: An improved microcapsule for zircon dissolution in U-Pb geochronology; Chemical Geology (Isotope Geoscience Section), v. 66, p. 99-102.

Parrish, R. R. and T. E. Krogh
1987: Synthesis and purification of 205Pb for U-Pb geochronology; Chemical Geology (Isotope Geoscience Section), 66, p. 103-110.

Parrish, R. R., Roddick, J. C., Loveridge, W. D., and Sullivan, R. W.
1987: Uranium-lead analytical techniques at the geochronology laboratory, Geological Survey of Canada; *in* Radiogenic agt and Isotopic Studies: Report 1 Geological Survey of Canada, Paper 88-2, p. 3-7.

Roddick, J.C.
1987: Generalized numerical error analysis with applications to geochronology and thermodynamics; Geochimica et Cosmochimica Acta, v. 51, p. 2129-2135.

Roddick, J.C., W.D. Loveridge, and R.R. Parrish
1987: Precise U/Pb dating of zircon at the sub-nanogram Pb level, Chemical Geology (Isot. Geosc. Sect.), 66, 111-121.

Saskatchewan Geological Survey
1987: Saskatchewan's Mineral Industry: Past and Present; *in* CIM Directory, 1987, Canadian Institute of Mining and Metallurgy, v. 21, p. 67-114.

Stacey, J.S. and Kramers, J.D.
1975: Approximation of terrestrial lead isotope evolution by atwo stage model; Earth and Planetary Science letters, 26, p. 207-221.

Thomas, D.J.
1987: Bedrock geological mapping, Bing Lake area (part of NTS 73P-7 and -10); *in* Summary of Investigations 1987, Saskatchewan Geological Survey; Saskatchewan Energy and Mines, Miscellaneous Report 87-4, p. 18-27.

Van Schmus, W.R. and Bickford, M.E.
1984: Preliminary U-Pb age data for the Trans-Hudson Orogen in northern Saskatchewan; *in* Summary of Investigations 1984, Saskatchewan Geological Survey; Saskatchewan Energy and Mines, Miscellaneous Report 84-4, p. 81-85.

1987: Chronology of the Trans-Hudson Orogen in Saskatchewan and Manitoba; Geological Association of Canada/Mineralogical Association of Canada, Joint Annual Meeting, Saskatoon, May 1987, Program with Abstracts, p. 99, (abstract).

Van Schmus, W.R., Bickford, M.E., Lewry, J.F., and Macdonald, R.
1987: U-Pb zircon geochronology in the Trans-Hudson Orogen, northern Saskatchewan, Canada; Canadian Journal of Earth Sciences, v. 24, p. 407-424.

Zwanzig, H.V.
1976: Laurie Lake area (Fox Lake project); *in* Report of Field Activities 1976; Manitoba Department of Mines Natural Resources, and Environmental Management, Mineral Resources Division, p. 26-32.

1977: Geology of the Fox Mine area; *in* Report of Field Activities 1977; Manitoba Department of Mines, Natural Resources, and Environmental Management, Mineral Resources Division, p. 21-26.

APPENDIX 1. ROCK DESCRIPTIONS.

OUROM LAKE META-ARKOSE (SAMPLE 8722-439)

At the sample locality this unit comprises predominantly thin- to medium-bedded, buff-weathering meta-arkose. Minor variations in biotite and magnetite content accentuate primary structures which include parallel laminations, crossbedding, scour surfaces and rare slump horizons. These rocks display a prominent foliation (S1) which varies from bedding-parallel to slightly oblique to bedding. North of the sample locality, east of Tabbernor Lake, a crenulation cleavage (S2) is common in this unit.

The sample has a granoblastic mosaic of mainly equant quartz and feldspar grains which average approximately 0.35 mm in diameter. Parallel alignment of biotite defines a good foliation. Its composition is quartz (40 %), plagioclase (40 %), microcline (17 %), biotite (5 %), muscovite (0.2 %), magnetite (1 %) and zircon (.1 %).

WOOD LAKE GRANODIORITE (SAMPLE 8722-438)

The Wood Lake granodiorite is a medium grained, buff- to light-grey-weathering, leucocratic granodiorite with rare centimetre-size amphibolitic xenoliths. It is massive to weakly foliated in contrast to the well developed foliation present at the margin of the intrusive to the west of the sample site (Fig. 2).

The sample has a bimodal grain size with a mosaic of quartz and feldspar grains averaging 0.6 mm in diameter hosting medium grained subhedra of plagioclase, anhedra of consertal textured quartz, scattered anhedra of hornblende and rare euhedra to subhedra of sphene. Biotite is present both as disseminations and clots. The sample is composed of plagioclase (61 %), quartz (17 %), microcline (9 %), hornblende (9 %), biotite (3 %), sphene (0.70 %), magnetite (0.20 %) and apatite (0.05 %).

Geochronology of the Taltson Magmatic Zone and its eastern cratonic margin, District of Mackenzie

H.H. Bostock[1] and W.D. Loveridge[1]

Bostock, H.H., and Loveridge, W.D., Geochronology of the Taltson Magmatic Zone and its eastern cratonic margin, District of Mackenzie; in Radiogenic Age and Isotopic Studies: Report 2, Geological Survey of Canada, Paper 88-2, p. 59-65, 1988.

Abstract

Geology of the Taltson Magmatic Zone and the margin of the hinterland to the east is reviewed. U-Pb ages on zircon are presented for two plutons intruding the hinterland gneisses: a megacrystic monzogranite to the north, 2436 ± 12 Ma and an equigranular monzogranite to the east, 2334 + 22/-18 Ma. A $^{207}Pb/^{206}Pb$ age of 1906 + 3/-1 Ma on monazite is believed to date the Benna Thy monzogranite. Near concordant $^{207}Pb/^{206}Pb$ ages were obtained on monazite from three structural phases of the Konth syenogranite: northwest zone, 1935 + 3/−1 Ma; southwest zone, 1938 + 3/−1 Ma; east zone 1936 + 2/−1 Ma. Both the eastern part of the Konth batholith and the coeval Natael granite (dated previously at 1935 ± 3 Ma) have local sinistral shear fabrics indicating that at least part of the sinistral shear did not predate this plutonism. Conversely, the Benna Thy pluton shows only dextral shear; the provisional 1906 + 3/−1 Ma age provides both a minimum for sinistral shear and a maximum for the dextral shear at that location.

Résumé

La géologie de la zone magmatique de Taltson et de la bordure de l'arrière-pays dans l'est est analysée. Les âges déterminés par la méthode U-Pb appliquée aux zircons de deux plutons recoupant les gneiss d'arrière-pays sont présentés: un monzogranite à macrocristaux au nord évalué à 2436 ± 12 Ma et un monzogranite isogranulaire à l'est évalué à 2334 +22/−18 Ma. L'âge du monzogranite de Benna Thy serait de 1906 + 3/−1 Ma selon une datation établie par la méthode $^{207}Pb/^{206}Pb$ appliquée à la monazite. Des âges $^{207}Pb/^{206}Pb$ presque concordants ont été obtenus sur la monazite pour trois phases structurales de syénogranite de Konth: zone du nord-ouest, 1935 + 3/−1 Ma; zone du sud-ouest, 1938 + 3/−1 Ma; zone de l'est, 1936 + 2/−1 Ma. La partie est du batholite de Konth ainsi que le granite contemporain de Natael (daté antérieurement à 1935 ± 3 Ma) présentent par endroits des fabriques de cisaillement sénestre indiquant qu'au moins une partie du cisaillement sénestre n'est pas antérieure à ce plutomisme. Au contraire, le pluton de Benna Thy n'affiche qu'un cisaillement dextre; l'âge provisoire de 1906 +3/−1 Ma constitue un âge minimal pour le cisaillement sénestre et un âge maximal pour le cisaillement dextre à cet endroit.

INTRODUCTION

This paper provides an interim report on the ongoing geochronological studies of Precambrian rock units along the exposed west margin of the Churchill Province, southeast of Great Slave Lake Shear Zone. It incorporates a brief review of work reported elsewhere (Bostock et al., 1987) and presents new U-Pb zircon and monazite dates, and their interpretations as currently viewed.

GENERAL GEOLOGY

The exposed west margin of Churchill Province incorporates two major Precambrian geological regimes, a hinterland comprising rocks probably predominantly of Archean age to the east, and the early Proterozoic Taltson Magmatic Zone to the west.

The hinterland may be further subdivided into an eastern zone of relatively more brittle deformation within which the rocks are thought to be primarily Archean, and a western zone of relatively more ductile deformation within which the gneisses and plutonic rocks may be primarily of younger Archean-early Aphebian age. Thus the hinterland comprises two zones in which the style of late deformation is different and the proportions of the various lithologies are at least in some respects different. Current geochronology indicates that the western zone is primarily composed of Archean

[1] Geological Survey of Canada, 601 Booth Street, Ottawa, Ontario K1A 0E8

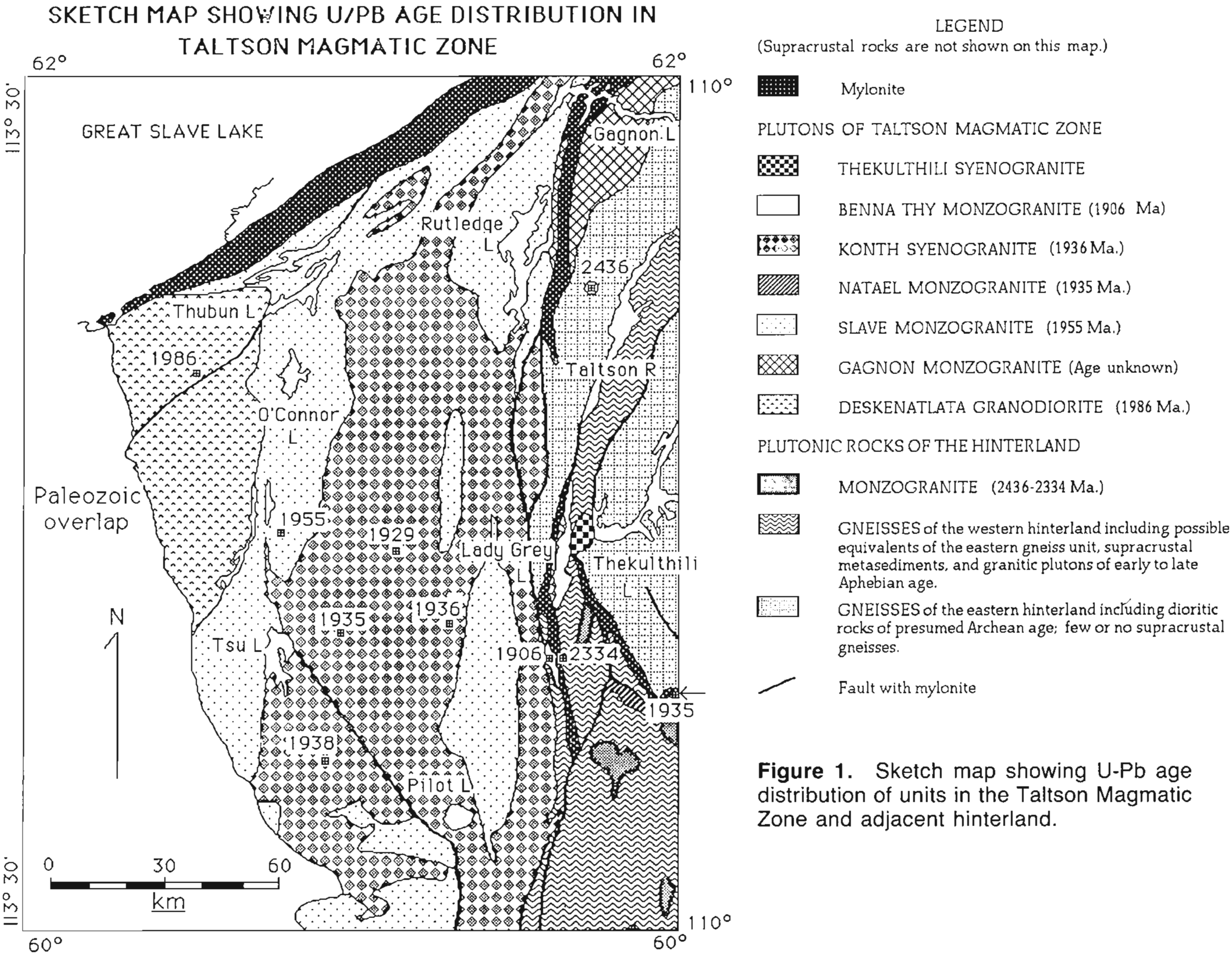

Figure 1. Sketch map showing U-Pb age distribution of units in the Taltson Magmatic Zone and adjacent hinterland.

rocks, supracrustal metasediments which may be of relatively early or late Archean age, and a greater proportion and variety of Aphebian granitic plutons. Remnants of two prograde Precambrian clastic sedimentary assemblages persist along the western margin of the eastern zone. The western zone is delimited on both sides by major faults and mylonite belts (Fig. 1).

The Taltson Magmatic Zone on the west comprises three major plutons. To the east an unknown number of minor granitic bodies are intruded mostly, so far as is known, within or at the margins of the western segment of the hinterland. Batholiths of the western Taltson Magmatic Zone progress from the oldest Deskenatlata granodiorite complex (1986.4 + 2.4/-2.0 Ma, Bostock et al., 1987) in the far northwest to the Slave monzogranite (1955 ± 2 Ma, Bostock et al., 1987) in the east. The latter is centrally intruded by the Konth syenogranite (ca. 1936 Ma, this study) whereas the coeval Natael monzogranite (1935 ± 3 Ma, Bostock et al., 1987) was intruded along the eastern fault margin of the western predominantly younger (late Archean-early Aphebian?) segment of the hinterland. The Gagnon monzogranite, in northeastern Taltson Magmatic Zone, is mineralogically more similar to Deskenatlata granodiorite than to either of the other two major plutons, but its relative age is currently unknown. A syenogranite stock at the southwest corner of Thekulthili Lake is probably at least as young as Konth syenogranite but it may be substantially younger.

The youngest granitic body so far recognized is the Benna Thy pluton, a small north- south elongate body of grey, medium grained, chlorite monzogranite which occupies the valley of Benna Thy Lake on Taltson River below Lady Grey Lake. Its most recent age is recognized in the field through its relations to regional north-south oriented sinistral and dextral shear (as described below).

Major zones of north-south oriented sinistral and dextral shear follow the east margin of Taltson Magmatic Zone. Lesser dextral shear zones of similar orientation have been found farther west along the contact zone between Deskenatlata and Slave granites. A second complex zone of northeasterly directed sinistral and dextral shears is evident but has not been completely mapped along the southeast margin of Great Slave Lake Shear Zone (Hanmer and Needham, 1988).

The regional but variably developed sinistral shear fabric along the eastern margin of Taltson Magmatic Zone affects the eastern part of Konth granite and the western part

Table 1. U-Pb isotopic data on zircon and monazite

Sample Fraction	Weight mg	U ppm	Pb* ppm	Measured $^{206}Pb/^{204}Pb$	Isotopic abundances ^{206}Pb = 100 ^{204}Pb	^{207}Pb	^{208}Pb	Isotopic ratios $^{206}Pb/^{238}U$	$^{207}Pb/^{235}U$	Age, Ma $^{207}Pb/^{206}Pb$
1. Northern megacrystic monzogranite										
a, -149+105 n-0.5°	0.0745	146.3	77.23	78.61	0.0078	15.72	20.18	0.45237	9.7442	2415
b, -74+64 n-0.5°	0.0388	142.5	73.71	4577	0.0124	15.76	17.53	0.45260	9.7343	2413
c, -105+74 n-0.5°	0.0548	150.5	77.51	11480	0.0023	15.59	17.16	0.45106	9.6790	2409
d, -64 n-0.5°	0.0347	156.2	80.59	4964	0.0104	15.68	17.80	0.45050	9.6593	2407
2. Eastern equigranular monzongranite										
a, +149 n0°	0.0010	193.4	117.9	314	0.1743	17.01	54.13	0.43074	8.7676	2319
b, +149 n0°	0.0248	356.6	168.0	16730	0.0020	14.09	20.84	0.40591	7.8700	2235
c, -64 n0°	0.0093	187.6	81.5	1224	0.0253	14.02	15.45	0.39341	7.4264	2188
d, -105+74 n0°	0.0403	227.1	98.8	9150	0.0046	13.65	16.08	0.39042	7.3151	2176
e, -74+64 n0°	0.0407	309.2	131.6	6375	0.0076	13.86	13.38	0.38988	7.3997	2198
3. Benna Thy monzogranite										
a, -105+62 n2°	0.0135	201.7	81.25	3390	0.0068	13.15	17.81	0.35823	6.4528	2107
b, +105 n2°	0.0051	116.9	50.21	260	0.3118	16.95	36.04	0.35830	6.3299	2072
c, -74+62 n2°	0.0175	783.5	309.3	4354	0.0150	12.68	15.34	0.36027	6.1983	2026
d, -62 n2°	0.0200	1253	491.6	3327	0.0256	12.88	16.21	0.35656	6.1638	2034
e, +105 n2°	0.0385	179.0	68.20	2460	0.0231	11.86	25.31	0.32511	5.1760	1887
f, +105 n2°	0.0089	155.0	56.16	602	0.1264	13.14	23.40	0.32184	5.0729	1869
g, Monazite	0.0131	6258	8077	25790	0.0014	11.69	323.2	0.34290	5.5176	1906
h, Monazite	0.0130	3661	5505	11590	0.0044	11.73	394.8	0.34287	5.5165	1906
4. Konth syenogranite										
a, Northwest zone										
Monazite	0.0064	8092	12640	31660	0.0005	11.86	406.0	0.34841	5.6952	1935
Monazite	0.0054	12425	22260	38790	0.0005	11.86	482.7	0.34796	5.6882	1935
b, Southwest zone										
Monazite	0.0020	10182	17210	6892	0.0078	11.98	446.2	0.34950	5.7233	1938
Monazite	0.0035	6009	9774	9772	0.0038	11.93	426.0	0.34922	5.7217	1939
c, East zone										
Monazite	0.0108	13677	12580	75050	0.0004	11.87	192.3	0.34977	5.7216	1936

Pb* = radiogenic Pb
Grain sizes are in micrometres
Fractions are zircon unless indicated otherwise
n = nonmagnetic at given angle
Zircon fractions are strongly abraded
Monazite fractions are lightly abraded

of the hinterland. The edge of the hinterland is marked and cut by major belts of sinistral mylonite. Sinistral shear is also expressed in the Natael Granite indicating that it is at least partly younger than both of these plutons. A more restricted zone of dextral shear has been recognized to extend from the mylonite belt at Gagnon Lake southward along the east margin of Taltson Magmatic Zone at least as far as Benna Thy Lake where it is tangential to a major sinistral mylonite belt. The Benna Thy pluton, which lies between these opposing belts of shear, shows only a dextral C and S fabric. Furthermore, dextral kink bands have been recognized within the sinistral mylonite. Dating of the Benna Thy pluton therefore provides a unique opportunity to determine both the minimum age of sinistral shear and the maximum age of dextral shear.

At least five zones of shear converge in the northern part of Taltson Magmatic Zone about Thubun Lakes. Four of these, including the Great Slave Lake Shear Zone itself, are northeasterly directed, and they truncate northerly oriented dextral shear along the west margin of Slave Granite. The four northeasterly trending zones may be conjugate shears related to movements along Great Slave Lake Shear Zone (Bostock, 1988). Further relations between these shear zones and the ages of shearing remain to be determined.

GEOCHRONOLOGY

Analytical considerations:

Results presented in this report (Table 1) were measured in 1987-88 using methods described by Parrish et al. (1987). Pb blanks for zircon are in the range 10-25 picograms; for monazite 30-45 picograms. Uncertainties in U-Pb isotope ratios are indicated in the concordia diagrams and reflect propagation of all analytical uncertainties (Roddick, 1987). Uncertainties generally approximate 0.20 % in $^{238}U/^{206}Pb$ and $^{235}U/^{207}Pb$ and 0.06 % in $^{207}Pb/^{206}Pb$ (2 sigma) but are higher in analyses of single zircon grains and where the quantities of zircon U and Pb are much lower than normal. Regression calculations have been done according to the method of York (1969).

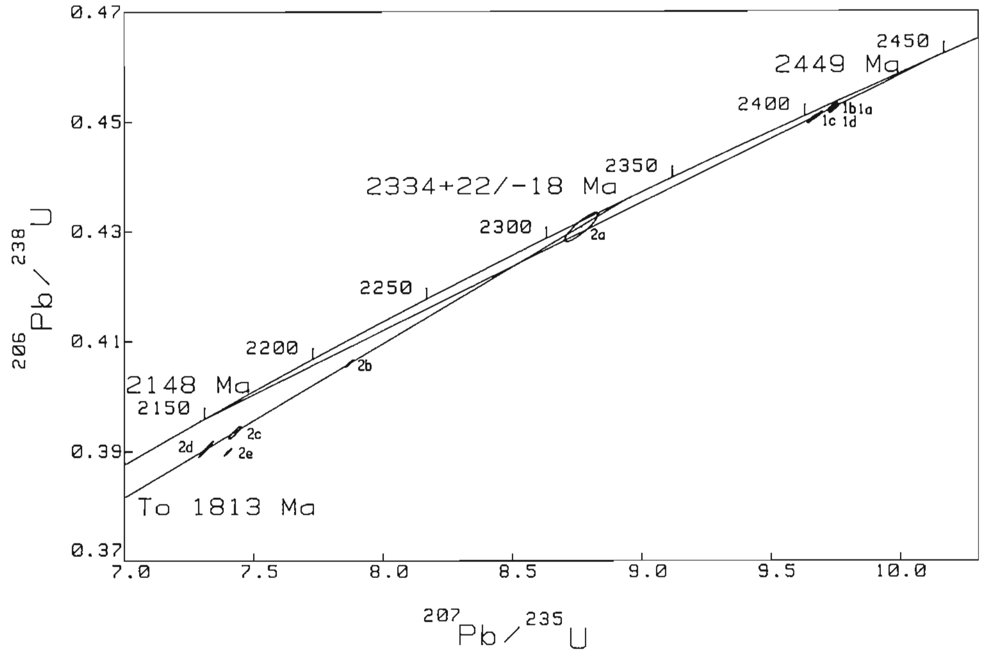

Figure 2. Isotope ratio plot for zircons from the northern megacrystic monzogranite (1a to 1d, see text for age interpretation) and the eastern equigranular monzogranite (2a to 2e).

Schärer (1984) has shown that the U decay series are not always in equilibrium in zircon, xenotime and monazite at the time of formation of these minerals. ^{230}Th, a member of the ^{238}U-^{206}Pb decay chain, is preferentially concentrated in monazite at the time of formation, due to the affinity of monazite for Th. The decay of this ^{230}Th produces excess ^{206}Pb which distorts the measured U-Pb age pattern, causing ^{238}U/^{206}Pb ages to be anomalously high (1-3 Ma excess being typical, R.R. Parrish, pers. comm., 1988) and ^{207}Pb/^{206}Pb ages to be correspondingly low.

The deficiency of measured ^{207}Pb/^{206}Pb ages relative to ^{207}Pb/^{235}U ages (the latter unaffected by excess ^{206}Pb) are greatest in rocks that: (a) are young, (b) have high Th/U in the monazite and (c) have low Th/U in the rock at the time of formation (Schärer, 1984; Parrish unpublished data). The amount of ^{208}Pb expressed as a percentage of the total radiogenic Pb may be used as an index of the monazite Th/U for near concordant monazite. For ages ca. 1900 Ma, Parrish has determined that the effect of ^{230}Th incorporation on ^{207}Pb/^{206}Pb age is likely to be less than 2 Ma for ^{208}Pb at about 70 % and less than 3 Ma for ^{208}Pb at approximately 80 %. Accordingly, the positive uncertainties in the monazite age results presented in this report have been increased to reflect these considerations. When monazites are highly thoriogenic (greater than 90 % ^{208}Pb), the deficiency in ^{207}Pb/^{206}Pb age relative to actual age can be several Ma or more (several tens of Ma are possible for extremely thoriogenic monazite).

MINOR PLUTONS OF THE HINTERLAND

Three granite plutons intruding the hinterland gneisses have been studied using the U-Pb zircon system and in one case coexistent monazite was also examined. The most northerly sample, sample 1, is from a deformed megacrystic granite within the northern belt of the eastern hinterland gneisses west of Taltson River (*see* Fig. 1). Many lithologically similar small plutons mostly within the western hinterland may be of similar age. Two other minor granites examined are equigranular and both are from plutons of the western hinterland. Zircons from these latter plutons have suffered variable degrees of lead loss but in both cases the U-Pb systematics show a reminance that is consistent with a component of about 2300-2450 Ma age.

Northern Megacrystic Monzogranite (sample 1)

Zircons from sample 1, from a small megacrystic granite pluton in the northeastern part of the area, are clear, colourless, euhedral to subhedral and generally elongate with L/B averaging 3.5. No cores were seen but euhedral zoning was evident. Inclusions and fractures were rare; this good quality concentrate resulted in low measured U contents and four collinear slightly discordant data points (Fig. 2). Regression analysis yields concordia intercept ages of 2449 + 60/−31 Ma and 2148 + 239/−269 Ma (chord shown in Fig. 2). We associate the lower intercept age with zircon Pb loss related to metamorphic effects of plutonic activity in the Taltson Magmatic Zone for which the documented time period is 1986.4 + 2.4/−2.0 Ma (Deskenatlata granodiorite, Bostock et al., 1987) to 1906 + 3/−1 Ma (Benna Thy monzogranite, this report). Since Pb loss may have been initiated by earlier metamorphism, or plutonism as yet undocumented, a range in lower intercept ages of 2100-1900 Ma is adopted. Regression analysis with lower intercept ages fixed at 1900 and 2100 Ma yields upper intercept ages 2428 ± 4 and 2442 ± 6 Ma, an extent equivalent to 2436 ± 12 Ma. Based on the euhedral zoning seen in the zircon crystals, this result is interpreted as the age of igneous crystallization of the northern megacrystic monzogranite.

Eastern Equigranular Monzogranite (sample 2)

Sample 2 was taken from a belt of sheared granite no more than a few hundred metres wide along the east margin of a major sinistral mylonite belt east of Benna Thy Lake on Taltson River. Zircon from sample 2 comprises clear, colourless euhedral to subhedral grains with L/B averaging 2.5 and sharp to rounded terminations. Etched polished sections reveal low U cores with medium U overgrowths. In larger grains typical of those picked for analysis, overgrowths are typically thin to absent, but are moderate in thickness in medium sized grains. Smaller grains show thin to relatively thick overgrowths (comparable to those on the larger grains) over low U cores, but rare, high U cores are present. Both cores and overgrowths are euhedrally zoned, indicating igneous origins.

Four of five data points (Fig. 2) are tightly collinear (probability of fit 93 %) yielding concordia intercept ages 2334 + 22/ − 18 and 1813 + 54/ − 57 Ma. Point 2a, which is only 5 % discordant, represents two smaller zircon grains from the +149 μm fraction; point 2b represents a single grain from the same fraction.

The U content of point 2e is 309 ppm compared with 188 and 227 ppm for points 2c and 2d respectively. Based upon this higher U content, it is possible that recent Pb loss has displaced the data point for this fraction although this was not the case for fraction 2b, a larger grain but with more U (357 ppm).

There is no evidence in these results for distinctly separate ages for the cores and overgrowths, unless the overgrowths developed at ca. 1813 Ma. This is considered unlikely as no major geological events are recognized at that time in the area. All zircon fractions were strongly abraded; it is possible that all overgrowths were abraded away. More probably, development of the overgrowths was immediately consecutive to the growth of the cores with the difference in time being small compared with the precision of measurement. Consequently, we relate the measured age, 2334 + 22/ − 18 ma to emplacement of eastern equigranular monzogranite. The granite is protolith to the shear zone and its date of intrusion provides a maximum age for major sinistral shear.

Benna Thy monzogranite (sample 3)

Sample 3 was taken from the Benna Thy granite, a small granite pluton largely confined to the valley of Taltson River at Benna Thy Lake. It is bordered on the east by the main belt of sinistral shear, and on the west by a lesser dextral mylonite belt.

Two monazite fractions were analyzed from sample 3. Monazite grains which are clear, pale yellow, rounded to flattened, mostly broken or subhedral, with no inclusions, cores or zoning noted, were moderately abraded. The monazite data points are almost concordant with essentially identical $^{207}Pb/^{206}Pb$ ages of 1906.1 and 1906.3 Ma. The proportions of ^{208}Pb in the monazite radiogenic Pb, 78 and 74 %, suggests only moderate deficiencies in the $^{207}Pb/^{206}Pb$ ages due to incorporation of excess ^{230}Th at the time of monazite genesis. Accordingly, the positive uncertainty in $^{207}Pb/^{206}Pb$ age is increased to 3 Ma.

The monazite age, 1906 + 3/ − 1 Ma is provisionally adopted as the age of emplacement of the Benna Thy monzogranite. The absence of sinistral shear in the Benna Thy pluton indicates that it is younger than the Natael granite, dated at 1935 ± 3 Ma (Bostock et al., 1987) where the sinistral shear is observed. Conversely, the presence of the monazite indicates that the Benna Thy pluton was in existence under monazite closure conditions at 1906 + 3/ − 1 Ma. Because this age is younger than monazites dated both to east and west, regional metamorphism capable of causing substantial monazite lead loss seems unlikely. This age probably reflects crystallization of monazite on intrusion.

The zircon results (Table 1) from the Benna Thy pluton are complex. In the fractions studied, a component of inherited Pb (2300-2500 Ma?) and/or unsupported radiogenic Pb (Williams et al., 1984) is indicated plus possible multiple stages of Pb loss. This pattern is not amenable to interpretation; we plan to re-collect for further zircon investigation.

Konth Syenogranite

Earlier work on the central zone of the Konth granite indicated that zircon in this pluton is scarce and commonly unsuitable for dating. Thus it was considered that the age of outlying parts of Konth batholith might best be investigated by dating the more abundant, inclusion-free, and generally near concordant monazite in this granite.

The central zone is characterized by a near vertical north-south foliation, common large inclusions of granulite facies metasediment, and a discontinuous border of vertical to inward dipping screens on either side. Age results on monazite and zircon from the central zone (Bostock et al., 1987) are further discussed below. Monazite was concentrated from three additional samples representing different structural phases of the batholith. The east zone (sample 4c) is characterized by vertical foliation; the northwest zone (4a) by moderate eastward dips and a less developed foliation; and the southwest zone (4b) by broad areas where the foliation is approximately horizontal. A major fault separates the southwestern flat lying zone from the rest of the batholith.

Monazite from these three samples is yellow, clear, rounded, L/B = 1 to 2, with no evident cores or zoning. Inclusions are rare except in 4c and were excluded by hand picking. Internal fractures are uncommon except in 4c but more than 50 % of grains were broken in concentrates from 4a and 4b compared with 25 % from 4c.

Northwest zone: Measurements on two monazite fractions from sample 4a (Fig. 3) resulted in slightly discordant data points yielding duplicate $^{207}Pb/^{206}Pb$ ages of 1934.6 ± 1.0 Ma. ^{208}Pb averages 80 % of radiogenic Pb; accordingly the positive uncertainty is increased to 3 Ma to reflect possible excess ^{206}Pb due to ^{230}Th incorporation. The resultant average monazite age is 1935 + 3/ − 1 Ma.

Figure 3. Isotope ratio plot of monazite from the Benna Thy monzogranite (3gh) and the Konth syenogranite (northwest zone, 4a; southwest zone, 4b; east zone, 4c).

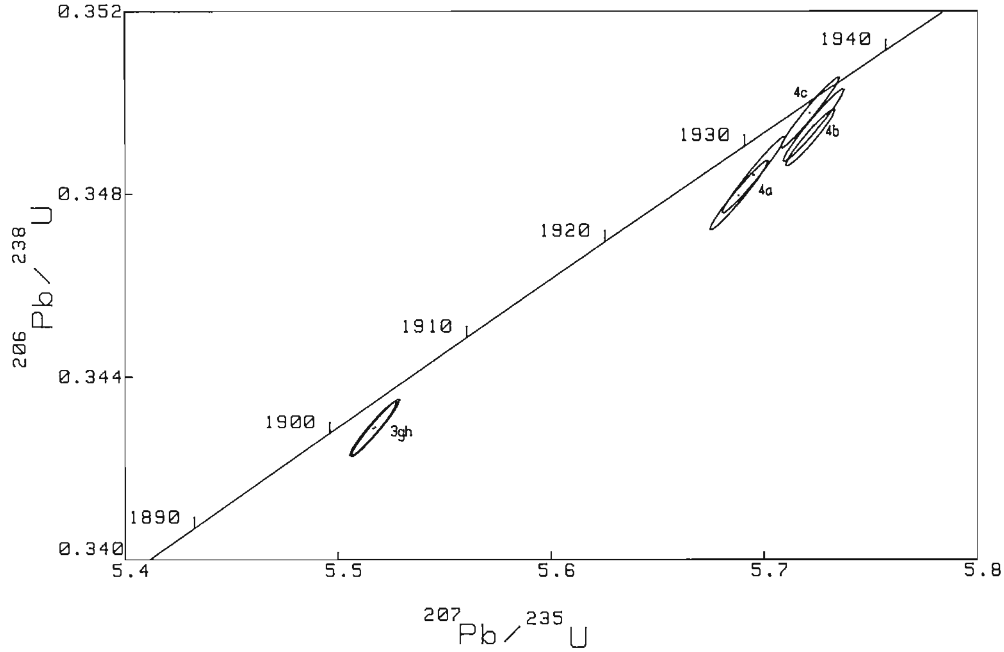

Southwest zone: Two monazite fractions from sample 4b were analyzed resulting in overlapping slightly discordant uncertainty envelopes (Fig. 3) and $^{207}Pb/^{206}Pb$ ages of 1937.8 ± 1.1 and 1938.7 ± 1.0 Ma. ^{208}Pb again averages 80 % of radiogenic Pb so the positive uncertainty is adjusted to 3 Ma and the average monazite age becomes 1938 + 3/ − 1 Ma.

East zone: A $^{207}Pb/^{206}Pb$ age of 1935.9 ± 1 Ma (4c, Fig. 3) was obtained from analysis of a single monazite fraction. The low ^{208}Pb content of 63 % of radiogenic Pb suggests that excess ^{230}Th played only a minor role in the U-Pb systematics. Accordingly, an age of 1936 + 2/ − 1 Ma is established for this monazite sample.

Central zone: In an earlier report (Bostock et al., 1987) we interpreted the results of analyses on three zircon and two monazite fractions from the central zone of the Konth syenogranite as indicating an age of emplacement of 1922 ± 2 Ma. In light of the studies by Parrish (Analytical considerations, this report) and the three monazite ages averaging 1936 Ma for the northwest, southwest and east zones of the Konth granite, an alternative interpretation of the results presented in 1987 is suggested.

The ^{208}Pb contents of the two monazite fractions analyzed in 1987 are both greater than 91 %. These levels of ^{208}Pb are high enough to indicate possible deficiencies of several Ma or greater in the monazite $^{207}Pb/^{206}Pb$ ages. Accordingly the age of monazite crystallization may be as high as 1936 Ma, with recent Pb loss having shifted the monazite data points from initial positions above the concordia curve (due to excess ^{206}Pb) to their present locations.

The zircon data presented for the central zone of the Konth granite in 1987 (op cit.) may be interpreted either as supporting a 1922 Ma age (assuming the coarsest fraction contains a component of older inherited zircon) or an age ca. 1936 Ma (the three zircon data points fit a 1936 — 982 Ma chord within analytical uncertainty). Further measurements on zircon from this sample are underway in order to resolve the ambiguities in interpretation.[1]

DISCUSSION

The geochronology of the hinterland east of the Taltson Magmatic Zone is still largely unknown. The presumed oldest rocks of the hinterland, consisting primarily of a mixed assemblage of mafic gneisses and amphibolite, variably intruded and engulfed by foliated to massive dioritic to granitic rocks, are probably of Archean age since 1) some of these rocks are intruded by the 2436 Ma megacrystic monzogranite (sample 1) and 2) very few or no remnants of supracrustal metasediment have been recognized within them. Supracrustal gneisses of high metamorphic grade, included with this older mixed assemblage in the western hinterland and engulfed within the major batholiths of the Taltson Magmatic Zone, are intruded by pegmatites of about 2500 Ma age in northeastern Alberta (Baadsgaard and Godfrey, 1972).

The two early Aphebian granites dated from the hinterland are similar to many other small plutons in the western hinterland. Assuming that the undated similar plutons are of similar ages, these two dates support the view that the early Aphebian was an important period of plutonism along

[1] Four additional zircon fractions have been analyzed since completion of this report. Results are complex but six of seven data points form a linear trend. The least discordant point (2 %) has a $^{207}Pb/^{206}Pb$ age of 1926 ± 1 Ma; no evidence was found for a component of inherited zircon. Regression analysis using the method of Davis (1982) for non linear data yields a concordia intercept age of 1929 + 10/ −6 Ma. This result is provisionally adopted pending further investigation.

the east margin of Taltson Magmatic Zone. The measured ages are similar to those found for the older Aphebian granites in the Beaverlodge area of northwestern Saskatchewan (van Schmus et al., 1986; Bickford et al., 1987). There, however, evidence exists that plutonism may have spanned the present gap between early Alphebian and Taltson magmatism (about 2334 — 1986 Ma). Further geochronological investigations will be required to see whether this gap is real in the northern part of Taltson Magmatic Zone.

The three monazites from outlying parts of the Konth Batholith provide similar ages suggesting that each of these parts was emplaced between 1934 and 1941 Ma, a period which corresponds with that of emplacement of Natael granite. Coeval intrusion of the major phase of Konth batholith and the outlying Natael granite suggest that 1935 Ma marks the culmination of major plutonism within Taltson Magmatic Zone. Furthermore, both the Natael granite and the eastern part of Konth batholith have local sinistral shear fabrics indicating that a significant part of the regional sinistral shear did not precede this plutonism. On the other hand, deformation in the Natael granite is not uniform, the northwestern part being locally reduced to mylonite, whereas the southeastern part, east of the map area in Figure 1, shows a more brittle deformation. This suggests that the great elongation of the pluton along the east boundary fault of the western hinterland (greater than 10 to 1) is not due to deformation alone. Emplacement of the pluton was in part controlled by the presence of this boundary. It is possible therefore that sinistral shear began slightly before and continued during at least the early part of Konth plutonism.

Monazite age results from Benna Thy granite suggest that it was emplaced at 1906 + 3/ − 1 Ma. This age is the youngest so far presented for plutonism in Taltson Magmatic Zone and corresponds closely to the age of youngest plutonism in Thelon Tectonic Zone (1908 ± 2 Ma, van Breemen et al., 1987). A similar age might be expected for the Thekulthili syenogranite stock (under investigation) which contains mylonite inclusions presumably derived from the adjacent sinistral mylonite. The 1906 Ma age provides a minimum age of regional sinistral shear along the east margin of Taltson Magmatic Zone and suggests that it did not continue after the end of plutonism within Taltson Magmatic Zone. It also provides a maximum for the age of the more restricted dextral shear along the east margin of the zone.

REFERENCES

Baadsgaard, H. and Godfrey, J.D.
1972: Geochronology of the Canadian Shield in northeastern Alberta II. Charles-Andrew-Colin Lake Area; Canadian Journal of Earth Sciences, v.9, p. 863-888.

Bickford, M.E., van Schmus, W.R., Colerson, K.D., and Macdonald, R.
1987: U-Pb zircon geochronology project: new results and interpretations; *in* Summary of Investigations 1987, Saskatchewan Geological Survey; Saskatchewan Energy and Mines, Miscellaneous Report 87-4, p. 76-79

Bostock, H.H.
1988: Geology of the north half of the Taltson Lake map area, District of Mackenzie; *in* Current Research, Part C, Geological Survey of Canada, Paper 88-1C, p. 189-198.

Bostock, H.H., van Breemen, O., and Loveridge, W.D.
1987: Proterozoic geochronology in the Taltson Magmatic Zone, N.W.T.; *in* Radiogenic Age and Isotopic Studies: Report 1, Geological Survey of Canada, Paper 87-2, p. 73-80.

Davis, D.
1982: Optimum linear regression and error estimation applied to U-Pb data; Canadian Journal of Earth Sciences, v. 19, p. 2141-2149.

Hanmer, S. and Needham, T.
1988: Great Slave Lake shear zone meets Thelon Tectonic Zone, District of Mackenzie, N.W.T.; *in* Current Research, Part C, Geological Survey of Canada, Paper 88-1C, p. 33-49.

Parrish, R.R., Roddick, J.C., Loveridge, W.D., and Sullivan, R.W.
1987: Uranium-lead analytical techniques at the Geochronology Laboratory, Geological Survey of Canada; *in* Radiogenic Age and Isotopic Studies: Report 1, Geological Survey of Canada, Paper 87-2, p. 3-7.

Roddick, J.C.
1987: Generalized numerical error analysis with applications to geochronology and thermodynamics; Geochimica et Cosmochimica Acta, v. 51, p. 2129-2135.

Schärer, U.
1984: The effect of initial ^{230}Th equilibrium on young U-Pb ages: the Makalu case, Himalaya; Earth and Planetary Science Letters, v. 67, p. 191-204.

van Breemen, O., Thompson, P.H., Hunt, P.A., and Culshaw, N.
1987: U-Pb zircon and monazite geochronology from the northern Thelon Tectonic Zone, District of Mackenzie; *in* Radiogenic Age and Isotopic Studies: Report 1, Geological Survey of Canada, Paper 87-2, p. 81-93.

van Schmus, W.R., Persons, S.S., Macdonald, R., and Sibbald, T.I.I.
1986: Preliminary results from U-Pb zircon geochronology of the Uranium City region, northwest Saskatchewan; *in* Summary of Investigations 1986, Saskatchewan Geological Survey; Saskatchewan Energy and Mines, Miscellaneous Report 86-4, p. 108-111.

Williams, I.S., Compston, W., Black, L.P., Ireland, T.R., and Foster, J.J.
1984: Unsupported radiogenic Pb in zircon: a cause of anomalously high Pb-Pb, U- Pb and Th-Pb ages; Contributions to Mineralogy and Petrology, v. 88, p. 322-327.

York, D.
1969: Least squares fitting of a straight line with correlated errors; Earth and Planetary Science Letters, v. 5, p. 320-324.

Early Proterozoic U-Pb zircon ages for granitoid rocks from the Moraine Lake transect, Thelon Tectonic Zone, District of Mackenzie

D.T. James[1], O. van Breemen[2], and W.D. Loveridge[2]

James, D.T., van Breemen, O., and Loveridge, W.D., Early Proterozoic U-Pb zircon ages for granitoid rocks from the Moraine Lake transect, Thelon Tectonic Zone, District of Mackenzie; in Radiogenic Age and Isotopic Studies: Report 2, Geological Survey of Canada, Paper 88-2, p. 67-72, 1988.

Abstract

U-Pb zircon analyses indicate Proterozoic emplacement ages for three granitoid intrusions within the Thelon Tectonic Zone east of a zone of abundant granulite facies rocks. A syntectonic hornblende granite yields an age of 1957 +9−5 Ma. The age of emplacement of extensive sheared megacrystic granite has been dated approximately at 1925 Ma, and a foliated biotite granite has been constrained between 2.0 and 1.9 Ga.

Résumé

Des analyses à l'aide de la méthode U-Pb appliquée aux zircons indiquent que, pendant le Protérozoïque, trois granitoïdes se seraient introduits dans la zone tectonique de Thelon, à l'est d'une zone où se trouve une abondance de roches à faciès des granulites. Un granite à hornblende syntectonique a donné un âge radiométrique de 1957 +9−5 Ma. L'âge de la mise en place du vaste granite cisaillé à macrocristaux a été établi à environ 1925 Ma et l'âge d'un granite à biotite feuilleté a été fixé entre 2,0 et 1,9 Ga.

INTRODUCTION

This study presents U-Pb zircon ages from the eastern end of a transect mapped by James (1985,1986) across part of the Thelon Tectonic Zone (Fig. 1, 2). The Moraine Lake transect extends southeastward from the southeast corner of the Healey Lake map sheet (NTS 76B) mapped by Henderson et al. (1982) and includes the extreme northeast corner of the Artillery Lake map sheet (NTS 75O) mapped by Henderson et al. (1987).

Mapping of the Healey Lake area revealed that Archean, low pressure metamorphic assemblages along the eastern margin of the Slave Province are progressively overprinted from west to east by a medium pressure facies Proterozoic metamorphism (Henderson and Thompson, 1980; 1981). The eastern limit of the metamorphic overprinting and of Slave Province lithologies is along a north-northeasterly striking, dextral strike-slip shear zone. East of the shear zone, the proposed contact between the Slave and Churchill structural provinces, are granulite facies rocks two samples of which have yielded Aphebian ages (van Breemen et al., 1987a). While the age of one granulite facies mylonite is bracketed between 1990 and 1950 Ma, a small, late-tectonic "Hanbury" granite in the northeast corner of the Artillery Lake map sheet was dated at 1920 ± 4 Ma.

Detailed, 1:50 000 scale, mapping of the 50 km long Moraine Lake transect has shown that the proposed Slave-Churchill contact is marked by significant changes in lithology, structural style and metamorphic grade. West of the contact the Slave Province includes Yellowknife Supergroup gneisses and granitoid gneisses, metamorphosed to upper amphibolite facies during the Archean, and overprinted by a kyanite-staurolite grade Proterozoic metamorphism. East of the contact is a heterogeneous group of supracrustal and plutonic rocks metamorphosed to granulite facies during the Proterozoic, as well as unmetamorphosed and variably deformed granitoid rocks that become increasingly abundant towards the eastern end of the transect.

The extreme eastern end of the transect is underlain entirely by megacrystic granodiorite that is associated with a prominent magnetic high that parallels the Thelon Tectonic Zone (one of the highest magnetic anomalies in the entire Canadian Shield). Aeromagnetic patterns suggest that the megacrystic granodiorite in the Moraine Lake transect extends to similar megacrystic rocks in the Overby Lake area, some 300 km to the north, mapped by Thompson et al. (1986), where the age is constrained in the 1980-1940 Ma interval (van Breemen et al., 1987b). The extent of this granite can only be inferred from interpretation of the

[1] Department of Geological Sciences, Queen's University, Kingston, Ontario K7L 3N6
[2] Geological Survey of Canada, 601 Booth Street, Ottawa, Ontario K1A 0E8

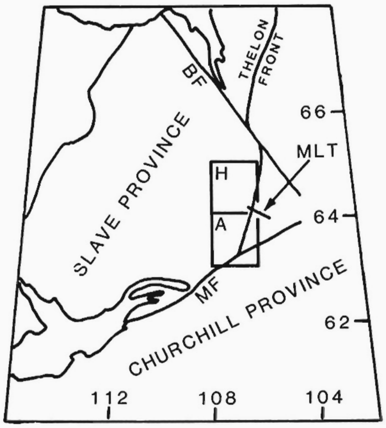

Figure 1. Location of the Moraine Lake transect. H, Healey Lake map sheet; A, Artillery Lake map sheet: BF, Bathurst Fault; MF, MacDonald Fault; MLT, Moraine Lake Transect.

aeromagnetic anomalies and from a few mapped occurrences of megacrystic granodiorite (eg. James, 1986; Henderson et al., 1987; Frith, 1982; Thompson et al., 1986). These have been interpreted to be part of a 80 by 1000 km batholith formed above an oblique east-dipping subduction zone, "The Thelon Magmatic Arc" (Hoffman et al., 1986; Hoffman, 1987).

In the Overby Lake map area the first eastward appearance of Proterozoic granitoid rocks coincides with the first occurrences of granulite facies rocks (Thompson et al., 1986). One of these, a clinopyroxene granodiorite has I-type chemical characteristics (Newman, 1986) and has an age also constrained in the 2020-1950 Ma interval (van Breemen et al., 1987b).

In order to test whether the zone of extensive Aphebian granites within the Thelon Tectonic Zone occurs to the south as well as to the north of the Bathurst Fault, three granitoid units have been collected from the eastern end of the Moraine Lake Transect. These units are:

(1) Darrell Granite — a clinopyroxene granite;
(2) megacrystic granodiorite — granite;
(3) Maze Lake Granodiorite — Granite.

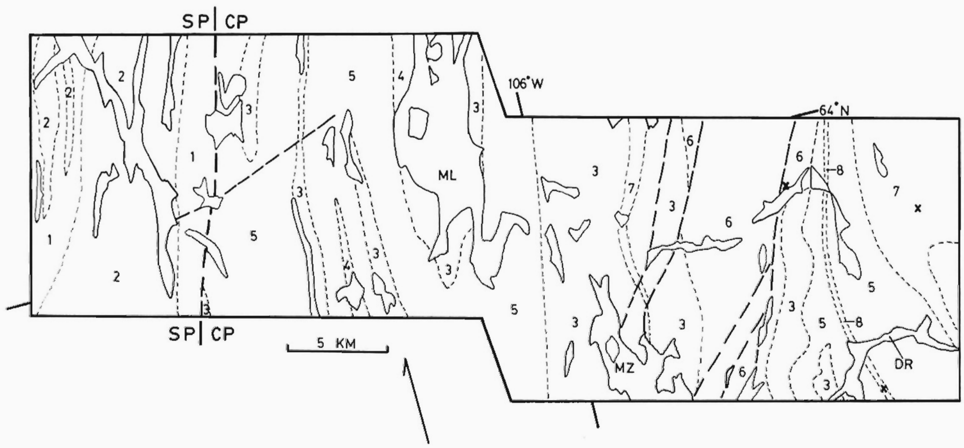

Figure 2. General geology of the Moraine Lake transect and sample locations: 8, Darrell River granite (x, sample 1); 7, megacrystic granodiorite — granite (x, sample 2); 6, Maze Lake granodiorite — granite (x, sample 3); 5, granulitic orthogneiss, migmatitic orthogneiss; 4, garnet granite; 3, granulite supracrustal gneiss; 2, Yellowknife Supergroup gneiss; 1, granitoid gneiss; SP I CP, proposed Slave -Churchill contact; x, geochronology sample location; ML, Moraine Lake; MZ, Maze Lake; DR, Darrell River.

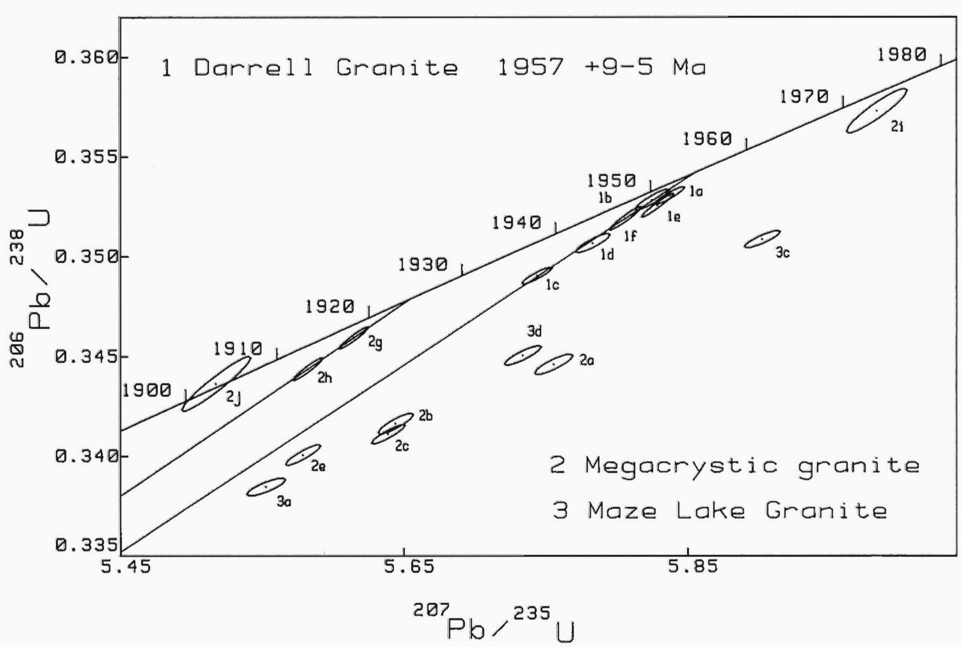

Figure 3. Isotope ratio plot for zircons from granitoids. Numbers and letters with data point correspond to those in Table 1.

Table 1. U-Pb zircon isotopic data

Sample and zircon fraction in microns	Weight (mg)	U (ppm)	Pb* (ppm)	Measured $^{206}Pb/^{204}Pb$	Isotopic abundances (^{206}Pb=1000) ^{204}Pb	^{207}Pb	^{208}Pb	Isotopic ratios $^{206}Pb/^{238}U$	$^{207}Pb/^{235}U$	Age, Ma $^{207}Pb/^{206}Pb$
1. Darrell granite (VK-86-ART51)										
a. +149,No.5,coarse	0.042	576.5	252.2	7355	0.060	120.7	316.7	0.35304	5.8373	1955.0
b, +149,No.5	0.019	417.0	173.3	2801	0.120	121.3	244.0	0.35283	5.8249	1952.3
c, −149+105,No.5	0.043	867.4	341.8	4071	0.196	122.0	185.0	0.34903	5.7439	1946.6
d, −105,No.5	0.033	602.4	248.7	2290	0.345	124.2	236.1	0.35066	5.7832	1950.5
e, +149,N1,S	0.072	454.3	203.6	20790	0.027	120.3	356.1	0.35255	5.8288	1954.9
f, +149,N1,S	0.017	560.3	241.5	9858	0.028	120.1	303.7	0.35190	5.8061	1951.2
2. Megacrystic granodiorite-granite (VK-86-ART50)										
a, +149,N1	0.031	309.7	126.1	1666	0.407	126.6	237.1	0.34461	5.7556	1973.0
b, +149,N1,ends	0.023	178.5	68.1	2038	0.168	122.1	183.7	0.34164	5.6442	1953.6
c, −149+105,N1	0.033	331.3	130.9	2339	0.252	123.3	217.2	0.34110	5.6389	1954.7
d, −149+105,N1,ends	0.019	241.8	84.8	902	0.787	129.4	151.0	0.32778	5.3706	1938.7
e, −105+74,N1	0.022	445.2	165.4	2077	0.288	122.8	141.1	0.34006	5.5788	1941.0
f, +74,N1	0.009	450.0	168.4	1666	0.206	122.6	180.5	0.33267	5.4963	1953.6
g. +149,M1,S	0.037	877.6	308.6	11150	0.025	118.1	65.03	0.34594	5.6145	1921.7
h, +149,M1,S	0.037	540.3	190.6	8210	0.025	117.9	74.13	0.34438	5.5822	1919.5
i, +149,M1,S	0.039	108.2	43.73	925	0.397	126.8	205.0	0.35728	5.9834	1977.8
j, +149,M1,S	0.039	119.0	48.15	788	0.357	121.2	262.3	0.34364	5.5175	1902.4
3. Maze Lake grandorite-granite (Y-27)										
a, +105,N3	0.025	1025	375.3	1400	0.639	127.6	117.0	0.33845	5.5528	1941.1
b, +105,N3	0.036	1716	606,8	1711	0.552	124.6	126.7	0.32545	5.2594	1914.1
c, −105+74,N3	0.017	1474	554.5	1880	0.457	128.1	109.1	0.35085	5.9028	1986.0
d, −62,N3	0.015	1018	380.1	1721	0.439	126.4	122.0	0.34505	5.7339	1964.0

* Radiogenic lead
N,M Respectively non-magnetic or magnetic at given side slope angle on Frantz magnetic separator
S Analyses of single crystals

CASE STUDIES

Sample localities are indicated on Figure 1. Analytical techniques of zircon preparation and U-Pb analysis have been described in Parrish et al. (1987). U-Pb isotopic data are presented in Table 1 and displayed on a concordia diagram (Fig. 3), although the boundaries of the latter exclude the most discordant data in Table 1.

Darrell Granite (sample 1; VK-86-ART51)

A thin sheet of clinopyroxene granite at the eastern end of the transect has been named the Darrell granite for exposures on the east side of the Darrell River. Contact with the surrounding granitoid gneisses is exposed at only one location, on the east side where it appears to be a fault marked by chlorite-grade cataclasite. Air photo lineaments suggest that all contacts along the granite are sharp. Outcrops of Darrell granite, including that from which the dated sample originates, are homogeneous and xenolith-free. They are consistently stongly foliated and sheared, with foliation defined by quartz lenticles, and elongate hornblende and sphene. Surrounding granitoid gneisses do not contain dykes of Darrell granite.

The granite contains fine grained orthoclase, quartz and plagioclase with straight to lobate grain boundaries, surrounded by very fine (less than 0.05 mm), recrystallized feldspars and quartz. A low percentage of quartz forms fine lenticles that parallel the foliation. Rocks contain up to 10 % clinopyroxene, variably overprinted by hornblende as rims or grains within clinopyroxene. Hornblende is also present with no obvious (or relict) overprinting relationship to clinopyroxene and forms fine to medium, well-formed and elongate grains that make up to 15 % of the granite. Rocks also contain several per cent sphene and lesser amounts of magnetite, apatite and zircon.

The outcrop pattern of the Darrell granite and the structural style - strong development of foliation, local protomylonitic structures and steep, east-plunging mineral lineations -suggest that the intrusion of this body was syntectonic with the strain in the granulites.

Zircons are clear and generally equidimensional with length to breadth (L:B) ratios of 1:1 to 1:2. Outlines are round to oval or of rounded irregular shape. Polished and etched sections show regularly zoned igneous cores surrounded by rims of irregular and discordant zoning (Fig. 4). Such zoning has been interpreted in terms of growth of zircon crystals impinging on surrounding crystals in a dynamic environment, such as a shear zone, either in a late magmatic (crystal mush; van Breemen and Hanmer, 1986) or in a solid state (van Breemen et al., 1987a). The latter is not supported by the absence of a sharp break between regular and discordant zoning nor by the absence of a mylonitic fabric in the hornblende granite. The ribbon outcrop pattern of the intrusion nevertheless suggests extreme attenuation, which in view of the discordant zircon zoning could, in part, have been produced by shear movements while the magma was in a semi-molten state.

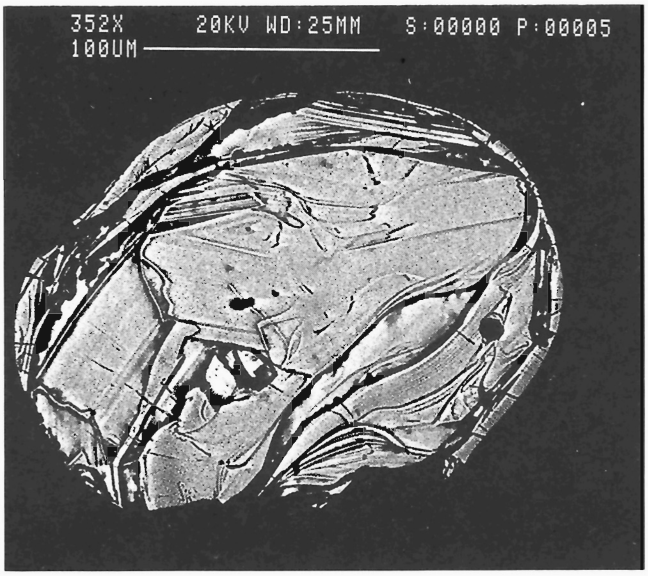

Figure 4. Scanning electron microscope image (backscattered electron mode) of polished and etched (HF) section of zircon. Note rounded shape and irregular zoning which in places is continuous with regular igneous zoning. The perimeter has a thin rim of presumably metamorphic zircon.

Although U concentrations for the zircon fractions analyzed are high (400 — 900 ppm), all four fractions analyzed plot near the concordia (Fig. 2). The distribution of data points suggests that the coarsest fraction (1a) may contain an older component. Two analyses of single zircons repeat this pattern, where an extremely coarse broken fragment (1e) of 350 μ average dimension yields a slightly older age than a smaller broken grain (1f), both being abraded to rounded forms. Regression of all six data points (Davis, 1982) yields an upper intercept age of 1959 +7/-3 Ma with a lower intercept near 1130 Ma and a probability of fit of 20 %, whereas the four data points excluding 1a and 1e yield upper and lower intercept ages of 1955 +6/−3 Ma and ca. 850 Ma with a probability of fit of 63 %. If the scatter of data points can be attributed to a small component of inheritance, the latter regression is appropriate. If, on the other hand, there has been a small component of later disturbance, the younger age is correct. As it is not possible to distinguish between these alternatives, an average age with full range of uncertainty is adopted, i.e. 1957 +9/−5 Ma. This age is interpreted in terms of the time of magma emplacement during tectonically active conditions.

Megacrystic granodiorite — granite (sample 2; VK-86-ART 50)

Megacrystic granodiorite and granite outcrop in three areas east of the proposed Slave — Churchill contact: (1) immediately east of the contact where they forms small lens-shaped bodies less than 1km long and 200 m wide; (2) in a long and narrow body that intrudes supracrustal granulite gneiss northeast of Maze Lake; and (3) as part of a major (?) intrusive body in the extreme east end of the transect. West of the large body of megacrystic rocks in the east end of the transect, there are abundant occurrences of megacrystic granodiorite that intrude the gneisses west and north of the Darrell River.

Outcrops are compositionally homogeneous and xenolith-free. Characteristically, rocks are red and black on fresh and weathered surfaces. Most rocks are megacrystic with orthoclase megacrysts, although a variety of textures and structures may be present. Rocks may be massive or strongly foliated and locally sheared. Highly strained rocks have a streaked appearance with a discontinuous gneissosity defined by elongated orthoclase megacrysts. Non-megacrystic, massive to foliated granodiorite and granite form a minor part of this unit.

Rocks have granodioritic and locally granitic compositions and are composed of up to 50 % medium-to coarse-grained megacrysts composed of single or multiple orthoclase grains. In relatively highly strained rocks megacrysts are polygonized to finer grains that retain megacrystic outlines or have relict coarse orthoclase cores surrounded by a fine grained, recrystallized microcline margin. Andesine and quartz in the matrix are fine grained with straight to embayed contacts. In all cases rocks contain fine-to medium-grained biotite and commonly hornblende. Common accessory minerals are magnetite, apatite and zircon.

The dated sample is from a strongly foliated outcrop with coarse alkali feldspar megacrysts and approximately 10 % fine-to coarse-grained hornblende and less than 5 % biotite. Accessory magnetite, apatite, sphene and zircon are present. Most megacrysts are elongated and composed of a fine grained aggregate of fine-to medium-grained orthoclase and minor microcline. The rock has a weak flaser structure defined by elongate (1 cm) quartz lenticles that surround deformed megacrysts.

Zircons range from equidimensional rounded to prismatic igneous shapes with L:B ratios varying from 2:1 to 5:1. Cracks are common, as are cores, and discordant internal zoning occurs near the outer margins of some crystals.

U concentrations for zircon concentrates analyzed range from 180 to 450 ppm. Data points corresponding to these fractions are strongly scattered, plotting slightly to the right of the chord for the hornblende granite (Fig. 3). A pre-magmatic component of zircon, as seen in the abundant cores, is likely to have contributed to this scatter, as cores are often not visible in transmitted light. For the two fractions (2b,2d) the ends of prismatic grains were broken off and abraded. Fraction 2b corresponds, however, to an older age than fraction 2e, so that the problem of inherited Pb was not entirely circumvented by this technique. It is also possible that the outer margins of the zircons have been affected by metamorphism and deformation following intrusion (cf. van Breemen et al., 1987b) although there is no evidence in the rocks for migmatitic segregation or granulite facies metamorphism. In a further attempt to resolve the above ambiguity, four single grains were analyzed individually using the improved micro-capsule for zircon dissolution (Parrish, 1987) now in routine use at the GSC. Grains g and h are broken fragments of zircon of ca 250 μ average dimension featuring regular igneous zonation, which were abraded to spheres of ca 180 μ diameter. These grains of high U content (Table 1) yield data points ca. 0.5 and 1 % discordant with $^{207}Pb/^{206}Pb$ model ages of 1922 and 1920

Ma respectively. A line drawn through these points yields upper and lower intercept ages of 1925 +7/ −4 Ma and 0.8 Ga repectively. Single grains i and j were 100 μ abraded spheres, survivors of broken prismatic grains originally ranging from 150 μ ends to 150 μ by 275 μ prisms. These grains of significantly lower U content yield concordant and semi-concordant data points with disparate $^{207}Pb/^{206}Pb$ ages of 1978 +/− 3 and 1902 +/− 3 Ma. The older age is interpreted in terms of an inherited age, in which case 1975 Ma represents the minimum age of a core, which because of its near concordance is clearly of Proterozoic age. The younger age is interpreted in terms of a metamorphic event for which 1905 Ma is an upper limit. Because of the concordance of this data point, this metamorphic event is not likely to be much younger than 1900 Ma. The 1925 +7−4 Ma age for fractions g and h is interpreted to approximate the time of emplacement of the megacrystic granite.

Maze Lake granodiorite — granite (sample 3; Y-27)

East of Maze Lake, outcrops of granodiorite and granite form an approximately 4 km wide, north-northeasterly striking body that continues beyond the transect to the north and south. Rocks are variably deformed, unmetamorphosed and intrusive into the supracrustal granulites along the west and east margins of the body. Contacts between the granitoid rocks and the granulites are gradational and are mapped where the proportion of ganitoid rocks is greater than granulite. The aeromagnetic signature of this unit is relatively low compared to the body of megacrystic granodiorite at the extreme east end of the transect.

This unit is a composite body composed predominantly of foliated, biotite (with or without hornblende) granodiorite with minor amounts of foliated, biotite-poor granite and local gradations into tonalite and quartz diorite. A wide range of textural and structural variations is also apparent. Outcrops may be massive, strongly foliated (sheared) and are locally poorly gneissic. Microcline megacrystic granodiorite and hornblende-glomeroblastic granodiorite form minor parts of the unit. All of the compositional, textural and structural variations of the unit are cut by the biotite-poor granite that locally forms foliation-parallel sills, discordant dykes and small plutons (several hundred metres in diameter) similar to the 1920 +/− 4 Ma Hanbury Granite of the Artillery Lake map sheet.

Zones with abundant xenoliths of granulite gneiss mark the eastern and western contacts of the body. Metre-sized, angular xenoliths of mafic gneiss are common throughout while xenoliths of hornblende granodiorite are local.

Rocks have "granitic" textures and are composed of microcline, plagioclase (An30-35), quartz, biotite and hornblende (biotite + hornblende = 10 to 20%). Accessory minerals include sphene (up to 5 %) (commonly with opaque — ilmenite (?) cores), epidote, apatite, ilmenite and zircon.

The dated sample is from a fine-to medium-grained, weakly foliated biotite granodiorite outcrop that is compositionally and texturally homogeneous and xenolith-free.

Zircons are cloudy and more paramagnetic than normal (Table 1). Crystals display simple igneous morphologies with L:B ratios of 4:1 to 2:1. Rounded cores are abundant.

U concentrations range from 1720 to 1020 ppm. Data points are not linearly aligned but follow a regular trend of increasing apparent age with increasing concordance. In view of the poor quality of the zircon population, single grain work was not considered feasible. Although a line through the lower two data points (3a and 3b; not on Fig. 3) yields an upper concordia intercept age of 1980 Ma, a line through data points 3c and 3d yields an upper intercept age of 2090 Ma. $^{207}Pb/^{206}Pb$ ages range from 1986 Ma to 1914 Ma. Given the combined possible effects of inherited cores and metamorphic disturbance, the granite emplacement age is tentatively placed in the 2.0-1.9 Ga range.

DISCUSSION

The new radiometric age data indicate that the zone of Proterozoic granulite facies gneisses gives way eastwards to extensive Proterozoic granitoid rocks which can be temporally correlated with megacrystic and I-type granites of similar age north of the Bathurst Fault. The megacrystic granite and Maze Lake granite contain extensive older memory. Although the age of this inherited component has not been constrained in general, one core from the megacrystic granite is clearly Proterozoic.

The 1957 +9/−7 Ma age for the hornblende granodiorite dates magmatism of intermediate composition as well as deformation in the form of shear movement during emplacement. A 1925 +7/−4 Ma age for two single crystals from the megacrystic granite is thought to indicate the approximate time of magma emplacement. Younger metamorphic zircon growth or Pb isotopic disturbance occurred close to 1900 Ma. The apparent emplacement age of the megacrystic granite is close to the 1920 +/− 4 Ma U-Pb monazite age for the strongly deformed Hanbury granite, intruded into migmatitic metasediments in the northeast of that Artillery Lake map area (Henderson et al., 1987; van Breemen et al., 1987a).

REFERENCES

Davis, D.
1982: Optimum linear regression and error estimation applied to U-Pb data; Canadian Journal of Earth Sciences, v. 19, p. 2141-2149.

Frith, R.A.
1982: Second preliminary report on the geology of the Beechey Lake-Duggan Lakes map areas, District of Mackenzie; *in* Current Research, Part A, Geological Survey of Canada, Paper 82-1A, p. 203-211.

Henderson, J.B. and Thompson, P.H.
1980: The Healey Lake map area (northern part) and the enigmatic Thelon Front , District of Mackenzie; *in* Current Research Part A, Geological Survey of Canada, Paper 80-1A, p. 165-169.
1981: The Healey Lake map area and the Thelon Front problem, District of Mackenzie; *in* Current Research, Part A, Geological Survey of Canada, Paper 81-1A, p. 175-180.

Henderson,J.B., McGrath,P.H., James, D.T., and Macfie, R.I.
1987: An integrated geological, gravity and magnetic study of the Artillery Lake area and the Thelon Tectonic Zone, District of Mackenzie; *in* Current Research, Part A, Geological Survey of Canada, Paper 87-1A, p. 803-814.

Henderson, J.B., Thompson, P.H., and James, D.T.
1982: The Healey Lake map area and the Thelon Front problem, District of Mackenzie; *in* Current Research, Part A, Geological Survey of Canada, Paper 82-1A, p. 191-195.

James, D.T.
1985: Geology of the Moraine Lake area and the Thelon Front, District of Mackenzie; *in* Current Research, Part A, Geological Survey of Canada, Paper 85-1A, p. 449-454.
1986: The geology of the Moraine Lake area, District of Mackenzie, part 2; a transect across part of the Thelon Tectonic Zone; *in* Current Research, Part A, Geological Survey of Canada, Paper 86-1A, p. 417-421.

Hoffman, P.F.
1987: Continental transform tectonics: Great Slave Lake shear zone (ca. 1.9 Ga), northwest Canada; Geology, v. 15, p. 785-788.

Hoffman, P.F., Culshaw, N.G., Hanmer, S.K., LeCheminant, A.N., McGrath, P.H., Tirrul, R., and van Breemen, O.
1986: Is the Thelon Front (NWT) a suture?; Geological Association of Canada, Program with Abstracts, Ottawa, 1986, p82.

Newman, R.M
1986: Petrology, geochemistry, and geochronology of a pluton in the Thelon Tectonic Zone, Northwest Territories; unpublished BSc thesis, McMaster University, 82 p.

Parrish, R.R.
1987: An improved micro-capsule for zircon dissolution in U-Pb geochronology; Isotope Geoscience, v. 66, p. 99-102.

Parrish,R.R., Roddick,J.C., Loveridge, W.D., and Sullivan,R.W.
1987: Uranium-lead analytical techniques at the geochronology laboratory, Geological Survey of Canada; *in* Radiogenic Age and Isotopic Studies: Report 1; Geological Survey of Canada, Paper 87-2, p. 3-7.

Thompson, P.H., Culshaw, N., Buchanan, J.R., and Manojlovic, P.
1986: Geology of the Slave Province and Thelon Tectonic Zone in the Tinney Hills-Overby Lake (west half) map area, District of Mackenzie; *in* Current Research, Part A, Geological Survey of Canada, Paper 86-1A, p. 275-289.

van Breemen,O. and Hanmer,S.
1986: Zircon morphology and U-Pb geochronology in active shear zones: studies on syntectonic intrusions along the northwest boundary of the Central Metasedimentary Belt, Grenville Province, Ontario; *in* Current Research, Part B, Geological Survey of Canada, Paper 86-1B, p. 775-784.

van Breemen,O., Henderson,J.B., Loveridge,W.D., and Thompson, P.H.
1987a: U-Pb zircon and monazite geochronology and zircon morphology of granulite and granite from the Thelon Tectonic Zone, Healey Lake and Artillery Lake map areas, N.W.T.; *in* Current Research, Part A, Geological Survey of Canada, Paper 87-1A, p.783-801.

van Breemen,O., Thompson,P.H., Hunt,P.A., and Culshaw,N.
1987b: U-Pb zircon and monazite geochronology from the northern Thelon Tectonic Zone, District of Mackenzie; *in* Radiogenic Age and Isotopic Studies: Report 1; Geological Survey of Canada, Paper 87-2, p. 81-93.

U-Pb zircon and monazite ages from the eastern Slave Province and Thelon Tectonic Zone, Artillery Lake area, N.W.T.

O. van Breemen[1] and J.B. Henderson[1]

van Breemen, O., and Henderson, J.B., U-Pb zircon and monazite ages from the eastern Slave Province, and Thelon Tectonic Zone, Artillery Lake area, N.W.T., in Radiogenic Age and Isotopic Studies: Report 2, Geological Survey of Canada, Paper 88-2, p. 73-83, 1988.

Abstract

In the western domain of the area, typical of much of the Slave Province, the Clinton-Colden rhyolite has yielded a U-Pb age of 2671 +2/-4 Ma. The proximate Tarantula tonalite has yielded a zircon age of 2622.0 +1.4/-1.2 Ma, and zircons and sphene have constrained the age of the related Charloit granodiorite at 2617 ± 7 Ma. Monazites from the two-mica Ptarmigan granite are younger at 2606 ± 5 Ma whereas to the south, the megacrystic Artillery Lake granite has yielded monazite ages of 2596 +3/-6 Ma. Most of the plutonism appears to be constrained in an interval 40-80 Ma after volcanism.

In the central domain, a structurally deeper exposed level of the Slave Province, the Smart orthogneiss has yielded a U-Pb zircon age of 2602 ± 2 Ma which is considered to date or slightly postdate igneous emplacement of the plutonic precursor. The megacrystic Musclow granite has yielded a U-Pb zircon emplacement age of 2603 +5/-4 Ma. In the eastern domain, part of the Thelon Tectonic Zone, the Sifton gneiss a granulite facies granitoid migmatite, has yielded zircon ages clustered around 1975 Ma which are interpreted as a mimimum age for a primary igneous event and a maximum age of a subsequent metamorphism. The megacrystic Critchell granite which postdates the granulite facies metamorphism has been dated at c.1.95 Ga.

Résumé

Dans le domaine ouest de la zone à l'étude, représentative d'une grande partie de la province des Esclaves, la rhyolite de Clinton et Colden a été datée par la méthode U-Pb à 2671 +2/−4 Ma. La tonalite voisine de Tarantula à 2622,0 +1,4/−1,2 Ma et la mesure des zircons et de la sphène ont donné un âge radiométrique basé sur les zircons de l'âge de la granodiorite Charloit associée à 2617 ± 7 Ma. Les monazites du granite à deux micas de Ptarmigan sont plus récentes (2606 ± 5 Ma) tandis qu'au sud, le granite à macrocristaux d'Artillery Lake a été daté à l'aide de la monazite à 2596 +3/−6 Ma. Le plutonisme semble avoir eu lieu, en grande partie, dans un intervalle de 40 à 80 Ma après le volcanisme.

Dans le domaine central, un affleurement structurellement plus profond de la province des Esclaves, l'orthogneiss de Smart, a été daté par la méthode U-Pb appliquée aux zircons à 2602 ± 2 Ma, ce qui coïnciderait avec l'intrusion ignée du précurseur plutonique ou la suivrait de peu. L'intrusion du granite à macrocristaux de Musclow a été datée par la méthode U-Pb appliquée aux zircons à 2603 +5/−4 Ma. La datation du gneiss de Sifton, une migmatite granitoïde à faciès des granulites, dans le domaine est au sein de la zone tectonique de Thelon, a produit des âges obtenus à partir de zircons regroupés autour de 1975 Ma, époque que l'on considère comme l'âge minimal d'un événement igné important et l'âge maximal d'un métamorphisme subséquent. Le granite à macrocristaux de Critchell, postérieur au métamorphisme à faciès des granulites, a été daté à 1,95 Ga.

INTRODUCTION

The Artillery Lake area straddles a 140 km long segment of the boundary between the Archean Slave Structural Province and the Thelon Tectonic Zone of the northwestern Churchill Province (Fig. 1) (Henderson et al., 1987a). This report is part of a series on the geochronology of the eastern Slave and western Thelon Tectonic Zone (van Breemen et al., 1987a,b,c; James et al., 1988).

North of the McDonald Fault the area has been divided into three domains. The western domain, west of the prominant series of faults east of Artillery and Clinton-Colden lakes, is typical of much of the Slave Province with its bulbous plutons, curvilinear structural style and large areas of Yellowknife Supergroup rocks at greenschist to amphibolite grade. The central zone is bounded on the east by the western margin of the Thelon Tectonic Zone (Fig. 1) and represents Slave Province rocks that are presently

1. Geological Survey of Canada, 601 Booth Street, Ottawa, Ontario K1A 0E8

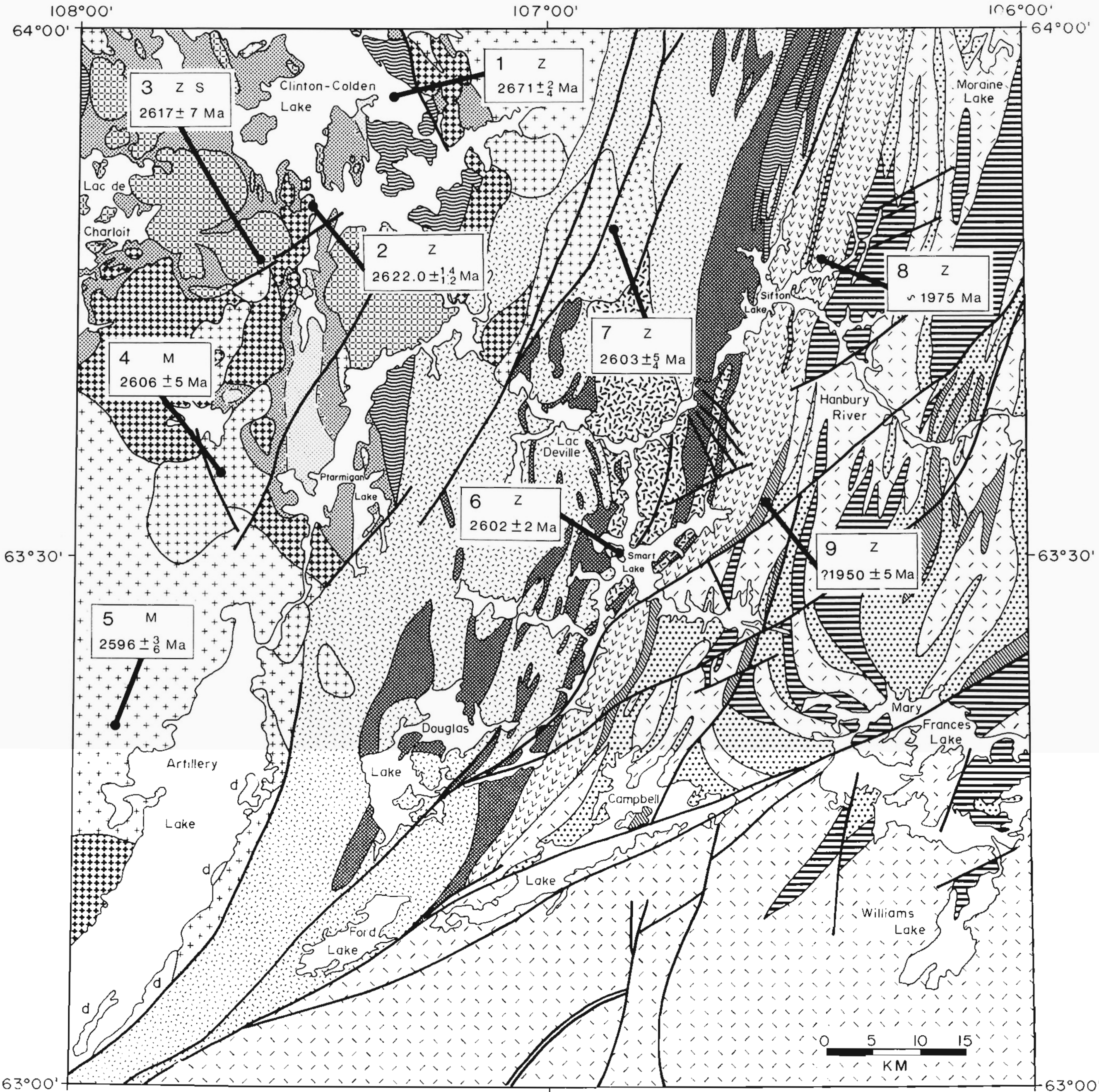

Figure 1. Geology of the Artillery Lake map sheet showing location of samples investigated from the southeastern Slave Structural Province and the Thelon Tectonic Zone. The main U-Pb age results are summarized at the various sample localities: Z, zircon age; M, monazite age; S, sphene age.

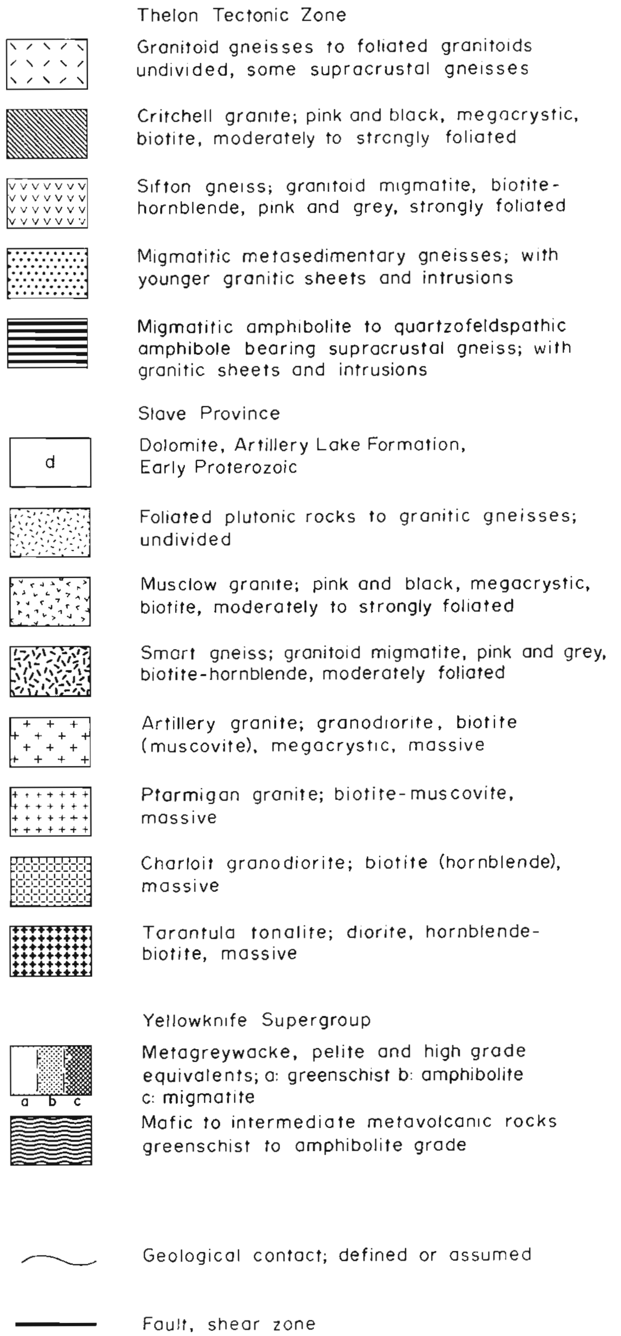

exposed at a much deeper structural level than those to the west so that all units are strongly foliated and metamorphosed, and all Yellowknife supracrustal rocks are migmatites. The eastern domain is part of the Proterozoic Thelon Tectonic Zone and is characterized by pronounced steep linear structure with abundant mylonite and high, commonly granulite metamorphic grade.

GEOCHRONOLOGY

In an attempt to extend our understanding of the ages of the Yellowknife supracrustal rocks and the intrusive granitoid rocks of the eastern Slave Province, samples for analysis of zircon, monazite and/or sphene were collected where possible from 5 units in the western domain. These include (sample 1) the Clinton-Colden rhyolite, (2) the Tarantula tonalite, (3) the Charloit granodiorite, (4) the Ptarmigan granite and (5) the Artillery granite. The strongly deformed and metamorphosed central zone is of considerable interest. Much of it is readily identifiable as part of the Slave Province in that a) it contains units in common with the western domain and b) the belt of highly deformed Yellowknife supracrustal rocks on its eastern margin can be followed continuously north into the Slave Province proper. However, the central zone does contain granitoid units that also have a marked lithological similarity to units in the Thelon Tectonic Zone. Two of these lithological pairs were dated to establish whether a) these units are lithological coincidences of different age, b) they are Proterozoic intrusions emplaced in both the Slave Province and the Thelon Tectonic Zone, or c) are Archean units of the Slave Province that have also been preserved as Archean relics in the Thelon Tectonic Zone, that up to now has yielded only Proterozoic ages. The units dated include (sample 6) the Smart gneiss and (7) Musclow granite from the central domain and the lithologically corresponding (8) Sifton gneiss and (9) Critchell granite respectively of the eastern domain.

Rock unit nomenclature used in this report is informal.

Analytical techniques for U-Pb zircon, monazite and sphene have been described in Parrish et al. (1987). Zircons have been strongly, and monazites lightly, abraded. Isotopic data are presented in Table 1 and displayed in isotope ratio plots (Fig. 2, 3, and 4).

Clinton-Colden rhyolite (sample 1; VK-86-ART130)

A major, dominantly mafic volcanic belt occurs along the northeast side of Clinton-Colden Lake, extending some 50 km from the Artillery Lake area into the Healey Lake area. As is commonly the case with Yellowknife Supergroup volcanic sequences, it contains relatively small centres of felsic volcanics, one of which occurs along the northeast shore of the lake at the map margin. These felsic volcanics are typically well bedded volcaniclastic units ranging from breccias to fine tuffs. However the site sampled on a small island in the lake is a massive rhyolite dome, either emergent or shallowly emplaced, that possibly represents the volcanic centre from which the adjacent volcaniclastics were derived.

Table 1. U-Pb isotopic

Sample and zircon fraction in microns	Weight (mg)	U (ppm)	Pb* (ppm)	Measured $^{206}Pb/^{204}Pb$	Isotopic abundances (^{206}Pb=1000)			Isotopic ratios		Age,Ma $^{207}Pb/^{206}Pb$
					^{204}Pb	^{207}Pb	^{208}Pb	$^{206}Pb/^{238}U$	$^{207}Pb/^{235}U$	
1. Clinton-Colden rhyolite (VK-86-ART130; 63 56.2 107 19.6)										
a, −149+105,N4	0.036	60.89	36.42	957	0.716	191.9	187.7	0.51533	13.0155	2681.8
b, −105+74,N4	0.026	58.35	33.88	685	0.995	194.1	167.4	0.51194	12.8422	2670.6
c, −105+74,N4	0.040	66.39	38.91	1029	0.701	190.8	174.6	0.51020	12.8181	2673.1
d, −74+62,N4	0.041	67.67	38.96	1897	0.257	184.6	147.0	0.50673	12.6792	2666.4
2. Tarantula tonalite (VK-86-ART21; 63 49.7 107 30.0)										
a, +105,N1	0.040	134.5	75.02	3365	0.131	178.5	150.1	0.48998	11.9465	2623.4
b, −105+74,N1	0.024	156.7	86.88	2986	0.092	177.2	140.4	0.49039	11.9054	2616.2
c, −74+62,N1	0.025	136.3	79.82	1079	0.674	185.1	196.2	0.50347	12.2679	2622.4
d, +62,N1	0.023	148.5	84.54	3792	0.086	177.6	163.3	0.49473	12.0439	2620.8
e, −105+74,M1	0.010	125.4	72.27	1682	0.235	179.5	169.0	0.50043	12.1825	2620.8
f, −74+62,M1	0.007	95.74	55.91	942	0.372	181.2	185.9	0.50225	12.2307	2621.3
3. Charloit granodiorite (VK-86-ART23; 63 47.3 107 37.3)										
a, −105+74,N1	0.022	189.8	101.2	2393	0.264	179.4	112.0	0.48440	11.7597	2616.2
b, −62+50,N1	0.013	142.0	76.67	1257	0.447	180.4	139.6	0.48246	11.6335	2604.9
c, −62+50,N1	0.009	194.9	102.7	824.4	0.823	184.3	142.7	0.47459	11.3921	2597.4
d, S, sphene	0.375	27.80	25.72	219.1	0.580	182.9	1043.9	0.48518	11.7530	2612.6
4. Ptarmigan granite (VK-86-ART25; 63 34.6 107 43.1)										
a, Monazite	0.0040	3412	4282	8068	0.000	174.6	1753	0.49597	11.9404	2602.3
b, Monazite	0.0045	142.7	376.3	5195	0.000	174.8	4998	0.49355	11.8968	2604.4
c, Monazite	0.0043	927.2	6105	2915	0.193	177.8	14009	0.49916	12.0689	2609.4
d, Monazite	0.0035	506.9	3059	2144	0.129	176.9	12790	0.49786	12.0364	2609.3
5. Artillery granite (VK-86-ART100; 63 21.3 107 53.3)										
a, Monazite	0.0020	759.6	1763	1315	0.000	172.7	4385	0.48231	11.4875	2584.4
b, Monazite	0.0019	1507	3424	3717	0.000	173.3	4201	0.48838	11.6668	2589.3
c, Monazite	0.0027	1824	2946	5062	0.073	174.7	2660	0.48694	11.6668	2594.3
d, Monazite	0.0039	2525	4831	12810	0.015	173.5	3358	0.48789	11.6575	2589.7
6. Smart gneiss (VK-86-142; 63 30.5 106 50.3)										
a, −105+74,N−3	0.016	94.66	55.71	854	0.516	181.1	239.7	0.48938	11.7882	2603.2
b, −105+74,N+2,	0.020	80.98	47.24	1399	0.388	179.4	214.3	0.49225	11.8481	2601.9
c, −74+62,N−3,R	0.015	89.07	50.29	1268	0.187	176.9	192.2	0.48190	11.6027	2602.4
7. Musclow granite (VK-86-ART82; 63 48.2 106 51.7)										
a, −149+105,N3	0.031	278.6	154.7	3903	0.140	176.4	156.8	0.48623	11.7099	2602.9
b, +74,N3	0.043	278.4	154.5	4224	0.150	176.1	182.3	0.47687	11.4581	2599.0
c, −74,N3	0.051	361.9	199.8	3062	0.207	176.5	161.0	0.48292	11.5840	2596.2
d, −74,M3	0.014	425.9	228.7	5073	0.087	174.9	141.8	0.47525	11.3893	2594.7
e, 74,M3	0.0036	190.6	113.4	423	1.71	195.9	269.2	0.49649	11.9593	2603.2
f, 74,M3	0.0025	164.0	94.68	478	0.964	186.4	226.1	0.48912	11.7626	2600.5
g, −74,M3,R	0.014	294.4	166.2	286	3.28	215.0	257.9	0.49347	11.8610	2599.6
8. Sifton gneiss (VK-86-ART77; 63 47.2 106 25.7)										
a, +105,N2	0.039	159.3	62.28	2089	0.244	124.7	163.2	0.35590	5.9604	1977.8
b, +105,N−2,R	0.037	146.5	57.78	1692	0.324	126.0	170.4	0.35757	5.9967	1980.3
c, −105+74,N−2	0.025	268.8	104.4	2665	0.158	123.2	159.6	0.35379	5.9081	1972.8
d, −105+74,N−2,R	0.032	156.8	61.77	1318	0.468	127.5	173.6	0.35770	5.9815	1975.1
e, −74+62,N−2,R	0.040	189.2	72.97	3882	0.109	122.8	143.1	0.35553	5.9464	1975.5
9. Critchell granite (VK-86-ART85; 63 33.1 106 33.0)										
a, +105,N−3	0.039	220.6	82.16	3702	0.125	121.8	114.9	0.35164	5.8259	1958.6
b, −105+74,N−3	0.036	228.2	85.81	3762	0.087	121.7	122.7	0.35233	5.8574	1964.8
c, −74+62,N−3	0.010	252.1	92.46	1006	0.422	125.3	108.4	0.35131	5.7939	1950.5
d, −62,N−3	0.030	226.9	83.56	2957	0.116	121.1	111.1	0.34896	5.7500	1948.9
e, −62,N−3	0.016	209.6	76.96	2434	0.141	121.4	102.8	0.35057	5.7765	1948.8

** Sample is zircon unless indicated otherwise
* Radiogenic lead
N,M Respectively non-magnetic or magnetic at given side slope angle on Frantz magnetic separator
R Ovoid or equidimensional shaped
S Sphene

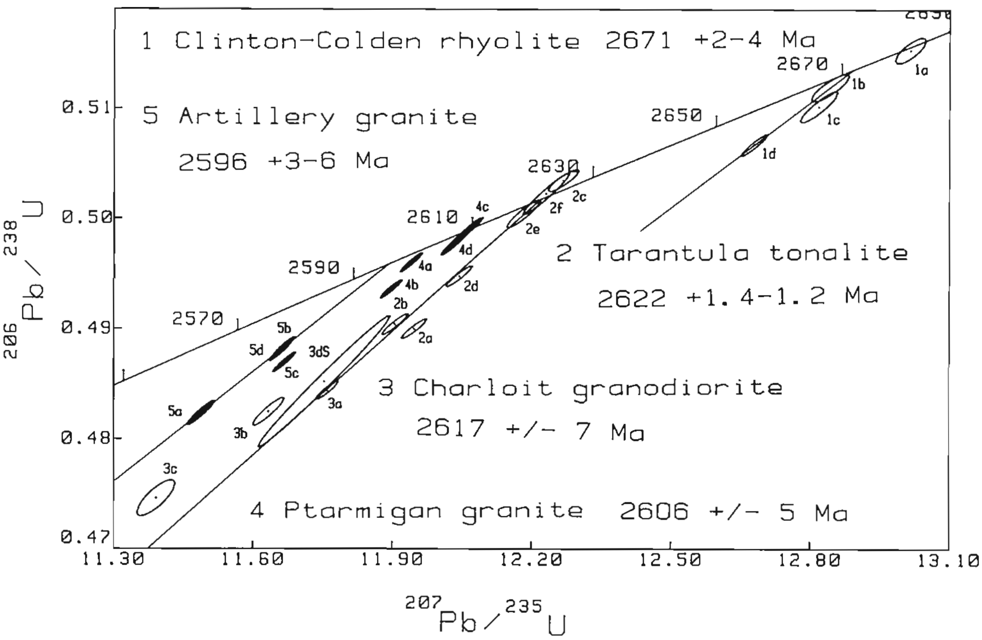

Figure 2. Isotope ratio plot for zircon (open error ellipses) and monazites (closed error ellipses) from: 1) Clinton-Colden rhyolite, 2) Tarantula tonalite, 3) Charloit granodiorite, 4) Ptarmigan granite and 5) Artillery granite. Numbers and letters identifying data points correspond to those of Table 1 (S denotes sphene). Note age gap between volcanism and plutonism.

The rock is a massive, structureless, very homogeneous, medium grained, pale greenish buff rhyolite porphyry with no visible mafic minerals. In thin section it has the texture of a densely packed porphyry with plagioclase phenocrysts up to 5 mm grading to a sparse, dominantly quartzofeldspathic matrix with a median grain size of about 0.2 mm. The albitic plagioclase phenocrysts occur in blocky, subhedral, slightly elongate, complexly twinned crystals that are commonly broken. Although presently homogeneous, there is a suggestion of original compositional zonation shown by the distribution of alteration products. The matrix consists of an anhedral assemblage of quartz, plagioclase, K-feldspar and completely altered minor mafic phases that are now represented by patches of various chlorites. The rock is at greenschist grade so that the original igneous texture is veiled by evenly distributed sericite-muscovite-chlorite alteration products. Sphene and zircon are accessory minerals.

Zircons are clear and pale-brown to purple. Crystals are generally euhedral with L:B (length to breadth ratios) of 2:1 and range from simple bipyramidal prisms to multifaceted shapes. Cores have not been distinguished and zoning is not prominent. Crystals contain some round fluid inclusions.

Four zircon fractions were analyzed. Uranium concentrations are low (ca. 60 ppm) and the two coarsest fractions are concordant, yielding $^{207}Pb/^{206}Pb$ model ages of 2682 (1a) and 2671 Ma (1b) respectively (Table 1), thus indicating a significant inherited component in the coarsest fraction 1a. A line through fractions 1b and 1d (the finest fraction) yields upper and lower intercept ages of 2672 and 873 Ma respectively (Fig. 2). A slight component of inherited Pb is indicated for fraction 1c with a $^{207}Pb/^{206}Pb$ model age of 2673 Ma. Given the possibility that a small component of inherited zircon is present in fraction 1b, the extrusive age of the volcanics is interpreted as 2671 +2/−4 Ma.

Tarantula tonalite (sample 2; VK-86-ART21)

Several plutons of the Tarantula suite occur in the vicinity of Clinton-Colden Lake and are part of an extensive suite of plutons that occur in the western half of both the Artillery Lake and Healey Lake area to the north. On the whole the suite grades from granodiorite in the northern Healey Lake area to tonalite in the south. A granodiorite pluton from the suite in the Healey Lake area was dated at 2617 +7/-6 Ma (van Breemen et al., 1987b). The nearby Charloit granodiorite, another unit discussed below, is also considered to be closely related to this suite of rocks.

The sample dated comes from near the contact between a small pluton of the tonalite and the Yellowknife metasedimentary country rock on Clinton-Colden Lake. The rock is a buff to grey, massive, homogeneous tonalite that locally contains sharply angular inclusions of the metasediment. In thin section it is a medium grained, somewhat inequigranular rock composed primarily of plagioclase (50 %) that is anhedral to subhedral, commonly zoned with minor oscillations and whose core zones are commonly altered to sericite and epidote. Mafic minerals form less than half the rock and include both coarse, brown flakes of only slightly chloritized biotite and irregular coarse aggregates of anhedral hornblende in approximately equal proportions. Quartz occurs as small, irregular, polygonized grains. Accessory and secondary minerals include illmenite, anhedral sphene that commonly, in part, overgrows the illmenite, apatite, zircon, sericite, epidote and chlorite.

Zircons are generally clear, brown, with a few cracks and inclusions, although cores are not evident. Crystals are mostly simple bipyramids with L:B of ca. 2:1.

Uranium concentrations range from 160-95 ppm with data points being concordant (2c,e,f) to 2 (2b) discordant (Table 1, Fig. 2). Fractions e and f, with the lowest U contents, consist of 3 and 4 grains respectively. The coarsest fraction, 2a, plots slightly to the right of the array of data points and may have an inherited component. A regression analysis (Davis, 1982) of the remaining 5 data points yields an upper intercept age of 2622 +1.4/-1.2 Ma and a lower intercept age of 0.5 Ga.

Charloit granodiorite (sample 3; VK-86-ART23)

The Charloit granodiorite forms small individual plutons to larger bulbous plutonic complexes east of Lac de Charloit and south of Clinton-Colden Lake (Fig.1). The bodies are typically homogeneous, massive to weakly foliated at their margins, faint pinkish grey to white, medium grained, even grained, biotite moderate to poor granodiorite. The biotite characteristically forms large single plates and the abundant quartz is commonly grey to brown. This unit is probably related to the previously described Tarantula plutonic suite but has been separated here because of the strong compositional contrast between the Charloit granodiorite and the nearby mafic tonalites of the southern Tarantula plutonic suite. Compositionally, texturally, and in its plutonic form, the Charloit granodiorite closely resembles the Defeat Plutonic Suite at Yellowknife (Henderson, 1985).

The Charloit granodiorite sample analyzed is a massive, somewhat inequigranular rock with abundant coarse quartz and to a lesser extent, plagioclase up to 5 or 6 mm. These phases grade abruptly into the average 1 to 2 mm grain size of the rock. Plagioclase, the dominant phase, consists of subhedral to anhedral, commonly zoned grains with minor oscillatory zoning. Alteration is concentrated in the originally more calcic zones. Quartz closely follows in abundance forming mainly coarse, anhedral, in many cases single, equidimensional, strained crystals but is also present as finer interstitial grains. Fine interstitial microcline forms about 10% of the rock. Mafic minerals constitute about 10% of the rock and consist of scattered, ragged, highly chloritized flakes of dark green to greenish- brown biotite and lesser amounts of hornblende. Accessory and secondary minerals include coarse, euhedral sphene up to 1.5 mm in size, an opaque phase, apatite, zircon, epidote and sericite.

The zircon population of this granodiorite is not of good quality with most grains being broken and quite cloudy. The best light golden brown primatic (L:B = 2) grains were picked from the finer fraction (Table 1). Uranium concentrations range from 190 to 140 ppm. Data points are discordant with the coarsest fraction appearing to contain an older Pb component. Fractions 3b and 3c appear to be slightly younger than zircons from sample 2 (Fig. 2). A fraction of sphene with a low U content of 28 ppm is ca. 3 % discordant. The $^{207}Pb/^{206}Pb$ age for this fraction is 2613 +/− 3 Ma. As it is unlikely that the sphene contains an inherited premagmatic component, the Pb model age is considered to provide a minimum age. If tonalite sample 2 provides a maximum age, the age for the Charloit granodiorite is constrained between 2624 and 2610 Ma, i.e. 2617 ± 7 Ma.

Ptarmigan granite (sample 4; VK-86-ART25)

The Ptarmigan granite is a two-mica granite that occurs in a series of moderate sized bodies in the northwestern part of the area. It is much more abundant in the Healey Lake area to the north where it also forms much larger bodies. There, it has recently been dated, using highly discordant zircon, as being emplaced between 2530 and 2600 Ma (van Breemen et al., 1987b). The Ptarmigan granite is similar to the Prosperous granite in the Yellowknife region (Henderson, 1985) even to the extent of also having rare lithium-mineral-bearing pegmatites.

The granite sampled is buff to white to pale yellow, massive, medium-to coarse-grained, generally equigranular and contains moderate amounts of biotite and muscovite. Rare euhedral crystals of muscovite in excess of 1 cm are also present. Muscovite-bearing pegmatite also occurs in the outcrop area. In thin section the rock is massive, coarse grained, with weakly developed microcline megacrysts and has a typical granitic texture. Microcline is the most abundant phase and occurs both as interstitial, typically inclusion-free grains and also as subhedral megacrysts (up to 7 mm) that typically contain inclusions (up to 1 mm) of plagioclase, biotite or quartz. The plagioclase forms blocky to anhedral grains that may be weakly zoned, and has a weak to moderately developed sericitic alteration, particularly in the cores. In many cases the plagioclase contains 0.5 mm plates of muscovite that are commonly crystallographically oriented. The plagioclase is commonly myrmekitic where in contact with microcline. Abundant quartz forms large, blocky, coarsely polycrystalline grains. Large undeformed flakes of biotite and muscovite are present in about equal proportions. The biotite is reddish brown and slightly chloritized. Accessory and secondary minerals include apatite, zircon, monazite, chlorite and sericite.

Zircons from this two-mica granite are scarce, of poor quality and contain abundant cores. Data points corresponding to 4 analyses of single monazite grains are concordant to one per cent discordant (Table 1, Fig. 2). Model $^{207}Pb/^{206}Pb$ ages range from 2602 to 2609 Ma. A small inherited monazite component cannot be ruled out (Parrish, 1988), although this is not supported by the agreement of the two concordant older data points 4c and 4d. The age adopted is the average model Pb age at 2606 ± 5 Ma.

Artillery granite (sample 5; VK-86-100)

The Artillery granite is a large megacrystic intrusion west and north of Artillery Lake. A lithologically similar body occurs northeast of Clinton-Colden Lake on the boundary between Artillery and Healey Lake map areas. The latter body was recently dated to have been emplaced at 2595 ± 10 Ma (van Breemen et al., 1987b).

The Artillery granite is a massive, homogeneous, pink to greyish pink, medium grained, megacrystic granite containing moderate amounts of biotite and a trace of muscovite. In thin section the rock that was analyzed is highly altered. The coarsest and most abundant phase is poikilitic anhedral orthoclase over 1 cm in size, with inclusions of plagioclase and biotite. The very fine, reddish brown alteration of the 2 to 3 mm grains of anhedral plagioclase almost obscures the original twinning of the mineral. Where in contact with quartz the plagioclase commonly has a thin clear albitic overgrowth. Quartz, for the most part, forms large equidimensional monocrystalline grains. Biotite is recrystallized along its margins and is commonly chloritized. Accessory and secondary minerals include zircon, monazite, chlorite, epidote and sericite.

Zircons from this granite are scarce and of poor quality. Data points corresponding to four analyses of single monazite grains are from one to two per cent discordant (Table 1, Fig.2). Fraction 5c appears to have an older component, which may be inherited . A regression analyis of the remaining three data points (Davis, 1982) yields an upper intercept age of 2596 +3/-6 Ma with a lower intercept of ca. 870 Ma and a 43 % probability of fit. The upper intercept age is likely to approximate the time of granite emplacement.

Smart gneiss (sample 6; VK-86-142)

The Smart gneiss is a granitoid migmatite near the eastern boundary of the central domain at and north of Smart Lake. It is of geochronological interest because of its lithological similarity on the whole to the much more severely deformed Sifton gneiss of the western Thelon Tectonic Zone discussed later.

The rock consists of a dominant, grey, medium grained, even grained to sparsely megacrystic, massive to well foliated, biotite moderate, meta-granodiorite to tonalite. Commonly present in highly varied proportions are veins to zones of a pink to white, mafic-poor, generally coarser grained leucosome phase that is commonly gradational with the grey phase and has been deformed with it.

The sample analyzed was the grey tonalitic phase. In thin section the tonalite has lost any igneous texture and now consists of a crushed granulated rock with clasts up to 5mm grading smoothly down to less than 0.1 mm. There is no preferred orientation of biotite. The dominant phase is unzoned and, in some cases, weakly antipertitic plagioclase that is weakly to moderately altered. Quartz forms irregular equidimensional grains up to 3 mm in size. Although typically polycrystalline, in some cases the large quartz masses are monocrystalline. Olive-green biotite occurs in aggregates of fine grained unaltered flakes that commonly tend to mantle some of the coarser phases. Epidote and sphene are particularly abundant accessories forming over 1 % of the rock in each case. Other minor phases include an opaque phase, apatite, zircon, muscovite and chlorite.

Zircons are generally small and clear with few inclusions. Although a range of morphologies is evident, two end members can be distinguished, namely long prismatic grains with L:B 3:1 to 6:1 and equidimensional more multifaceted types. Cores and rims have not been distinguished, and it is not clear that the equidimensional grains are of igneous or metamorphic origin. U concentrations are low (95-80 ppm; Table 1)) so that polished sections cannot be etched with HF.

The two prismatic fractions (6a and 6b) are slightly discordant and the equidimensional fraction (6c) is 3 % discordant (Fig. 3). All three fractions fit a regression line (MSWD = 0.7) with an upper intercept of 2602 $\pm$ 2 Ma and a lower intercept near 0 Ma (York, 1969). Given the agreement of apparent ages of the prismatic and equidimensional grains and indication of only slight recent Pb loss, there is no evidence for significantly younger metamorphic zircon growth. Also, in view of the strong abrasion of the prismatic fraction, the upper intercept age is interpreted to be close to igneous crystallization. However, in view of the migmatitic aspect of this unit, the plutonic emplacement age may be somewhat older.

Musclow granite (sample 7; VK-86-ART82)

The Musclow granite occurs in the northern part of the central domain. Like the Smart gneiss it has a lithological analogue in the Proterozoic Thelon Tectonic Zone to the east: the Critchell granite. The Musclow granite is a fairly homogeneous, generally weakly to moderately foliated augen granite. It is characterized by concentrated pink to red feldspar megacrysts up to several centimetres long in a sparse, typically dark grey to black, biotite-rich matrix. On the west side of the body, adjacent to the domain boundary fault, the large quartz lenticles in the rock become sugary, resulting in a rather spectacular red, white and black rock.

The sample analyzed is from the west side of the unit and is a strongly deformed granite that in thin section consists of coarse abraded anhedral porphyroblasts of slightly perthitic microcline with inclusions of plagioclase, quartz and biotite and somewhat smaller anhedral, only minimally altered plagioclase or aggregates of plagioclase in a foliated, fine, inequigranular matrix of quartz, two feldspars and biotite, The quartz forms elongate, pure, finely polycrystalline aggregates, in some cases mantled by finer heterogeneous matrix components. The olive-green biotite forms ragged aggregates of fine flakes that are only rarely chloritized and are commonly associated with fine granular epidote. Of the accessory minerals, sphene, apatite and an opaque phase are particularly abundant with lesser amounts of metamict allanite that is commonly overgrown by epidote, and zircon.

Zircons are colourless to pink, and range from prismatic grains with L:B of ca. 3:1 to equidimensional shapes with simple faceting. The latter are generally clearer. Cracks and inclusions including fluid inclusions are evident as well as cores. Zircons with apparent cores were removed during hand-picking.

Zircon fractions picked were prismatic with the exception of fraction 7g which consists of equidimensional grains. Uranium concentrations range from 430 to 160 ppm. The two smallest zircon fractions, 7e and 7f have the lowest U

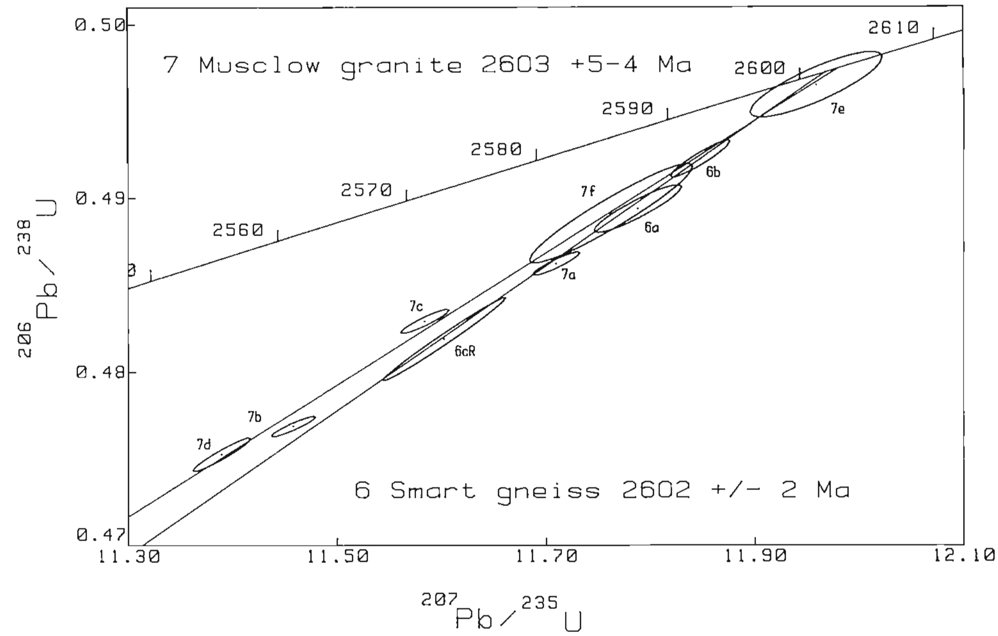

Figure 3. Isotope ratio plot for zircons from 6) Smart gneiss and 7) Musclow granite. Numbers and letters identifying data points correspond to those of Table 1.

concentrations and the largest analytical uncertainties, but are the most concordant (Fig. 3). Data point 7a, corresponding to the coarsest size fraction, plots slightly to the right of the main data point array and is interpreted in terms of slight zircon inheritance. Fraction 7g (not plotted) corresponding to equidimensional grains has a $^{207}Pb/^{206}Pb$ age and uncertainty of 2600 $\pm$ 5 Ma and is indistinguishable from the data point array. A regression analysis of the five data points 7e to 7f yields an upper intercept age of 2603 +5/-4 Ma, and a lower intercept age of 0.4 Ga with a probability of fit of 51 % (Davis, 1982). The upper intercept age is interpreted in terms of granite emplacement.

Sifton gneiss (sample 8; VK-86-ART77)

The Sifton gneiss is a relatively homogeneous, strongly deformed, granitoid migmatite that is the dominant unit along the western boundary of the Thelon Tectonic Zone. Smaller, similar units occur elsewhere within the area to the east. It has a strong positive aeromagnetic expression and is almost always associated with the other gneisses and supracrustal gneisses that are commonly granulite grade. Where best preserved, it consists of a grey, relatively finer grained biotite and/or hornblende-moderate granodiorite to tonalite with wispy lenses to layers of pink, mafic-poor, coarser grained granite leucosome. Where mylonitized, which is commonly the case, the rock is a pink and grey layered gneiss with porphyroclasts of coarser grey feldspar and black hornblende.

The sample analyzed is a tonalite from one of the least deformed parts of the unit on Sifton Lake. The rock is massive to weakly foliated, medium grained, inequigranular. and is dominated by anhedral equidimensional grains of plagioclase with somewhat finer hornblende and quartz with similar habit. The hornblende in some cases forms aggregates. Quartz is commonly monocrystalline although there is a complete range to finely polycrystalline aggregates. The coarser phases grade abruptly into the fine, inequigranular, sutured, mainly quartzofeldspathic minerals of the matrix. Brown, weakly to moderately chloritized biotite, a relatively minor mafic phase, occurs in ragged patchy aggregates and in some instances has a weak tendancy to overgrow some of the hornblende. No pyroxenes were noted. Accessory and secondary minerals include magnetite, apatite, sphene, zircon, chlorite, carbonate and sericite. No igneous textures are preserved.

The sample contains abundant zircons (8 gm recovered from 80 kg). Zircons consist of prismatic subhedral shapes with L:B of about 1:3 as well as ovoid multifaceted types. Crystals are clear with very few inclusions. Polished and etched sections show a three-fold zoning with a) inner cores which generally show regular igneous zoning, when visible, b) an inner mantle with discordant zoning which commonly has an igneous aspect and 3) an outer mantle of apparently uniformly low U content showing little zoning (Fig. 5). This pattern of zoning is identical to that of the tonalitic granulite gneiss (sample 1 of van Breemen et al., 1987a) at Moraine Lake, an extension of the eastern domain of the Artillery Lake map sheet (Henderson et al., 1982) The zonation may reflect the regional geology in terms of a precursor of unknown but probably igneous origin, followed by migmatization during tectonically active conditions, followed by granulite facies metamorphism.

In an attempt to separate primary igneous from metamorphic ages, a fraction of prismatic crystals was selected from two of the fractions composed of the more ovoid types. On an isotope ratio plot, data points are clustered and range from concordant to one percent discordant. Ovoid grains (indicated by 'R' on Fig. 4) do not show a bias towards younger ages. The 1975 Ma $^{207}Pb/^{206}Pb$ model age of concordant fraction 8d is taken to be be a minimum age for the igneous precursor and a maximum age for the granulite facies metamorphism. The ca. 1975 Ma zircon age is likely to be close to the time of growth of the inner mantle, which has a higher U content and hence radiogenic Pb content.

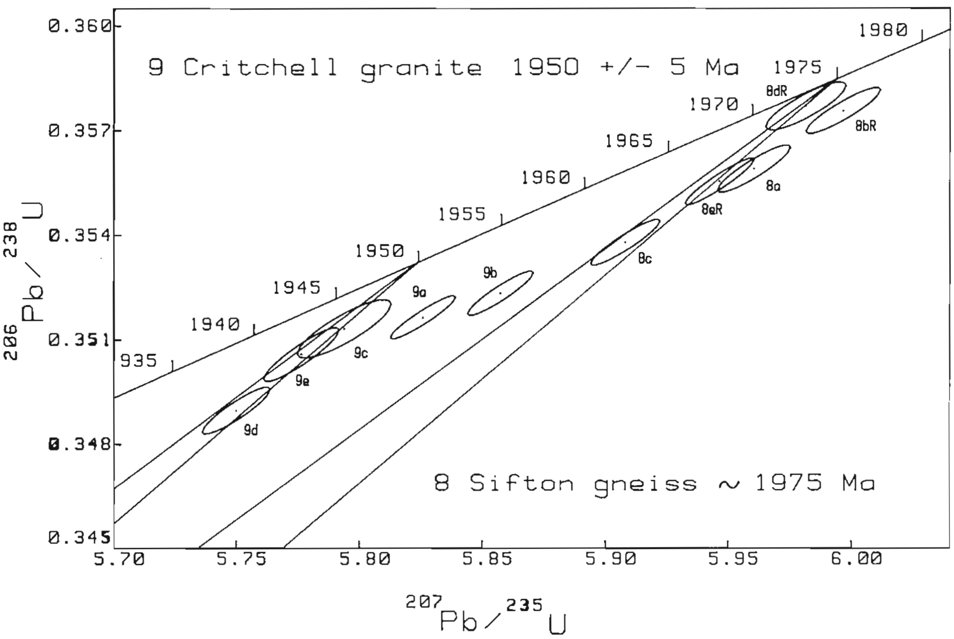

Figure 4. Isotope ratio plot for zircons from 8) Sifton gneiss and 9) Critchell granite. Numbers and letters identifying data points correspond to those of Table 1.

Critchell granite (samle 9; VK-86-ART85)

The Critchell granite occurs in a series of elongate lensoid bodies up to 3 km wide and 20 km long throughout the area mapped in the Thelon Tectonic Zone. The granite is everywhere a strongly deformed, pink and black, megacrystic rock that has a strong positive aeromagnetic expression in the central and western part of the domain. It has a strong lithological resemblance to the Musclow granite in the central domain as well as to the megacrystic granite dated by James et al. (1988) from a locality immediately northeast of the present map area. Although it is associated with granulite grade gneisses, it does not appear to have ever been at granulite grade itself. Henderson et al. (1987a) noted that the association of these granites with tectonic boundaries between subdomains within the Telon Tectonic Zone suggested a possible causal relationship.

The rock analyzed is strongly deformed and porphyroclastic, consisting mainly of coarse, weakly altered, anhedral to granulated orthoclase and some microcline porphyroclasts with inclusions of quartz and plagioclase, and lesser amounts of weakly to moderately altered, weakly zoned plagioclase of similar morphology but smaller size. Finely polycrystalline, coarse, very irregular, amoeboid masses of quartz show no preferred orientation. Hornblende, with smaller size but similar habit to the feldspar porphyroclasts, is the dominant mafic mineral. Brown scattered open aggregates of fine, essentially unaltered biotite is also present. There is also a weak tendancy for biotite to overgrow hornblende. The matrix is a fine, equigranular, broken assemblage of the porphyroclastic components with scattered open concentrations of biotite. Accessory minerals include abundant magnetite, apatite, sphene, zircon and allanite.

Zircons are colourless euhedral to subhedral, and generally with simple sharp terminations and L:B of 3:1. Igneous zoning and some cores are visible. Such cores could be more easily avoided in the clearest fine fractions.

Of the five fractions analyzed, the two coarsest (9a,b) show evidence of a component of inherited Pb (Fig. 4). The three remaining fractions are clustered with $^{207}Pb/^{206}Pb$ model ages ranging from 1950.5 to 1948.8 Ma. Given the near concordance of data points and apparent absence of cores in the finest fraction, the age of granite crystallization is placed at 1950 ± 5 Ma.[1]

DISCUSSION

Within the Archean of the Slave Province, a consistent pattern is appearing. First of all, volcanic ages in the eastern and southwestern Slave Province are accumulating in the 2695-2660 Ma age range. Although an earlier date appeared to indicate that the volcanism in the east was some 20 Ma older than volcanism in the west (van Breemen et al., 1987b), in view of the 2671 +2/-4 Ma age for the Clinton-Colden rhyolite, there may be a ca. 30 Ma range to the period of volcanism in the province.

[1] A caveat is added following additional U-Pb analysis of two strongly abraded single grains from the +149 μ fraction. Both analyses are concordant within large error envelopes and have $^{207}Pb/^{206}Pb$ ages of 1979 ± 9 Ma and 1980 ± 7 Ma. These identical model ages could be interpreted in terms of an inherited zircon Pb component. Sm-Nd whole-rock isotope data indicate a large older crystal component (unpublished data, E. Hegner). One cannot, however, exclude the hypothesis that magma emplacement was at 1980 Ma and that smaller zircons partially record a metamorphic event after 1950 Ma.

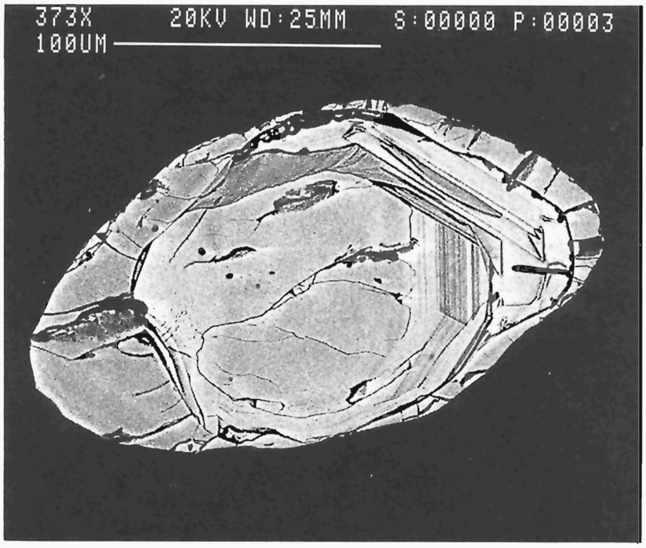

Figure 5. Scanning electron microscope image (backscattered electron mode) of polished and etched (HF) section of zircon from Sifton gneiss (sample 8). Partially resorbed core in which zoning is not visible is followed by an inner mantle of iregularly zoned zircon and an outer mantle of unzoned zircon with a rounded perimeter. The strong etching of the inner mantle reveals a higher U content.

Evidence is also accumulating for a significant, 40-50 Ma break between the end of volcanism and the onset of major plutonism. In the eastern part of the Slave Province, the earliest reliably dated, clearly post-volcanic igneous units are the tonalites of the Tarantula plutonic suite, dated at 2616 +7/−6 Ma in the Healey Lake map area and at 2622.0 +1.4/−1.2 Ma in the Artillery Lake area. Emplacement of the Charloit granodiorite at 2617 +/− 7 Ma appears to be part of the same plutonic event. Comparable ages have been obtained from the Defeat Plutonic suite in the southwestern Slave Province near Yellowknife (Henderson et al., 1987b).

The U-Pb monazite ages from the two-mica Ptarmigan granite at 2606 ± 5 Ma and the megacrystic Artillery Lake granite at 2596 +3/− 6 Ma appear to mark the end of plutonism in the Artillery Lake region. A megacrystic granodiorite in the southwestern Healey Lake map sheet has yielded an identical age of 2695 ± 10 Ma. North of the Bathurst Fault, two-mica granites have been dated (U-Pb monazite) at 2597 +5/−3 and 2585 ± 2 Ma (Tinney Hills-Overby Lakes area; Thompson et al., 1986; van Breemen et al., 1987c). Thus although the two-mica granites are generally late in the plutonic evolution, they do not appear to constitute part of a separate pulse, as their ages overlap with ages of the megacrystic granites. Continuous igneous activity from the time of emplacement of the earlier tonalite-granodiorite suite is also apparent but remains to be proved. A considerable proportion of the plutonism so far dated in the Slave Province is thus bracketed in the 2625-2585 Ma time interval with as yet no apparent regional recognizable age variation.

Gneiss and megacrystic granite from the central domain in the Artillery Lake area, characterized by foliated plutonic rocks and gneisses that are not at granulite facies, yield ages of about 2.6 Ga. The 2603 +5/−4 Ma age of the megacrystic Musclow granite cannot be distinguished from the ages of megacrystic granite to the west. Plutonic ages from the central domain of the Artillery Lake map sheet are also comparable to the grey and pink gneiss north of the Bathurst Fault, situated west of the terrane of abundant Yellowknife Supergroup outcrop and east of the first appearance of granulite facies rocks and Proterozoic granitoids (Thompson et al., 1986; van Breemen et al., 1987c). These terranes, therefore, both north and south of the Bathurst Fault, appear to be deeper levels of the Slave Craton, largely denuded of high-level Slave-type metasediments, involved in Proterozoic metamorphism, but forming terranes generally of the same age as the main magmatic event in the Slave Province.

The eastern edge of the wide shear zone at the eastern margin of the central zone involving both Archean supracrustal and granitoid rocks, forms the break between Slave Craton of the central zone and younger rocks of the Thelon Tectonic Zone, and is consistent with the break in rock types specified in the southwestern Healey Lake map sheet by James (1985). The 1950 ± 5 Ma age for the megacrystic Critchell granite appears to be about 25 Ma older than a U-Pb zircon age obtained from the more extensive megacrystic granite in the eastern extension of the mapping traverse of James (1986), but is in agreement with a 1957 +9/-5 Ma age for a syntectonic hornblende granite from the same area (James et al,, 1988). The 1950 Ma age for the Critchell megacrystic granite provides a minimum age for granulite facies metamorphism in the easten Artillery Lake area, while the 1975 Ma age for the concordant zircon fraction of the Sifton gneiss appears to provide a maximum age. Such an age bracket is consistent with the evidence from the southeastern Healey Lake map sheet (Henderson et al., 1982) where granulite facies metamorphism has been bracketed in the 1990-1950 Ma interval (van Breemen et al., 1987a). As in the Healey Lake and Tinney Hills Overby lake map sheets, the eastern region of granulite facies rocks has not provided evidence for Archean precursors equivalent in age to the Slave Province.

REFERENCES

Davis, D.

1982: Optimum linear regression and error estimation applied to U-Pb data; Canadian Journal of Earth Sciences, v. 19, p. 2141-2149.

Henderson, J.B.

1985: Geology of the Yellowknife-Hearne Lake area, District of Mackenzie: a segment across an Archean basin; Geological Survey of Canada, Memoir 414, 135 p.

Henderson, J.B. McGrath, D.T. James, and Macfie, R.I

1987a: An integrated geological, gravity and magnetic study of the Artillery Lake area and the Thelon Tectonic Zone, District of Mackenzie; *in* Current Research, Part A, Geological Survey of Canada, Paper 87-1A, p. 803-814.

Henderson, J.B., Thompson, P.H., and James, D.T.

1982: The Healey Lake map area and the Thelon Front problem, District of Mackenzie; *in* Current Research, Part A, Geological Survey of Canada, Paper 82-1A, p. 191-195.

Henderson, J.B., van Breemen, O., and Loveridge, W.D.

1987b: Some U-Pb zircon ages from Archean basement, supracrustal and intrusive rocks, Yellowknife-Hearne Lake area, District of Mackenzie; *in* Radiogenic Age and Isotopic Studies: Report 1; Geological Survey of Canada, Paper 87-2, p.111-121.

James, D.T.

1985: Geology of the Moraine Lake area and the Thelon Front, District of Mackenzie; *in* Current Research, Part A, Geological Survey of Canada, Paper 85-1A, p. 449-454.

1986: The geology of the Moraine Lake area, District of Mackenzie, part 2; a transect across part of the Thelon Tectonic Zone; *in* Current Research, Part A, Geological Survey of Canada, Paper 86-1A, p. 417-421.

James, D.T., van Breemen, O., and Loveridge, W.D.

1988: Early Proterozoic U-Pb zircon ages for granitoid rocks from the Moraine Lake transect, Thelon Tectonic zone, District of Mackenzie; *in* Radiogenic Age and Isotopic Studies: Report 2, Geological Survey of Canada, Paper 88-2.

Parrish, R.R.

1988: U-Pb systematics of monazite and a preliminary estimate of its closure temperature based on natural examples (abstract); Geological Association of Canada, MAC, CGU, Program with Abstracts, v. 11, p. 139.

Parrish, R.R., Roddick, J.C., Loveridge, W.D., and Sullivan, R.W.

1987: Uranium-lead analytical techniques at the geochronology laboratory, Geological Survey of Canada; *in* Radiogenic Age and Isotopic Studies: Report 1; Geological Survey of Canada, Paper 87-2, p. 3-7.

Thompson, P.H., Culshaw, N., Buchanan, J.R. and Manojlovic, P.

1986: Geology of the Slave Province and Thelon Tectonic Zone in the Tinney Hills-Overby Lake (west half) map area, District of Mackenzie; *in* Current Research, Part A, Geological Survey of Canada, Paper 86-1A, p. 275-289.

van Breemen, O., Henderson,J.B., Loveridge, W.D., and Thompson, P.H.

1987a: U-Pb zircon and monazite geochronology and morphology of granulites and granite from the Thelon Tectonic zone, Healey Lake and Artillery Lake map area, N.W.T.; *in* Current Research, Part A, Geological Survey of Canada, Paper 87-1A, p. 783-801.

van Breemen, O., Henderson, J.B., Sullivan, R.W., and Thompson, P.H.

1987b: U-Pb, zircon and monazite ages from the eastern Slave Province, Healey Lake area, N.W.T.; *in* Radiogenic Age and Isotopic Studies: Report 1; Geological Survey of Canada, Paper 87-2, p. 101-110

van Breemen, O., Thompson, P.H.,Hunt, P.A., and Culshaw, N.

1987c: U-Pb zircon and monazite geochronology from the northern Thelon Tectonic Zone, District of Mackenzie; *in* Radiogenic Age and Isotopic Stuies: Report 1; Geological Survey of Canada, Paper 87-2, p. 81-93.

York, D.

1969: Least squares fitting of a straight line with correlated errors; Earth and Panetary Science Letters, v. 5, p. 320

U-Pb zircon ages for felsic volcanism in Slave Province, N.W.T.

J.K. Mortensen[1], R.I. Thorpe[1], W.A. Padgham[2], J.E. King[1] and W.J. Davis[3]

Mortensen, J.K., Thorpe, R.I., Padgham, W.A., King, J.E., and W.J. Davis, U-Pb zircon ages for felsic volcanism in Slave Province, N.W.T.; in Radiogenic Age and Isotopic Studies: Report 2, Geological Survey of Canada, Paper 88-2, p. 85-95, 1988.

Abstract

U-Pb zircon dating of felsic volcanic rocks from widely separated sites in the eastern, central and northern Slave Province, together with previously published age data, have shown that volcanism occurred in two main episodes, at 2698-2687 Ma and at 2671-2663 Ma. Preliminary data for a sample from Point Lake suggest that supracrustal rocks greater than 2827 Ma in age may be present in this area. Supracrustal sequences elsewhere in the western Slave Province may also include rocks substantially older than are recognized in the rest of the province. Two ages for units interpreted as possible volcanics, in the Izok and Concession lakes areas, are 60 Ma younger than the end of major volcanic activity. If these units are extrusive, they would indicate that deposition of the Yellowknife Supergroup strata lasted considerably longer than previously thought. However, an alternative hypotheses, that the units represent relatively late, high-level intrusions, is equally possible given the available data.

These data demonstrate that there were at least two episodes of formation of volcanogenic massive sulphide deposits in the Slave Province, and provide constraints for evaluating the various models that have been proposed for the tectonic evolution of the province.

Résumé

Une datation par la méthode U-Pb appliquée aux zircons de roches volcaniques felsiques provenant d'endroits éloignés dans l'est, le centre et le nord de la province des Esclaves, ainsi que des datations antérieurement publiées, ont montré que le volcanisme s'est produit pendant deux principaux épisodes, entre 2698 et 2687 Ma et entre 2671 et 2663 Ma. Des données préliminaires sur un échantillon provenant du lac Point semblent indiquer qu'il pourrait se trouver dans cette région des roches supracrustales antérieures à 2827 Ma. Des séquences supracrustales, ailleurs dans l'ouest de la province des Esclaves, pourraient également contenir des roches beaucoup plus anciennes que ce que l'on a établi dans le reste de la province.

Deux datations d'unités interprétées comme pouvant être des roches volcaniques au sein de la région des lacs Izok et Concession indiquent que ces dernières sont 60 Ma plus récentes que la fin de la principale activité volcanique. S'il s'agit d'unités extrusives, elles pourraient indiquer que la sédimentation des couches du supergroupe de Yellowknife a duré bien plus longtemps qu'il n'avait auparavant été établi. Toutefois, les données dont on dispose permettent l'examen d'une autre hypothèse, selon laquelle ces unités représentent des intrusions de haut degré relativement récentes.

Selon ces données, il y aurait eu au moins deux épisodes de formation de gisements de sulfure massif d'origine volcanique dans la province des Esclaves. Elles limitent aussi l'évaluation de différents modèles proposés de l'évolution tectonique de cette province.

[1] Geological Survey of Canada, 601 Booth Street, Ottawa, Ontario K1A 0E8

[2] Geology Division, Department of Indian Affairs and Northern Development, Box 1500, Yellowknife, N.W.T. X1A 2R3

[3] Department of Earth Sciences, Memorial University of Newfoundland, St. John's, Newfoundland A1B 3X5

INTRODUCTION

The Slave Province is an Archean cratonic block in the northwestern part of the Canadian Shield. Although similar to other Archean cratons in most respects, the Slave Province is unusual in that the supracrustal rocks (collectively assigned to the Yellowknife Supergroup) consist predominantly of metasediments (about 80 %) and metavolcanic rocks are much less abundant (McGlynn and Henderson, 1970). The metavolcanic rocks occur mainly in three discontinuous zones (Fig. 1), an eastern zone (Artillery Lake-Back River-Hackett River-Canoe Lake-High Lake areas), a central zone (Yellowknife-Turnback Lake-eastern Point Lake-Takijuq Lake areas), and a western zone (Russell Lake-Indin Lake areas). The eastern zone includes abundant rocks of intermediate to felsic composition, whereas the central and western zones tend to consist predominantly of mafic rocks (e.g. Padgham, 1985).

Four main tectonic scenarios have been proposed to explain the origin of the Slave Province and the proportion and present disposition of volcanic rocks with respect to sediments. McGlynn and Henderson (1970) and Henderson (1981, 1985) suggested that the major sedimentary sequences of the Slave Province were deposited in intracontinental rift basins, with volcanism localized along marginal faults. Kusky (1988, pers. comm., 1988) divided the Slave Province into four separate terranes, the Hackett River volcanic terrane (magmatic arc), Contwoyto terrane (accretionary prism), Anton terrane (microcontinental fragment), and Sleepy Dragon terrane (possibly equivalent to Anton terrane). In this model, the Slave Province is considered to have evolved as a west-facing subduction complex, which subsequently collided with the Anton microcontinent. Helmstaedt et al. (1986) argued that at least parts of the Slave Province, and in particular some of the volcanic sequences around Yellowknife, represent the products of Archean seafloor spreading. Fyson and Helmstaedt (1988), in an extension of the model of Helmstaedt et al. (1986), suggested early rifting of pre-3 Ga sialic crust to produce oceanic crust now preserved as the mafic-dominated greenstone belts (ophiolitic assemblages) in the central and western Slave Province. Subsequent closure of this ocean basin by subduction along an east dipping subduction zone resulted in arc magmatism in the eastern volcanic belt, and eventual collision of the previously rifted sialic block with the subduction complex. Hoffman (1986 and in press) suggested that the Slave province evolved as a prograding arc-trench system (direction unspecified), and comprises a collage of arc volcanic and plutonic rocks, fore-arc basin deposits, and exotic blocks (possibly including seamounts, ophiolitic fragments and microcontinental blocks) scraped off the subducting plate.

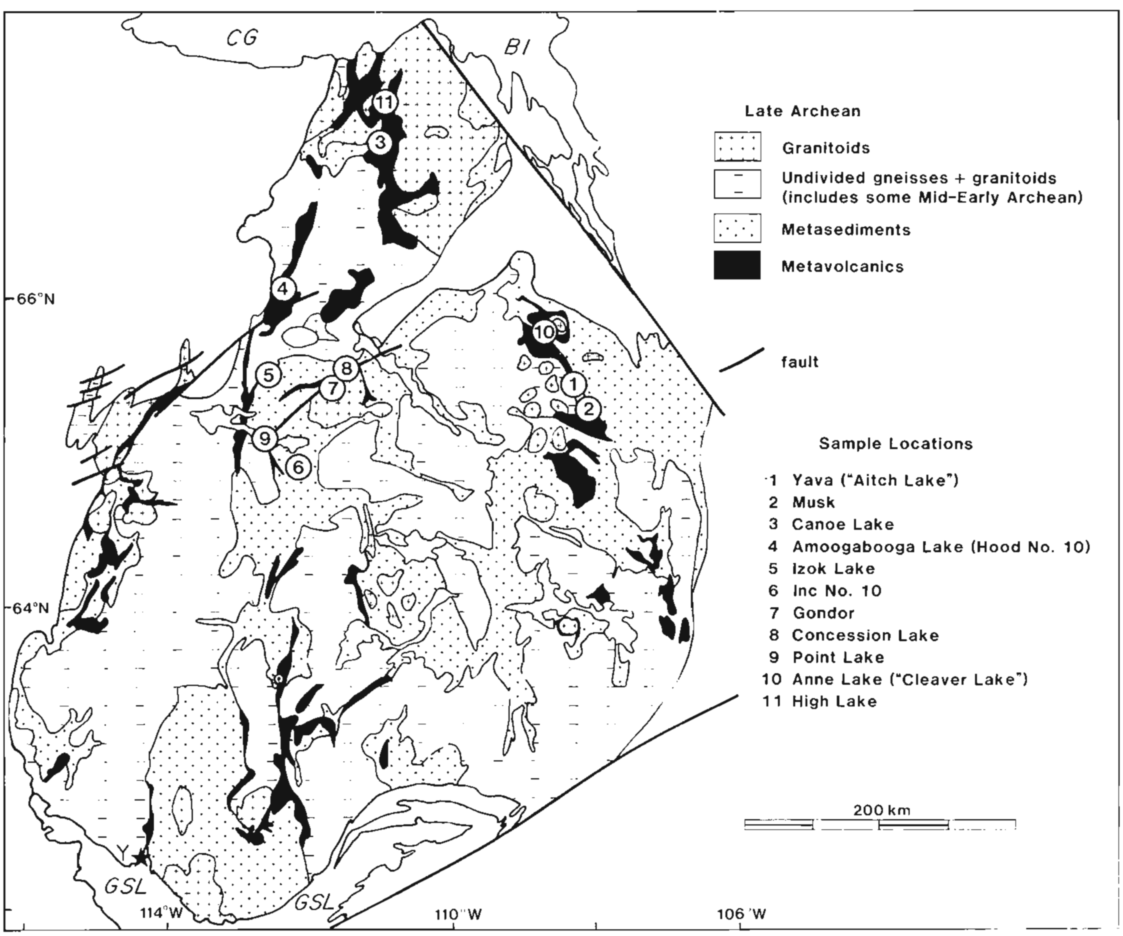

Figure 1. Generalized geological map of the Slave Province (excluding that part northeast of Bathurst Inlet), simplified from Padgham (1985). Large bodies of water: BI = Bathurst Inlet; CG = Coronation Gulf; GSL = Great Slave Lake. Location of Yellowknife shown as "Y". Localities of samples dated for this study are shown as numbered dots. Samples 10 (Anne Lake) and 11 (High Lake) are in the process of being dated.

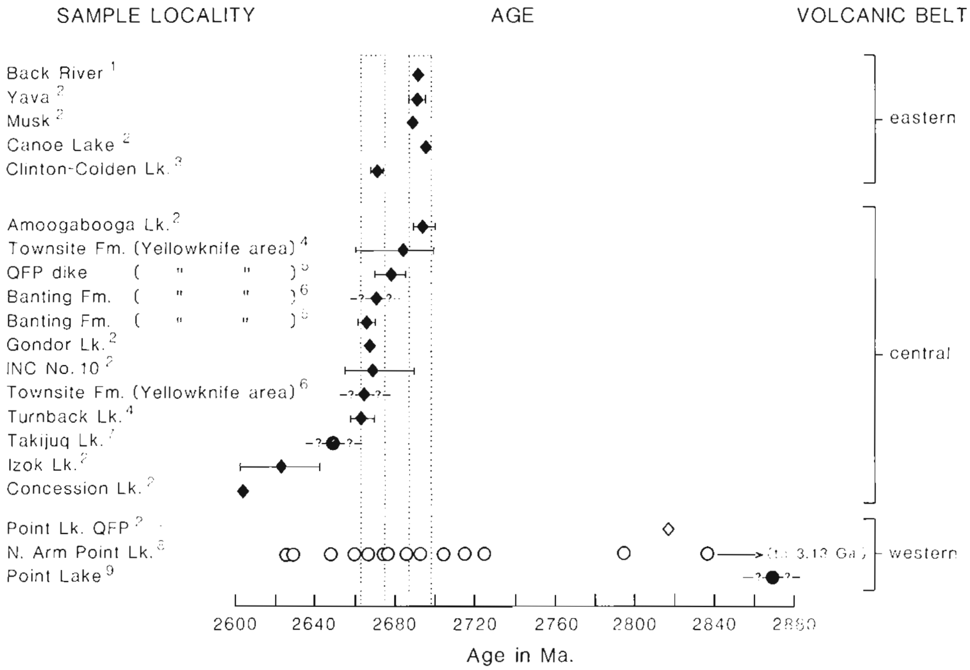

Figure 2. Summary of reliable U-Pb zircon age data for supracrustal rocks in Slave Province. Solid diamonds and error bars are volcanic ages and assigned errors. Open diamonds are Pb/Pb zircon minimum ages for volcanic rocks. Solid circles are ages of cobbles in conglomeratic units, and open circles are Pb/Pb zircon minimum ages for detrital grains in sediments. Dotted vertical bars represent age ranges for the two main episodes of volcanism in Slave Province (2698-2687 Ma and 2675-2663 Ma; see text for explanation). Data sources are: 1) van Breemen et al., 1987a; 2) this study; 3) van Breemen and Henderson, 1988; 4) Henderson et al., 1987; 5) Bowring (*in* Padgham, 1985); 6) Bowring and Padgham, 1987; 7) Krogh (*in* Padgham, 1985); 8) Scharer and Allegre, 1982; 9) Krogh and Gibbins, 1978.

Although the results of the present study do not conclusively prove or disprove any of the above scenarios, they expand considerably the database required to evaluate the relative merits of each model.

Very few U-Pb zircon ages are available for the supracrustal sequences in the Slave Province. Available reliable age data are summarized in Figure 2. Model lead ages for galena specimens from volcanogenic massive sulphide deposits distributed throughout the province suggest that the host volcanic sequences are mainly in the range of ca. 2.69-2.66 Ga (Frith and Loveridge, 1982; Franklin and Thorpe, 1982; Thorpe, 1982 and unpublished data). An exception is an older model age of about 2725 Ma for a small zone of base metal mineralization reported by Henderson (1975) on the south shore of Point Lake.

In this study, U-Pb zircon geochronology has been undertaken on 9 specimens of felsic to intermediate volcanic and metavolcanic rocks from the eastern, north-central and northern Slave Province (Fig. 1). Most of the specimens are from sites in the vicinity of volcanogenic massive sulphide deposits. The purpose of the study is threefold; first, to establish crystallization ages for volcanic units in Slave Province as a basis for regional stratigraphic correlation and tectonic synthesis; second, to determine ages for volcanogenic massive sulphide deposits, as a contribution to regional metallogenic studies of the Slave Province; and third, to establish an age framework with which to construct lead isotopic evolution models for Slave Province using isotopic analyses of galena from the base metal deposits.

ANALYTICAL TECHNIQUES

Zircons were separated from 10 to 25 kg samples using standard Wilfley table and heavy liquid techniques. Details of zircon selection, abrasion, dissolution and analysis are reviewed by Parrish et al. (1987). A Finnegan MAT 261 solid source mass spectrometer was employed for the analyses. Total procedural Pb blanks ranged from 0.007 to 0.015 nanograms and U blanks were about 0.001 nanograms. Errors assigned to isotopic ratios and calculated ages were determined using the numerical error propagation technique of Roddick (1987). Concordia intercept ages were obtained using the line-fitting technique of Davis (1982) (unless otherwise noted) and the algorithm of Ludwig (1980). All errors are quoted at the 2 sigma level (95 % confidence interval).

SAMPLE DESCRIPTIONS AND ANALYTICAL RESULTS

1. YAVA. The sample was collected from the northern shore of Friday (Aitch) Lake about 2.5 km southeast along strike from, and at approximately the same stratigraphic level as, the Yava massive sulphide deposit (Fig. 1). It is a massive, unfoliated quartz feldspar porphyry showing minor sericite and carbonate alteration, and is typical of unit 3a in this area as mapped by Padgham et al. (1975). Zircon in the sample is clear and colourless to pale pink, forming stubby square prisms with simple terminations. Many of the grains show resorbed surfaces. Five fractions were analyzed

Table 1. U-Pb zircon analytical data

Fraction, Size[1]	Weight (mg)	U (ppm)	Pb[2] (ppm)	$^{206}Pb/^{204}Pb$ [3]	Pb_c[4] (pg)	^{208}Pb[2] (%)	$^{206}Pb/^{238}U$ +/−SEM%[5]	$^{207}Pb/^{235}U$ +/−SEM%[5]	$^{207}Pb/^{206}Pb$ +/−SEM%[5]	$^{207}Pb/^{206}Pb$ age, error (Ma)[6]
1. YAVA (62°36′39″N; 107°56′12″W)										
A NM1,+149,a	0.043	39.0	22.5	4193	12.8	10.1	0.51076 (.087)	12.8452 (.100)	0.18240 (.030)	2674.8 (0.5)
B NM1,-149+105, <M,a	0.028	42.5	25.6	1681	14.6	12.7	0.51579 (.135)	13.0711 (.144)	0.18380 (.037)	2687.4 (0.6)
C NM1,-149+105, >M,a	0.037	65.7	39.0	5317	14.9	11.8	0.51374 (.088)	12.9748 (.100)	0.18317 (.030)	2681.8 (0.5)
D NM2,+149,a	0.078	27.0	14.9	2286	28.5	10.6	0.48693 (.094)	12.1425 (.108)	0.18086 (.034)	2660.7 (0.6)
E NM2,-149+105,a	0.016	48.0	27.8	1315	19.2	10.9	0.50518 (.120)	12.8950 (.132)	0.18440 (.042)	2692.8 (0.7)
2. MUSK (65°19′20″N; 107°36′00″W)										
A NM1,+149,a	0.007	20.6	12.9	5062	10.0	15.7	0.51938 (.395)	13.1522 (.396)	0.18366 (.088)	2686.2 (1.5)
B NM1,-149+105,a	0.046	69.7	41.7	7041	14.7	12.9	0.51129 (.087)	12.9508 (.099)	0.18371 (.029)	2686.6 (0.5)
C NM2,+149,a	0.033	14.2	8.6	1327	11.3	14.3	0.50855 (.137)	12.9137 (.145)	0.18381 (.044)	2687.5 (0.7)
D NM2,-149+105,a	0.020	82.1	44.4	2626	18.1	12.0	0.46708 (.098)	11.8312 (.109)	0.18371 (.031)	2686.7 (0.5)
E NM5,+105,a	0.023	69.8	38.3	2887	17.0	12.1	0.50947 (.098)	12.9218 (.109)	0.18395 (.034)	2688.8 (0.6)
F NM1,-105+74,a	0.027	54.0	32.1	3084	15.2	11.7	0.51633 (.087)	13.0999 (.106)	0.18401 (.032)	2689.3 (0.5)
3. Canoe Lake (67°08′33″N; 111°03′08″W)										
A NM2,-149+74,a	0.024	121	71.4	4556	20.7	11.1	0.51475 (.088)	13.0975 (.100)	0.18454 (.030)	2694.1 (0.5)
B NM2,-74+62,a	0.020	155	91.7	5506	17.8	12.5	0.50781 (.088)	12.8730 (.100)	0.18386 (.032)	2688.0 (0.5)
C NM5,-74+62,a	0.027	157	89.8	4315	30.6	12.7	0.48854 (.085)	12.4313 (.098)	0.18455 (.031)	2694.2 (0.5)
4. Amoogabooga Lake (66°04′18″N; 112°42′25″W)										
A NM1,+74, <M,a	0.032	295	174.8	8800	34.5	11.6	0.51383 (.084)	12.9689 (.092)	0.18305 (.029)	2680.7 (0.5)
B NM1,+74, >M,a	0.016	284	167.1	9882	14.5	11.4	0.51241 (.089)	12.9342 (.101)	0.18307 (.028)	2680.9 (0.5)
C NM2,+93,a	0.036	237	139.6	6858	39.8	11.4	0.51343 (.083)	12.9582 (.096)	0.18305 (.029)	2680.7 (0.5)
D NM5,+93,a	0.054	277	160.5	13810	34.1	12.1	0.50166 (.088)	12.4383 (.100)	0.17983 (.028)	2651.3 (.05)
5. Izok Lake (65°37′41″N; 112°40′12″W)										
A NM5,+62, <M,a	0.017	2248	1168	4034	264.1	14.4	0.44059 (.097)	10.4573 (.110)	0.17214 (.035)	2578.6 (0.6)
B NM5,-62, >M,a	0.011	1691	819.5	4907	98.5	14.8	0.41096 (.087)	9.4577 (.100)	0.16691 (.032)	2526.9 (0.6)
C NM7,-105+74,a	0.009	2227	845.4	1781	216.9	17.9	0.30659 (.098)	6.4641 (.122)	0.15292 (.060)	2378.8 (1.0)
D NM7,+105,a	0.030	1834	703.6	685	1447	27.3	0.28249 (.124)	5.6351 (.207)	0.14467 (.144)	2283.9 (2.5)
E NM7,+105,a,6 gr.	0.007	2083	744.7	1228	215.3	21.5	0.28435 (.086)	5.7108 (.129)	0.14566 (.079)	2295.6 (1.4)
F NM7,+105,a,3 gr.	0.011	1401	512.5	1583	174.4	19.8	0.29490 (.085)	6.3287 (.115)	0.15565 (.060)	2408.9 (1.0)
G NM7,-105+74,clr,a	0.038	463	179.1	1769	200.1	18.7	0.31673 (.084)	6.7089 (.111)	0.15362 (.056)	2386.7 (1.5)
6. INC No. 10 (65°05′30″N; 112°15′00″W)										
A NM2,+93,t,a	0.031	796	450.6	14520	53.9	10.8	0.49787 (.084)	12.2555 (.096)	0.17853 (.028)	2639.3 (.05)
B NM2,+149,a	0.018	1348	764.6	2211	345.8	10.8	0.49920 (.085)	12.2687 (.085)	0.17825 (.044)	2636.6 (0.7)
C NM2,-149+105,p,a	0.029	686	357.8	7338	84.3	5.9	0.48515 (.083)	11.7300 (.097)	0.17536 (.029)	2609.5 (0.5)
D NM2,-149+105, <M,a	0.059	864	481.0	18470	85.6	10.1	0.49384 (.083)	12.1065 (.102)	0.17780 (.028)	2632.5 (0.5)
E NM5,+93,t,a	0.017	789	444.5	3772	108.8	10.3	0.49843 (.083)	12.2668 (.098)	0.17850 (.034)	2638.9 (0.6)
F NM5,+105,p,a	0.020	1155	638.3	26720	26.8	9.1	0.49595 (.089)	12.0927 (.101)	0.17684 (.028)	2623.5 (0.5)
7. Gondor Lake (65°34′N; 111°48′W)										
A NM1,+105,a	0.024	78.1	46.3	4761	76.3	13.0	0.50694 (.088)	12.6746 (.100)	0.18132 (.031)	2665.0 (0.5)
B NM1,-149+93, <M,a	0.022	97.1	58.2	3424	19.7	13.4	0.50988 (.089)	12.7061 (.102)	0.18150 (.033)	2666.7 (.06)
C NM1,-149+93, >M,a	0.013	89.1	53.1	1631	76.5	13.0	0.51041 (.095)	12.7663 (.112)	0.18140 (.046)	2665.7 (0.8)
D NM2,-149+105,a	0.024	80.9	47.6	5549	11.1	12.6	0.50669 (.090)	12.6637 (.102)	0.18127 (.029)	2664.5 (0.5)
E NM2,-105+74,a	0.014	98.0	58.0	3722	12.2	12.7	0.50793 (.090)	12.7009 (.103)	0.18135 (.030)	2665.3 (0.5)
8. Concession Lake (65°42′N; 11134″W)										
A NM5,-105+74,p,a	0.041	363	206.0	5869	76.5	14.6	0.47622 (.084)	12.0385 (.097)	0.18334 (.030)	2683.3 (0.5)
B NM5,-149+105,r,a	0.005	275	172.4	573	58.4	32.9	0.41807 (.114)	9.6791 (.181)	0.16791 (.116)	2537.0 (2.0)
C NM2,-105+74,clr,a	0.040	54.3	28.7	3222	21.1	5.6	0.49311 (.094)	11.8804 (.107)	0.17474 (.032)	2603.5 (0.5)
D NM2,-105+74,p,a	0.037	71.3	42.8	5995	14.7	9.8	0.52750 (.087)	14.0992 (.099)	0.19385 (.029)	2775.1 (0.5)
E NM2,-149+105, <M,s,a	0.052	48.8	25.7	4605	17.3	4.7	0.49633 (.102)	11.9592 (.113)	0.17476 (.030)	2603.7 (0.6)
F NM2,-149+105, <M,s,a	0.015	44.1	23.0	1293	16.4	4.2	0.49498 (.149)	11.9234 (.165)	0.17471 (.037)	2603.3 (0.6)
G NM2,-149+105, >M,s,a	0.017	8.3	4.3	252	18.4	4.0	0.49354 (.603)	11.8646 (.660)	0.17435 (.108)	2599.9 (1.8)
H NM2,-149+105, >M,s,a	0.015	118	59.4	3847	14.6	2.5	0.48664 (.104)	11.7158 (.116)	0.17461 (.030)	2602.3 (0.5)
9. Point Lake (65°13′30″N; 11252′15″W)										
A NM1,+74,a	0.017	251	157.0	4376	32.3	11.1	0.53832 (.090)	14.8542 (.102)	0.20013 (.030)	2827.2 (0.5)
B NM1,-74+62,a	0.009	374	230.4	2277	48.9	14.3	0.51601 (.092)	13.5068 (.098)	0.18938 (.037)	2740.8 (0.5)
C NM2,+74,a	0.034	316	174.2	8721	37.5	10.5	0.48445 (.083)	12.2236 (.096)	0.18300 (.029)	2680.2 (0.5)
D NM5,+74,a	0.018	469	289.8	4057	66.0	17.9	0.49512 (.084)	12.9280 (.098)	0.18938 (.032)	2736.7 (0.5)

Notes: [1]sizes (-74+62) refer to length aspect of zircons in microns (i.e. through 74 micron sieve but not the 62 micron sieve); NM1,2,5,7=non-magnetic cut with Frantz at 1, 2, 5 or 7 degrees side slope; <M, >M=non-magnetic,magnetic with cobalt magnet; t=tablets; p=prismatic grains; r=round grains; s=single grain; a=abraded; [2]radiogenic Pb; [3]measured ratio, corrected for spike and fractionation; [4]total common Pb in analysis corrected for fractionation and spike; [5]corrected for blank Pb and U, common Pb, errors quoted are one sigma in per cent; [6]corrected for blank and common Pb, errors are one sigma in Ma; decay constants used are those of Steiger and Jäger (1977); initial common Pb compositions from Cumming and Richards (1975); for analytical details see Parrish et al. (1987).

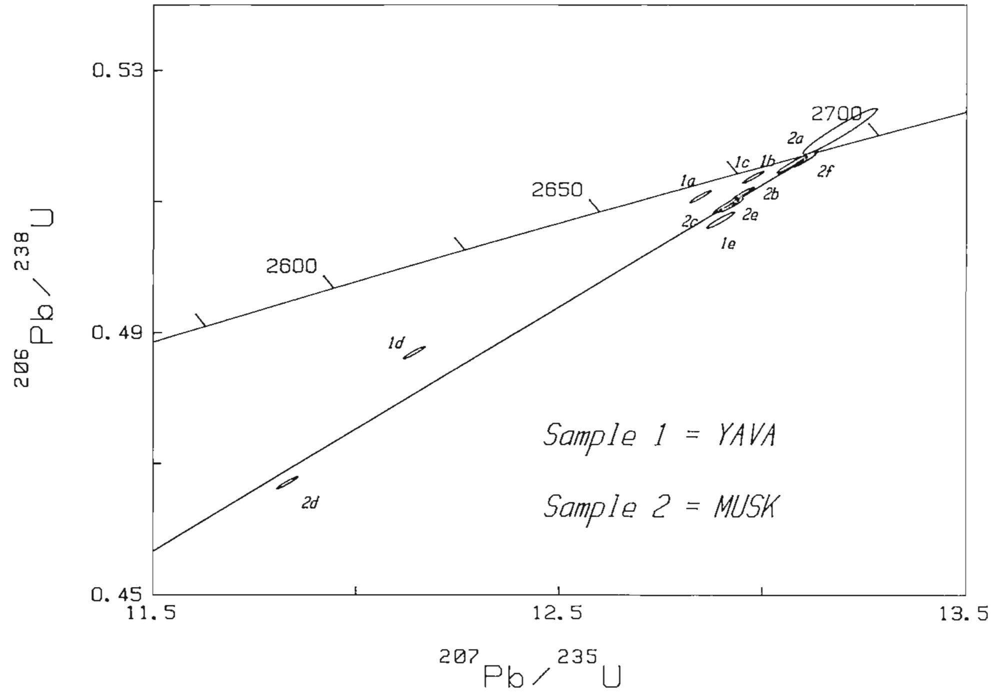

Figure 3. U-Pb concordia plot of zircon data from samples 1 (YAVA) and 2 (MUSK). Discordia line fit to 5 of the 6 MUSK analyses is shown.

(Table 1). One fraction (1b) is nearly concordant, and the remaining fractions form a non-linear array with up to 8 % discordance (Fig. 3). The cause(s) of this scatter are probably complex. Fraction 1e is 5.9 % discordant, but yields an older Pb-Pb age than the nearly concordant fraction, suggesting that there may be a small amount of inheritance present in at least fraction 1e. Discordia lines through fraction 1b and other single analyses yield lower intercept ages as old as 1970 Ma. This may indicate that significant Pb loss of Early Proterozoic age has occurred, in addition to recent Pb loss effects that have not been entirely avoided by abrasion. It is not possible to establish a precise crystallization age for the sample from such scattered data points; however, the age can reasonably be bracketed between the Pb-Pb age of the most concordant fraction (2687.4 Ma) and the oldest upper intercept age for a two-point discordia line through this fraction (2695.8 Ma). More single crystal analyses are planned to better define the age of this sample.

2. MUSK. The sample is a recrystallized intermediate to felsic volcanic rock containing rare preserved fine quartz phenocrysts and clots of dark green amphibole. It was collected from immediately south of the southeast shore of a small, horseshoe-shaped lake located about 5.5 km west of the Musk massive sulphide deposit (Fig. 1). Zircons from the sample form clear, pale pinkish, stubby prisms with simple terminations and locally resorbed surfaces. Six fractions were analyzed (Table 1, Fig. 3). One relatively imprecise analysis (fraction a) falls slightly above concordia. This was a very small sample of low-uranium zircon, and the analysis indicated a Pb content of only 95 picograms. As a result, the calculated parent daughter ratios are very sensitive to the compositions assumed for blank and common leads. The other five analyses form a linear array with calculated upper and lower intercept ages of 2689.3 +2.4/-1.8 Ma and 231.1 Ma, respectively. The upper intercept age is considered to be the crystallization age of the rock, and the lower intercept age indicates mainly recent Pb loss. The error envelope for fraction a overlaps the calculated regression line, but the analysis for this fraction was not included in the regression due to its larger associated errors and reverse discordance.

3. Canoe Lake. The sample was collected from an exposure assigned to unit 8 (quartz-feldspar porphyry) by Yeo et al. (1983). It consists of an unfoliated, fine grained mass of quartz, feldspar, biotite and trace muscovite, with rare strained and partially recrystallized quartz phenocrysts. The sample site is 2.6 km northeast of the east end of Canoe Lake (Fig. 1), and about 4.1 km from where massive sulphide-type mineralization and galena-bearing boulders were discovered near the western end of the lake. Zircon recovered from the rocks is clear, almost colourless, and forms stubby prisms, most of which display smoothly resorbed surfaces. Three fractions were analyzed (Table 1, Fig. 4). They range from 0.6 to 5.6 % discordant, but do not define a linear array. As the zircon appears to represent a single, homogeneous population with no evidence for inherited cores or xenocrysts, the crystallization age should be bracketed by the Pb-Pb age of the most concordant point (2691.4 Ma) and the oldest upper intercept age calculated for a two point discordia line through this point (2698.5 Ma). More analyses are planned to better constrain the age of this rock.

4. Amoogabooga Lake (Hood River No. 10). The sample was taken from a site on the east shore of a southward-projecting arm of the lake (Fig. 1), about 2.5 km east-northeast of the small Hood River No. 10 massive sulphide deposit (located 4.3 km ESE of the southeast shore of Takijuq Lake; Gill, 1977). It is from unit 3a felsic volcanic flows as mapped by Hyde et al. (1976). The rock is a weakly deformed quartz-feldspar porphyry, with subhedral feldspar and strongly resorbed quartz phenocrysts

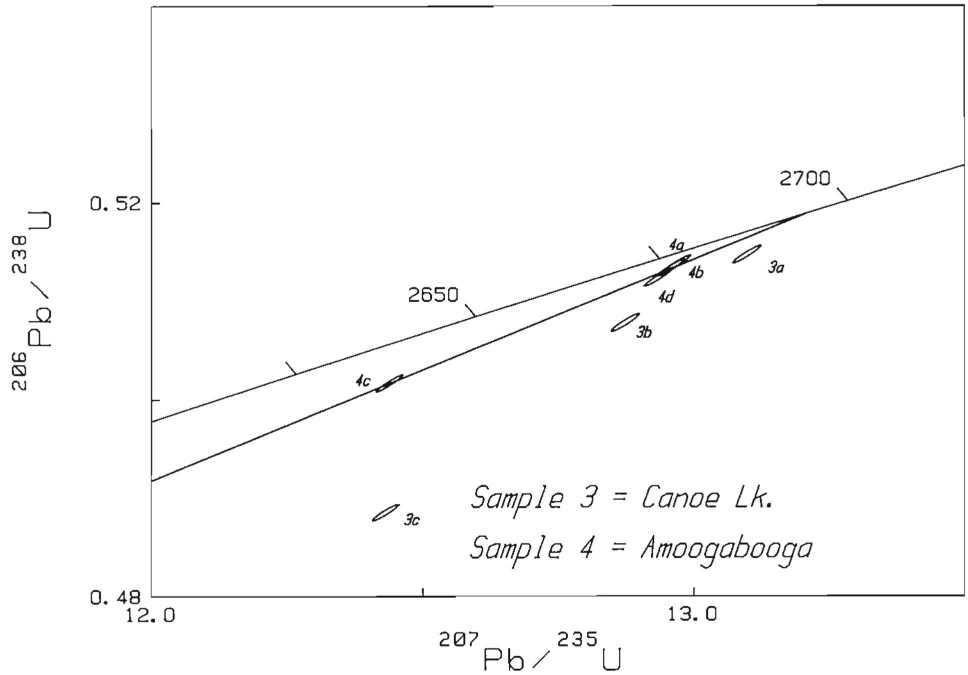

Figure 4. U-Pb concordia plot of zircon data from samples 3 (Canoe Lake) and 4 (Amoogabooga Lake). Best-fit line to Amoogabooga Lake data is shown.

in a slightly sericitized and chloritized groundmass. Zircon in the sample consists of very pale pinkish brown, stubby, euhedral grains with square cross-sections and simple terminations. Analyses of four fractions (Table 1, Fig. 4) define a linear array with upper and lower intercepts of 2694.4 +7.0/-4.5 Ma and 1946 Ma. The upper intercept gives the crystallization age of the rock, and the lower intercept reflects a Pb loss event of Early Proterozoic age.

5. Izok Lake. The specimen for dating was obtained from the south shore of Izok Lake (Fig. 1) from a felsic volcanic unit (unit 3 as mapped by Bau et al. 1979; *see also* Bostock, 1980). This site is approximately 0.6 km west-southwest from the Izok Lake massive sulphide deposit. Supracrustal rocks in this area are highly strained and metamorphosed, and protoliths are generally not easily recognizable. The sample is a thinly layered schist, consisting of a fine grained equigranular assemblage of quartz, feldspar and minor biotite and muscovite. Clots of fibrolitic sillimanite occur locally. Although no relict igneous textures are preserved, the rock resembles other felsic metavolcanic rock units in the area (H.H.Bostock, pers. comm., 1987).

Zircons recovered from the sample show a uniform morphology, forming stubby, subhedral to euhedral grains with large, sharp-edged facets with no evidence of metamorphic overgrowths. All grains are strongly paramagnetic, and display well developed internal growth zoning and pervasive microfracturing. A variation from clear and colourless to deep reddish brown and nearly opaque is common, often within single crystals. No inherited cores were observed. Seven fractions of the best quality zircon were analyzed (Table 1). Measured uranium contents were very high (463 to 2248 ppm), and all fractions are more than 15 % discordant (Fig. 5). Six of the seven analyses define a linear array with upper and lower intercept ages (calculated using a modified York-II regression as described by Parrish et al., 1987) of 2623 ± 20 Ma and 802 Ma, respectively. The seventh fraction plots somewhat above this array. The calculated upper intercept age may represent the crystallization age of the sample; however, because of the extreme discordance of the analyses and the high degree of scatter about the regression line, this age must be interpreted very cautiously. The very high uranium contents and resultant pronounced Pb loss preclude obtaining a more precise age.

6. INC No. 10. The Inc No. 10 massive sulphide deposit is located on the Coppermine River near the eastern end of Point Lake (Fig. 1). The main mineralized zone is exposed at about 65° 02′40″ N, 112° 16′10″ W and can be traced around the nose of a north-plunging antiform (Falls, 1979). The mineralized zone is hosted by biotite-quartz-feldspar gneiss, interpreted by Falls to represent felsic and mixed tuffs of the Point Lake Formation, and is overlain by calc-silicate gneiss interpreted as a carbonate exhalite unit. The host rocks were sampled 2.2 km to the north at about 65° 05′ N, 112° 15′ W, in close proximity to what appears to be an extension of the INC sulphide horizon that recurs at surface along a continuation of the same antiform. The sample is a fine grained, thinly banded quartz-K-feldspar-plagioclase-biotite gneiss that is interlayered with hornblende-plagioclase orthogneiss and pelitic schist. P-T estimates in this general area are in the range of 4.3–5.4 kbar and 675-750°C (King, 1982).

Zircon in the sample is in the form of stubby prisms with large, sharp-edged facets. There in no evidence of inherited cores or metamorphic overgrowths, although some of the grains have slightly resorbed surfaces. Grains range from nearly colourless to medium brown and measured U contents are relatively high (686-1348 ppm, Table 1). Individual analyses range from 7.3 to 14.5 % discordant. Five of the six analyses form a linear array (Fig. 5) with upper and lower intercept ages (using a modified York-II

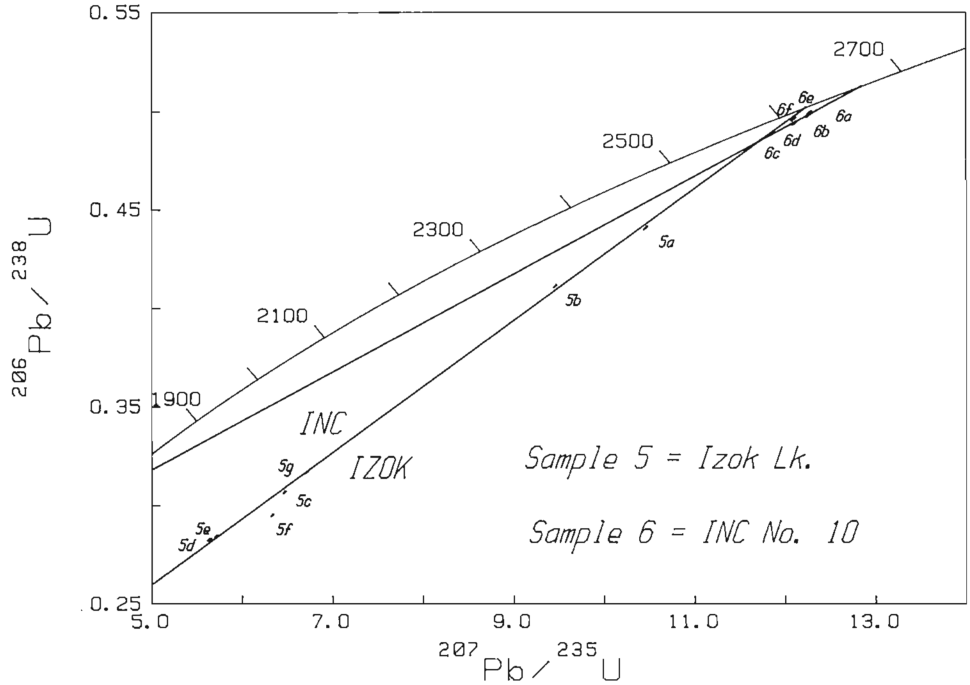

Figure 5. U-Pb concordia plot of zircon data from samples 5 (Izok Lake) and 6 (INC No. 10). Lines IZOK and INC represent best-fit lines to the Izok and INC data, respectively.

regression) of 2668.4 +21.4/−12.8 Ma and 1695.1 Ma. The sixth analysis falls above this regression line. The calculated upper intercept age is tentatively interpreted to represent the crystallization age of the volcanic protolith. More analyses are planned to constrain this age and to determine the cause of the marked scatter of the data.

7. Gondor Lake. This sample is from a well exposed sequence of intermediate to felsic volcanics 1 km west of the Gondor massive sulphide deposit (Bubar and Heslop, 1985) and 300 m northwest of Gondor Lake (Fig. 1). The unit sampled is a schistose, plagioclase porphyritic rhyolite, which is interbedded with aphyric and hornblende-plagioclase porphyritic mafic volcanics, plagioclase porphyries of intermediate composition (dacite?) and massive to autoclastic rhyolite. The sample is well-banded and is considered to be tuffaceous in origin. Bubar and Heslop (1985) have shown that volcanic rocks in the area are sub-alkaline to calc-alkaline. Pelitic rocks in the area contain sillimanite and muscovite, and have therefore experienced middle amphibolite metamorphic conditions (King et al., 1988).

Zircon in the sample represents a single population, and is generally euhedral, forming stubby prisms with simple and rare multifaceted terminations. The grains are pale pink, and contain abundant clear rods, tubes, and bubbles. Five fractions of abraded zircon were analyzed (Table 1). The analyses range from 0.5 to 1.4 % discordant, and define a discordia line with upper and lower intercepts of 2667.6 +3.0/−1.6 Ma and 578.6 Ma (Fig. 6). The upper intercept represents the crystallization age of the rock.

8. Concession Lake. This sample is from a unit that was interpreted as a felsic tuff of dacitic to rhyolitic composition that outcrops 500 m south of the southwest shore of Concession Lake (Fig. 1). The unit is 1m thick and is characterized by a fine siliceous matrix with approximately 5 % plagioclase phenocrysts. Its interpretation as a tuffaceous unit (as opposed to a high level porphyritic sill, several of which occur in the immediate area) was based on the observation of apparent grading of the feldspar phenocrysts. Rocks containing the tuff unit are biotite-grade turbiditic mudstones of the Contwoyto Formation (Bostock, 1980; King et al, 1988). Minor iron-formation is also interbedded with the mudstones at this location, but is not closely spatially associated with the felsic tuff bed.

Zircon grains recovered from the sample have a range of characteristics. Clear, pale pink fragments predominate, locally displaying one or more preserved facets and/or smoothly rounded, resorbed surfaces. Also present are stubby subhedral prisms with vaguely to well developed internal zoning, and a variety of coarse, subhedral to anhedral, strongly coloured grains. Because of the inferred tuffaceous nature of the sample, and the somewhat heterogeneous appearance of the zircon concentrate, it was suspected that a detrital zircon component might be present. To test this, a total of eight zircon fractions were analyzed (Table 1, Fig. 6), consisting of four single crystals, and four multiple-grain fractions. Five of the clear, pink, generally anhedral fractions plot close to concordia (0.3 to 2.4 % discordant) and form a well defined linear array with upper and lower intercept ages of 2603.9 +0.9/-0.8 Ma and 178.6 Ma, respectively. The three other fractions, including grains with visible internal zoning and strongly coloured grains, are considerably more discordant and yield Pb-Pb ages as great as 2775 Ma. The data indicate an age of 2604 Ma for a major component of zircon in the sample. This represents a minimum age for the sample, and it is very probable that it is the true age of the rock. The analyses also confirm the presence of older zircon grains, either as detrital grains or as xenocrysts from the parent magma of the unit.

9. Point Lake. The sample was collected from a small island near the south shore of Point Lake 3 km east of

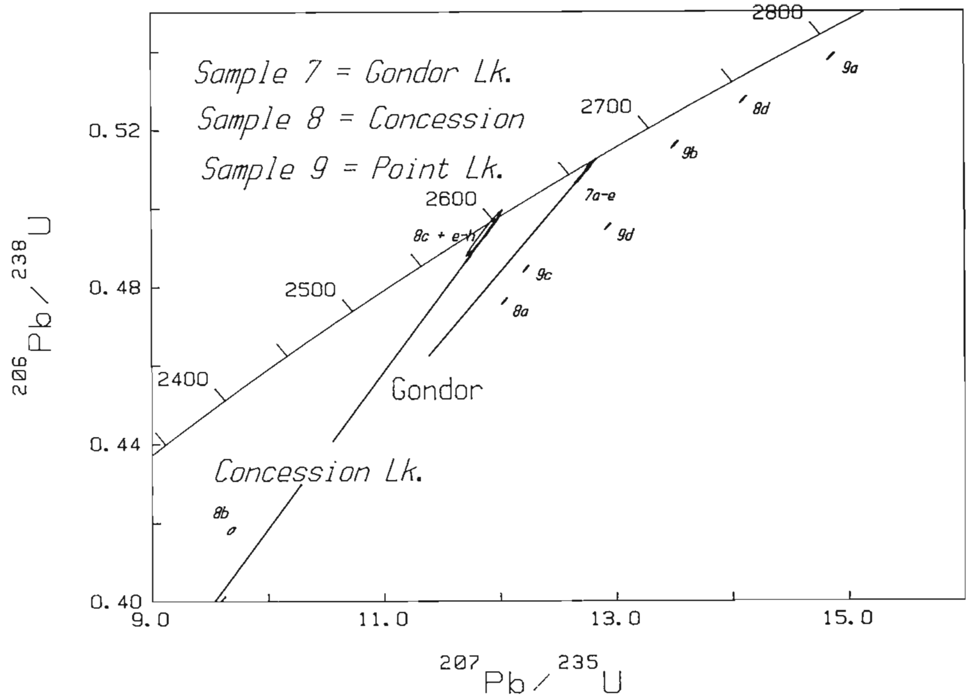

Figure 6. U-Pb concordia plot for zircon data from samples 7 (Gondor Lake), 8 (Concession Lake) and 9 (Point Lake). Best-fit lines to all Gondor Lake data, and to 5 of the Concession Lake analyses are shown (see text for discussion). The most discordant analysis from the Concession Lake sample (fraction 8b) plots off the diagram.

Keskarrah Bay (Fig. 1). It consists of a massive to weakly foliated quartz-feldspar porphyry with strongly strained quartz and plagioclase phenocrysts in a weakly sericitized and chloritized aphanitic groundmass. The sample site is about 11.5 km east of a small massive sulphide occurrence described by Henderson (1975). The zircon concentrate consists of pale brownish, euhedral, stubby grains with large, sharp-edged facets. No cores were visible, and the zircon appears to represent a single population. Although many of the grains were broken, there is no evidence that any are xenocrystic. Four fractions of zircon were analyzed (Table 1). The analyses are all relatively discordant and do not form a linear array (Fig. 6). Pb-Pb ages for individual fractions range from 2680 to 2827 Ma. If the zircons represent a single population of igneous, non-xenocrystic grains, then the data appear to indicate a minimum age of crystallization of 2827 Ma for the porphyry. More zircon fractions, including single crystals, will have to be analyzed to confirm this.

The minimum age inferred for the porphyry sample is considerably older than has been obtained from volcanic rocks elsewhere in the Slave Province. Older U-Pb ages have been obtained from basement(?) granitoid gneisses, and for cobbles and single detrital zircons in the western Point Lake area (e.g. Krogh and Gibbins, 1978; Henderson et al., 1982; Schärer and Allègre, 1982), and it is likely that relatively old supracrustal rocks, perhaps including the sample dated in this study, have also been preserved in the area. The Point Lake area is structurally complex, however, and many contacts within and between basement and cover sequences are presently interpreted to be faults of uncertain sense and/or magnitude of displacement (e.g. Easton, 1985; Kusky, 1987, pers. comm., 1988). Because of this structural complexity, the porphyry sample dated in this study cannot be directly correlated with the host rocks for the base metal occurrence described by Henderson (1975).

Further geochronological investigations at Point Lake now in progress by C. Isachson (Washington University, St.Louis) will provide additional constraints on the age(s) of supracrustal rocks in the area.

DISCUSSION OF RESULTS

Obtaining precise crystallization ages for igneous rocks in the Slave Province is complicated in some cases by the combined effects of minor inheritance (mainly by incorporation of xenocrystic zircon), and Pb loss of both Early Proterozoic (1.9-2.0 Ga) and relatively recent age. In addition, the high degree of strain and moderately high grade of metamorphism have at several sample sites obscured the character of protolith lithologies. The capability of analyzing very small samples of zircon, including single crystals, has been shown to be critical to resolving the resulting complex U-Pb isotope systematics. Indications of a significant Early Proterozoic Pb loss event is not surprising, since the Slave craton is bounded on the east, south and west by mid-Proterozoic orogenic belts, and samples for which this older Pb loss event is postulated (e.g. MUSK, Canoe Lk.) were collected within 100 km of such orogenic belts.

U-Pb zircon age data reported here for widely distributed felsic volcanic units in Slave Province, together with previously published data, indicate a distinctly bimodal distribution of ages for volcanic activity in the eastern and central parts of the Slave Province, one episode ranging from about 2698-2687 Ma, and another episode from 2675-2663 Ma (Fig. 2). Volcanogenic massive sulphide deposits are associated with both episodes. There is also now a suggestion of volcanism both considerably older and younger than either of these two episodes.

Preliminary data for a felsic porphyry at Point Lake suggest a crystallization age in excess of 2827 Ma. In view of the structural complexity in the Point Lake area, it is possible that the sample dated in this study may be structurally and perhaps petrogenetically separate from the rest of the central volcanic belt. Although the timing of volcanism elsewhere in the western part of the Slave Province is at present almost completely unknown, the Point Lake data and the documented presence of old (>3 Ga) crystalline basement in the area suggest that supracrustal sequences substantially older than those recognized in the central and eastern parts of the province may be present.

Portions of the western volcanic belt are, however, closely similar in some ways to supracrustal sequences of the central belt. For example, the stratigraphic section described by Lord (1942) at Wijinnedi Lake in the southern Indin Lake belt, and specifically the presence of limestone at the transition from volcanic to sedimentary sequences, is very similar to those in central and eastern Slave Province. Also, arsenide-gold mineralization in amphibolitic sulphide-silicate-facies iron-formation near Russell Lake (Bunner and Taylor, 1987) resembles Lupin-type iron-formation hosted gold occurrences in the Contwoyto Lake area and elsewhere in the province. Thus the western Slave Province may include supracrustal rocks of both considerably older and of comparable age to those in the central and eastern volcanic belts. Sampling in 1988 is planned in the western belt to test this hypothesis. Volcanic rocks as old as 2739 Ma also appear to be present within stratigraphically lower portions of the Yellowknife belt (C. Isachson, pers. comm., 1988).

The significance of the 2604 Ma age obtained for the Concession Lake sample is equivocal. Although originally interpreted in the field as a tuff, it is equally possible that the dated sample is from a strongly tectonized felsic sill. Conditions of exposure and the amount of strain that the sampled unit has experienced have obscured critical textural evidence. Evidence for a tuffaceous origin includes the apparent grading of small feldspar phenocrysts in the unit and the presence of at least two distinct populations of zircons recovered from the sample. One of these populations has clearly been incorporated into the sample as detrital grains and/or xenocrysts. Another population appears to be a homogeneous suite of igneous grains displaying strongly resorbed surfaces similar to those commonly found in felsic volcanic rocks. Interpreting the sample as a tuff, however, would require sedimentation to have occurred over at least 60 Ma for the Contwoyto Formation alone, considerably longer-lived deposition than had previously been postulated for rocks of the Yellowknife Supergroup. On the other hand, there are numerous instances of plutonic rocks yielding U-Pb ages of about 2600 Ma in the Slave Province (e.g. Krogh and Gibbins, 1978; Frith et al., 1986; van Breemen et al., 1987a, b; Henderson et al., 1987; van Breemen and Henderson, 1988), and swarms of porphyry sills intruding the Contwoyto Formation immediately east of Contwoyto Lake were recognized during the 1988 field season. It is presently considered more likely that the Concession Lake sample represents a sill rather than a tuff. Further sampling for U-Pb dating and examination of similar units in the area are being carried out to resolve the nature of the Concession Lake sample and the age of the adjacent sedimentary rocks.

The age obtained for the felsic meta-igneous unit at Izok Lake (2623 $\pm$ 20 Ma) presents a similar problem as that at Concession Lake. The Izok Lake sample is too thoroughly recrystallized to preserve textural evidence which would prove whether the rock is of extrusive or intrusive origin, and the significance of the age data with respect to other supracrustal rocks in the area is thus uncertain. The lead isotope composition for galena from the nearby Izok Lake massive sulphide deposit (Franklin and Thorpe, 1982) suggests that the associated volcanic rocks should be a minimum of about 2660 Ma. More work is needed in this area as well.

IMPLICATIONS FOR TECTONIC EVOLUTION OF SLAVE PROVINCE

Geochronological data compiled and newly reported here for volcanic rocks in the central and eastern Slave Province provide constraints on how these sequences have evolved through time and space. Volcanism in the age range 2698 to 2687 Ma occurred mainly in a northwesterly-trending zone in the eastern and northern Slave Province. This zone includes the Artillery Lake, Back River, Hackett River and Canoe Lake portions of the eastern volcanic belt as well as the Amoogabooga Lake area (Takijuq greenstone belt) at the northern end of the central volcanic belt. Volcanism was dominantly felsic in the southeast, but included substantial mafic to intermediate material in the northwestern portion. Minor volcanism at this time is also represented by parts of the Kam Formation and crosscutting porphyry dykes in the Yellowknife area (Bowring, *in* Padgham, 1985; Bowring and Padgham, 1987; C. Isachson, pers. comm., 1988). After an apparent hiatus of 15-20 Ma, mafic to intermediate volcanism resumed over a broad area of central and southern Slave Province. Deposition of turbiditic sediments occurred concurrently with this latter stage of volcanism (e.g. Padgham, 1985; J.E. King and H. Helmstaedt, pers. comm., 1988). Both the older and younger phase of volcanism appear to be represented in the Takijuq belt. Zircon geochronology by Krogh (reported by Padgham, 1985) indicates that the Takijuq granite near Takijuq Lake, and a large quartz monzonite boulder in a polymictic conglomerate within the volcanic sequence, both have ages of about 2650 Ma. This was interpreted to indicate that the Takijuq granite was a subvolcanic intrusion that was uplifted and unroofed during a later phase of volcanism (Padgham, 1985).

The disposition of volcanic belts in the central and eastern Slave Province into two subparallel zones of distinctly different age places important constraints on tectonic models for the province. For example, the accretionary complex-magmatic arc model proposed by Kusky (1988 and pers. comm., 1988) is inconsistent with the age data, because fragments of ophiolite incorporated into an accretionary prism must be of equivalent age or older than the magmatic arc with which they are associated; this is the reverse of the observed age relationship. Age control for the Slave Province supracrustal rocks is still fragmentary, however, and the presence of volcanic rocks in the Yellowknife belt belonging to both the older and younger episodes suggests that other volcanic belts may be the result of long-lived magmatism.

In view of the structural complexity and high grade of metamorphism in parts of the Slave Province, as well as poor exposure and the lack of regionally continuous marker horizons, a precise chronostratigraphic framework for the supracrustal sequences will be critical to understanding the tectonic evolution of the province.

ACKNOWLEDGMENTS

The results of this study could not have been obtained without the technical expertise of the staff of the Geochronology Section, particularly Klaus Santowski and Dale Loveridge. We thank John Henderson and Hewitt Bostock for helpful discussions concerning regional stratigraphy in the Slave Province. The manuscript was critically reviewed by Otto van Breemen, John Henderson and Charles Jefferson. We also thank Clark Isachson for collecting the Point Lake sample.

REFERENCES

Bau, A.F.S., Goff, S.P., and Yakey, M.J.
1979: Preliminary geology of NTS 86H/9, 10, 11 (3 maps with marginal notes); Department of Indian and Northern Affairs, Geology Division, EGS 1979-2.

Bostock, H.H.
1980: Geology of the Itchen Lake area, District of Mackenzie; Geological Survey of Canada, Memoir 391, 101 p.

Bowring, S.A. and Padgham, W.A.
1987: New U-Pb zircon dates from the Yellowknife volcanic belt: stratigraphic gold deposit model implications; Geological Association of Canada, Yellowknife '87 Summer Field Meeting, Program with Abstracts, p. 25. (abstract).

Bubar, D.S. and Heslop, J.B.
1985: Geology of the Gondor volcanogenic massive sulphide deposit, Slave Province, N.W.T.; Canadian Institute of Mining and Metallurgy, Bulletin, v. 78, no. 876, p. 52-60.

Bunner, D.P. and Taylor, R.P.
1987: Characteristics of auriferous iron formation in the Russell Lake region; Geological Investigations and Abstracts of Papers, 15th Annual Geoscience Forum, Department of Indian Affairs and Northern Development, Yellowknife, N.W.T., p. 19-20, (abstract).

Cumming, G.L. and Richards, J.R.
1975: Ore lead ratios in a continually changing earth; Earth and Planetary Science Letters, v. 28, p. 155-171.

Davis, D.
1982: Optimum linear regression and error estimation applied to U-Pb data; Canadian Journal of Earth Sciences, v. 19, p. 2141-2149.

Easton, R.M.
1985: The nature and significance of pre-Yellowknife Supergroup rocks in the Point Lake area, Slave Structural Province, Canada; *in* Evolution of Archean Supracrustal Sequences, ed. L.D. Ayres, P.C. Thurston, K.D. Card and W. Weber; Geological Association of Canada, Special Paper 28, p. 153-167.

Falls, R.M.
1979: Geology and metamorphism of the Inc 10 sulphide occurrence, Coppermine River area, N.W.T.; unpublished M.Sc. thesis, University of Western Ontario, 144 p.

Franklin, J.M. and Thorpe, R.I.
1982: Comparative metallogeny of the Superior, Slave and Churchill provinces; *in* Precambrian Sulphide Deposits, Geological Association of Canada, Special Paper 25, p. 3-90.

Frith, R.A. and Loveridge, W.D.
1982: Ages of Yellowknife Supergroup volcanic rocks, granitoid intrusive rocks and regional metamorphism in the northeastern Slave Structural Province; *in* Current Research, Part A, Geological Survey of Canada, Paper 82-1A, p. 225-237.

Frith, R.A. Loveridge, W.D., and van Breemen, O.
1986: U-Pb ages on zircon from basement granitoids of the western Slave Structural Province, northwestern Canadian Shield; in Current Research, Part A, Geological Survey of Canada, Paper 86-1A, p. 113-119.

Fyson, W.K. and Helmstaedt, H.
1988: Structural patterns and tectonic evolution of supracrustal domains in the Archean Slave Province, Canada; Canadian Journal of Earth Sciences, v. 25, p. 301-315.

Gill, J.W.
1977: The Takiyuak metavolcanic belt: geology, geochemistry and mineralization; unpublished Ph.D. thesis, Carleton University, 210 p.

Helmstaedt, H., Padgham, W.A., and Brophy, J.A.
1986: Multiple dikes in Lower Kam Group, Yellowknife greenstone belt: evidence for Archean sea-floor spreading?; Geology, v. 14, p. 562-566.

Henderson, J.B.
1975: Sedimentological studies of the Yellowknife Supergroup in the Slave Structural Province; *in* Report of Activities April to October 1974, Geological Survey of Canada, Paper 75-1, Part A, p. 325-330.
1981: Archaean basin evolution in the Slave Province, Canada; *in* Precambrian Plate Tectonics, ed. A. Kroner; Elsevier, Amsterdam, p. 213-236.
1985: Geology of the Yellowknife-Hearne Lake area, District of Mackenzie: a segment across an Archean basin; Geological Survey of Canada, Memoir 414, 135 p.

Henderson, J.B., Loveridge, W.D., and Sullivan, R.W.
1982: A U-Pb study of zircon from granitic basement beneath the Yellowknife Supergroup, Point Lake, District of Mackenzie; *in* Rb-Sr and U-Pb Isotopic Age Studies, Report 5, Geological Survey of Canada, Paper 82-1C, p. 173-178.

Henderson, J.B., van Breemen, O., and Loveridge, W.D.
1987: Some U-Pb zircon ages from Archean basement, supracrustal and intrusive rocks, Yellowknife-Hearne Lake area, District of Mackenzie; in Radiogenic Age and Isotopic Studies: Report 1, Geological Survey of Canada, Paper 87-2, p. 111-121.

Hoffman, P.F.
1986: Crustal accretion in a 2.7 — 2.5 Ga "granite-greenstone" terrane, the Slave Province, NWT: a prograding trench — arc system? (abstract); *in* Workshop on the Tectonic Evolution of Greenstone Belts, ed. M.J. de Wit and L. Ashwal; Lunar and Planetary Institute, Technical Report 86-10, p. 33. (in press), On accretion of granitoid-greenstone terranes; Nature.

Hyde, R.S., McLeod, H.A., Sribbins, B.J., and Taylor, S.L.
1976: Preliminary geology maps of Takijuq Lake, 86L/1, 2, District of Mackenzie; Department of Indian Affairs and Northern Development, Geology Division, EGS 1976-17 and 1976-18.

King, J.E.
1982: Low-pressure regional metamorphism and progressive deformation in the eastern Point Lake area, Slave Province, N.W.T.; unpublished M.Sc. thesis, Queen's University, Kingston, Ontario.

King, J.E., Davis, W.J., Relf, C., and Avery, R.W.
1988: Deformation and plutonism in the western Contwoyto Lake map area, central Slave Province, District of Mackenzie, N.W.T.; *in* Current Research, Part C, Geological Survey of Canada, Paper 88-1C, p. 161-176.

Krogh, T.E. and Gibbins, W.
1978: U-Pb isotopic ages of basement and supracrustal rocks in the Point Lake area of the Slave Structural Province, Canada; Geological Association of Canada, Abstracts with Program, v. 3, p. 438 (abstract).

Kusky, T.M.
1987: An Archean fold-and-thrust belt at Point Lake, NWT; Geological Association of Canada, Yellowknife '87 Summer Field Meeting, Program with Abstracts (abstract).
1988: Accretion of the Archean Slave Province; Journal of the Geological Society of India, v. 31, no. 1, p. 63-65.

Lord, C.S.
1942: Snare River and Ingray Lake map-areas, Northwest Territories; Geological Survey of Canada, Memoir 235, 55 p.

Ludwig, K.R.
1980: Calculation of uncertainties of U-Pb isotopic data; Earth and Planetary Science Letters, v. 46, p. 212-220.

McGlynn, J.C. and Henderson, J.B.
1970: Archean volcanism and sedimentation in the Slave Structural Province; *in* Symposium on Basins and Geosynclines of the Canadian Shield, ed. A.J. Baer; Geological Survey of Canada, Paper 70-40, p. 31-44.

Padgham, W.A.
1985: Observations and speculations on supracrustal successions in the Slave Structural Province; *in* Evolution of Archean Sequences, ed. L.D.Ayres, P.C.Thurston, K.D.Card and W.Weber; Geological Association of Canada, Special Paper 28, p. 133-151.

Padgham, W.A., Bryan, M.P.D., Jefferson, C.W., Ronayne, E.A., and Sterenberg, V.Z.
1975: Preliminary geology of Agricola Lake area, NTS 76G/12 (map with marginal notes); Department of Indian and Northern Affairs, Geology Division, EGS 1975-2.

Parrish, R.R., Roddick, J.C., Loveridge, W.D., and Sullivan, R.W.
1987: Uranium-lead analytical procedures at the geochronology laboratory, Geological Survey of Canada; *in* Radiogenic Age and Isotopic Studies: Report 1, Geological Survey of Canada, Paper 87-2, p. 3-7.

Roddick, J.C.
1987: Generalized numerical error analysis with application to geochronology and thermodynamics; Geochimica et Cosmochimica Acta, v. 51, p. 2129-2135.

Schärer, U. and Allègre, C.J.
1982: Investigation of the Archean crust by single grain dating of detrital zircon: a greywacke of the Slave Province, Canada; Canadian Journal of Earth Sciences, v. 19, p. 1910-1918.

Steiger, R.H. and Jäger, E.
1977: Subcommission on geochronology: convention on the use of decay constants in geo- and cosmochronology; Earth and Planetary Science Letters, v. 31, p. 359-362.

Thorpe, R.I.
1982: Lead isotope evidence regarding Archean and Proterozoic metallogeny in Canada; Revista Brasileira de Geociencias, v. 12, p. 510-521.

van Breemen, O., Henderson, J.B., Sullivan, R.W., and Thompson, P.H.
1987a: U-Pb zircon and monazite ages from the eastern Slave Province, Healey Lake area, N.W.T.; *in* Radiogenic Age and Isotopic Studies: Report 1, Geological Survey of Canada, Paper 87-2, p. 101-110.

Thompson, P.H., Hunt, P.A., and Culshaw, N.
1987b: U-Pb zircon and monazite geochronology from the northern Thelon Tectonic Zone, District of Mackenzie; *in* Radiogenic Age and Isotopic Studies: Report 1, Geological Survey of Canada, Paper 87-2, p. 81-93.

van Breemen, O. and Henderson, J.B.
1988: U-Pb zircon and monazite ages from the eastern Slave Province and Thelon Tectonic Zone, Artillery Lake area, N.W.T.; *in* Radiogenic Age and Isotopic Studies: Report 2, Geological Survey of Canada, Paper 88-2.

Yeo, G.M., Bailey, G., Crux, J., Fischer, B., Jackson, V., Relf, C., and Wahlroth, J.
1983: Preliminary geology of western Hepburn Island map area, N.W.T., NTS 76M/3-6, 11-14; Department of Indian Affairs and Northern Development, Geology Division, EGS 1983-8.

Age constraints on the evolution of the Quetico Belt, Superior Province, Ontario

J.A. Percival[1] and R.W. Sullivan[1]

Percival, J.A., and Sullivan, R.W., Age constraints on the evolution of the Quetico Belt, Superior Province, Ontario; in Radiogenic and Isotopic Studies: Report 2, Geological Survey of Canada, Paper 88-2, p. 97-107, 1988.

Abstract

Metasedimentary and associated rocks of the 1200 km long Quetico Belt form a prominent 10-100 km wide subprovince bounded to the north and south by volcanic-plutonic subprovinces. U-Pb zircon geochronology suggests that the sediments were deposited and accreted in the interval between 2702±4 and 2687±19/13 Ma, shortly after major calc-alkaline volcanic activity in the adjacent belts. Major metamorphism and plutonism, dated by U-Pb on monazites in granites with inherited zircon, occurred at 2671-2667 Ma and was followed by late pegmatite injection at about 2653 Ma. A cobble from a Seine-equivalent conglomerate at Max Creek gave an age of 2687±3 Ma, not allowing distinction of the ages of the Quetico and Seine sedimentary sequences.

Résumé

Les roches métasédimentaires et associées de la zone de Quetico s'allongeant sur 1200 km forment une importante sous-province de 10 à 100 km de largeur, limitée au nord et au sud par des sous-provinces volcaniques plutoniques. Une géochronologie établie à l'aide de la méthode U-Pb appliquée aux zircons semble indiquer que les sédiments ont été mis en place et accumulés entre il y a 2702±4 et 2687±19/13 Ma, après une intense activité volcanique de nature calco-alcaline dans les zones adjacentes. D'après des résultats obtenus par la méthode U-Pb appliquée aux monazites de granites avec zircon hérité, un métamorphisme et un plutonisme importants se sont produits, entre 2671 et 2667 Ma, suivis d'une injection tardive de pegmatite il y a environ 2653 Ma. Un galet provenant d'un conglomérat équivalent aux roches de Seine, à Max Creek, a été daté à 2687±3 Ma, ce qui ne permet pas de distinguer les âges des séquences sédimentaires de Quetico et de Seine.

INTRODUCTION

U-Pb zircon geochronology on greenstone-granite belts of the Superior Province (e.g. Davis et al., 1987; in press; Mortensen, 1987) have provided important constraints on the timing of events and consequently, on large-scale tectonic processes. The interval between 2.75 and 2.68 Ga was a period of active volcanism and plutonism throughout the southern Superior Province, attesting to rapid crustal growth. In detail, individual linear greenstone-granite subprovinces, separated by metasedimentary subprovinces, are characterized by temporally discrete deformational sequences (Stott and Corfu, 1988; Davis, 1988), suggestive of sequential north to south accretion of volcanic arcs (Langford and Morin, 1976; Card, 1986; Percival and Williams, in press.). Although determination of the timing of events in these belts is equally important in the interpretation of regional tectonic evolution, geochronological control on events in the metasedimentary subprovinces is lacking owing to the scarcity of dateable primary depositional units. Hence, to provide a time framework, U-Pb ages were determined on zircon, sphene and monazite from several rock types in the Quetico subprovince.

REGIONAL GEOLOGY

Superior Province forms the Archean nucleus of the Canadian shield and consists of high grade terranes in the north and south, and a central zone of easterly-trending subprovinces (Card and Ciesielski, 1986). Volcano-plutonic, plutonic and metasedimentary subprovinces, alternating on 50-200 km scale, comprise the central zone (Fig. 1). Here we consider the Quetico metasedimentary subprovince, bounded to the north over 1200 km of strike length by the Wabigoon and to the south by the Wawa subprovince.

Originally distinguished from adjacent volcano-plutonic terranes by the linear character of its internal structure

[1] Geological Survey of Canada, 601 Booth Street, Ottawa, Ontario K1A 0E8

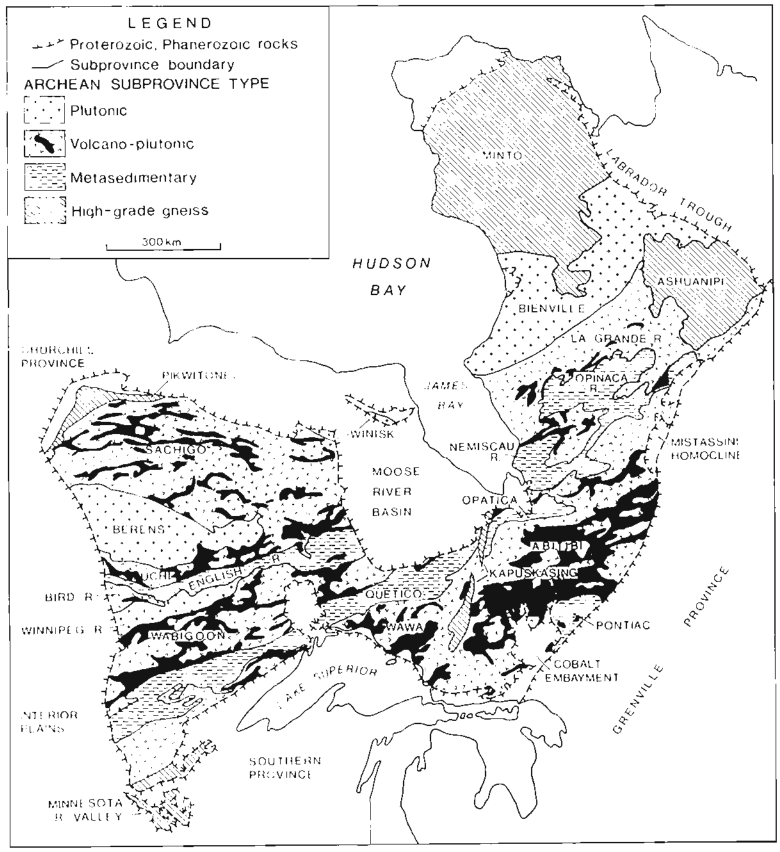

Figure 1. Generalized geological map of the Superior Province showing distribution of subprovinces (modified after Card and Ciesielski, 1986).

(Stockwell, 1964), the Quetico was subsequently recognized as being lithologically distinct as well, consisting of greywacke-argillite metasedimentary rocks, derived migmatite and granite. The linear, 10-100 km wide belt has symmetrical internal metamorphic zonation, grading from greenschist facies near the margins, to amphibolite and local granulite facies migmatite in the axis (Pirie and Mackasey, 1978; Percival, in press). Steep faults with both reverse dip-slip and dextral transcurrent displacement bound the Quetico to the north and south (Williams, 1987; Mackasey et al., 1974). A prominent easterly cleavage and foliation (S_2) transects earlier folds (F_1) of variable style and orientation (Percival, in press). Open F_3 folds, developed in the high grade parts of the belt, have axes parallel to a pervasive, gently east-plunging stretching lineation.

Intrusive rocks of variable composition and age cut the metasedimentary sequence. Some of the earliest intrusions recognized are rare, fine grained granodiorite sills with chilled appearance, which occur sporadically near the southern margin (Percival, 1983). Pods of mafic, alkaline rock, generally of less than mappable size (Smith and Williams, 1980; Schulz, 1982) may be related to larger alkaline complexes such as Poohbah Lake (Sage et al., 1979). Both the pods and complexes are cut by leucogranites which comprise two suites: an older, white, peraluminous muscovite leucogranite and a younger, pink biotite-magnetite leucogranite (Percival, 1988). The leucogranites are medium — to coarse — grained, massive to locally weakly foliated, and are cut by dykes of pink leucocratic pegmatite.

To the north, the Wabigoon subprovince consists of at least two volcanic-plutonic sequences. In the Atikokan area, an older (2.99 Ga; Davis and Jackson, 1988) mafic- felsic volcanic- tonalite sequence is overlain unconformably by the Steep Rock Group (Wilks and Nisbet, 1988). The relationship between the older rocks and the younger, 2.77-2.68 Ga cycle of volcanic and intrusive rocks, (Davis et al., in press) which makes up most of the subprovince, is not known. Major deformation is bracketed at 2.702-2.695 Ga (Davis et al., 1982). Along the southern margin of the Wabigoon, polymictic conglomerate and arkose of the Seine Group have been interpreted as proximal equivalents of the Quetico greywackes (Wood, 1980) or pull-apart basin deposits in a dextral wrench zone (Poulsen, 1986). Deformation of the Seine Group is bracketed at 2.695-2.685 Ga (D.W. Davis pers. comm., 1988).

In the Wawa subprovince, south of the Quetico, major volcanism occured at 2.77-2.695 Ga (Corfu and Stott, 1986; Turek et al., 1984), followed by late plutons of 2.695-2.675 Ga (Frarey and Krogh, 1986). An earlier sequence (2.89 Ga) is recognized locally (Turek et al., 1988). D_1 deformation, bracketed at 2.695-2.689 Ga, predated deposition of "Timiskaming" type alkaline volcanic and fluviatile sedimentary rocks (2.689-2.685 Ga; Corfu and Stott, 1986). D_2 deformation followed, at 2.685-2.675 Ga.

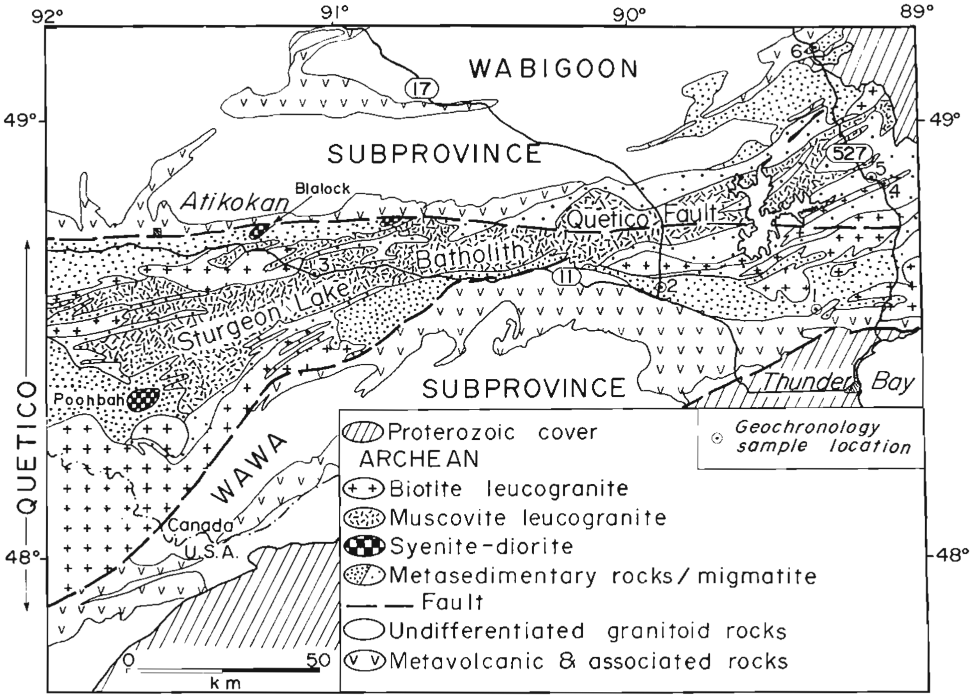

Figure 2. Geological map of the Quetico subprovince in western Ontario (modified after Percival, 1988; in press), showing locations of samples analyzed.

SAMPLING STRATEGY AND SAMPLE DESCRIPTIONS

One of the major objectives of the geochronology program was to bracket the age of sediment deposition, as felsic volcanic layers are not present to date deposition directly. Two samples were therefore collected: 1) a low grade metagreywacke, containing detrital zircon, and 2) an early granodiorite sill. The age of major intrusive, and by inference, metamorphic events is represented by samples of the two major leucogranite types (peraluminous muscovite leucogranite no. 3; biotite-magnetite leucogranite no. 4) and by late pegmatite no. 5. In order to obtain an estimate of the source area for Seine-type conglomerate, a tonalitic boulder (sample no. 6) was extracted from conglomerate at Max Creek.

Sample no. 1 Metagreywacke, Lappe, Ont.

This 25 kg sample was taken from the most southerly exposure of Quetico sediments (Fig. 2). Thick-bedded greywackes have preserved graded bedding, rip-up clasts and flame structures. The sample, from the coarse base of a Bouma ''A'' bed, contains quartz and fine grained rock fragments, set in a matrix of chlorite and sericite.

The detrital zircon population is generally euhedral with euhedral internal growth zonation and with slightly rounded shapes. Some rounded unzoned zircons and zircons with cores are also present. A variety of zircons was selected for single and multigrain analysis.

Sample no. 2 Granodiorite sill, Hwy 17, 2 km north of Shabaqua Corners.

Irregular sills of fine grained granodiorite, 0.3- 2 m thick, are generally parallel to bedding in biotite grade metagreywacke (Fig.3). Thin apophyses which cut bedding demonstrate that the bodies are sills rather than flows, and the fine grain size suggests chilling upon intrusion into cool sediments. The sills are present intermittently over a strike length of 25 km and have also been reported from the Vermilion area, 400 km to the west (Southwick, 1972). The bodies consist mainly of quartz and feldspar with minor biotite and accessory sphene, rutile and zircon. Two samples of 25 kg were collected from different sills in the same outcrop. Both yielded small amounts of zircon, which were combined to obtain sufficient zircon to analyze. Zircons are typically euhedral to subhedral, clear to somewhat translucent, slightly coloured, some with visible internal zonation, all suggestive of an igneous origin. Cores were not observed. Pale yellow subhedral sphene is common, and was also analyzed from one sill.

Sample no. 3 Peraluminous muscovite leucogranite, Windigoostigwan Lake.

This 25 kg sample was collected from a blasted outcrop on Hwy 11 (Fig.2) within the Sturgeon Lake batholith, an irregular elongate body measuring about 10 by 100 km (Percival et al., 1985). The rock is a coarse grained, white, leucocratic granite with garnet, coarse muscovite and local aggregates of sillimanite. Large variations in grain size from fine to coarse are common within single outcrops. Zircons are abundant and consist of pale to dark yellow grains. Most contain visible cores, such that a core-free population was impossible to select. Some zircons have clear, colourless overgrowths with rounded protruding terminations on purple-tan cores. Abundant monazite occurs as clear pale yellow euhedral crystals and rounded grains.

Sample no. 4 Biotite-magnetite leucogranite, near Pace Lake.

A 25 kg sample of slightly foliated, pink biotite granite was collected from a blasted outcrop (Fig. 2). The rock is medium — to coarse — grained, with 2-3 % aligned biotite and abundant accessory magnetite and zircon and small amounts of monazite. Zircon grains are amber to brown, altered and contain a high proportion of core material. Parallel growth twins and zircon aggregates are also present. Monazite occurs as a homogeneous population of clear, round, yellow grains.

Figure 3. Aphanitic granodiorite sills (white) cutting low grade Quetico metasedimentary rocks (grey), 2 km north of Shabaqua corners, Ontario. Note apophyses of granodiorite. GCS 204430-N

Sample no. 5 Massive granite pegmatite, near Pace Lake.

A sample of massive pegmatite cutting foliated granite (sample no. 4) was collected with the aim of bracketing deformation, however, the sample was found to be devoid of good quality zircon. A second sample, collected from an outcrop where pegmatite cuts massive biotite leucogranite, contained euhedral zircon. The 25 kg sample consists of coarse quartz and feldspar with accessory biotite, magnetite, zircon, apatite and monazite. Zircon generally occurs as elongate, yellow to brown, cracked, altered grains. Small nebulous cores are visible in some grains. Cuniform and parallel growth twins, and a few triplets occur. Some zircons also have clear rounded protruding terminations. These features have been interpreted in terms of synneusis and early crystalization around zircon xenocrysts (Jocelyn and Pidgeon, 1974). Monazite occurs as clear, yellow, round grains.

Sample no. 6 Tonalite boulder, Max Creek.

The Max Creek conglomerate occurs over a strike length of about 30 km (Pye, 1968), near the boundary between the Wabigoon and Quetico subprovinces. It contains a variety of clast types,which range up to 35 cm in diameter and include gabbro, basalt, iron — formation, chert, tonalite and granodiorite. A 30 cm diameter clast of massive to weakly foliated hornblende-biotite tonalite was extracted and trimmed of matrix rind. The tonalite contains accessory zircon, magnetite, apatite and sphene. Zircon comprises a homogeneous population of dark yellow to brown, subhedral grains with internal coarse zonation and a moderate degree of alteration. Polished and HF etched grain mounts show euhedral growth zones with a larger, low uranium, inner zone surrounded by finer, high uranium outer zones, possibly representing rapid growth. Fine apatite inclusions are also present. Subhedral sphene is generally dark amber.

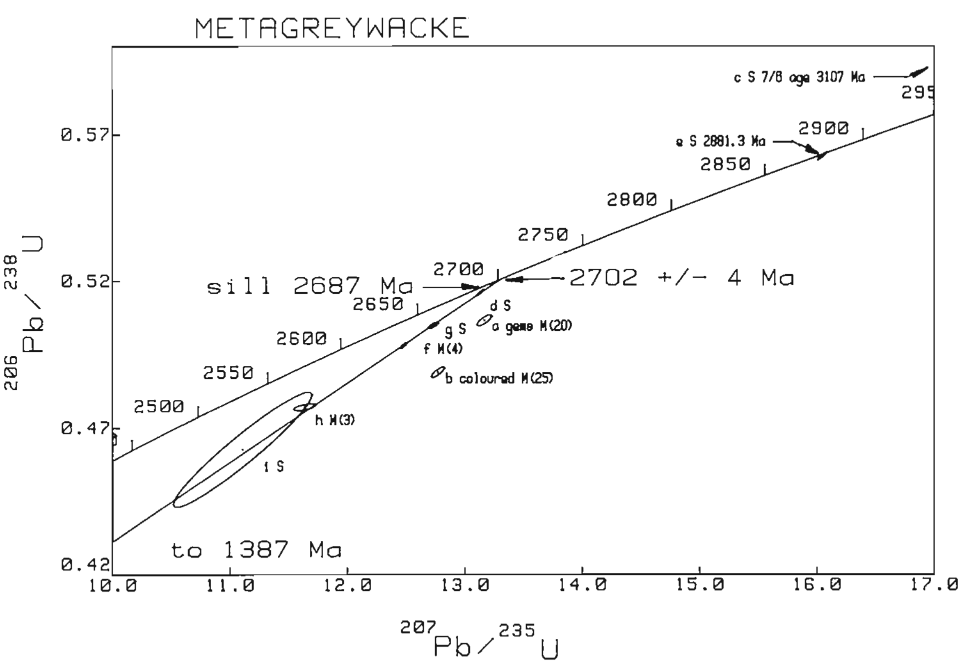

Figure 4. U-Pb concordia diagram showing single, S and multigrain, M(no. of grains) analyses of detrital zircons from metagreywacke (sample 1). The points have Pb-Pb ages ranging from 2598 to 3107 Ma with one concordant point at 2881.3 +/ − 1.2 Ma. Points d,f,g,h,i are colinear and yield 2702 Ma for a maximum age of sedimentation. The minimum age of sedimentation is estimated from the granodiorite sill (sample 2) at 2687 +/− 19/13 Ma. Multigrain fractions a and b represent detrital zircons of mixed age. The grain which gave 3107 Ma had an obvious core.

Table 1. U-Pb isotopic data on zircon, monazite and sphene: Quetico subprovince, Ontario

Sample and fraction[3]	Weight (mg)	U (ppm)	Pb* (ppm)	Measured[1] $^{206}Pb/^{204}Pb$	Isotopic abundances[2] (^{206}Pb=1000) ^{204}Pb	^{207}Pb	^{208}Pb	Isotopic ratios $^{206}Pb/^{238}U$	$^{207}Pb/^{235}U$	Age,Ma $^{207}Pb/^{206}Pb$
1. Metagreywacke: PBA-82-398 (48°33′55″N 89°21′47″W)										
Detrital zircons										
a, −105+62,gems,A	0.103	157.4	94.8	570	1.670	208.80	243.72	0.50652	13.16676	2729.4
b, -105+62,col'd,A	0.118	305.2	173.7	704	1.381	206.18	205.99	0.48897	12.77175	2737.3
c, sing XL,core,A	0.006	——[4]	189.5	1244	0.390	242.4	174.3	——[4]	——[4]	3107.0
d, single XL,A	0.0065	249.8	156.0	1855	0.259	187.8	228.5	0.51596	13.13188	2694.6
e, single XL,A	0.0116	125.7	89.8	1624	0.330	210.8	278.4	0.56246	16.04407	2881.3
f, 4 XL'S,A	0.0095	222.9	134.6	1082	0.705	190.4	248.0	0.49809	12.48119	2668.8
g, single XL,A	0.0111	305.2	174.1	623	1.472	200.9	176.4	0.50488	12.73149	2679.3
h, 3 XL's,A	0.0115	394.0	218.5	229	4.267	229.5	305.3	0.47709	11.63660	2624.0
i, single XL,A	0.005	464.6	250.3	98	4.613	231.0	320.7	0.46269	11.10959	2597.6
2. Granodiorite sill: Q-84-7,8 (48°37′46″N 89°53′50″W)										
S1, dark,A	0.2481	86.2	48.2	1010	0.879	191.9	154.5	0.49693	12.40935	2663.1
S2, pale	0.2518	40.8	23.1	389	2.342	208.9	259.3	0.48907	12.14752	2654.2
S3, pale	0.2006	39.4	22.8	336	2.687	213.0	276.8	0.48816	12.11297	2652.6
S4, pale	0.259	37.0	21.3	382	1.481	197.8	239.7	0.48635	12.04495	2649.4
S5, pale	0.253	38.7	22.2	379	1.520	198.2	238.9	0.48604	12.03354	2648.9
ZIR1, −74,A,NM	0.118	330.3	166.1	2007	0.351	180.5	189.5	0.43127	10.47808	2617.5
ZIR2, −74,"best"	0.042	273.5	134.2	681	0.970	186.0	207.0	0.42207	10.13101	2597.3
ZIR3, −74,A,M	0.123	510.7	228.4	911	0.998	179.8	206.6	0.38676	8.92493	2531.5
3. Peraluminous musc. leucogranite: Q-84-10 (48°39′49″N 91°04′07″W)										
X, mon., fragments	0.184	8779.3	12268.5	22997	0.119	182.0	1994.5	0.508962	12.75333	2668.7
Y, monazite, XL's	0.017	11946.9	16528.4	3676	0.226	184.7	1947.2	0.511658	12.83431	2670.5
4. Biot.-magnetite leucogranite: Q-84-3 (48°52′30″N 89°11′49″W)										
A, monazite	0.119	5292.8	8071.3	14304	0.023	180.9	2489.1	0.480489	11.96534	2658.5
B, monazite	0.0143	3273.3	5941.5	6182	0.033	182.3	3046.9	0.496028	12.43847	2670.0
C, monazite	0.0126	3906.6	7153.2	24570	0.008	181.5	2964.3	0.510450	12.76915	2666.0
D, monazite	0.004	11371.9	11785.9	50117	0.000	181.3	1176.7	0.508955	12.71955	2664.4
ZIR1, prisms,A	0.0060	647.5	255.4	1850	0.034	159.7	101.1	0.364231	7.99672	2447.5
ZIR2, cored,A	0.0253	310.3	127.0	1163	0.628	173.6	94.1	0.383859	8.77280	2515.2
ZIR3, robust,A	0.0280	282.2	144.4	1504	0.472	184.8	124.1	0.461795	11.39489	2643.3
5. Massive granite pegmatite: PBA-84-215 (48°53′10″N 89°11′53″W)										
M6, monazite	0.0189	9911.9	15710.9	54544	0.012	180.1	2423.9	0.508498	12.61817	2652.6
M7, monazite	0.0261	6757.3	12290.0	97250	0.007	179.8	2955.7	0.508164	12.59369	2650.5
M8, monazite	0.0322	6468.4	10680.0	65790	0.012	180.3	2578.7	0.507739	12.61203	2654.3
Z1, −74+62,A	0.071	2837.8	1185.6	883	1.118	177.3	48.8	0.413595	9.31111	2489.9
Z2, −105+74	0.104	3232.9	1324.5	906	1.092	176.4	43.1	0.407595	9.14341	2483.9
Z3, −105+74,A	0.138	3173.7	1284.6	1039	0.953	172.9	38.2	0.403350	8.94876	2465.2
Z4, −74+62,A	0.174	3031.5	1229.1	876	1.136	175.3	45.8	0.403338	8.95854	2467.1
6. Tonalite boulder: Q-84-6 (49°10′08″N 89°21′10″W)										
S1, sphene	0.282	71.8	37.6	1877	0.079	282.6	8.5	0.512211	12.93194	2681.2
S2, sphene	0.119	98.4	48.5	1004	0.163	181.2	15.1	0.477860	11.80960	2645.8
Z1, −74+62,A	0.116	1618.1	768.0	9733	0.073	172.0	107.2	0.432450	10.20016	2568.1
Z2, −62+44	0.318	1395.8	657.4	5272	0.133	172.6	110.2	0.428792	10.10654	2566.9
Z3, −105+74	0.464	2176.6	885.1	2221	0.444	165.7	111.9	0.375830	8.29793	2457.0

NOTES: * radiogenic Pb; 1 corrected for fractionation and spike; 2 corrected for Pb,U blank and common Pb; 3 size in microns; 4 no uranium analyses
A abraded; NM,M relative non-magnetic, magnetic separation using iron needle with cobalt-REE magnet

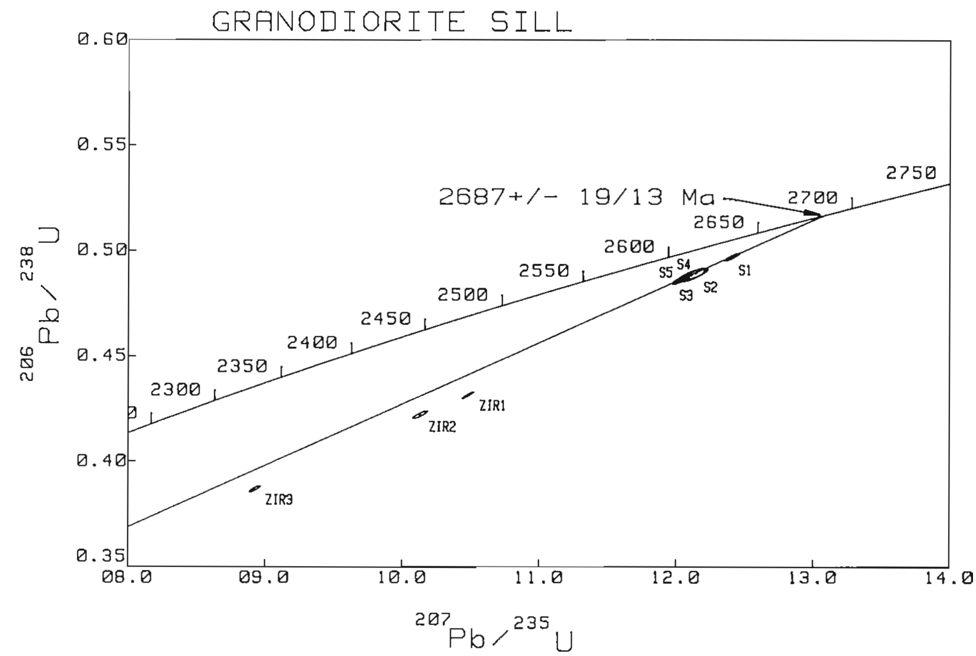

Figure 5. U-Pb concordia diagram showing analyses of zircon and sphene from granodiorite sill (sample 2). The upper intercept age is generated from the five sphene data only and taken as the best estimate for the age of the sill (minimum age of sedimentation). The zircons probably have an inherited zircon component (*see* text).

ANALYTICAL PROCEDURES AND RESULTS

Zircon, monazite and sphene fractions were selected and analyzed according to procedures similar to those outlined in Parrish et al. (1987). Monazite and sphene were not abraded or only lightly abraded to remove gangue, but acid washed as for zircon. Analytical data are reported in Table 1 and plotted on concordia diagrams (Fig. 4 to 7). Age calculations and regression of data sets are as described in Parrish et al. (1987). All quoted errors are at the two sigma level.

Sample no 1 Nine single and multigrain fractions of crack-free, weakly coloured zircons were selected from the metagreywacke sample. A few grains with cores were also selected for analysis after severe abrasion. The zircons were typically euhedral to subhedral, internally zoned crystals of 149-74 μm size. Most of the fractions were dissolved using the micro capsule technique (Parrish, 1987). The resulting analyses, plotted on Figure 4, yield Pb-Pb ages ranging from 2598-3107 Ma. Most of the grains are in the range 2700-2800 Ma with one concordant point at 2881.3 ± 1.2 Ma.

Similar ages of detrital zircon have been reported from the Pontiac sediments (Gariepy et al., 1984) and the northern Quetico (D.W. Davis pers. comm., 1988). The older population may have been derived from sequences like those exposed in the Atikokan area (Davis and Jackson, 1988), whereas the younger grains are probably the product of erosion of volcano-plutonic sequences like those exposed throughout the Wabigoon and Wawa subprovinces. The younger detrital zircons, in the 2700 Ma age range, place an upper limit on the age of deposition of the sediments. Five fractions (d,f,g,h and i) which were carefully selected for uniformity and lack of visible cores, and which had 1,4,1,3,1 grains respectively, produced a colinear data set. The regression (MSWD=1.3) gave upper and lower intercept ages of 2701.7 ± 3.9/3.4 Ma and 1387 ± 100 Ma respectively. It would appear that this colinear data set is from a single age population and that multigrain fractions a and b are mixed ages. This colinearity and the near concordant point d, with Pb-Pb age of 2694.6 Ma are considered valid reasons for assigning 2702 ± 4 Ma as a low error estimate for the maximum age of sedimentation. It is apparent that within the resolution of this technique, similar source terranes are represented on the northern and southern margins of the Quetico subprovince. The presence of zircon of 2.88 Ga age suggests that sources such as the Hawk Lake volcano-plutonic complex of the Wawa area (Turek et al., 1988) were exposed at the time of sediment deposition.

Sample no. 2 Three fractions of low-colour, crack-free zircon without visible cores were selected from the granodiorite sill population for analysis. Despite careful selection of small numbers of high-quality grains and strong abrasion prior to analysis, the points are very discordant (Fig. 5), defining a line with an upper intercept of 2743±12 Ma . Five sphene analyses from the sill are much less discordant; when regressed they give an upper intercept of 2687+/−19/13 Ma (Fig. 5). In view of the small size of the sill, and the relatively high closure temperature of the U-Pb system for sphene (Ghent et al., 1988), the sphene age should be very close to the true age of the intrusion.

The purpose of dating the sill was to provide a minimum age for sediment deposition. Taken at face value, the zircon age would suggest deposition of some sediments before 2743 Ma ago, in clear conflict with the evidence from the detrital suite. It is possible, but unlikely, that two ages of sediments are intercalated; those older than 2743 and those younger than 2700 Ma. It is more likely that an inherited zircon component (possibly as xenocrysts) is present, although cores were not observed in the zircon population.

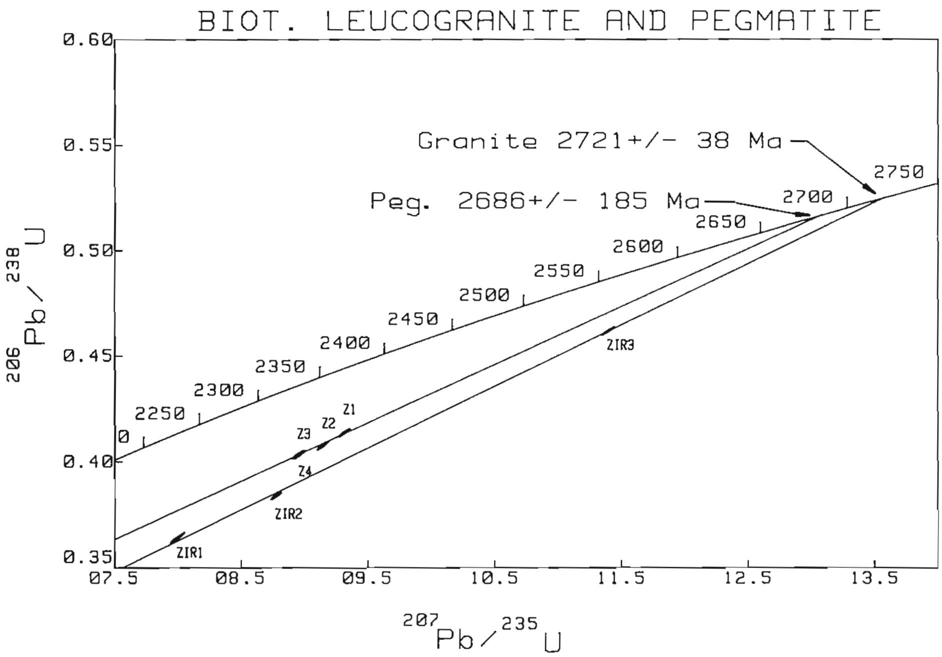

Figure 6. U-Pb concordia diagram showing analyses of zircons from sample 4, biotite leucogranite (ZIR1-ZIR3) and sample 5 , pegmatite (Z1-Z4). Points are very discordant and suffer from an inherited component. Monazite from these rocks provided near concordant points.

Zircons with cores were observed from a similar sill (sampled but not analyzed) cutting metagreywacke at a different location. If there is an inherited zircon component, the upper intercept age is meaningless with respect to estimating the age of the sill. Similar sills cutting low grade "Coutchiching" sediments in the Rainy Lake area of the Wabigoon subprovince contain inherited components ranging from 2.73-4.0 Ga (D.W. Davis pers. comm., 1988). The best estimate for the age of the sill and hence the minimum age of sedimentation is from the sphene data at 2687±19/13 Ma. Sedimentation is therefore bracketed between 2702 and 2687 Ma.

Sample no. 3 Zircons from peraluminous leucogranite are generally altered and contain cores within euhedral, well zoned igneous overgrowths. In light of the potential inheritance, zircon is unlikely to provide an accurate estimate of the age of crystallization and analyses were not pursued. Small fractions of monazite, however, were analyzed and yielded 2 nearly concordant points (Fig. 7). The best estimate for the age is 2670.5±2.0 Ma based on the $^{207}Pb/^{206}Pb$ age of fraction Y which is concordant within analytical error.

Interpretation of monazite ages is clouded by the potential for inheritance (Sawka et al., 1986; Rapp et al., 1987) and/or high-temperature diffusive lead loss. Rocks with a rapid cooling history or shallow emplacement level should not be susceptible to the latter problem. Quetico granites were probably intruded at high structural levels, based on low-pressure metamorphic assemblages developed in adjacent metasedimentary lithologies (Percival, in press). Inheritance is possible for low-temperature melts which do not exceed the closure temperature for monazite (650-700°C; Parrish, 1988). Although Quetico granitoids are leucocratic, they contain high-temperature phases such as sillimanite, which suggest relatively high crystallization temperatures (Percival et al., 1985). The monazite date therefore probably accurately reflects the time of crystallization of the body.

Sample no. 4 Zircons from biotite leucogranite are generally altered and consist of rounded cores surrounded by euhedral growth zones. Three fractions with and without apparent cores were selected, abraded and analyzed. The zircons have moderately high U contents, are severely but variably discordant and are not colinear within analyical error. When regressed the points yield an upper intercept age of 2721 ± 38 Ma (Fig. 6). Four monazites with very high U and Pb contents yielded much more concordant points, 0.3 to 6 % discordant, with Pb-Pb ages of 2658-2670 Ma which, when regressed, give an upper intercept age of 2666 ± 4 Ma. Although the age could be as old as 2670 Ma, the best estimate of the age of crystallization is considered to be the average Pb-Pb age of the two most concordant monazite analyses (C,D, Fig. 7) which overlap within error, yielding 2665 ± 2 Ma.

The monazite age for sample 4 is slightly younger than that for sample 3, in agreement with rare crosscutting relationships. Mixing between granite types was not observed, suggesting derivation from distinct magma types.

Sample no. 5 Zircons in this pegmatite are generally altered and contain a small nebulous core component. Four fractions without visible cores have high U concentrations (2838-3233 ppm) and define an array with an upper intercept of 2686±185/100 Ma. These highly discordant data are difficult to interpret, particularily in light of the possible presence of an inherited component in some or all of the fractions. Three monazite fractions from sample 5, however, yielded a near concordant point (M8), and two concordant (within error) points (M6,M7, Fig. 7). It is not certain what has produced the small scatter in these results. It is possible that this monazite population contains varying amounts of inclusions (e.g. thorite) that have different closure temperatures, although none have been observed. The best estimate for the age of the pegmatite is considered to be the average of the three Pb-Pb ages with a graphically estimated error, namely 2653 ± 3/4 Ma.

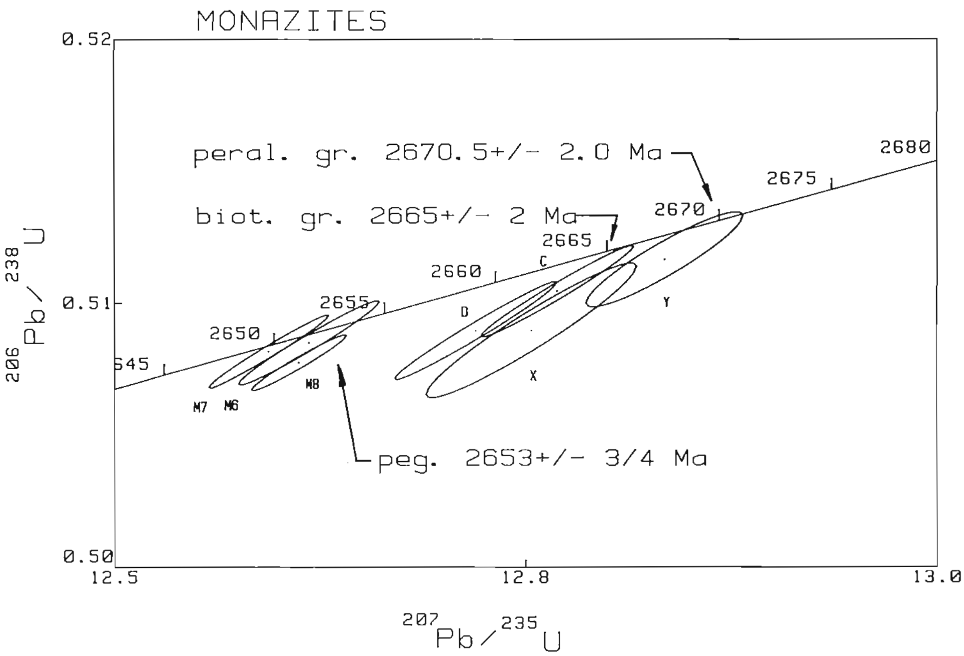

Figure 7. U-Pb concordia diagram showing analyses for monazite from sample 3, peraluminous muscovite granite (X,Y); sample 4, biotite leucogranite (C,D) and sample 5, pegmatite (M6, M7, M8). Monazite results represent the best estimate of the age of these samples. The reason for the small scatter in results for sample 5 is not known (*see* text).

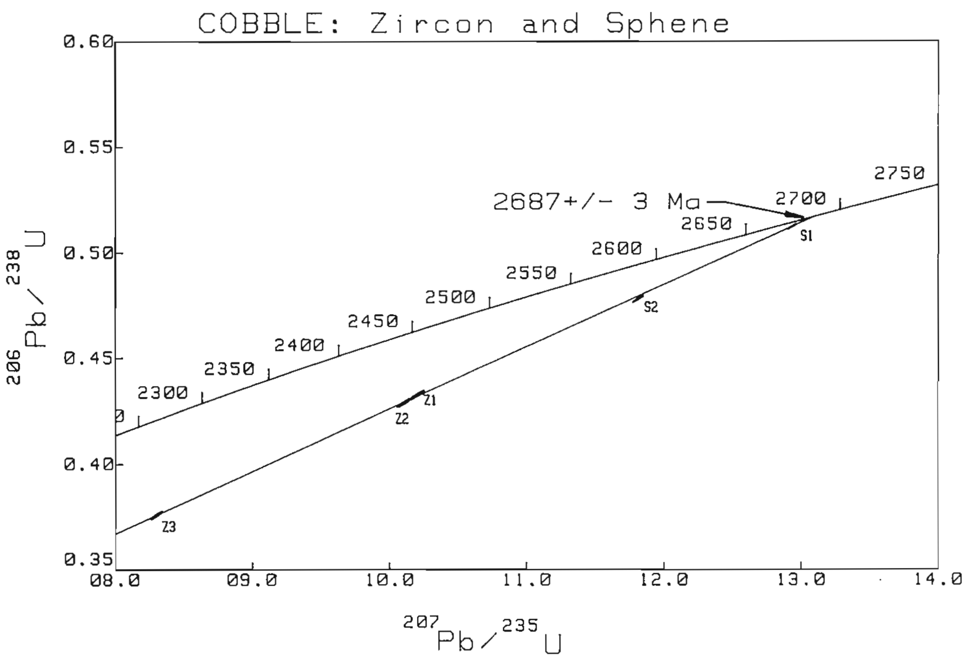

Figure 8. U-Pb concordia diagram showing analyses from sphene (S) and zircon (Z) from a tonalite boulder, sample 6, in Max Creek conglomerate. The best estimate of the age is from the regression of all five data (*see* text).

Sample no. 6 Three fractions of low-colour, subhedral zircon from the tonalite boulder were selected and analyzed. The high uranium zircon yielded a discordant, linear-trending data set which intersects concordia at 2681 ±29/24 Ma (Fig. 8). Two sphene analyses are more concordant and appear to be essentially colinear with the zircon data. A line through the 2 sphene data yields an upper intercept age of 2685.6 ± 1.9 Ma. Employing the Davis (1982) model for regression of non-linear data, the 5 analyses together give an upper intercept age of 2687 ± 3 Ma (Fig. 8) and is taken as the best estimate for the age of the boulder. This provides a maximum age for deposition of the conglomerate. Cobbles as young as 2695 Ma were dated in the type Seine conglomerate by D.W. Davis (pers. comm., 1988), suggesting a similar age to the Max Creek occurrence.

GEOLOGICAL HISTORY

The oldest event recognized in the Quetico subprovince is deposition of the sedimentary protoliths of the paragneiss-migmatite sequence. Although the sediments have not been dated directly, the presence of detrital zircons from an apparent single age population at 2702 ± 4 Ma indicates deposition after this time. A minimum age for sediment deposition is provided by the sphene data from the intrusive granodiorite sill at 2687 ± 19/13 Ma.

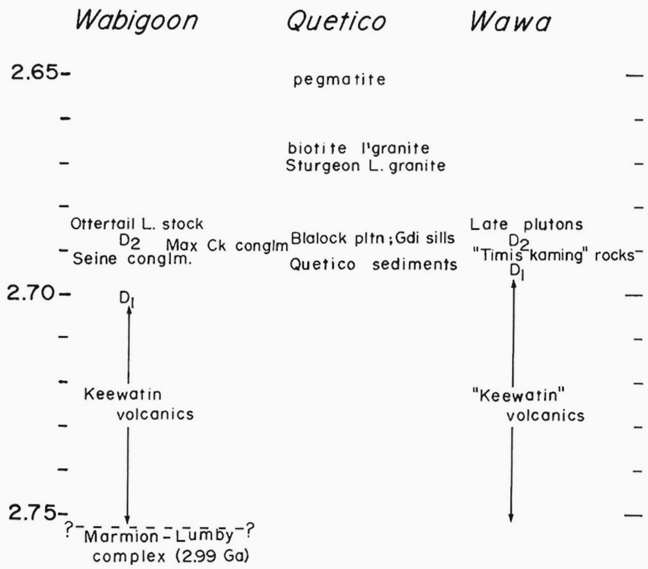

Figure 9. Age summary of events for Wabigoon, Quetico and Wawa subprovinces from this and previous studies.

Conglomerate at Max Creek could be similar in age to the Quetico sediments, or it may be younger, based on the age of 2687 ± 3 Ma for the tonalite clast. Deformation of Seine conglomerate in the Wabigoon subprovince was bracketed between 2695 Ma, the age of a tonalitic clast in the type area, and 2685 Ma, the age of the post-tectonic Ottertail Lake stock (D.W. Davis, pers. comm. 1988). The Max Creek clast age may suggest a slightly younger sequence of deposition and deformation than in the type Seine area, however, the precision of the age is not sufficient to prove this. It is more prudent to conclude that the ages of the sequences overlap, within error.

Deformation (D_1, D_2) of the sedimentary wedge occurred prior to metamorphism and pluton emplacement (Pirie and Mackasey, 1978; Sawyer and Robin, 1986). According to Williams (1987) and Percival and Williams (in press), early deformation resulted from thrusting and recumbent folding in an accretionary environment whereas steep D_2 foliation formed during a transpressional event.

Early intrusions, including the alkaline Poohbah Lake (2700 Ma K-Ar date; Mitchell, 1976; Tilton and Kwon, 1984) and Blalock (2688 Ma; U-Pb zircon; D.W. Davis, pers. comm., 1988) plutons predate granites and provide a lower limit on the time of sediment deposition.

Symmetrical patterns of regional metamorphism appear to be directly related to the presence of granitic plutons, with the highest grade assemblages and migmatites adjacent to leucocratic intrusions (Percival et al., 1985). The leucocratic plutons appear to result from partial melting of tonalitic and metasedimentary sources at depth during the metamorphism (Percival, in press; Sawyer, 1987), therefore linking metamorphism and plutonism closely together in time.

Minor D_3 structures warp the high grade portions of the belt. The minor foliation present in some leucogranites may be a manifestation of this event. Alternatively, the foliation could be a local effect of deformation zones such as the Quetico fault (Fig. 2). Whatever the cause, the event is bracketed by the age of samples 4 and 5, at 2665-2653 Ma. The sequence of events in the Quetico subprovince, incorporating results of this as well as previous studies, is summarized in Figure 9.

CONCLUSION

Several key events in the evolution of the Quetico subprovince have been bracketed using U-Pb zircon, monazite and sphene geochronology. Sediment deposition, possibly on mafic, oceanic basement (Devaney and Williams, in press), occurred after 2702 Ma ago, with provenance ages ranging from 2702-3107 Ma, including a precisely dated source of 2881.3 ± 1.2 Ma. Both the 2702 and 2881 Ma sources are represented in the volcanic rocks of the Wawa subprovince; volcanic rocks of 2702 Ma age are also known from the Wabigoon subprovince (Davis et al., 1982). Sources of 3.1 Ga detritus have not been identified from the Wawa or Wabigoon subprovinces although zircons of this age have been identified in detrital suites from elsewhere in the Quetico (D.W. Davis, pers. comm., 1988), Pontiac (Gariepy et al., 1984) and Ashuanipi (Percival et al., 1988) subprovinces. Granodiorite sills, inferred to be early intrusions on the basis of chilled textures, probably contain an inherited zircon component resulting in an anomalously old age of 2743 ± 12 Ma. Sphene data from the sill provide an age of 2687 + 19/13 Ma. This is similar to the age of the Blalock pluton, 2688 Ma (D.W. Davis, pers. comm., 1988), and provides a lower age limit for sediment deposition. Sediments were deposited and tectonically stacked in an accretionary prism (Percival and Williams, in press) prior to major transpressional deformation (Williams, 1987) at 2684-2679 Ma (Corfu and Stott, 1986). Regional metamorphism and associated leucogranite plutonism followed deformation closely. Peraluminous muscovite leucogranite of the Sturgeon Lake batholith contains zircon with xenocrystic cores, however, monazite provides an age of 2670.5 ± 2.0 Ma. Biotite leucogranite also contains an inherited zircon component and monazite which gives an age of 2665 ± 2 Ma. Late pegmatite postdates minor deformation of granite; it yields discordant zircon analyses suggestive of probable inheritance, and monazite which is dated at 2653 ± 3/4 Ma.

Several common events can be recognized in the Quetico and adjacent volcano-plutonic subprovinces. Quetico sediments are probably derived from erosion of volcanic and plutonic units, based on similar ages of zircon populations, as well as stratigraphic (Devaney and Williams, in press) and sedimentological (Ojakangas, 1985) considerations. Common transpressional deformation along the Quetico-Wawa (Corfu and Stott, 1986) and Quetico-Wabigoon (D.W. Davis pers. comm. 1988) boundaries suggests structural contiguity by about 2685 Ma ago. Major plutonism in the Quetico subprovince, at 2671-2665 Ma, is significantly later than that in the adjacent volcano-plutonic subprovinces, which peaked at about 2680 Ma in the Wawa subprovince and earlier in the Wabigoon.

ACKNOWLEDGMENTS

K.D. Card and O. van Breemen provided valuable advice in the field and through later discussions. J.K. Mortensen is thanked for helpful discussion of the data and review of the manuscript.

REFERENCES

Card, K.D.
1986: Tectonic setting and evolution of late Archean greenstone belts of Superior Province, Canada: *in* Tectonic Evolution of Greenstone Belts, Lunar and Planetary Institute, Technical Report 86-10, p.74-76.

Card, K.D. and Ciesielski, A.
1986: Subdivisions of the Superior Province of the Canadian Shield: Geoscience Canada, v.13, p.5-13.

Corfu, F. and Stott, G.M.
1986: U-Pb ages for late magmatism and regional deformation in the Shebandowan belt, Superior Province, Canada: Canadian Journal of Earth Sciences, v.23, p. 1075-1082.

Davis, D. W.
1982: Optimum linear regression and error estimation applied to U-Pb data; Journal of Earth Sciences, v. 19, p. 2141-2149.
1988: Are Archean greenstone belts the product of rifting or subduction? New evidence from geochronology in the Wabigoon subprovince, N.W. Ontario; Geological Association of Canada/Mineralogical Association of Canada, Program with Abstracts, v. 13, p. A30. (abstract).

Davis, D.W. and Jackson, M.C.
1988: Geochronology of the Lumby Lake greenstone belt: A 3 Ga complex within the Wabigoon subprovince, northwest Ontario; Geological Society of America, Bulletin, v. 100, p. 818-824.

Davis, D.W., Blackburn, C.E. and Krogh, T.E.
1982: Zircon U-Pb ages from the Wabigoon-Manitou Lakes region, Wabigoon subprovince, northwest Ontario; Canadian Journal of Earth Sciences, v. 19, p. 254-266.

Davis, D.W., Sutcliffe, R.H. and Trowell, N.F.
Geochronological constraints on the tectonic evolution of a late Archean greenstone belt, Wabigoon subprovince, northwestern Ontario, Canada; Precambrian Research, (in press).

Devaney, J.R. and Williams, H.R.
Evolution of an Archean subprovince boundary: A sedimentological and structural study of part of the Wabigoon-Quetico boundary in northern Ontario; Canadian Journal of Earth Sciences, (in press).

Frarey, M.J. and Krogh, T.E.
1986: U-Pb zircon ages of late internal plutons of the Abitibi and eastern Wawa subprovinces, Ontario and Quebec; *in* Current Research, Part A, Geological Survey of Canada Paper 86-1A, p.43-48.

Gariepy, C., Allègre, C.J. and Lajoie, J.
1984: U-Pb systematics in single zircons from the Pontiac sediments, Abitibi greenstone belt; Canadian Journal of Earth Sciences, v. 21, p. 1296-1304.

Ghent, E.D., Stout, M.Z. and Parrish, R.R
1988: Determination of metamorphic pressure-temperatue-time (P-T-t) paths, *in* Heat, Metamorphism and Tectonics, ed. E.G. Nisbet and C.M.R. Fowler; Mineralogical Association of Canada, Short Course, v. 14, p. 155-188.

Jocelyn, J. and Pidgeon, R.T.
1974: Examples of twinning and parallel growth in zircons from some Precambrian granites and gneisses; Mineralogical Magazine, v. 39, p. 587-594.

Langford, F.F. and Morin, J.A.
1976: The development of the Superior Province of northwestern Ontario by merging island arcs; American Journal of Science, v. 276, p. 1023-1034.

Mackasey, W.O., Blackburn, C.E., and Trowell, N.F.
1974: A regional approach to the Wabigoon-Quetico belts and its bearing on exploration in northwestern Ontario; Ontario Division of Mines, Miscellaneous Paper 58, 30p.

Mitchell, R.H.
1976: Potassium-argon geochronology of the Poohbah Lake alkaline complex, northwestern Ontario; Canadian Journal of Earth Sciences, v. 13, p. 1456-1459.

Mortensen, J.K.
1987: Preliminary U-Pb ages for volcanic and plutonic rocks of the Noranda-Lac Abitibi area, Abitibi Subprovince, Quebec; *in* Current Research, Part A, Geological Survey of Canada, Paper 87-1A, p. 581-590.

Ojakangas, R.W.
1985: Review of Archean clastic sedimentation, Canadian shield: Major felsic volcanic contributions to turbidite and alluvial-fluvial facies associations, *in* Evolution of Archean Supracrustal Sequences, ed. L.D. Ayres et al., Geological Association of Canada, Special Paper 28, p. 23-47.

Parrish, R.R.
1987: An improved micro-capsule for zircon dissolution in U-Pb geochronology; Chemical Geology v. 66, p. 99-102.
1988: U-Pb systematics of monazite and a preliminary estimate of its closure temperature based on natural examples; Geological Association of Canada, Program with Abstracts v. 13, p. A94. (abstract).

Parrish, R.R., Roddick, J.C., Loveridge, W.D., and Sullivan, R.W.
1987: Uranium-lead analytical techniques at the geochronology laboratory, Geological Survey of Canada; *in* Radiogenic Age and Isotopic Studies: Report 1, Geological Survey of Canada, Paper 87-2, p. 3-7.

Percival, J.A.
1983: Preliminary results of geological synthesis in the western Superior Province, *in* Current Research, Part A, Geological Survey of Canada Paper 83-1A, p. 125-131.
1988: Geological compilation of Quetico (52B); Geological Survey of Canada, Map 1682A.
A regional perspective of the Quetico belt, Superior Province, Canada, Canadian Journal of Earth Sciences, (in press).

Percival, J.A. and Williams, H.R.
The late Archean Quetico accretionary complex, Superior Province, Canada, Geology, (in press).

Percival, J.A., Stern, R.A., and Digel, M.R.
1985: Regional geological synthesis of western Superior Province, Ontario; *in* Current Research, Part A, Geological Survey of Canada, Paper 85-1A, p. 385-397.

Percival, J.A., Mortensen, J.K., and Roddick, J.C.M.
1988: Evolution of the Ashuanipi granulite complex: conventional and ion probe U-Pb data; Geological Association of Canada, Program with Abstracts, v. 13, p. A97. (abstract)

Pirie, J.A. and Mackasey, W.O.
1978: Preliminary examination of regional metamorphism in parts of Quetico metasedimentary belt, Superior Province, Ontario; *in* Geological Survey of Canada, Paper 78-10, p. 37-48.

Poulsen, K.H.
1986: Rainy Lake wrench zone: An example of an Archean subprovince boundary in northwestern Ontario: *in* Tectonic Evolution of Greenstone Belts; Lunar and Planetary Institute, Technical Report 86-10, p. 177-179.

Pye, E.G.
1968: Geology of the Lac des Iles area; Ontario Department of Mines, Geological Report 64, 47p.

Rapp, R.P., Ryerson, F.J., and Miller, C.F.
1987: Experimental evidence bearing on the stability of monazite during crustal anatexis; Geophysical Research Letters, v. 14, p. 307-310.

Sage, R.P., Wright, W., Chamois, P., and Higgins, C.
1979: Poohbah Lake alkalic complex, District of Rainy River; Ontario Geological Survey, Map P-2219.

Sawka, W.N., Banfield, J.F., and Chappell, B.W.
1986: A weathering-related origin of widespread monazite in S-type granites; Geochimica et Cosmochimica Acta, v. 50, p. 171-175.

Sawyer, E.W.
1987: The role of partial melting and fractional crystallization in determining discordant migmatite leucosome compositions; Journal of Petrology, v. 28, p. 445-473.

Sawyer, E.W. and Robin, P.Y.F.
1986: The subsolidus segregation of layer-parallel quartz-feldspar vein in greenschist to amphibolite facies metasediments; Journal of Metamorphic Geology, v. 4, p. 237-260.

Schulz, K.J.
1982: The nature and significance of Archean alkaline magmatism, southern Superior Province; Geological Association of Canada, Program with Abstracts, v. 7, p. 80 (abstract).

Smith, I.E.M. and Williams, J.G.
1980: Geochemical variety among Archean granitoids in northwestern Ontario; *in* The Continental Crust and its Mineral Deposits, ed. D.W. Strangway; Geological Association of Canada, Special Paper 20, p. 181-192.

Southwick, D.L.
1972: Vermilion granite-migmatite massif; *in* Geology of Minnesota, a centenial volume, ed. P.K. Sims and G.B. Morey; Minnesota Geological Survey, p. 108-119.

Stockwell, C.H.
1964: Fourth report on structural provinces, orogenies and time classification of rocks of the Canadian Precambrian shield; *in* Age Determinations and Geological Studies, Part II; Geological Survey of Canada, Paper 64-17, p.1-21.

Stott, G.M. and Corfu, F.
1988: Whither the Kenoran orogeny?; Geological Association of Canada/Mineralogical Association of Canada, Program with Abstracts, v. 13, p. A120 (abstract).

Tilton, G.R. and Kwon S.T.
1984: Geochemical evolution of Precambrian mantle in Superior Province, Canadian Shield; Geological Society of America, Abstracts with Program, v. 16, p. 676 (abstract).

Turek, A., Smith, P.E., and Van Schmus, W.R.
1984: U-Pb zircon ages and the evolution of the Michipicoten plutonic-volcanic terrane of the Superior Province, Ontario; Canadian Journal of Earth Sciences, v. 21, p. 457-464.

Turek, A., Van Schmus, W.R., and Sage, R.P.
1988: Extended volcanism in the Michipicoten greenstone belt, Wawa, Ontario; Geological Association of Canada, Program with Abstracts, v. 13, p. A127 (abstract).

Wilks, M.E. and Nisbet, E.G.
1988: Stratigraphy of the Steep Rock Group, northwest Ontario: a major Archaean unconformity and Archaean stromatolites; Canadian Journal of Earth Sciences, v. 25, p. 370-391.

Williams, H.R.
1987: Structural studies in the Wabigoon and Quetico Subprovinces; Ontario Geological Survey, Open File Report 5668, 163p.

Wood, J.
1980: Epiclastic sedimentation and stratigraphy in the North Spirit Lake and Rainy Lake areas: A comparison; Precambrian Research, v. 12, p. 227-255.

Use of zircon U-Pb ages of felsic intrusive and extrusive rocks in eastern Wabigoon Subprovince, Ontario, to place constraints on base metal and gold mineralization

C.D. Anglin[1], J.M. Franklin[1], W.D. Loveridge[1], P.A. Hunt[1], and S.A. Osterberg[2].

Anglin, C.D., Franklin, J.M., Loveridge, W.D., Hunt, P.A., and Osterberg, S.A., Use of zircon U-Pb ages of felsic intrusive and extrusive rocks in eastern Wabigoon Subprovince, Ontario, to place constraints on base metal and gold mineralization; in Radiogenic Age and Isotopic Studies: Report 2, Geological Survey of Canada, Paper 88-2, p. 109-115, 1988.

Abstract

The Eastern Wabigoon Subprovince contains numerous base metal and gold deposits. The principal base metal occurrences have stratigraphic and alteration characteristics indicative of a synvolcanic origin, and are thus similar to volcanic-associated massive sulphide deposits. They occur near Onaman Lake,Ontario, in the central, volcanic-dominated portion of the subprovince. The gold deposits occur near Geraldton and Beardmore, Ontario, at the southern margin of the Subprovince, and are vein and replacement bodies in highly deformed iron formation, felsic porphyritic intrusions, and sedimentary rocks.

Rhyolite that is host to the Onaman massive sulphide occurrences is 2769+6/-5 Ma. This deposit is significantly older than the somewhat similar deposits at Sturgeon Lake, Ontario, but similar to the age of volcanic rocks in the Manitou-Stormy Lakes area of western Wabigoon Subprovince.

A porphyritic intrusion near Geraldton is 2691 +3/−2 Ma. This is significantly younger than any volcanic rocks in Wabigoon. As gold mineralization cuts the porphyry, the mineralization is obviously not synvolcanic.

Résumé

La sous-province est de Wabigoon contient de nombreux gisements de métaux communs et d'or. Les principaux gîtes de métaux de base présentent une stratigraphie et une altération indiquant une origine synvolcanique et sont, de ce fait, semblables aux gisements de sulfure massif associés à des roches volcaniques. Ces gisements se trouvent près d'Onaman Lake, en Ontario, dans la partie d'origine surtout volcanique au centre de la sous-province. Les gisements aurifères se trouvent près de Geraldton et Beardmore, en Ontario, à la bordure sud de la sous-province. Il s'agit de massifs filoniens et de substitution dans une formation ferrifère très déformée, d'intrusions porphyritiques felsiques et de roches sédimentaires.

La rhyolite qui est la roche encaissante des gîtes de sulfure massif d'Onaman date de 2769 +6/−5 Ma. Ce gisement est beaucoup plus ancien que les gisements quelque peu semblables que l'on trouve à Sturgeon Lake, en Ontario, mais du même âge que les roches volcaniques de la région des lacs Manitou et Stormy dans la sous-province ouest de Wabigoon.

Une intrusion porphyritique près de Geraldton date de 2691 +3/−2 Ma. Il s'agit donc d'une intrusion beaucoup plus récente que toutes les roches volcaniques de Wabigoon. Comme la minéralisation d'or traverse le porphyre, la minéralisation est évidemment plus récente et n'est pas d'origine synvolcanique.

[1]Geological Survey of Canada, 601 Booth Street, Ottawa K1A 0E8
[2]Department of Geology, University of Minnesota, Duluth, Minnesota 55812

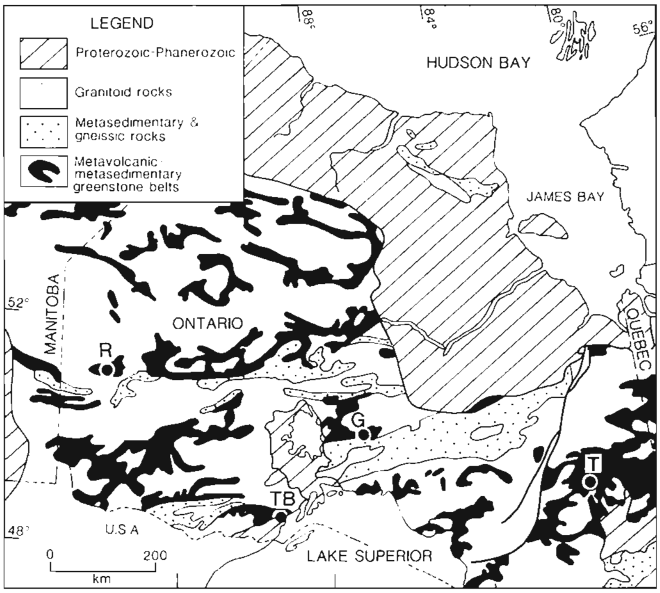

Figure 1. Location map. G = Geraldton, T = Timmins, TB = Thunder Bay, SL = Sturgeon Lake, R = Red Lake, dashed line = outline of Wabigoon Subprovince.

INTRODUCTION

The eastern Wabigoon Subprovince contains numerous gold and base metal deposits and occurrences (Fig. 1). Gold mines in the Beardmore and Geraldton areas, along the southeastern margin of the subprovince, produced approximately 2 900 000 oz of gold from 1934 to 1968 (Mason et al., 1985). The Onaman-Tashota metavolcanic belt to the north contains numerous occurrences of massive base metal sulphides, and porphyry copper-molybdenum and vein gold deposits. 250 km to the west, within the western extension of the Wabigoon Subprovince, the Sturgeon Lake camp contains five base-metal massive sulphide mines. Placing absolute age constraints on these various types of mineralization is important in determining stratigraphic and genetic relationships between districts and deposit types. In this report, the two most economically significant deposit types, base-metal massive sulphide and lode-gold deposits, are examined.

In the Geraldton area, gold mineralization is in veins and fracture zones in sedimentary rocks (including iron-formation), mafic and felsic intrusions, and mafic volcanic rocks. The felsic intrusive rocks cut all other lithologies except for diabase dykes and rare lamprophyre dykes, both of which cut gold-bearing structures (Horwood and Pye, 1955). Several hypotheses have been proposed to explain the gold mineralization; 1) because a significant proportion of the gold at Geraldton occurred in iron-formation, the mineralization might be related to a volcanogenic-hydrothermal process; 2) the felsic porphyritic intrusions which host significant gold might represent magma from which gold-rich fluids were derived; and 3) the gold-bearing fluids were transmitted along major faults and gold was emplaced in structurally-controlled sites, probably relatively late in the geological history of the area.

At the Headway-Coulee prospect near Onaman Lake, Thurston (1980) reported chloritoid alteration of subaerial felsic volcanic rocks associated with unusual, vein-hosted, Pb-Zn-Ag mineralization. The alteration and rock types are similar to those of the Mattabi deposits at Sturgeon Lake (Franklin et al., 1975). A significant proportion of the Onaman Lake Zn-Cu-Pb-Ag sulphides occurs in veins. Although their attendant alteration is metamorphosed they may not have been emplaced penecontemporaneously with their host rocks. Comparison of the crystallization age of these rocks with model lead ages of the sulphides may elucidate this problem. In addition, comparison of the ages of the deposits in the Onaman and Sturgeon Lake areas will establish if seafloor hydrothermal venting occurred at more than one time during the development of the Wabigoon volcanic complexes.

As part of a continuing study of the metallogeny of the Wabigoon belt, intensive investigations of stratigraphic, structural and geochemical aspects were undertaken in both the Geraldton and Onaman areas (Anglin, 1987; Osterberg, 1985). As part of these studies, samples for radiogenic isotope determinations were obtained to; 1) establish the age of the felsic volcanic sequence at Onaman Lake for comparison with the age of the texturally and compositionally similar subaerial felsic volcanic sequence at Sturgeon Lake; 2) determine the age of felsic porphyritic intrusive rocks in the Geraldton area to establish whether these rocks are contemporaneous with the volcanism in the eastern Wabigoon, and to place a maximum age constraint on the age of gold mineralization, and 3) obtain model Pb ages on galena from base metal mineralization for comparison with the U-Pb ages. In this contribution we present the results of the U-Pb zircon dating studies and discuss their implications with respect to the timing of base and precious metal mineralization in the two study areas.

REGIONAL GEOLOGY

The Wabigoon Subprovince (WS) in northwestern Ontario is a typical Archean granite-greenstone terrane consisting of a supracrustal assemblage of predominantly volcanic rocks and lesser amounts of sedimentary rocks, into which were emplaced plutons ranging in composition from granite to syenite and gabbro (Card, 1983; Blackburn et al., 1985; see Fig. 1). The WS extends in an east-west direction for approximately 900 km and attains widths as great as 150 km. It is bounded to the north by the English River and Winnipeg River subprovinces, and to the south by the Quetico Subprovince. Thurston (1980) and Mason and White (1986) divided the eastern WS (east of Lake Nipigon) into two belts; the Beardmore-Geraldton belt, south of the Paint Lake Fault, and the Onaman-Tashota metavolcanic belt north of this fault.

Geology of the Onaman area

The Onaman Lake greenstone area, located in the central part of the eastern WS (Fig. 2), is an elongate zone of volcanic and minor sedimentary rocks, approximately 4 km wide, situated between two very large plutons of biotite-hornblende trondhjemite and granodiorite. The volcanic

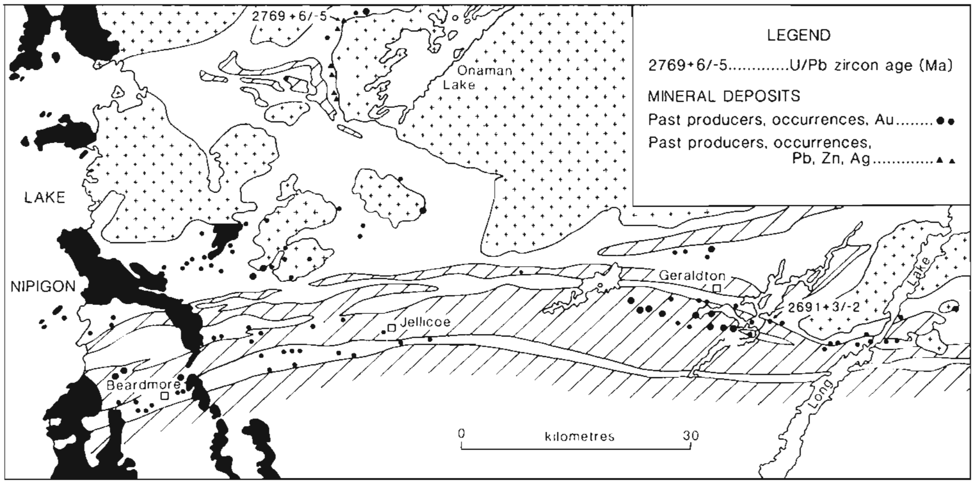

Figure 2. Geological map of the eastern Wabigoon Subprovince (after Pye et al., 1965) showing the Beardmore-Geraldton and Onaman-Tashota belts. Gold past-producers and occurrences are shown in large and small solid circles respectively; Pb-Zn past-producers and occurrences are shown in large and small solid triangles respectively. The locations of samples for U-Pb zircon study are indicated by an arrow from the age obtained on the sample. Rock types: Proterozoic diabase dykes and sills, solid pattern; granitic and gneissic rocks, crosses; metasedimentary rocks, diagonal lines; metavolcanic rocks, no pattern.

area is a north-facing homocline of pillowed basalt, with 200 to 300 m of felsic volcanic and sedimentary rocks near the centre of the volcanic pile (Thurston, 1980). Discontinuous iron-formations are intercalated with the basalt and the felsic tuff. The volcanic sequence is much thicker to the southeast in the Con Creek area (Amukun, 1980).

Felsic volcanic rocks and associated quartz-feldspar porphyry bodies, along with sedimentary strata, occur near the stratigraphic top of many of the sequences (Thurston, 1980). Granitic intrusions are a major component of this part of the belt, generally forming the boundaries to the crescent-shaped greenstone domains.

Massive sulphide mineralization was discovered in the Onaman River area in 1949 by Headvue Mines Ltd.. This occurrence contains more than 600 000 tonnes of zinc-lead mineralization (Shklanka, 1969) in chloritoid and sericite-bearing felsic and mafic volcanic rocks. Copper vein occurrences occur in the underlying mafic volcanic flows, approximately 200m below the Pb-Zn-Ag zones. A few kilometres to the east, gold was mined from the Tashota-Nipigon Mine.

The felsic rocks consist of ash tuff and porphyritic flows, and are interlayered with polymictic diamictite (Osterberg, 1985). The tuff beds formed as hydrovolcanic eruption products, in shallow subaqueous conditions (Osterberg, 1985).

A porphyritic rhyolite flow unit (sample 83FRA-602) from the Onaman Lake area was sampled for U-Pb zircon study to establish the age of the host rock sequence to the base metal mineralization. Osterberg (1985) described two felsic lava flows which occur near the top of the volcanic sequence in the Onaman area. The flow sampled for this study (*see* samples 1, 246 *in* Osterberg, 1985) was predominantly massive, with local flow-banded and brecciated portions. It contains 7-8 % round blue quartz phenocrysts (0.5-2mm diameter) and 3 % sericitized K-feldspar phenocrysts, set in a matrix of quartz, albite, sericite, and chlorite, with accessory carbonate and pyrite. Some spherulites are present. The fragments are slightly flattened, the phenocrysts have cataclastic margins, and the micas define a regional cleavage. Alteration is slight to moderate, with 3-10 % carbonate present, and some sodium depletion. The unit is unusually rich in K_2O (1.3-2.3 wt. %) compared to most Archean felsic lavas (e.g Goodwin, 1977).

Geology of the Geraldton area

Gold was first discovered in the Geraldton area of northwestern Ontario in the early 1930s. The camp was active intermittently from then until 1968, producing almost 3 million ounces of gold from 10 mines (Mason et al., 1985). The gold mineralization is superimposed on all Archean rock types in the area, including the youngest Archean lithologies, feldspar and quartz-feldspar porphyries. Unmetamorphosed Proterozoic diabase dykes, compositionally similar to Keweenawan dykes and sills near Lake Nipigon crosscut gold mineralization.

Sedimentary rocks, which dominate the Geraldton area, consist of greywacke-siltstone turbidites, conglomerate and iron-formation. This assemblage is bounded to the north by a panel of mafic volcanic rocks and to the south, across the Bankfield-Tombill Fault (BTF), by a sequence of homogeneous greywacke-siltstone turbidites. The BTF is the most prominent fault in the camp. North of the BTF the sedimentary and volcanic rocks have been intruded by hornblende-bearing mafic dioritic and gabbroic bodies of which the largest have been emplaced into the volcanic units. Feldspar and quartz-feldspar porphyries have also intruded the sequence north of the BTF and crosscut the mafic intrusions. They are preferentially localized within the northern sedimentary assemblage, but crosscut the volcanic rocks at several locations east of Geraldton.

The majority of gold occurrences and all the major mines in the Geraldton area are within the heterogeneous assemblage of sedimentary rocks. The deposits are spatially closely associated with the BTF and the felsic porphyritic intrusions. At several of the mines, including Hard Rock, MacLeod-Cockshutt, and Bankfield, the quartz-feldspar porphyries were important host rocks for quartz and quartz-carbonate veins and disseminated pyrite ore.

The felsic porphyritic intrusive dykes and sills represent the youngest lithologies in the area to be crosscut by gold mineralization and therefore can be used to place a maximum age constraint on the time of this mineralization. Their close spatial association with the gold deposits, both at Geraldton and at many of the largest gold camps in Superior and Churchill provinces, has been interpreted to indicate a possible genetic relationship between gold and these intrusions (Hodgson and MacGeehan, 1982).

To establish the absolute timing of intrusion, and therefore a maximum age for the gold mineralization, a large sample of relatively unaltered feldspar porphyry was collected for zircon separation and U-Pb isotopic analysis. Determination of the absolute age of ore formation is more difficult, as the veins contain no minerals useful for conventional radiometric isotopic age determinations.

A minimum relative age may be placed on the mineralization on the basis of diabase dykes which crosscut the mineralization. These dykes are unmetamorphosed, unaltered and undeformed (other than a dextral offset of approximately 650 m for some dykes crosscutting the BTF (Horwood and Pye, 1955)). Two types of diabase dykes are present. One set is oriented slightly east or west of north and is mineralogically similar to the Matachewan diabase dykes of eastern Superior Province. They are distinguished from the younger Keweenawan dykes by their porphyritic texture (Horwood and Pye, 1955). The age of these dykes has not been determined in the Geraldton area, but a recent U-Pb zircon age of 2454 Ma has been obtained on a Matachewan-type dyke at Hearst (Heaman, 1988). The other dykes are more abundant, oriented north-south, and are though to be correlative with mineralogically similar Keweenawan dykes and sills exposed in the vicinity of Lake Nipigon (Horwood and Pye, 1955). These dykes near Lake Nipigon are 1109.7 ± 2 Ma (Davis and Sutcliffe, 1984); this is the minimum time of gold introduction.

The sample of porphyritic intrusion for age determination was collected from an outcrop approximately 5 km southeast of Geraldton (Wods-Mac property, sample 83FRA-209; sample location and age indicated on Figure 2). Petrographic inspection revealed that this porphyry body is the least deformed and altered of all of those sampled in the Geraldton area. To the east and west of this location the porphyries have significant carbonate, sericite and pyrite alteration and are variably strained and foliated.

The Wods-Mac porphyry consists of plagioclase phenocrysts (5-8mm) that form up to 30% of the rock. The phenocrysts are both twinned and untwinned, and zoned and unzoned. The zoning, where present, is oscillatory, and compositions range from An_{25-35} (Anglin, 1987). The phenocrysts are euhedral to subhedral, but are variably altered to sericite and minor carbonate. The groundmass, which makes up approximately 70% of the rock, is composed of fine grained quartz and plagioclase, with minor sericite, carbonate, chlorite and biotite. The Wods-Mac sample is only weakly foliated.

U-PB ZIRCON ISOTOPE PROCEDURES

Approximately 40 kg of rock were collected at each locality sampled for zircon studies. Procedures used for concentration of zircon and preparation of zircon fractions, chemical extraction of U and Pb from zircon and isotopic analyses of U and Pb are described in van Breemen et al. (1986). Fraction 12 was analyzed using refined mass spectrometric techniques (Roddick et al., 1986).

U-Pb ages have been calculated using the uranium decay constants and isotopic composition recommended by Steiger and Jaeger (1977). Linear regression of the U-Pb data and error estimation is based on Davis (1982). Davis' model for non linear data (op. cit.) was used for regression of 83-FRA-602 data where the data points were not collinear within analytical uncertainty. The U-Pb data are presented in Table 1 and Figure 3.

Geraldton felsic porphyry (samples 83-FRA-209)

Five fractions were analyzed, two abraded and three not abraded. The data points are collinear and regression analysis of the five analyses yields upper and lower intercept ages of 2691+3/−2 and 328+79/−74 Ma. The zircon crystals display continuous internal growth zoning and euhedral habit; accordingly the upper intercept age is interpreted as the age of intrusion of the porphyritic felsic intrusion.

Porphyritic rhyolite, Onaman Lake area, (sample 83-FRA-602)

Coarse and fine non-magnetic fractions were picked from the zircon concentrate. Each fraction was split and one part was abraded. Analytical results are presented in Table 1 and depicted in Figure 3. The data points for the abraded fractions are considerably more concordant than those of their unabraded twins. U contents of all fractions are relatively low (less than 260 ppm) and U appears to be concentrated near the surface as the abraded fractions have 60% and 20% less U than their unabraded counterparts.

Table 1. Analytical data, U-Pb analyses of zircon.

Size and characteristics	Weight (mg)	U (ppm)	Pb* (ppm)	Measured $^{206}Pb/^{204}Pb$	Isotopic abundances $^{206}Pb=100$ ^{204}Pb	^{207}Pb	^{208}Pb	Isotopic ratios $^{206}Pb/^{238}U$	$^{207}Pb/^{235}U$	Age, Ma $^{207}Pb/^{206}Pb$
Wods Mac feldspar porphyry, 83-FRA-209										
1a - 105+74 NOA	0.019	301.5	167.0	2528	0.0107	18.526	8.961	0.50685	12.856	2689
1b - 105+74 MOA	1.54	228.8	123.6	1842	0.0435	18.853	11.160	0.49041	12.390	2682
1c - 105+74 MO	0.68	733.6	390.1	3234	0.0220	18.557	10.843	0.48129	12.136	2679
1d - 74+62 M-1	3.15	297.0	157.8	6531	0.0120	18.459	11.133	0.47837	12.078	2681
1e - 62+35 N-2	3.17	245.3	129.1	5380	0.0174	18.503	12.040	0.47127	11.885	2679
Onaman Lake rhyolite, 83-FRA-602										
2a - 105+74 NIA	0.38	105.0	64.40	1362	0.0166	19.429	18.797	0.51799	13.734	2762
2b - 74+62 NIA	0.69	179.5	110.07	1172	0.0651	19.961	22.366	0.51054	13.501	2758
2c - 105+74 NI	1.21	260.4	147.6	767	0.1213	20.398	23.809	0.47360	12.366	2737
2d - 74+62 NI	1.11	223.9	124.7	634	0.1356	20.572	25.078	0.46247	12.073	2736

Size fractions are given in μm; N = non magnetic, M = magnetic at given angle; A = hand picked and abraded, all others are hand picked; Pb*ppm = radiogenic Pb content; Pb isotopic abundances are given after correction for mass spectrometer discrimination (fractionation) and Pb blank.

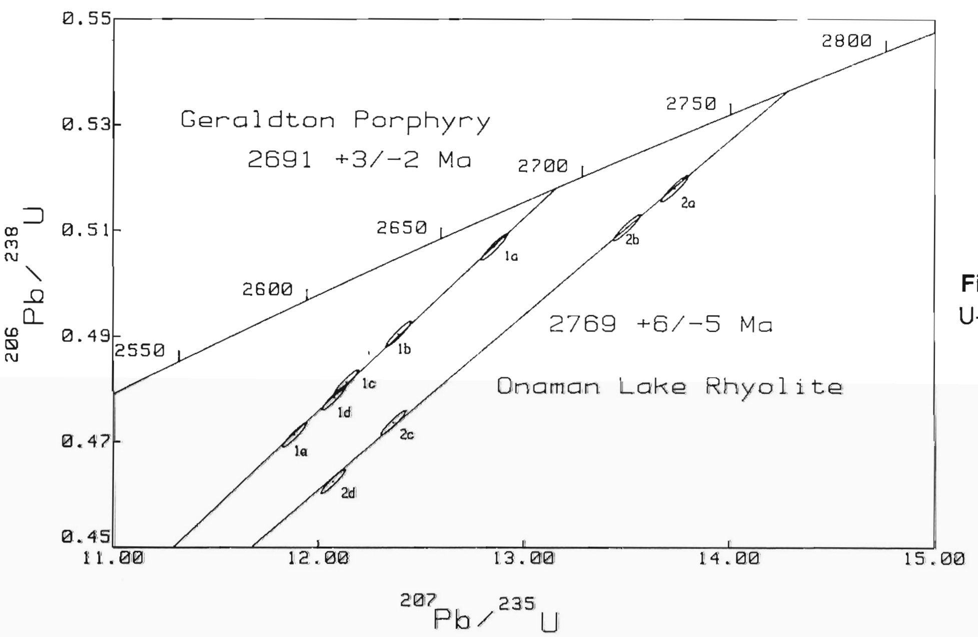

Figure 3. Concordia plot of U-Pb analyses.

The four points are not quite collinear within analytical uncertainty. Regression using Davis' (1982) method for non-linear data, results in concordia intercept ages of 2769+6/-5 and 539 Ma. The fine, unabraded fraction (d) is most discordant. Although it has a lower bulk U content than fraction (c), its higher surface to volume ratio would be expected to make it more susceptible to surface-correlated lead-loss. The data points for the other three fractions are collinear and yield upper and lower intercept ages of 2771+4/-3 and 606 Ma. Although excluding the fine, unabraded, most discordant fraction from the regression may well be valid, we adopt the more conservative upper intercept age of 2769+6/-5 Ma as the age of extrusion of the rhyolite.

DISCUSSION OF RESULTS

Onaman sulphide deposits:

The U-Pb zircon crystallization age of 2769+6/-5 Ma for the porphyritic rhyolite flow from the Onaman Lake area is clearly significantly older than the similar-looking volcanic sequence at Sturgeon Lake, 245 km to the west (lower cycle = 2735 Ma, uppermost cycle = 2718 Ma, Davis et al., 1985; Blackburn et al., 1985). The Onaman age is relatively old for extrusive volcanic activity in the WS as a whole (see compilation of western WS age dates by Blackburn et al., 1985, p.107, Fig. 16). They state that "the oldest age so far obtained from the supracrustal sequences is 2755 Ma, a minimum age from the Thundercloud porphyry which intruded the upper part of the tholeiitic Wapageisi Group in the Manitou-Stormy Lakes area. The group is 8000 m thick, and basal members thus may be considerably older." (Blackburn et al., p.107). It may be that the volcanic rocks in the Manitou-Stormy Lakes area are correlative with those in the Onaman Lake area, and these may represent an older section of the Wabigoon greenstone belt.

Geraldton porphyritic intrusions and their relationship to gold deposits.

The crystallization age of 2691 +3/-2 Ma for the Wods-Mac porphyritic intrusion in the Geraldton area illustrates that these rocks are clearly not contemporaneous with the volcanism in the Onaman Lake area. Although no other ages have been obtained on volcanic rocks in the Beardmore-Geraldton or Onaman-Tashota belts, none of the ages of extrusive rocks in the western WS (Blackburn et al., 1985) are as young as this porphyry age. The 2691 Ma age correlates very well, however, with other post-volcanic felsic intrusive events in the western WS. For example, in the Manitou-Stormy Lakes area the post-tectonic Taylor Lake Stock is 2695 $\pm$ 3.6 Ma old. In the Geraldton area the feldspar porphyry bodies are locally highly deformed and this deformation may have occurred over a much longer time interval than in other parts of the subprovince. However, the age, composition and setting of the felsic porphyritic rocks at Geraldton are very similar to those of similar plutons at Timmins (Marmont and Corfu, 1988).

As gold mineralization clearly cuts the porphyry bodies at Geraldton, it must have occurred later than the time of intrusion, and therefore is definitely not contemporaneous with volcanism in the southeastern WS. If it is valid to extrapolate an age of 2454 Ma (Heaman, 1988) for a Matachewan-type dyke at Hearst to dykes that cut ore at Geraldton, then gold mineralization is constrained to the range 2691 to 2454 Ma.

CONCLUSIONS

1) Rhyolite in the Onaman Lake area is older than most of the volcanic rocks in the Wabigoon Subprovince for which age data are available. The Wabigoon greenstone belts probably formed over a longer interval than most of those in the Abitibi Subprovince (Mortensen, 1987).

2) The Onaman Lake sulphide deposits are distinctly older than the deposits at Sturgeon Lake. Seafloor hydrothermal activity was thus not constrained to a single period of volcanism within the Wabigoon Subprovince.

3) The Geraldton porphyritic intrusion is younger than any of the Wabigoon volcanic sequences for which age determinations exist. Its age relationships to surrounding rocks are generally similar to those of the porphyry bodies at Timmins (Marmont and Corfu, 1988). It was probably emplaced at the same time as many of the large syn- to post-tectonic felsic batholiths that separate the greenstone belts in the Wabigoon Subprovince. Although the temporal and genetic relationships between the gold mineralization and the porphyries has not been clearly established in the Geraldton area, the gold mineralization was emplaced syn- to post-intrusion and therefore is 2691 Ma old or younger.

APPENDIX.

MORPHOLOGY OF ZIRCON POPULATIONS

82-FRA-209, Wods Mac feldspar porphyry: This zircon concentrate consists of more or less uniform purple translucent, euhedral crystals with fine zoning. Length to breadth ratios fall in the 3:1 to 4:1 range but many crystals are broken, particularly in the larger size fractions. Clear bubble inclusions and fractures are common. Some crystals show overgrowths of a clearer lighter colour on terminations; a few have multiple terminations. Some crystals have darker purple inner domains and lighter coloured, coarse euhedral, zoned rims while others are more uniform. Etched sections indicate that the inner domains are not cores of inherited zircon, but rather central enclaves defined by a U-rich zone. Zoning is continuous from the central domain through the surrounding zircon and into the clear overgrowths.

83-FRA-602, Onaman Lake rhyolite: This zircon population consists of a wide size range of clear to translucent, euhedral crystals. Length to breadth ratios range from unity to 4:1. Clear rod and bubble inclusions are prevalent; some dark inclusions were noted. No cores were seen and fractures are rare. All crystals are euhedral but terminations are somewhat rounded or frosted and the facets are indistinct. Up to 50 % of the crystals are broken, particularly in the large grain sizes.

REFERENCES

Amukun, S.E.,
1980: Geology of the Conglomerate Lake area, District of Thunder Bay; Ontario Geological Survey, Report 197, 101 p. (accompanied by map 2429, scale 1:31680).

Anglin, C.D.,
1987: Geology, Structure and Geochemistry of Gold Mineralization in the Geraldton area, Northwestern Ontario; unpublished, MSc thesis, Memorial University of Newfoundland, 283 p.

Blackburn, C.E., Bond, W.D., Breaks, F.W., Davis, D.W., Edwards, G.R., Poulsen K.H., Trowell, N.F., and Wood, J.
1985: Evolution of Archean volcanic-sedimentary sequences of the Western Wabigoon Subprovince and its margins: a review; *in* Evolution of Archean Supracrustal Sequences, Ed. L.D. Ayres, P.C. Thurston, K.D. Card, and W. Weber, Geological Association of Canada, Special Paper 28.

Card, K.D.
1983: Regional geological synthesis, central Superior Province: reconnaissance investigations in the Nakina area, Ontario; *in* Current Research, Part A, Geological Survey of Canada, Paper 83-1A, p.25-27.

Davis, D.W.
1982: Optimum linear regression and error estimation applied to U-Pb data; Canadian Journal of Earth Sciences, v. 19, no. 11, p. 2141-2149.

Davis, D.W. and Sutcliffe, R.H.
1984: U-Pb ages from the Nipigon Plate; *in* Geological Association of Canada/ Mineralogical Association of Canada Joint Annual Meeting, Program with Abstracts, v. 9, p. 57

Davis, D.W., Krogh, T.E., Hinzer, J., and Nakamura, E.
1985: Zircon dating of polycyclic volcanism at Sturgeon Lake and implications for base metal mineralization; Economic Geology, v. 80, p. 1942-1952.

Franklin, J.M., Kasarda, J., and Poulsen, K,H.
1975: Petrology and chemistry of the alteration zone of the Mattabi massive sulphide deposit; Economic Geology, v. 70, p. 63-79.

Goodwin, A.M.
1977: Archean volcanism in Superior Province, Canadian Shield, *in* Volcanic Regimes in Canada, Ed. W.R.A. Baragar, L.C. Coleman, and J.M. Hall; Geological Association of Canada, Special Paper 16, p.205-241.

Heaman, L.M.
1988: A precise U-Pb zircon age for a Hearst dyke; *in* Geological Association of Canada, Mineralogical Association of Canada, Joint Annual Meeting, Program with Abstracts v. 13.

Hodgson, C.J. and MacGeehan, P.J.
1982: Geological characteristics of gold deposits in the Superior Province of the Canadian Shield, *in* Geology of Canadian Gold Deposits, Ed. R.W. Hodder, and W. Petruk; Canadian Institute of Metallurgy and Minning, Special Volume 24.

Horwood, H.C. and Pye, E.C.
1955: Geology of Ashmore Township, Ontario Department of Mines, Annual Report, v. 60, part 5, 105 p.

Krogh, T.E.
1982: Improved accuracy of U-Pb zircon ages by the creation of more concordant systems using an air abrasion technique; Geochimica et Cosmochimica Acta, v. 46, p. 637-649.

Marmont, S. and Corfu, F.
1988: Timing of gold introduction in the late Archean tectonic framework of the Canadian Shield: evidence from U-Pb zircon geochronology of the Abitibi Subprovince; Bicentennial Gold 88, Melbourne, May 1988.

Mason, J. and White, G.
1986: Gold occurences, prospects and deposits of the Beardnote — Geraldton area, districts of Thunder Bay and Cochrane; Ontario Geological Survey, Open File Report 5630, 680 p.

Mason, J., White, G., and McConnell, C.
1985: Field guide to the Beardmore-Geraldton metasedimentary-metavolcanic belt; Ontario Geological Survey, Open File Report 5538, 73p.

Montensen, J.K.
1987: Preliminary U-Ph zircon ages for volcanic and plutonic rocks of the Noranda — Lac Abitibi area, Abitibi Subprovince, Québec; *in* Current Research, Part A, Geological Survey of Canada, Paper 87-1A, p. 581-590.

Osterberg, S.A.
1985: Stratigraphy and Hydrothermal Alteration of Archean Volcanic Rocks at the Headway-Coulee Massive Sulfide Prospect, Northern Onaman Lake area, Northwestern Ontario; unpublished MSc thesis, University of Minnesota at Duluth, 114 pp.

Pye, E.G., Harris, F.R., Fenwick, K.G., and Baillie, J.
1965: Tashota-Geraldton Sheet, Thunder Bay and Cochrane Districts; Ontario Department of Mines, Geological Compilation Series Map 2102, (scale 1 inch to 4 miles or 1:253 440).

Roddick, J.C., Loveridge, W.D., and Parrish, R.
1986: Precise U/Pb dating of sub-milligram quantities of zircon; Sixth International Conferences on Geochronology, Cosmochronology and Isotope Geology, Cambridge U.K.

Shklanka, R.
1969: Copper, Nickel, Lead and Zinc Deposits of Ontario, Ontario Department of Mines, Mineral Resources Circular No. 12.

Steiger, R.H. and Jaeger, E.
1977: Subcommission on Geochronology: convention on the use of decay constants in geo- and cosmochronology; Earth and Planetary Science Letters, v. 36, p. 359-362.

Thurston, P.C.
1980: Geology of the Northern Onaman Lake area, District of Thunder Bay; Ontario Geological Survey, Report 208, 81 p. (accompanied by Map2411, scale 1:31 680, and Chart A).

van Breemen, O., Davidson, A., Loveridge, W.D., and Sullivan, R.W.
1986: U-Pb zircon geochronology of Grenville tectonites, granulites, and igneous precursors, Parry sound, Ontario; *in* The Grenville Province, ed. J.M. Moore, A. Davidson and A.J. Boer; Geological Association of Canada, Special Paper 31 p. 191-207.

U-Pb zircon and monazite ages from the Precambrian Shield of Ellesmere and Devon islands, Arctic Archipelago

Thomas Frisch and P.A. Hunt

Abstract

Frisch, T. and Hunt, P.A., U-Pb zircon and monazite ages from the Precambrian Shield of Ellesmere and Devon islands, Artic Archipelago; in Radiogenic Age and Isotopic Studies: Report 2, Geological Survey of Canada, Paper 88-2, p. - , 1988.

U-Pb dating of rocks from the granulite facies terrane of the northernmost Canadian Shield yields the following results.

(1) Zircons from interlayered gneisses indicate that Archean crust is present in southern Devon Island.

(2) Zircon from gneissic orthopyroxene tonalite in Ellesmere Island, interpreted to have grown during granulite metamorphism, has a concordia upper intercept age of 1960 ± 5 Ma. Monazites from the same rock and from a closely associated granite give ages around 1930 Ma, a minimum age for the metamorphism.

(3) A small monzonorite intrusion, probably of deep crustal derivation, in eastern Ellesmere Island is precisely dated at 1912 ± 2 Ma, showing that post-metamorphic magmatism was locally active.

The distribution of isotopic ages — Archean in the south (Devon Island), Proterozoic in the north (Ellesmere Island) — corresponds broadly to that in the Precambrian Shield of Greenland on the opposite side of northern Baffin Bay.

Résumé

Des datations U-Pb provenant de roches du terrain granulitique à l'extrême nord du Bouclier canadien donnent les résultats suivants:

(1) Les zircons extraits des gneiss interlités indiquent la présence d'une croûte archéenne dans le sud de l'île Ellesmere.

(2) Les zircons d'une tonalite gneissique à orthopyroxène sur l'île Ellesmere, interpretés comme un produit du métamorphisme granulitique, ont une intersection supérieure sur concordia à 1960 ± 5 Ma. Les monazites de la même roche et celles d'un granite associé donnent des âges autour de 1930 Ma, âge minimum du métamorphism.

(3) Une petite intrusion de monzonorite, probablement d'origine infracrustale, dans l'est de l'île Ellesmere est datée précisément à 1912 ± 2 Ma, signe d'un magmatisme post-métamorphique localement actif.

La répartition des âges isotopiques — archéen dans le sud (île Devon), protérozoïque dans le nord (île Ellesmere) — correspond schématiquement à celle du bouclier précambrien du Groënland, côté opposé de la baie de Baffin du nord.

INTRODUCTION

The northernmost exposures of the Canadian Shield occur on eastern Devon Island, Coburg Island and southeastern Ellesmere Island in the eastern High Arctic. This remote and rugged terrain was little known geologically until regional reconnaissance mapping was undertaken in the period 1977-82. Prior to the work reported here, a single K-Ar determination on biotite from a gneiss constituted the sum total of our geochronological knowledge of the crystalline rocks of this 60 000 km^2 area.

GEOLOGICAL SETTING

The Precambrian Shield of the region, conveniently referred to as the Ellesmere-Devon terrane, consists of highly deformed, granulite facies, meta-igneous and metasedimentary rocks, which are overlain by unmetamorphosed Neohelikian and lower Paleozoic strata (Fig. 1). An account of the geology has recently been published (Frisch, 1988). Isotopic data and interpretations contained in that report are superseded by the present paper.

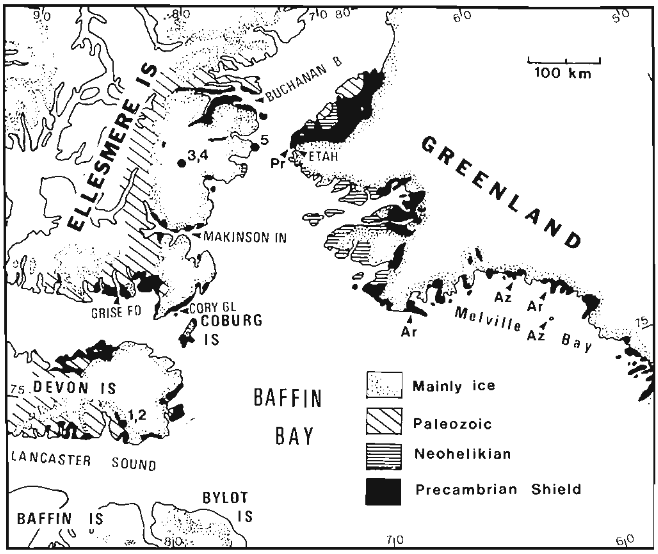

Figure 1. Geological sketch map of northern Baffin Bay, showing sample localities. 1,2 - FS-78-25 and 26; 3,4 - FS-77-331 and 332; 5 — FS-84-101. A and P refer to Archean and Proterozoic U-Pb zircon (z) and Rb-Sr whole-rock (r) ages (Dawes et al., 1988).

Major units of the crystalline terrane are orthopyroxene-bearing quartzofeldspathic gneiss and migmatitic garnet-sillimanite-cordierite-biotite gneiss. Marble and quartzite are common, if subordinate, members of the supracrustal assemblage on Ellesmere and Coburg islands; they are scarce on Devon Island. The quartzofeldspathic gneiss, which is predominantly tonalitic, may be of both intrusive and supracrustal origin and may include rocks older than the metasediments. However, no basement-cover relationship has been recognized. The gneisses and metasediments are interpreted to represent a metamorphosed continental margin sequence of shales, greywackes, shallow-water carbonates and volcanogenic rocks. Mineralogical thermobarometers indicate pressures and temperatures of 0.7 to 0.3 GPa and about 750° (locally higher) to 500°C, largely reflecting decompression and cooling following the metamorphic climax. Maximum paleopressures appear to be slightly higher on Devon Island than elsewhere.

Another major group of rocks includes granitoids of plutonic aspect, ranging from pyroxene-bearing tonalite-quartz norite to several varieties of granite. Dark weathering, generally massive and fresh, noritic to tonalitic bodies, commonly with clinopyroxene and hornblende in addition to orthopyroxene, outcrop at a number of places on Ellesmere and Coburg islands but are volumetrically minor components of the plutonic suite. One important variety of granite is felsic and carries abundant perthite phenocrysts and orthopyroxene. This rock would be termed charnockite by some workers but we prefer to use the terminology of Streckeisen (1974) and call such rocks orthopyroxene granite. Retrogression is locally common and resulted in replacement of orthopyroxene by biotite. Another variety of granite, particularly abundant on Ellesmere Island, is a peraluminous S-type with garnet, cordierite and/or sillimanite. The occurrence of this granite in bodies ranging from veins in garnet-sillimanite-cordierite gneiss to stocks with schlieren of gneiss attests to its generation by anatexis of aluminous metasediments.

Although commonly massive or only crudely gneissic, virtually all the granitoid bodies show evidence of deformation and some are strongly gneissic. Clear evidence of intrusion is generally lacking: contacts are concordant, chilled margins absent, and xenoliths of country rock rare. At a few localities, however, field relations such as inclusions of granulite facies gneiss in massive orthopyroxene granite (Frisch, 1988, Fig. 64) and contact effects in marble at borders of granitoid bodies demonstrate an intrusive origin for the latter. Furthermore, no rock so far examined from the Ellesmere-Devon terrane shows evidence that the granulite facies mineralogy represents an overprint on a lower grade assemblage. Hence the bulk of the granitoid rocks are thought to have intruded pre- or syntectonically under granulite facies conditions.

Lithological and gneissic trends are predominantly north-south on Ellesmere and Coburg islands but east-west on Devon Island. Coupled with the lithological differences mentioned above, the contrasting structural trends suggest that Devon Island may not belong to the same tectonic block as Ellesmere and Coburg islands. There is, however, a strong overall similarity in lithology and metamorphic grade between all three islands.

The Precambrian Shield outcropping extensively in northwestern Greenland (Fig. 1) is probably an extension of the Ellesmere-Devon terrane. Correlations between Greenland and adjacent Canada have been made on the basis of not only lithology and metamorphic grade but also chronological and tectonic history (Frisch and Dawes, 1982).

K-Ar mineral ages from metamorphic rocks of the region cluster around 1.7 $\pm$ 0.1 Ga. They include a biotite age of 1760 Ma from a gneiss in southeastern Ellesmere Island (Lowdon et al., 1963, p. 30) and hornblende and biotite ages of 1740 $\pm$ 47 and 1769 $\pm$ 24 Ma from tonalite and granite gneisses, respectively, in southern Devon Island (GSC 87-138 and 139 *in* Hunt and Roddick, 1987). A number of similar K-Ar ages have been obtained from northwest Greenland (Larsen and Dawes, 1974).

A suite of rocks for U-Pb geochronology was collected during reconnaissance mapping of the Ellesmere-Devon terrane. The major aims of the present study were to determine the protolith age of quartzofeldspathic gneisses on Devon Island and the age of granitoid magmatism and metamorphism on Ellesmere Island. The samples dated comprise two gneisses from Devon Island and five plutonic granitoid rocks from Ellesmere Island. Two of the latter — orthopyroxene granite from Grise Fiord and S-type anatexite from Makinson Inlet (Fig. 1) — contained strongly zoned zircons of mixed ages giving highly discordant and inconclusive results and are not considered further.

Table 1. U-Pb zircon and monazite data

Fraction, Size[1]	Weight (mg)	U (ppm)	Pb[2] (ppm)	$^{206}Pb/^{204}Pb$[3]	Pb_c[4] (pg)	^{208}Pb[2] (%)	$^{206}Pb/^{238}U$ +/-SEM%[5]	$^{207}Pb/^{235}U$ +/-SEM%[5]	$^{207}Pb/^{206}Pb$ +/-SEM%[5]	$^{207}Pb/^{206}Pb$ age, error (Ma)[6]
Devon Island										
Orthopyroxene tonalite gneiss FS-78-25 (74°43′N, 82°33′W)										
1a +105 NMO abr	0.0664	349.5	177.9	9630	68	11.7	0.45060 (.12)	9.9294 (.17)	0.15982 (.06)	2453.7 (.7)
1b +105 NMO abr	0.0222	217.1	114.4	2350	60	13.3	0.45752 (.24)	10.1531 (.25)	0.16095 (.05)	2465.6 (.8)
1c -105+74 NMO abr	0.068	289.2	145.4	4998	109	13.0	0.43987 (.16)	9.4652 (.17)	0.15606 (.04)	2413.5 (.7)
1d -105+74 NMO abr	0.073	307.2	149.2	6444	93	12.6	0.42745 (.18)	9.0558 (.19)	0.15365 (.04)	2387.0 (.7)
Granite gneiss FS-78-26 (74°43′N, 82°33′W)										
2a +74 NMO abr	0.0672	772.9	326.7	3013	425	8.3	0.39120 (.15)	8.1844 (.17)	0.15174 (.05)	2365.6 (.9)
2b +74 MagO abr	0.0717	807.7	355.7	4537	325	8.8	0.40437 (.16)	8.5848 (.18)	0.15398 (.04)	2390.5 (.7)
2c -74+62 MagO abr	0.0269	853.5	390.7	3570	168	9.8	0.41442 (.18)	9.0450 (.19)	0.15830 (.05)	2437.5 (.8)
Ellesmere Island										
Pink granite FS-77-331 (78°8′30″N, 79°56′W)										
3a +74 MagO abr	0.0320	878.9	321.0	1592	378	11.0	0.33756 (.12)	5.5550 (.16)	0.11935 (.07)	1946.6 (1.3)
3b +74 NMO abr	0.0248	890.5	313.3	1929	241	9.0	0.33292 (.11)	5.4167 (.14)	0.11800 (.06)	1926.2 (1.1)
3ma monazite	0.0129	1697.2	7605.0	11640	41	92.5	0.34752 (.09)	5.6623 (.09)	0.11817 (.03)	1928.7 (0.6)
3mb monazite	0.0199	1940.7	8607.0	12660	67	92.4	0.34865 (.11)	5.6951 (.12)	0.11847 (.03)	1933.3 (0.5)
Orthopyroxene tonalite FS-77-332 (78°8′30″N, 79°56′W)										
*4a +74	1.86	679.9	207.5	6969	986	8.4	0.29139 (.25)	4.6376 (.25)	0.11543 (.05)	1886.5 (.9)
*4b -62	1.26	375.5	116.8	6875	2014	6.2	0.31894 (.25)	5.1670 (.25)	0.11750 (.05)	1918.5 (.9)
*4c -74+62	2.24	279.4	91.6	6958	589	7.4	0.31582 (.25)	5.1157 (.25)	0.11748 (.05)	1918.2 (.9)
4d -74+62 abr	0.015	513.7	189.8	1545	109	10.1	0.34485 (.25)	5.6868 (.32)	0.11960 (.07)	1950.3 (1.2)
4ma monazite	0.0260	2299.3	5159.0	21440	62	84.9	0.35026 (.09)	5.7329 (.10)	0.11817 (.03)	1935.8 (.5)
4mb monazite	0.0139	2728.3	7792.0	22290	37	88.2	0.34702 (.12)	5.6528 (.12)	0.11814 (.03)	1928.3 (.5)
Two-pyroxene monzonorite FS-84-101 (78°19′30″N, 75°4′W)										
5a +149 NM-4 abr	0.1135	109.3	44.6	624	442	18.8	0.34453 (.10)	5.5648 (.22)	0.11715 (.16)	1913.1 (1.4)
5b -149+105 NM-4 abr	0.1637	89.9	36.3	3177	101	18.3	0.34406 (.09)	5.5548 (.12)	0.11709 (.05)	1912.3 (.43)
5c -105+74 NM-4 abr	0.0677	81.5	32.7	3382	36	17.3	0.34529 (.09)	5.5738 (.11)	0.11708 (.05)	1912.1 (.8)
5d -74 NM-4 abr	0.0865	87.5	35.1	2016	82	17.4	0.34425 (.09)	5.5542 (.12)	0.11702 (.06)	1911.2 (.5)

Notes: [1]sizes (-74+62) refer to length aspect of zircons in microns (i.e. through 74 micron sieve but not the 62 micron sieve); abr=abraded, NM1=non-magnetic cut with Frantz at 1 degree side slope, MagO=magnetic cut with Frantz at 0 degree side slope; [2]radiogenic Pb; [3]measured ratio, corrected for spike and fractionation; [4]total common Pb in analysis corrected for fractionation and spike; [5]corrected for blank Pb and U, common Pb, errors quoted are one sigma in percent; [6]corrected for blank and common Pb, errors are one sigma in Ma; fractions marked with * used a 208 spike for analysis; decay constants used are those of Steiger and Jäger (1977); for analytical details see Parrish et al. (1987).

ANALYTICAL PROCEDURES

Methods of analysis for U-Pb in zircon and monazite used in this work follow those outlined by Parrish et al. (1987). Analytical results are presented in Table 1. Errors on individual analyses were propagated numerically and are quoted at the one sigma level.

Also included are data of 1980 vintage, whose methodology is outlined in Sullivan and Loveridge (1980). These fractions are identified with an asterisk in Table 1 and utilized a ^{208}Pb-^{233}U-^{235}U spike. Errors were estimated to be 0.25 % at the one sigma level for both $^{207}Pb/^{235}U$ and $^{206}Pb/^{238}U$ ratios.

Most zircon fractions were abraded by the method of Krogh (1982) prior to dissolution, in order to remove overgrowths on grains and to decrease the amount of surface-correlated Pb loss.

Discordia line fitting used a modified York II type regression and concordia intercept, and associated errors were calculated using the algorithm of Ludwig (1980) (*see* Parrish et al., 1987 for discussion). Errors quoted for the concordia intercept ages are given at the two sigma level.

INTERLAYERED TONALITE AND GRANITE GNEISSES, DEVON ISLAND (samples 1 and 2)

Mafic orthopyroxene tonalite gneiss (sample 1:FS-78-25) and felsic granite gneiss (sample 2:FS-78-26), interlayered on the scale of a metre or so, occur 16 km east of Croker Bay, southern Devon Island (Fig. 1). Although more mafic than usual, the tonalite gneiss is otherwise representative of the orthopyroxene-bearing quartzofeldspathic gneiss that underlies much of the southern coastal region of Devon Island. The rocks typically are highly deformed in belts that probably represent ductile shear zones (Frisch, 1988, Fig. 83).

In the outcrop sampled, both gneiss types are fine grained and mylonitic and contacts between them are concordant. Because granite veining is a common feature in the Ellesmere-Devon terrane, it seems likely that granite intruded tonalite and both were deformed together.

The tonalite gneiss consists of ferrohypersthene, brownish green horblende, brown biotite, plagioclase (An_{32}), and quartz; small garnets occur sporadically. The granite gneiss is made up of hematite-dusted K-feldspar, ribbon quartz and minor brown biotite.

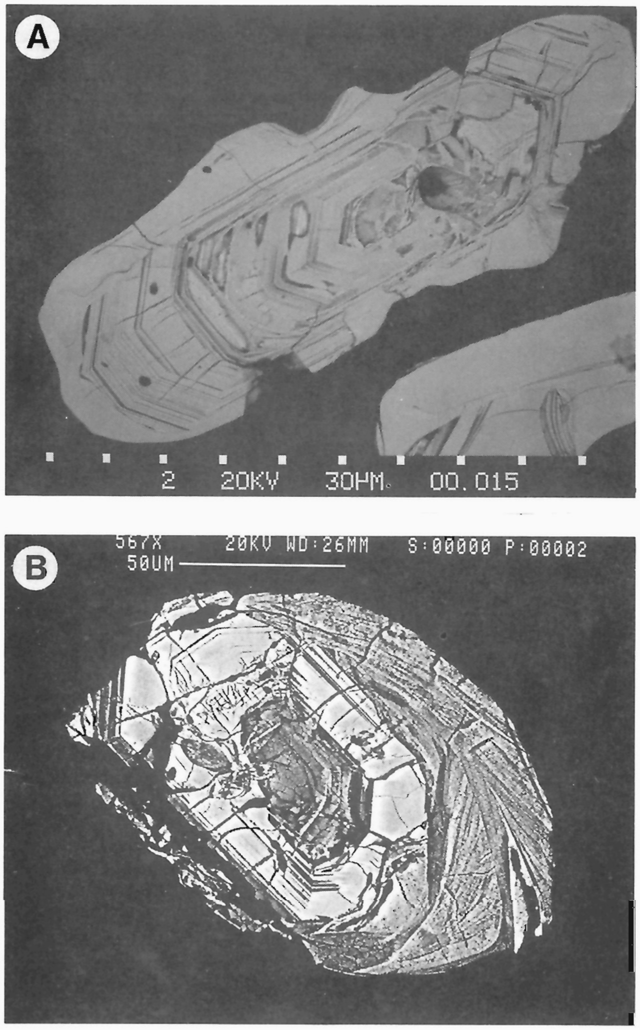

Figure 2. Scanning electron microscope images of zircon grains in polished and etched (HF) sections. All images were taken in the backscatter electron mode. A) Zircon from orthopyroxene tonalite gneiss (sample 1:FS-78-25) shows a high-U igneous core with euhedral zoning, which is truncated by a thin, resorbed, metamorphic rim. B) Zircon from granite gneiss (sample 2:FS-78-26) has a high-U igneous core truncated by a high-U metamorphic outer rim, attributed to growth in an active shear zone.

Zircons separated from the tonalite gneiss (sample 1, Table 1) are generally brown to colourless and of poor clarity. The grains are highly fractured and heavily zoned with abundant inclusions. They are euhedral to subhedral with rounded terminations and have an aspect ratio of 3:1. Polished and etched grains confirm the presence of zoned cores and thin, low-U, resorbed overgrowths that are probably metamorphic in origin (Fig. 2A).

Four abraded zircon fractions, each less than 0.1 mg, (1a,b,c,d in Fig. 3) scatter about a regression line with an upper intercept of 2518 +56/−33 Ma and a lower intercept of 1724 Ma, with a MSWD of 9.2. These points are discordant but are nearly collinear within two sigma error limits. The upper intercept of 2518 Ma is a minimum age for the emplacement of the tonalite, assuming that most of the metamorphic overgrowth was removed during abrasion. Interestingly, the lower intercept age of 1724 Ma agrees within error limits with K-Ar ages of hornblende from the same rock and biotite from the interlayered granite gneiss (see above).

Zircons selected from the granite gneiss (sample 2, Table 1) are subhedral to euhedral with slightly to completely rounded terminations. They are clear to light brown, have abundant inclusions, and are highly fractured. Polished and etched grain mounts clearly indicate a two-stage zircon crystallization history. The etched grains show a zoned igneous core with an extensive metamorphic overgrowth of a number of zones at varying orientations (Fig.2B). The inner core has been resorbed and igneous zoning has been truncated by the outer mantle. This type of mantle is attributed to metamorphic growth in an active shear environment such as a mylonite zone (van Breemen and Hanmer, 1986).

Three abraded zircon fractions, each less than 0.1 mg, were analyzed. They are high in U (800 ppm), discordant, and are not collinear(2a,b,c in Fig. 3). It is impossible to deduce an exact age from this scattered, highly discordant array of points but the >2400 Ma $^{207}Pb/^{206}Pb$ ages for individual zircon fractions from the granite gneiss, and the zircon morphology, suggest that an Archean protolith was metamorphosed in an active shear zone.

The main significance of the data from these two gneisses is the indication of Archean crust in southern Devon Island. Further analyses on selected zircon cores and rims from this suite of samples are needed to determine the age of granulite facies metamorphism.

PINK GRANITE AND INCLUDED ORTHOPYROXENE TONALITE, SOUTHERN PRINCE OF WALES MOUNTAINS, ELLESMERE ISLAND (samples 3 and 4)

Pink granite intrusive into greenish, orthopyroxene-bearing granitoid rock is one of the major lithological associations in the Ellesmere-Devon terrane. A cliff face, 24 km northwest of the head of Trinity Glacier in the southern Prince of Wales Mountains, Ellesmere Island (Fig. 1), shows the result of disruptive intrusion of pink, retrograded orthopyroxene granite into dark orthopyroxene tonalite (Fig. 4). Both rock types are gneissic and less than 1 km away, they appear coarsely interlayered as a lit-par-lit gneiss, illustrating the pre- or syntectonic nature of granitoid intrusive activity in the region.

In the pink granite (sample 3: FS-77-331) orthopyroxene has been totally replaced by a fine grained mixture of biotite and chlorite, K-feldspar shows the faint grid twinning of incipient microcline, and quartz is strongly strained. Orthopyroxene in the tonalite (sample 4: FS-77-332) is little altered and accompanied by fresh, zoned, antiperthitic plagioclase (An_{27-33}), subordinate perthite, a little biotite and strained quartz. Garnet is present in outcrop, erratically distributed in both granite and tonalite. The textures of both

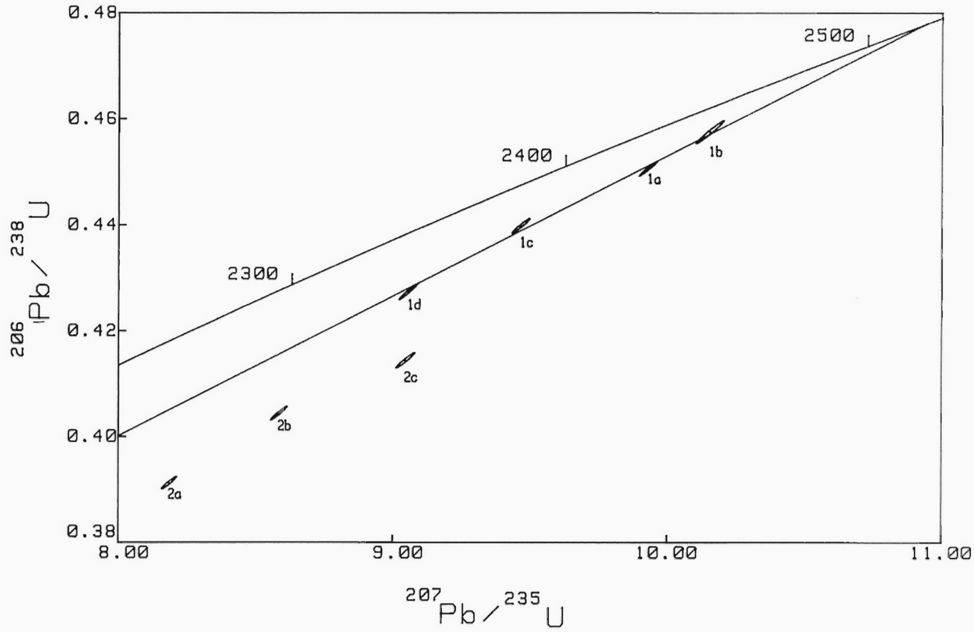

Figure 3. Concordia plot of zircons from orthopyroxene tonalite gneiss FS-78-25 (1a-d) and granite gneiss FS-78-26 (2a-c), southern Devon Island.

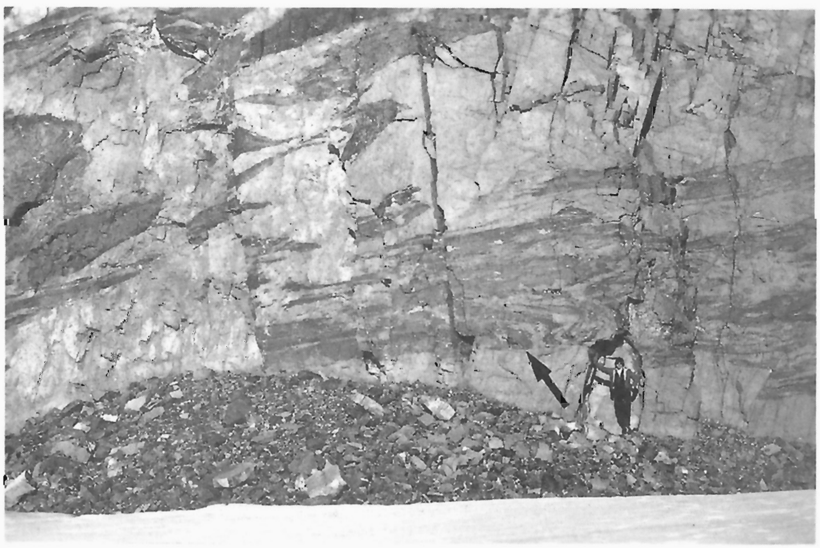

Figure 4. Gneissic, retrograded orthopyroxene granite with layers and lenses of gneissic orthopyroxene tonalite, southern Prince of Wales Mountains, Ellesmere Island. Sample 4:FS-77-332 was taken from the lens arrowed, sample 3:FS-77-331 from below it. (GSC 203740-T)

rocks have been modified by cataclasis, particularly in the case of the granite. It is uncertain whether the orthopyroxene tonalite belongs to the quartzofeldspathic gneisses or the plutonic suite.

Zircons separated from the pink granite (sample 3, Table 1) are cloudy, highly fractured and strongly zoned with an aspect ratio of 2:1 to 3:1. Grains are subhedral with completely rounded terminations.

Two fractions from the least magnetic cut were heavily abraded. They are strongly discordant (3a,b in Fig. 5), reflecting their high U contents of almost 900 ppm. The $^{207}Pb/^{206}Pb$ ages for the two fractions are 1947 and 1926 Ma. Most of this sample was used up in the preparation of five fractions, each heavier than 2 mg, previously analyzed in 1980. Most of these were unabraded and represented large bulk fractions of probably mixed populations. They formed a highly discordant cluster of points and were essentially meaningless.

Two fractions of monazite from the granite are slightly discordant (3ma,3mb in Fig. 5) with $^{207}Pb/^{206}Pb$ ages of 1929 $\pm$1 and 1933 $\pm$1 Ma at two sigma (Table 1). The significance of these data is discussed below.

Zircons from the orthopyroxene tonalite (sample 4, Table 1) are clear to slightly cloudy with little or no zoning. The grains were subhedral to anhedral and well rounded with an aspect ratio of 2:1 to 1:1. In morphology, they resemble metamorphic zircons.

Four fractions were analyzed. Three of these (4a,b,c in Fig. 5) each weighed 1 to 2 mg and were analyzed prior to 1981 and not abraded. These yielded strongly discordant results. The most recently analyzed fraction was abraded but remained fairly discordant (4d, in Fig. 5). All four fractions are collinear within analytical uncertainty (MSWD=1.41). The calculated upper intercept for this array is 1960 $\pm$ 5 Ma, and the lower intercept is 587 Ma. Two monazite fractions have $^{207}Pb/^{206}Pb$ ages of 1928 $\pm$1 and 1936 $\pm$1Ma, the older age being concordant (4ma,mb in Fig. 5, Table 1).

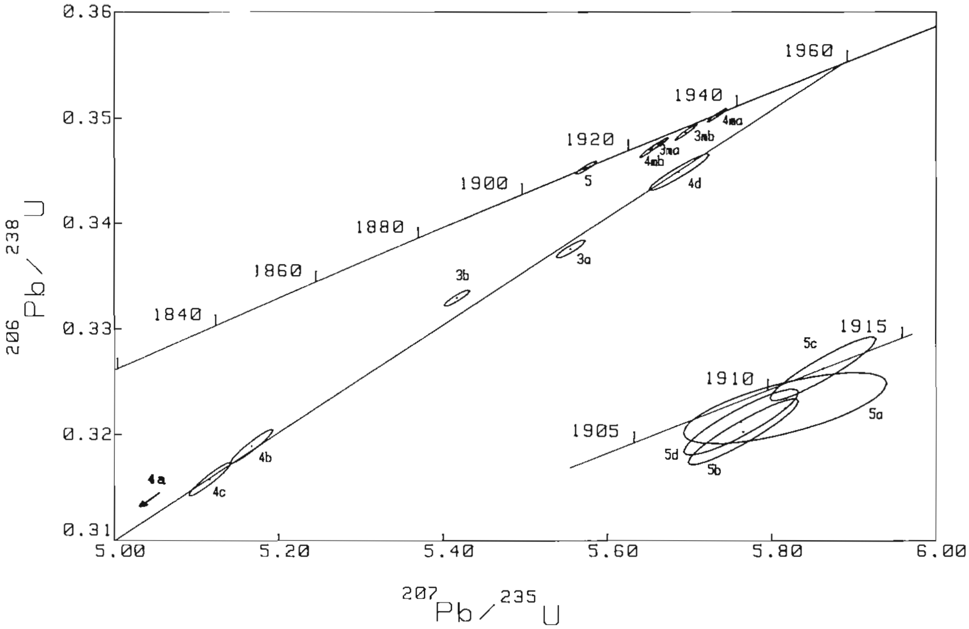

Figure 5. Concordia plot of zircons and monazites (m) from retrograded orthopyroxene granite FS-77-331 (3a,b;3ma,mb) and orthopyroxene tonalite FS-77-332 (4a-d;4ma,mb), Ellesmere Island; and of zircon from monzonorite FS-84-101 (5a,b,c,d, inset), Cape Isabella, Ellesmere Island.

As both tonalite and granite underwent granulite grade metamorphism, the 1928-1936 Ma monazite ages probably represent the cooling age of monazite following the metamorphism. A temperature of 650-700°C has recently been suggested as an approximate closure temperature of monazite (Parrish, 1988). Thus the monazite results provide a minimum for the age of granulite metamorphism in this region of Ellesmere Island, ca. 1.93 Ga. If the zircon of the orthopyroxene tonalite grew during metamorphism, the concordia upper intercept age of 1960 Ma should date the metamorphic climax more closely.

TWO-PYROXENE MONZONORITE, CAPE ISABELLA, ELLESMERE ISLAND (sample 5)

Massive monzonorite has intruded marble and gneiss at Cape Isabella on the east coast of Ellesmere Island (Fig. 1,6). The intrusion outcrops as two bodies, one 0.8 × 0.4 km, the other much smaller, separated by a narrow septum of marble. The intrusive rock is a brown weathering, clinopyroxene-bearing monzonorite characterized by mafic clots, 1-2 cm across, rich in hornblende and pyroxene. The texture of the sample dated (sample 5: FS-84-101) is largely granoblastic-polygonal, with grain size typically 1 mm but hornblende crystals commonly exceed 5 mm in length. Plagioclase (An_{26}) predominates over perthite; orthopyroxene and pale green clinopyroxene are present in approximately equal amounts but brown hornblende is the major mafic mineral. Brown biotite and quartz are minor constituents and Fe-Ti oxide and apatite are major accessory minerals.

The zircons from this rock are exceptionally clear with an aspect ratio of 3:1 and slightly rounded terminations. The fractions were strongly abraded to remove any rim material even though none was observed. The pristine nature of the zircon crystals has resulted in a very precise U-Pb age.

Of the four fractions analyzed, one is concordant and gives a $^{207}Pb/^{206}Pb$ age of 1912.1 ± 1.6 Ma (Table 1, Fig. 5). The other three points are very slightly discordant, probably due to recent lead loss. The $^{207}Pb/^{206}Pb$ age of 1912 Ma is interpreted as the time of crystallization of the monzonorite.

DISCUSSION

The following conclusions may be drawn from the isotopic results presented above.

(1) Zircon ages from gneiss indicate the presence of Archean crust in southern Devon Island.

(2) According to data from Ellesmere Island, a granulite grade thermotectonic event occurred in the latter part of Aphebian time. Zircon of apparent metamorphic origin from a gneissic orthopyroxene tonalite crystallized 1.96 Ga ago. Ages of monazite from the same rock and from a closely associated retrograded orthopyroxene granite cluster around 1.93 Ga, providing a minimum age for the granulite metamorphism, and suggesting relatively slow cooling from peak metamorphic conditions.

(3) Late- to post-tectonic igneous activity in Ellesmere Island is represented by a 1912 Ma monzonorite intrusion.

The isotopic data from Ellesmere Island provide little information on the temporal relationship between granitoid intrusion and high grade metamorphism. If the inference from fieldwork that the two processes were coeval is correct, then the major granitoid magmatism occurred ca. 1.96 Ga ago.

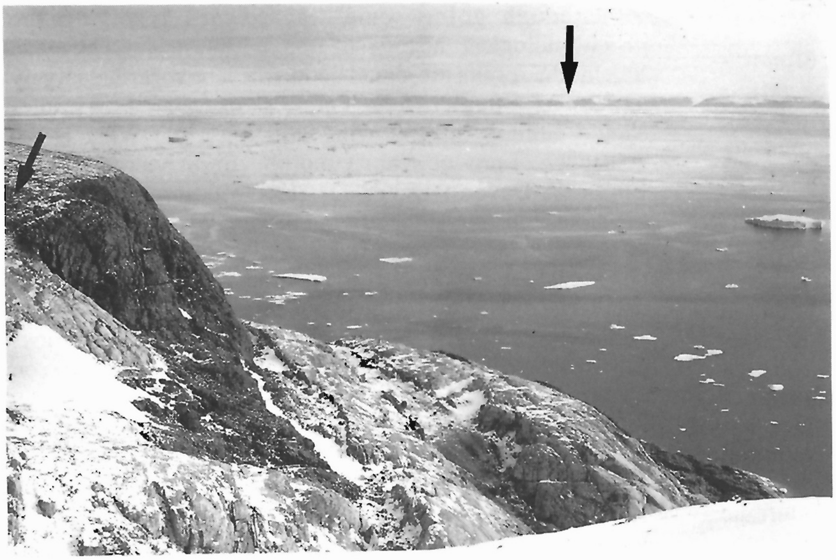

Figure 6. Part of the monzonorite body (dark rock at left) intrusive into layered, pale marble at Cape Isabella, east coast of Ellesmere Island. Left arrow marks the locality of sample FS-84-101. Right arrow indicates Sunrise Point on the coast of Greenland, "type locality" of the Etah meta-igneous complex. (GSC 204074-V)

Significance of the monzonorite

An unexpected result was the clearly post-metamorphic age, 1912 Ma, of the monzonorite at Cape Isabella. Although relatively undeformed rocks do occur in the Ellesmere-Devon terrane, they neither are sufficiently abundant nor have a unifying characteristic to constitute a widely recognizable post-tectonic suite.

In its geological setting, lithology and petrography, the monzonorite is typical of the late-stage, Fe- and K-enriched, intrusive ferrodiorite/jotunite suite of the anorthosite-quartz mangerite-rapakivi granite association (Emslie, 1985). An example of an area where the suite is abundantly developed and has been intensively studied is the Rogaland district of southern Norway. There, rocks of the suite, called jotunites, form smaller bodies and dykes intrusive into larger massif anorthosites and granulite grade gneisses (Demaiffe and Michot, 1985). Monzonorite from the Hidra body, which intrudes gneiss, has a U-Pb zircon age close to 930 Ma, whereas the granulite facies metamorphism in the area is estimated, mainly on the basis of monazite ages, at 1000-1050 Ma (Pasteels and Michot, 1975, Demaiffe and Michot, 1985). Interestingly, zircons from the Rogaland monzonorites, like those from the Cape Isabella rock, typically are clear, unzoned and low in U (Duchesne et al., 1987). Although the origin of the ferrodiorite/jotunite suite has not been entirely resolved, there is general agreement that deep crustal material was involved in the parent melt (Emslie, 1985). Pyroxene crystallization temperatures of the Rogaland jotunite suite are estimated to have been in the order of 1000°C (Rietmeijer, 1979). Obviously, despite the metamorphic peak having been passed, heat sources in the Rogaland district were active several tens of millions of years later, suggestive of a protracted thermal event. Similarly, the Cape Isabella monzonorite should be regarded as a manifestation of magmatic activity in the waning stages of a major thermotectonic event, not as an unrelated, anorogenic intrusion.

Analogy with the Rogaland district and other areas in which the ferrodiorite/jotunite suite occurs suggests that other members of the anorthosite-quartz mangerite-rapakivi granite association may be present in the Ellesmere-Devon terrane. Massif anorthosites have not been, and are unlikely to be, found, but certain granitoid bodies may be related to the Cape Isabella monzonorite. The most likely candidates are dykes of retrograded orthopyroxene granite-granodiorite on the southern shore of Buchanan Bay, north of Cape Isabella (Fig. 1), described by Frisch (1988, p. 76). The dyke rock is made up of antiperthitic plagioclase An_{25-30}, perthite, quartz, olive-green hornblende, brown biotite and pseudomorphs of intergrown biotite and hornblende after orthopyroxene. The mafic minerals tend to be aggregated in clots. Although the dykes are strongly discordant and little deformed, neither chill zones nor thermal effects in the country rocks (orthopyroxene granite and metasedimentary gneiss) were seen and the dykes were interpreted as post-tectonic, high temperature intrusions into still-hot rock (Frisch, 1988). Chemical analysis of one dyke indicated high Fe, K and Zr, relative to massive orthopyroxene granite in the area (Frisch, 1988). These chemical features are characteristic of intermediate-acid rocks related to anorthosite-quartz mangerite associations (Duchesne et al., 1987). Late- to post-tectonic charnockite dykes occur in the Rogaland district, e.g. cutting the Hidra body (Demaiffe and Michot, 1985).

Other plutonic rocks that may be coeval with the Cape Isabella monzonorite are (1) the massive, black norite-tonalite, commonly with two pyroxenes and hornblende, that outcrops on Coburg Island and in the Prince of Wales Mountains (west of Cape Isabella) on Ellesmere Island; and (2) a coarse grained, leucocratic granite near Cory Glacier, southeastern Ellesmere Island (Frisch, 1988). The granite has a miarolitic structure and weathers to grus (Frisch, 1988, Fig. 65). It contains microcline perthite as the predominant feldspar, biotite as the only mafic silicate and accessory fluorite (Frisch, 1988). These are all features of the classic Fennoscandian rapakivi granite suite (Simonen, 1980).

Correlation with Greenland

Recent isotopic work on the Precambrian Shield of northwest Greenland is broadly in agreement with the results from the Ellesmere-Devon terrane (Dawes et al., 1988). Large parts of the shield in the Melville Bay region are Archean, according to both U-Pb zircon and Rb-Sr whole-rock analyses (Fig.1).

Farther north in Greenland, only Rb-Sr whole-rock results from the meta-igneous Etah complex are available. The complex consists chiefly of mafic to felsic granitoid rocks, with and without orthopyroxene, intruding gneisses and metasediments. Rocks assigned to the Etah complex include both gneissic and massive types and transitions between the two. Emplacement of the Etah complex has been considered to predate granulite metamorphism and deformation, and correlations have been drawn with the granitoid plutonic suite of the Ellesmere-Devon terrane (Frisch and Dawes, 1982).

Etah complex rocks at Sunrise Point, near the abandoned settlement of Etah (Fig. 1,6), are predominantly massive and include dark, orthopyroxene-bearing granitoids (including quartz norite) intruded by pink, leucocratic granite and pegmatite (Frisch and Dawes, 1982). The complex itself intrudes marble and other metasediments (Frisch and Dawes, 1982). Analytical data for a varied suite of plutonic rocks from this locality show considerable scatter about a Rb-Sr errorchron corresponding to an age of 1800 $\pm$ 45 Ma with an initial $^{87}Sr/^{86}Sr$ ratio of 0.7032 $\pm$ 0.0005 (Dawes et al., 1988). These results suggest that the Etah complex is Proterozoic and does not represent reworked Archean crust.

Similar lithology and field relations leave little doubt that the monzonorite at Cape Isabella, less than 50 km from Sunrise Point, is correlative with the Etah complex (Frisch and Dawes, 1982). If so, at least part of the Etah complex was emplaced 1.91 Ga ago after granulite facies metamorphism. As both pre- and post-metamorphic intrusive granitoid rocks appear to be present in the shield of northwest Greenland, the Etah complex probably needs redefinition and caution must be exercised in applying the term to rocks far from the "type locality" near Etah.

As Dawes et al. (1988) admit, the ca. 1800 Ma Rb-Sr "age" of the Etah complex has little significance beyond being an indication of Proterozoic, rather than Archean, emplacement. The Rb-Sr system was probably disturbed by some later thermal event.

Nevertheless, the broad correspondence in ages between the shield terranes of Ellesmere-Devon and northwest Greenland is noteworthy: Archean crust is identifiable on Devon Island and in Melville Bay, whereas a Proterozoic component is prominent farther north. These data provide further support for inferences derived from fieldwork concerning correlation of shield terranes on both sides of northern Baffin Bay (Frisch and Dawes, 1982).

Although going some way toward resolving the geochronological history of the northernmost Canadian Shield, the results presented herein must be regarded largely as a basis for further work. Future geochronological studies should address the following questions: (1) What is the actual age of pre- or synmetamorphic intrusive rocks in the Ellesmere-Devon terrane? (2) How widespread was post-metamorphic igneous activity in the area? (3) Is the absence of Archean ages from Ellesmere Island (and Greenland north of Melville Bay) real or simply due to insufficient data? The answer to the third question bears directly on the significance of the lithological and tectonic contrasts between the Ellesmere and Coburg islands block and Devon Island.

ACKNOWLEDGMENTS

We are grateful to J.K. Mortensen, J.C. Roddick, R.R. Parrish and O. van Breemen for review of the manuscript and useful discussions. R.F. Emslie gave valuable insights into the significance of the monzonorite. P.R. Dawes kindly provided geochronological results from northwest Greenland prior to their publication.

REFERENCES

Dawes, P.R., Larsen, O. and Kalsbeek, F.
1988: Archean and Proterozoic crust in North-West Greenland: evidence from Rb-Sr whole-rock age determinations; Canadian Journal of Earth Sciences, v. 25, p. 1365-1373.

Demaiffe, D. and Michot, J.
1985: Isotope geochronology of the Proterozoic crustal segment of Southern Norway: a review; *in* The Deep Proterozoic Crust in the North Atlantic Provinces, ed. A.C. Tobi and J.L.R. Touret; D. Reidel, Dordrecht, p. 411-433.

Duchesne, J.C., Caruba, R. and Iacconi, P.
1987: Zircon in charnockitic rocks from Rogaland (southwest Norway): Petrogenetic implications; Lithos, v. 20, p. 357-368.

Emslie, R.F.
1985: Proterozoic anorthosite massifs; *in* The Deep Proterozoic Crust in the North Atlantic Provinces, ed. A.C. Tobi and J.L.R. Touret; D. Reidel, Dordrecht, p. 39-60.

Frisch, T.
1988: Reconnaissance geology of the Precambrian Shield of Ellesmere, Devon and Coburg islands, Canadian Arctic Archipelago; Geological Survey of Canada, Memoir 409, 102 p.

Frisch, T. and Dawes, P.R.
1982: The Precambrian Shield of northernmost Baffin Bay: correlation across Nares Strait; *in* Nares Strait and the Drift of Greenland: a Conflict in Plate Tectonics, ed. P.R. Dawes and J.W. Kerr; Meddelelser om Grønland, Geoscience 8, p. 79-88.

Hunt, P.A. and Roddick, J.C.
1987: A compilation of K-Ar ages, Report 17; *in* Radiogenic Age and Isotopic Studies: Report 1; Geological Survey of Canada, Paper 87-2, p. 142-210.

Krogh, T.E.
1982: Improved accuracy of U-Pb zircon ages by the creation of more concordant systems using an air abrasion technique; Geochimica et Cosmochimica Acta, v. 46, p. 637-649.

Larsen, O. and Dawes, P.R.
1974: K/Ar and Rb/Sr age determinations on Precambrian crystalline rocks in the Inglefield Land-Inglefield Bredning region, Thule district, western North Greenland; Grønlands Geologiske Undersøgelse, Rapport 66, p. 5-8.

Lowdon, J.A., Stockwell, C.H., Tipper, H.W. and Wanless, R.K.
1963: Age determinations and geological studies; Geological Survey of Canada, Paper 62-17, p. 140.

Ludwig, K.
1980: Calculation of uncertainties of U-Pb isotope data; Earth and Planetary Science Letters, v. 46, p. 212-220.

Parrish, R.R.
1988: U-Pb systematics of monazite and a preliminary estimate of its closure temperature based on natural examples; Geological Association of Canada/Mineralogical Association of Canada, Program with Abstracts, v. 13, p. A94 (abstract).

Parrish, R.R., Roddick, J.C., Loveridge, W.D., and Sullivan, R.W.
1987: Uranium-lead analytical techniques at the geochronology laboratory, Geological Survey of Canada; *in* Radiogenic Age and Isotopic Studies: Report 1; Geological Survey of Canada, Paper 87-2, p. 3-7.

Pasteels, P. and Michot, J.
1975: Geochronologic investigation of the metamorphic terrain of southwestern Norway; Norsk Geologisk Tidsskrift, v. 55, p. 111-134.

Rietmeijer, F.J.M.
1979: Pyroxenes from iron-rich igneous rocks in Rogaland, S.W. Norway; Geologica Ultraiectina, no. 21, 341 p.

Simonen, A.
1980: The Precambrian in Finland; Geological Survey of Finland, Bulletin 304, 58 p.

Steiger, R.H. and Jäger, E.
1977: Subcommission on geochronology: convention on the use of decay constants in geo- and cosmochemistry; Earth and Planetary Science Letters, v. 36, p. 359-362.

Streckeisen, A.
1974: How should charnockitic rocks be named?; *in* Géologie des Domaines crystallines, ed. J. Belliere et J.C. Duchesne; Société géologique de Belgique, Liège, p. 349-360.

Sullivan, R.W. and Loveridge, W.D.
1980: Uranium-lead age determinations on zircon at the Geological Survey of Canada: current procedures in concentrate preparation and analysis; *in* Current Research, Part C; Geological Survey of Canada, Paper 80-1C, p. 164.

van Breemen, O. and Hanmer, S.
1986: Zircon morphology and U-Pb geochronology in active shear zones: studies on syntectonic intrusions along the northwest boundary of the Central Metasedimentary Belt, Grenville Province, Ontario; *in* Current Research, Part B; Geological Survey of Canada, Paper 86-1B, p. 775-784.

A COMPILATION OF K-AR AGES REPORT 18

P.A. Hunt[1] and J.C. Roddick[1]

Hunt, P.A. and Roddick, J.C., A compilation of K-Ar ages, Report 18; in Radiogenic Age and Isotopic Studies: Report 2, Geological Survey of Canada, Paper 88-2, p.127-153, 1988.

Abstract

One hundred and five potassium-argon age determinations carried out by the Geological Survey of Canada are reported. Each age determination is accompanied by a description of the rock and mineral concentrate used; brief interpretative comments regarding the geological significance of each age are also provided where possible. The experimental procedures employed are described in brief outline. An index of all Geological Survey of Canada K-Ar age determinations published in this format has been prepared using NTS quadrangles as the primary reference.

Résumé

Les auteurs présentent 105 datations au potassium-argon effectuées par la Commission géologique du Canada. Chaque datation est accompagnée d'une description de la roche ou du concentré mineral utilisé ainsi que d'une bréve interprétation touchant l'aspect géologique. Les méthodes expérimentales qui ont servi aux datations sont aussi résumées. De plus, à l'aide de quadrilatéres du SRCN, un index de toutes les datations au potassium-argon a été publié par la Commission géologique du Canada.

INTRODUCTION

This compilation of K-Ar ages determined in the Geochronological Laboratories of the Geological Survey of Canada is the latest in a series of reports, the last of which was published in 1987 (Hunt and Roddick, Paper 87-2). In this new contribution 105 determinations are reported. The format of this compilation is similar to the previous reports with data ordered by province or territory and subdivided by map sheet number. In addition to the GSC numbers, laboratory numbers (K-Ar xxxx) are also included for internal reference.

Experimental procedures

The data compiled here represent analysis over a period of time from 1985 to 1986. Potassium was analyzed by atomic absorption spectrometry on duplicate dissolutions of the samples. Argon extractions were carried out using an RF vacuum furnace with a multi-sample loading system capable of holding six samples. The extraction system is on-line to a modified A.E.I. MS-10 with a 1.8 KG magnet. An atmospheric Ar aliquot system is also incorporated to provide routine monitoring of mass spectrometer mass discrimination. While computer acquisition and processing of data has been in operation since 1978, complete computer control of the mass spectrometer was initiated in 1986. Further details are given in Roddick and Souther (1987). Decay constants recommended by Steiger and Jäger (1977) are used in the age calculations.

The complete series of reports including the present one is as follows:

		Determinations
GSC Paper 60-17,	Report 1	59-1 to 59-98
GSC Paper 61-17,	Report 2	60-1 to 60-152
GSC Paper 62-17,	Report 3	61-1 to 61-204
GSC Paper 63-17,	Report 4	62-1 to 62-190
GSC Paper 64-17,	Report 5	63-1 to 63-184
GSC Paper 65-17,	Report 6	64-1 to 64-165
GSC Paper 66-17,	Report 7	65-1 to 65-153
GSC Paper 67-2A,	Report 8	66-1 to 66-176
GSC Paper 69-2A,	Report 9	67-1 to 67-146
GSC Paper 71-2,	Report 10	70-1 to 70-156
GSC Paper 73-2,	Report 11	72-1 to 72-163
GSC Paper 74-2,	Report 12	73-1 to 73-198
GSC Paper 77-2,	Report 13	76-1 to 76-248
GSC Paper 79-2,	Report 14	78-1 to 78-230
GSC Paper 81-2,	Report 15	80-1 to 80-208
GSC Paper 82-2,	Report 16	81-1 to 81-226
GSC Paper 87-2,	Report 17	87-1 to 87-245
GSC Paper 88-2	Report 18	88-1 to 88-105

REFERENCES

Hunt, P.A. and Roddick, J.C.
1987: A compilation of K-Ar ages, Report 17; in Radiogenic Age and Isotopic Studies: Report 1, Geological Survey of Canada, Paper 87-2, p. 143-210.

Roddick, J.C. and Souther, J.G.
1987: Geochronology of Neogene volcanic rocks in the northern Garibaldi Belt, B.C.; in Radiogenic Age and Isotopic studies: Report 1, Geological Survey of Canada, Paper 87-2, p. 25-32.

Steiger, R.H. and Jäger, E.
1977: Subcommission on Geochronology: Convention on the use of decay constants in Geo- and Cosmo-chronology; Earth and Planetary Science Letters, v. 36, p. 359-362.

[1] Geological Survey of Canada, 601 Booth Street, Ottawa, Ontario K1A 0E8

BRITISH COLUMBIA
(GSC 88-1 to GSC 88-34)

GSC 88-1 Whole rock
84±3 Ma

Wt % K=1.940
Rad. Ar=6.494x10^{-6} cc/gm
K-Ar 3766 % Atmos. Ar=11.0

From a diabasic mafic dyke.
Prominant outcrop 1 km west of mouth of Allandale Creek, north
(82 F/5) shore Lower Arrow Lake, B.C.
UTM 11U, 437600E, 5465800N.
Sample TSP015. Collected and interpreted by Ted Irving and R. Parrish.

Sample is a relatively coarse interior part of a mafic dyke, trending 010/68E, which cuts the 52 Ma Coryell Syenite, the U-Pb age of which is published in Parrish et al. (1988). The age of 84±3 Ma is clearly excessive, and the most logical explanation is that of significant excess argon. The dyke is likely Middle Eocene in age.

REFERENCES

Parrish, R.R., Carr, S.D., and Parkinson, D.L.
1988: Eocene extensional tectonics and geochronology of the southern Omineca Belt, British Columbia and Washington; Tectonics, v. 7, p. 181-212.

GSC-88-2 Hornblende
60±1 Ma

Wt % K=1.011
Rad. Ar=2.409×10^{-6} cc/gm
K-Ar 3747 % Atmos. Ar=11.4

From a foliated hornblende
(82 F/5) granodiorite on the west side of Sentinel Mountain on a logging road, 6 km north-northeast of Castlegar, B.C. UTM 11U, 454100E, 5468200N, Sample PCA-93-85. Collected and interpreted by R.R. Parrish and S.D. Carr.

This is a sample of the Nelson batholith which underlies most of Sentinel Mountain. The sample is within the Valkyr shear zone but is in the hanging wall of the Slocan Lake normal fault, as detailed by Carr (1985) and Carr et al. (1987). The 60 Ma age represents total degassing of Jurassic hornblende during shearing on the Valkyr shear zone during the Early Eocene extensional development of Valhalla Complex.

REFERENCES

Carr, S.D.
1985: Ductile shearing and brittle faulting in Valhalla gneiss complex, southeastern British Columbia; *in* Current Research, Part A, Geological Survey of Canada, Paper 85-1A, p. 89-96.

Carr, S.D., Parrish, R., and Brown, R.L.
1987: Eocene structural development of the Valhalla complex, southeastern British Columbia; Tectonics; 6, p. 175-196.

GSC 88-3 Vhole rock
62±3 Ma

Wt % K=2.120
Rad. Ar=5.235×10^{-6} cc/gm
K-Ar 3706 % Atmos. Ar=40.3

From a mafic dyke.
(82 F/5) Railroad cut, south shore Lower Arrow Lake 1.8 km west of Hugh Keenleyside Dam west of Castlegar, B.C. UTM 11U 442100E, 5464950N. Sample Late Dyke. Collected and interpreted by R.R. Parrish.

The sample is a mafic dyke with gabbroic and ultramafic xenoliths which trends 000/75E and cuts foliated dioritic rocks of the southern Valhalla Complex. Because all other mineral K-Ar dates from rocks of Valhalla Complex have ages ranging from about 50-60 Ma, the 62±3 Ma age on this dyke is interpreted as reflecting significant excess argon. This dyke is part of a swarm which cuts the foliated ca. 58 Ma Ladybird granite on the opposite shore, and it cannot be older than 58 Ma.

A similar dyke (TSP 015) on the opposite shore has an even older K-Ar date, despite the fact that it cuts 52 Ma syenite, and confirms that excess Ar is a problem in these dyke rocks (see GSC-88-1).

GSC-88-4 Biotite
49±1 Ma

Wt % K=7.129
Rad. Ar=1.376x10^{-5} cc/gm
K-Ar 3736 % Atmos. Ar=13.8

From a 2-mica granite.
(82 F/13) 300 m east of south Nemo Lake at head of Nemo Creek, Valhalla Range, B.C. UTM 11U, 455500E, 5531900N. Sample PCA-226-85. Collected and interpreted by R.R. Parrish and S.D. Carr.

This ca. 57 Ma granite (U-Pb zircon age, published in Parrish et al., 1988) is part of the Ladybird granite of Valhalla Complex. The 49±1 Ma biotite and 50±1 Ma muscovite (GSC 88-5) ages reflect final cooling below about 300°C in the Middle Eocene during extensional tectonic denudation along Slocan Lake normal fault (Carr et al., 1987).

REFERENCES

Carr, S.D., Parrish, R., and Brown, R.L.
1987: Eocene structural development of the Valhalla complex, southeastern British Columbia; Tectonics, v. 6, 175-196.

Parrish, R.R., Carr, S.D., and Parkinson, D.L.
1988: Eocene extensional tectonics and geochronology of the southern Omineca Belt, British Columbia and Washington; Tectonics, v. 7, p. 181-212.

GSC 88-5

Muscovite
50±1 Ma

Wt % K=8.437
Rad. Ar=1.675×10^{-5} cc/gm
K-Ar 3737 % Atmos. Ar=28.0

(82 F/13) From a 2-mica granite. For locations and interpretation see GSC-88-4. Sample PCA-226-85. Collected and interpreted by R.R. Parrish and S.D. Carr

GSC-88-6

Hornblende
136±4 Ma

Wt % K=0.950
Rad. Ar=5.222×10^{-6} cc/gm
K-Ar 3735 % Atmos. Ar=13.1

(82 F/13) Ridge crest 3 km north-northwest of Avis Lakes, northern Valhalla Ranges, B.C. UTM 11U, 449100E, 5531700N. Sample PCA-251-85. Collected and interpreted by R.R. Parrish and S.D. Carr.

This sample of hornblende-biotite granodiorite comes from the immediate hangingwall of the Valkyr shear zone which forms the upper boundary of the Valhalla complex. The rock lithologically resembles the Nelson batholith to the east of the complex. Most rocks in the hangingwall of the Valkyr shear zone have early Cretaceous and older K-Ar cooling dates (Carr et al., 1987). This sample probably underwent substantial Ar loss while the Valkyr shear zone was active, either because of shearing or because of a thermal disturbance due to juxtaposition of hot Valhalla complex rocks. The 136±4 Ma date is in contrast to ca. 60 Ma dates within Valhalla complex which represent complete outgassing or quenching in the Late Paleocene to Early Eocene.

REFERENCES

Carr, S.D., Parrish, R., and Brown, R.L.
1987: Eocene structural development of the Valhalla complex, southeastern British Columbia; Tectonics, v. 6, p. 175-196.

GSC 88-7

Hornblende
74±3 Ma

Wt % K=0.945
Rad. Ar=2.767×10^{-6} cc/gm
K-Ar 3730 % Atmos. Ar=49.5

(82 F/13) From a hornblende — biotite granodiorite. Roadcut along Highway 6, 5 km east of Caribou Point along the shore of Lower Arrow Lake, B.C., UTM 11U, 433100E, 5534600N. Sample PCA-WHAT-83. Collected and interpreted by R.R. Parrish.

This sample is generally representative of hornblende± biotite granitic rocks which underly a region extending from Lower Arrow Lake to west of Whatshan Lake, informally termed the Whatshan batholith. U-Pb zircon ages on two related samples are ca. 80 Ma. The hornblende age of 74±3 Ma reflects a small degree of Ar loss related to Eocene tectonic (and plutonic) activity adjacent to the Columbia River Fault to the northeast of this sample.

GSC 88-8

Hornblende
58±2 Ma

Wt % K=1.445
Rad. Ar=3.306×10^{-6} cc/gm
K-Ar 3725 % Atmos. Ar=18.5

(82 F/13) From a foliated hornblende-biotite-granodiorite- gneiss, 1.5 km northwest of Gladsheim Peak, elev. 2256 m. B.C. UTM 11U, 453600E/5515400N. Sample PCA-121-84A. Collected and interpreted by R.R. Parrish and S.D. Carr.

The granodioritic Mulvey gneiss of the Valhalla complex (Carr et al. 1987), is particularly deformed adjacent the ductile Gwillim Creek shear zones, interpreted as Late Mesozoic thrusts. This sample comes from Mulvey gneiss in the immediate hanging wall of the upper Gwillim Creek shear zone and it is thoroughly mylonitized and annealed. The U-Pb zircon age is ca. 100 Ma, and this hornblende date of 58 Ma, shown in Carr et al. (1987), is interpreted as a cooling age. The age is consistent with all other hornblende dates in Valhalla Complex which fall near 60 Ma, and collectively they imply rapid cooling below about 500°C during Eocene uplift and tectonic denudation of the complex.

REFERENCES

Carr, S.D., Parrish, R., and Brown, R.L.
1987: Eocene structural development of the Valhalla complex, southeastern British Columbia; Tectonics, v. 6, p. 175-196.

GSC 88-9

Hornblende
158±2 Ma

Wt % K=1.276
Rad. Ar=8.197×10^{-6} cc/gm
K-Ar 3700 % Atmos. Ar=10.5

82 K/4) From a hornblende-biotite granodiorite. Roadcut along logging road 4 km east of Scalping Knife Mountain, B.C., UTM 11U 441600E, 5547300N. Sample Ruby Range West. Collected and interpreted by R.R. Parrish.

This is a sample from the west end of the elongate E-W trending pluton of the Ruby Range extending across Meadow Mountain south of Nakusp, B.C. in the hanging wall of the Rodd Creek (Columbia River) Fault (Hyndman, 1968) and the Valkyr shear zone (Carr et al., 1987). The 158±2 Ma date confirms its Middle Jurassic age, consistent with unpublished U-Pb zircon data of R. Parrish. The preservation of the Jurassic age suggests no significant younger thermal disturbance in this rock, and this is consistent with its being confined to the hangingwalls of the major Eocene normal faults of the region.

REFERENCES

Carr, S.D., Parrish, R., and Brown, R.L.
1987: Eocene structural development of the Valhalla complex, southeastern British Columbia; Tectonics, v. 6, p. 175-196.

Hyndman, D.W.
1968: Petrology and structure of Nakusp Map-Area, British Columbia; Geological Survey of Canada Bulletin 161, 95 p.

GSC 88-10 Muscovite

47±1 Ma

Wt % K=8.580
Rad. Ar=1.593×10^{-5} cc/gm
K-Ar 3703 % Atmos. Ar=22.5

(82 K/5) From roadcut in mylonitic leuco-granite, north side of bridge over Pingston Creek on main logging road, west side of Upper Arrow Lake, B.C.; UTM 11U, 431100E, 5587700N. Sample Pingston Creek. Collected and interpreted by R.R. Parrish and S.D. Carr.

This sample is a mylonitic leucogranite with conspicuous muscovite porphyroclasts from the footwall of the Columbia River normal fault. The muscovite is not a primary igneous mineral but formed during retrograde greenchist facies mylonitization. The granite protolith, the Early Eocene Ladybird granite suite, is ca. 56 Ma old (U-Pb zircon, Parrish et al., 1988). The K-Ar age, of 47±1 Ma is a cooling age, interpreted as the time the rock passed below ~300-350°C, the approximate temperature of Ar closure for muscovite. Cooling in this sample has resulted from tectonic denudation on the nearby Columbia River Fault, a major east dipping normal fault of Eocene age.

REFERENCES

Parrish, R.R., Carr, S.D., and Parkinson, D.L.
1988: Eocene extensional tectonics and geochronology of the southern Omineca Belt, British Columbia and Washington; Tectonics, v. 7, p. 181-212.

GSC 88-11 Muscovite

46±1 Ma

Wt% K=8.650
Rad. Ar=1.55×10^{-5} cc/gm
K-Ar 3704 % Atom. Ar=25.6

(82 L/8) From a mylonitic granite outcrop along logging road 1 km southeast of confluence of Fosthall and Vanstone creeks, west side of upper Arrow Lake, B.C., UTM 11U, 428800E, 5583400N. Sample Fosthall #1. Collected and interpreted by R.R. Parrish and S.D. Carr.

The interpretation and geological setting are identical to that of sample PINGSTON CREEK (GSC-88-10), with the additional constraint that a published U-Pb zircon age from this locality is ca. 56 Ma (Parrish et al., 1988).

REFERENCES

Parrish, R.R., Carr, S.D., and Parkinson, D.L.
1988: Eocene extensional tectonics and geochronology of the southern Omineca Belt, British Columbia and Washington; Tectonics, v. 7, p. 181-212.

GSC 88-12 Muscovite

47±1 Ma

Wt% K=8.510
Rad. Ar=1.579×10^{-5} cc/gm
K-Ar 3705 % Atmos. Ar=20.9

(32 L/8) From a mylonitic granite within metres of sample Fosthall #1 (GSC 88-11). For location and interpretation see GSC 88-11 and GSC 88-10. Sample Fosthall #2. Collected and interpreted by R.R. Parrish and S.D. Carr.

GSC 88-13 Hornblende

459±17 Ma

Wt% K=1.358
Rad. Ar=2.755×10^{-5} cc/gm
K-Ar 3701 % Atmos. Ar=2.8

(82N) From a nepheline syenite. 51°08′N, 116°26′W. Rerun of GSC 87-181. Sample Ice River. Collected by W.C. Gussow, interpreted by R. Parrish.

This is a re-run of a hornblende separate reported earlier which yielded a K-Ar age of 421 Ma (Hunt and Roddick, 1987), (GSC 87-181). In a detailed study on this sample (Parrish et al., 1987), a $^{40}Ar/^{39}Ar$ age spectra showed that this hornblende has large amounts of excess argon. The actual age of the rock is 368±4 Ma, based on U-Pb and $^{40}Ar/^{39}Ar$ analyses.

REFERENCES

Parrish, R.R., Heinrich, and Archibald, D.
1987: Age of the Ice River Complex, southeastern British Columbia, *in* Radiogenic Age and Isotopic studies, Report 1; Geological Survey of Canada, Paper 87-2, p. 33-37.

Hunt, P.A. and Roddick, J.C.
1987: A compilation of K-Ar ages, Report 17, *in* Radiogenic Age and Isotopic Studies: Report 1, Geological Survey of Canada, Paper 87-2, p. 192.

GSC 88-14 Hornblende

52±5 Ma

Wt% K=0.193
Rad. Ar=3.972×10^{-7} cc/gm
K-Ar 3702 % Atmos. Ar=67.4

(92 B/5) From agmatitic trondhjemite. Southeast slope of Broom Hill, southern Vancouver Island, B.C., UTM 444400E, 5358750N. Sample NWM-8430010. Collected by N. Massey, interpreted by R. Parrish.

This trondhjemite is intrusive into the Broom Hill gabbro and Lower Eocene Metchosin sheeted dyke complex. Xenoliths of gabbro and diabase are recrystallized to amphibolite. The material dated is hornblende from amphibolitic xenoliths since no mafics are present in the trondhjemite. The age of 52±5 Ma reflects a middle Eocene age of intrusion and development of amphibolite, only slightly younger than the Lower Eocene age of the host rocks.

GSC 88-15 Hornblende
120±3 Ma

Wt% K=0.433
Rad. Ar=2.095×10^{-6} cc/gm
K-Ar 3786 % Atmos. Ar=11.4

From a quartz diorite.
(92 H/12) Logging road north of Cogburn Creek, el. 2500', bearing N209° from Mount Urquhart at distance of 7 km. 49°34'10"N, 121°41'30"W. Sample MV85-211. Collected and interpreted by J.W.H. Monger.

Sample is from a discrete intrusion which ranges in composition from quartz diorite to gabbro. The lithology is typical of the Spuzzum Batholith, which lies 5 km to the southeast, and from which it is separated by a screen of high-grade metamorphic rocks and a possible Tertiary fault. The date is older than those from the type Spuzzum Batholith, which yields K-Ar dates of 81-103 Ma (Richards and McTaggart, 1976) and one discordant U-Pb date of 110 Ma (R.L. Armstrong, in Irving et al., 1985).

REFERENCES

Richards, T.A. and McTaggart, K.C.
1976: Granitic rocks of the Southern Coast Plutonic Complex and Northern Cascades of British Columbia; Geological Society of America, Bulletin, v. 87, p. 935-953.

Irving, E., Woodsworth, G.J., Wynne, P.J. and Morrison, A.
1985: Paleomagnetic evidence for displacement from the south of the Coast Plutonic Complex, British Columbia; Canadian Journal of Earth Sciences, v. 22, p. 584-598.

GSC 88-16 Biotite
39± 1 Ma
Wt% K=6.087
Rad. Ar=9.334×10^{-6} cc/gm
K-Ar 3787 % Atmos. Ar=27.1

From a biotite —
(92 H/5) hornblende granodiorite. From a logging road on north side of Bear Creek, el. 1100', 0.85 km east of east shore of Harrison Lake. 49°28'20"N, 121°44'10"W. Sample MV-85-124. Collected and interpreted by J.W.H. Monger.

The dates resemble some from the Yale Intrusions, east of Hope, which is 30 km to the southeast, and appear to be part of an earliest Tertiary plutonic suite in the southeastern Coast Belt, Cascade Range.

GSC 88-17 Hornblende
53±2 Ma

Wt% K=0.268
Wt% K=0.268
Rad. Ar=5.653×10^{-7} cc/gm
K-Ar 3788 % Atmos. Ar=44.1

From a granodiorite.
(92 H/5) See GSC 88-16 for location and interpretation. 49°28'20"N, 121°44'10"W. Sample MV-85-124. Collected and interpreted by J.W.H. Monger.

GSC 88-18 Hornblende
186±3 Ma

Wt% K=0.467
Rad. Ar=3.55×10^{-6} cc/gm
K-Ar 3713 % Atmos. Ar=18.7

From a biotite —
(92 H/8) hornblende granodiorite. Roadcut on Old Hedley Road, north side of Similkameen River, 7.5 km west of Hedley, B.C. 49°22'55"N, 120°10'15"W. Sample MV-84-41. Collected and interpreted by J.W.H. Monger.

Sample is a typical lithology from the rim of the granitic complex called the Okanagan Plutonic Complex; the new name is the Bromley Batholith. The U-Pb date from this locality is approx. 205 Ma (unpublished data); the hornblende and biotite dates (GSC 88-19) were probably partially reset during intrusion of the Osprey Lake Batholith, which is exposed 7 km to the north and east. See also GSC 88-20, 21.

GSC 88-19 Biotite
173±5 Ma

Wt% K=6.360
Rad. Ar=4.5×10^{-5} cc/gm
K-Ar 3714 % Atmos. Ar=5.4

From a biotite —
(92 H/8) hornblende granodiorite. See GSC 88-18 for location and interpretation. Sample MV-84-41. Collected and interpreted by J.W.H. Monger.

GSC 88-20 Hornblende
154±3 Ma

Wt%K=0.444
Rad. Ar=2.784×10^{-6} cc/gm
K-Ar 3711 % Atmos. Ar=12.1

From a megacrystic
(92 H/9) granite-granodiorite. Roadcut in Hayes Creek road, approx. 20 km NE of Princeton, B.C. 49°37'36"N, 120°21'31"W. Sample MV-84-5. Collected and interpreted by J.W.H. Monger.

Sample is a typical lithology from the core of the granitic complex variously named Okanagan Plutonic Complex, Pennask Batholith, Similameen Batholith. Recent GSC, BCGS and UBC mapping and isotopic dating has resulted in revision of these names: the revisions will appear on the 1:250 000 scale Hope map sheet (92H; in prep.) and in the new Geology of Canada publication. This sample is typical of the core of the complex, now called the Osprey Lake Batholith, which is petrogenetically unrelated to the older, surrounding, rocks.

The hornblende and biotite (GSC 88-21) ages are thought to be close to the crystallization age (U-Pb zircon age from the core is about 160 Ma, unpublished data).

GSC 88-21

Biotite
149±2 Ma

Wt% K=7.580
Rad. Ar=4.563×10^{-5} cc/gm
K-Ar 3712 — % Atmos. Ar=2.3

(92 H/9) — From a megacrystic granite-granodiorite. See GSC 88-20 for location and interpretation. Sample MV-84-5. Collected and interpreted by J.W.H. Monger.

GSC 88-22

Muscovite
51±2 Ma

Wt% K=8.845
Rad. Ar=1.77×10^{-5} cc/gm
(93 B/9) — % Atmos. Ar=21.9

(93 B/9) — From a granitic pegmatite. NE shore of North Arm of Quesnel Lake, 3.2 km NE of mouth of Long Creek, B.C.; 52°41.75″N; 120°55.8″W. Sample JG-80-36. Collected by J.S. Getsinger and interpreted by J.K. Mortensen.

The three samples (SG-139A (GSC 88-23), SG-417 (GSC 88-24) and JG-80-36) are representative of a suite of coarse grained to pegmatitic muscovite (±tourmaline, ±garnet) granite dykes and sills that occur within medium to high grade metamorphic rocks of the Snowshoe Group in the Barkerville Terrane of the Quesnel Highlands. These bodies were intruded both during the second phase of deformation in this area (as recognized by Ross et al., 1985) and immediately following this event. Some pegmatite bodies (e.g. samples SG-417 and JG-80-36) clearly postdate the major F2 deformation whereas other bodies (e.g. SG-139A) have been folded and boudinaged by the F2 event. Sample JG-80-36 previously yielded a Rb-Sr muscovite age of 86±3 Ma (Getsinger, 1985). The three K-Ar muscovite ages, which date cooling through about 350°C , range from latest Cretaceous to mid-Eocene. The considerably older Rb-Sr muscovite age (closure temperature about 500°C) obtained for one sample suggests that the K-Ar ages are only cooling ages, and are much younger than actual emplacement ages. It is presently unclear whether the Late Cretaceous to Eocene K-Ar ages reflect very prolonged cooling of this region following the F2 event or the effects of Eocene thermal resetting of the K-Ar mineral systematics. Field evidence suggesting a syn-F2 emplacement for the pegmatites, and independent isotopic age studies that indicate a mid-Jurassic age for the F2 event (e.g. Mortensen et al., 1987) make the latter explanation most probable.

REFERENCES

Getsinger, J.S.
1985: Geology of Three Ladies Mountain-Mount Stevenson area, Quesnel-Highland, British Columbia; unpublished Ph.D. thesis, University of British Columbia.

Mortensen, J.K., Montgomery, J.R., and Filipone, J.
1987: U-Pb zircon, monazite and sphene ages for granitic orthogneiss of the Barkerville Terrane, east-central British Columbia; Canadian Journal of Earth Sciences, v. 24, p. 1261-1266.

Ross, J.V., Filipone, J., Montgomery, J.R., Elsby, D.C. and Bloodgood, M.A.
1985: Geometry of a convergent zone, central British Columbia; Tectonophysics, v. 119, p. 285-297.

GSC 88-23

Muscovite
69±2 Ma

Wt% K=7.512
Rad. Ar=2.041×10^{-5} cc/gm
K-Ar 3795 — % Atmos. Ar=21.6

(93 B/9) — From a granitic pegmatite. 4.4 km SW of Niagara Peak. B.C.; 52°39.69′N., 120°35.78′W. Sample SG-139-A. Collected by S. Garwin and interpreted by J.K. Mortensen.

See GSC 88-22 for description and interpretation.

GSC 88-24

Muscovite
57±2 Ma

Wt% K=8.729
Rad. Ar=1.971×10^{-5} cc/gm
K-Ar 3796 — % Atmos. Ar=12.4

(93 B/9) — From a granitic pegmatite. 2 kW. SW of Niagara Peak, B.C.; 52°40.51′N., 120°34.09′W. Sample SG-417. Collected by S. Garwin and interpreted by J.K. Mortensen.

See GSC 88-22 for description and interpretation.

GSC 88-25

Biotite
92±3 Ma

Wt% K=7.760
Rad. Ar=2.852×10^{-5} cc/gm
K-Ar 3727 — % Atmos. Ar=3.1

(94 E/8) — From a muscovite-biotite quartz monzonite. South side of Whudzi Mountain, Swannel Ranges, northern British Columbia. UTM 9V, 652800E, 6358500N. Sample PCA-160-83. Collected and interpreted by R.R. Parrish.

The sample is from the mid-Cretaceous Whudzi granite, an intrusion of 2-mica granite in the core of the Swannell Antiform of the Omineca Crystalline Belt. The granite has dextral strike-slip kinematic indicators related to nearby northwest-trending strike-slip Finlay fault to the west. The 92±3 Ma age is interpreted as a cooling age following intrusion about 10 Ma earlier.

GSC 88-26 Muscovite

98±2 Ma

Wt. % K=8.590
Rad. Ar=3.347×10^{-5} cc/gm
K-Ar 3726 % Atmos. Ar=11.3

(94 E/8) From a muscovite-biotite quartz monzonite. See GSC 88-25 for location. Sample PCA-160-83. Collected and interpreted by R.R. Parrish

The muscovite age of 98±2 Ma is slightly older than the 92 Ma biotite age on the same sample and both reflect cooling through respective closure temperatures in the mid-Cretaceous.

GSC 88-27 Biotite

41±1 Ma

Wt% K=7.240
Rad. Ar=1.169×10^{-5} cc/gm
K-Ar 3729 % Atmos. Ar=5.3

(94 F) From a mylonitic muscovite-biotite granitic orthogneiss. Ridge crest in central Cormier Range, west-southwest of peak labelled 5431, B.C.; 57°30′40″N, 125°47′30″W. Sample PCA-108-83. Collected and interpreted by R.R. Parrish.

This sample is from a sheet of orthogneiss in central Cormier Range which has a southerly plunging lineation and a moderately dipping mylonitic foliation. The gneiss is thought to be remobilized crystalline basement. The biotite age of 41±1 Ma reflects cooling below closure temperatures of about 300°C in Late Eocene time, probably related to uplift of the range between strands of major strike slip faults.

GSC 88-28 Muscovite

42±2 Ma

Wt% K=8.480
Rad. Ar=1.398×10^{-5} cc/gm
K-Ar 3728 % Atmos. Ar=17.3

(94 F) From a mylonitic muscovite-biotite granitic orthogneiss. See GSC 88-27 for location. Sample PCA-108-83. Collected and interpreted by R.R. Parrish.

The muscovite age of 42±2 Ma is interpreted as a cooling age of the Cormier gneiss. See GSC 88-27 for further explanation.

GSC 88-29 Hornblende,

165±3 Ma

Wt% K=1.46
Rad. Ar=9.832×10^{-6} cc/gm
K-Ar 3715 % Atmos. Ar=3.4

(93 G) From a granite. Approximately 7 km south-southwest of Ste. Marie Lake, British Columbia, 54°35′22″N, 122°23′45″W. Map unit 7B, GSC Map 49-1960. Sample SCB-84-10, collected by L.C. Struik.

The K-spar megacrystic hornblende quartz monzonite intrudes dark grey argillite, phyllite and fine grained volcanic derived greywackes of Takla Group affinity in east-central British Columbia. Surrounding the pluton is a hornfelsed aureole approximately 3 to 10 m thick. The border zones are from 10 to 200 m thick, consisting mainly of finer grained equivalents of the pluton as sills throughout the country rock. The 165±3 Ma age for the hornblende confirms an earlier determination of 176 Ma (Wanless et al., 1968). Except for the hornblende the intrusive is texturally and compositionally similar to the biotite quartz monzonite of the 100 Ma Naver pluton immediately to the south. The pluton is locally disturbed by alteration and shear but is mainly undeformed and fresh.

REFERENCES

Wanless, R.K., Stevens, R.D., Lachance, G.R., and Edmonds, C.M.
1968: Age determinations and geological studies, K-Ar Isotopic ages, Report 8; Geological Survey of Canada, Paper 67-2, Part A, p. 25-26.

GSC 88-30 Biotite

98±3 Ma

Wt% K=7.230
Rad. Ar=2.837×10^{-5} cc/gm
K-Ar 3717 % Atmos. Ar=6.7

(93 G/8) From a granite. Roadcut at Mary Lake, central British Columbia. UTM 10, 545645E, 5908080N., 53°19′06″N, 122°18′53″W. Sample SCB-84-56. Collected and interpreted by L.C. Struik.

Interpretation and References: The composition of SCB84-56 is determined from one macroscopic point count as; 38 % quartz, 33 % potassium feldspar, 38 % plagioclase and 4 % biotite. Texture is defined by orthoclase phenocrysts (up to 2 cm long, euhedral to subhedral) in an equigranular matrix of plagioclase and quartz. Veins (up to 12 cm wide) of finely crystalline granite transect approximately 5 % of the outcrop area. Faults of metre spacing, steep dip and southeast trend cut much of the exposure. The U-Pb age from the same sample as determined from 2 zircon analyses is 109.6±1 Ma (R.R. Parrish, written communication, 1986).

The two samples sites (SCB84-54 and 56 (GSC 88-31)) are connected by intervening granite of the Naver Pluton and demonstrate continuity of composition and isotopic age between the sites. The ages are similar to those determined previously for nearby samples collected by H.W. Tipper (GSC 66-23, GSC 66-24, Wanless et al., 1968) and strongly suggest that approximately 100 Ma is the closure age of biotite systematics for the Naver Pluton. The Naver Pluton intrudes the Eureka Thrust which carries Quesnel Terrane and therefore provides a minimum age of 100 Ma for the emplacement of the terrane.

GSC 88-31 Biotite
101±2 Ma

Wt% K=7.820
Rad. Ar=98.32×10^{-7} cc/gm
K-Ar 3716 % Atmos. Ar=12.5

From a granite.
(93 G/9) West of Jerry Creek 9 km south of its junction with the Willow River, B.C. UTM, 10, 555825E, 5928950N. 53°30'30"N, 122°09'30". Sample SCB-84-54. Collected and interpreted by L.C. Struik.

Interpretation and References: The sample is from the Naver Pluton and contains 19% plagioclase, 43% potassium feldspar, 36% quartz, and 2% biotite. The Naver Pluton is generally potassium feldspar megacrystic, but this sample was equigranular with 2 to 4 mm crystals. Thin veins of aplite and pegmatite cut the granite of the sample area. The sample is from the margin of the pluton near its contact with Snowshoe Group metamorphosed immature sands, muds and minor carbonate. The U-Pb age on three zircons and a monazite from the same sample is 110+3.5/−3.5 Ma; some lead loss is suspected and the age may be older than stated but within the range of error (R.R. Parrish, written communication, 1986).

GSC 88-32 Hornblende
262±8 Ma

Wt% K=0.347
Rad. Ar=3.801×10^{-6} cc/gm
K-Ar 3732 % Atmos. Ar=37.0

From a diorite.
(104 I) 5 km north-northeast of the east end of Beale Lake, Cry Lake map area northern British Columbia; 58°56'N; 129°05'W. Sample GA-84-31A. Collected and interpreted by H. Gabrielse.

The sample is a disctinctly foliated hornblende diorite intrusive into argillite, chert and volcanics of the Mississippian to Triassic Sylvester Group. A leucocratic body of markedly different lithology (granite) adjoining the diorite to the west has yielded a biotite K-Ar age of 266.5±3.9 Ma (GSC 87-240). A U-Pb zircon age on a tonalite body that cuts a thrust fault in the Sylvester Group is 276±6 Ma (Harms, 1986).

The K-Ar date reported here thus confirms Permian plutonism in the Sylvester Group. Structural relationships between the various granitoid bodies are unknown but they clearly represent different plutonic episodes on the basis of their petrology.

REFERENCES

Harms, T.A.
1986: Structural and tectonic analysis of the Sylvester Allochthon, northern British Columbia: explorations for paleogeography and accretion; unpublished Ph.D. thesis, University of Arizona, Tucson.

GSC 88-33 Biotite
167±3 Ma

Wt% K=6.187
Rad. Ar=4.199×10^{-5} cc/gm
K-Ar 3734 % Atmos. Ar=8.1

From a biotite granite.
(104 N/12) 7.8 km SE of Atlin, B.C. In valley midway between Union and Monarch mountains; 59°32'15"N; 133°35'20"W. Sample DY-2958. Collected and interpreted by K.M. Dawson.

A small granite stock, about 750 m in diameter, was located during mineral deposit studies in the Atlin area. It was not mapped previously by Aitken (1959).

The rock is a porphyritic K-feldspar-biotite granite that contains: pale pink K-feldspar phenocrysts up to 2 cm (40%); in a medium grained matrix of quartz (35%0); white plagioclase (An10-15) (15%); brown biotite (unaltered) 8%; accessory sphene, magnetite (2%).

The stock intrudes andesitic greenstone, serpentinized periodotite, cherts and argillite of the Pennsylvanian and Permian Cache Creek Group. The stock is intruded by aplite and hornblende porphyry dykes, and is veined by six quartz-molybdenite-pyrite veins enveloped by sericite (160±2 Ma, GSC 88-34).

A shear zone, 120/90°, adjacent to the stock contact contains an assemblage of quartz-pyrite-galena-minor Au similar to other lode Au occurrences in the Atlin area. Galena-Pb isotopes from this occurrence are similar to galena-Pb from 3 other Au veins in the camp.

The granite stock and Mo mineralization are of Middle Jurassic age, notably older than the phases of the Surprise Lake batholith associated with the Adanac porphyry Mo deposit, 22 km to the northeast that were dated by P.A. Christopher (K-Ar, biotite, average of 7 dates, 71 Ma, 1982).

Au-Pb mineralization is interpreted to be related to the Middle Jurassic stock and/or dykes. Au-bearing veins occur on nearby Monarch and Union mountains, associated with undated minor granitoid intrusions and hosted by rocks of the Cache Creek Group. The stock may be a northwestern extension of the Middle Jurassic Three Sisters plutonic suite (G.J. Woodsworth, pers. comm., 1988).

REFERENCES

Aitken, J.C.
1959: Atlin map-area, British Columbia (104N); Geological Survey of Canada, Memoir 307, 89 p.

Christopher, P.A.
1982: Geology of the Ruby Creek-Boulder Creek area (Adamac Molybdenum Deposit); British Columbia Ministry of Energy, Mines and Petroleum Resources, Preliminary Map No. 52.

GSC 88-34 Sericitic, muscovite

160±2 Ma

Wt% K=8.899
Rad. Ar=5.791×10^{-5} cc/gm
K-Ar 3733 % Atmos. Ar=8.6

From a sericite alteration envelope
(104 N/12) on a Mo vein. 7.8 km SE of Atlin, B.C. In valley midway between Union and Monarch mountains; 59°32′15″N; 133°35′20″W. Sample DY-2957. Collected and interpreted by K.M. Dawson.

A small, previously unmapped granite stock that intrudes Cache Creek Group greenstone, serpentinized peridotite, chert and argillite was dated (167±3 Ma, GSC 88-33), along with sericite envelopes from one of six quartz-molybdenite-pyrite veins; 130-140/90°. Mineralization is apparently slightly younger than the host pluton. Mo mineralization at Adanac porphyry Mo deposit 22 km to northeast is notably younger: Mo bearing phases of the Surprise Lake batholith average 71 Ma (Christopher, 1982). The stock may be a northwestern extension of the Middle Jurassic Three Sisters plutonic suite (G.J. Woodworth, pers. comm., 1988).

YUKON
(GSC 88-35 to GSC 88-43)

GSC 88-35 Whole-Rock

75±2 Ma

Wt% K=2.900
Rad. Ar=8.601×19^{-6} cc/gm
K-Ar 3720 % Atmos. Ar=7.5

From a sericitized sandstone.
(104 O) Midway silver-lead-zinc deposit, 90 km west of Watson Lake, Yukon Territory and 9 km south of the Yukon-B.C., border, 59°54′24″N, 130°20′00″W. Sample SYA85-91 from Regional Resources Ltd. drill hole B82-1 at a depth of 284.2 m, collected and interpreted by W.D. Sinclair.

The sample is from altered, sericitic and pyritic sandstone of the Upper Devonian-Lower Mississippian Earn Group (Nelson and Bradford, 1987). The sericitic and pyritic alteration appears to be part of an extensive zone of hydrothermal alteration that is probably related to a granitic intrusion at depth. The 75±2 Ma date indicates a Late Cretaceous age for the emplacement of this postulated intrusion and the associated alteration. Bradford and Godwin (1988) obtained a slightly younger date of 65.4±2.3 Ma from sericite from hydrothermally-altered Earn Group sedimentary rocks at Brinco Hill about 1 km to the east and probably part of the same alteration zone.

The zone of alteration represented by the sample occurs about 1 km south of the Midway silver-lead-zinc deposit which consists of massive sulphide bodies that have filled open spaces in, and in part replaced, mid-Devonian McDame Group carbonates. The Midway deposit appears to be genetically related to the alteration zone (Bradford and Godwin, 1988) and thus likely is also Late Cretaceous in age.

REFERENCES

Bradford, J.A. and Godwin, C.I.
1988: Midway silver-lead-zinc manto deposit, northern British Columbia (104O/16); *in* Geological Fieldwork, 1987; British Columbia Ministry of Energy, Mines and Petroleum Resources, Paper 1988-1, p. 353-360.

Nelson, J.A. and Bradford, J.A.
1987: Geology of the area around the Midway deposit, northern British Columbia (104O/16); *in* Geological Fieldwork, 1986; British Columbia Ministry of Energy, Mines and Petroleum Resources, Paper 1987-1, p. 181-192.

GSC 88-36 Whole-rock

150±5 Ma

Wt% K=4.410
Rad. Ar=2.69×10^{-5} cc/gm
K-Ar 3718 % Atmos. Ar=9.2

From a phyllite.
(105 A) 1.5 km southeast of the peak of Mount Hundere, elevation 4500′, Watson Lake map area, Yukon; 60°31′45″N, 128°53′57″W. Sample SYA85-38B, collected and interpreted by W.D. Sinclair

The sample is a very fine grained phyllite composed mainly of quartz and muscovite-type mica (based on X-ray diffraction). The phyllite belongs to a lower Cambrian sequence which includes carbonate rocks that host the nearby Mount Hundere zinc-lead-silver deposit (Abbott, 1981). The date from the phyllite probably reflects a mid- to Late Jurassic regional metamorphic event that predated the intrusion of Tertiary granitic rocks associated with the Mount Hundere deposit (cf. GSC 88-37).

REFERENCE

Abbott, J.G.
1981: A new geological map of Mt. Hundere and the area north; *in* Yukon Exploration and Geology 1979-80; Department of Indian Affairs and Northern Development (Canada), Northern Affairs Program, Exploration and Geological Services Division, Whitehorse, p. 45-50.

GSC 88-37 Whole-rock

53±2 Ma

Wt% K=2.810
Rad. Ar=5.91×10^{-6} cc/gm
K-Ar 3769 % Atmos. Ar=21.2

From a quartz-feldspar porphyry.
(105 A) 2.4 km north-northeast of the peak of Mount Hundere, elevation 4500′, Watson Lake map area, Yukon; 60°32′47″N, 128°52′49″W. Sample SYA85-40B, collected and interpreted by W.D. Sinclair.

The sample is from a 1 to 2 m wide quartz-feldspar porphyry dyke that has intruded lower Cambrian marble and phyllite. The porphyry is pervasively sericitized and fluoritized, probably as a result of magmatic-hydrothermal alteration associated with emplacement of the dyke. The porphyry dyke is closely associated with zinc-lead-silver occurrences in the adjacent sedimentary rocks. Related intrusions are likely associated with the nearby Mount Hundere zinc-lead-silver deposit which consists of sphalerite and argentiferous galena in actinolite-hedenbergite-garnet skarn zones in lower Cambrian carbonate rocks.

The Eocene date of the altered porphyry represents the age of intrusion of the prophyry and is probably the age of formation of the associated Mount Hundere deposit. The date is consistent with an Eocene extensional event in the region which has been documented by Gabrielse (1985). Similar dates of 50.8±0.8 Ma from the Fiddler tungsten prospect (GSC 87-154 *in* Hunt and Roddick, 1987) and 53 Ma from the YP silver-lead-zinc prospect (Abbott, 1985) have been recorded from the nearby Rancheria district in southern Yukon and northern B.C. These dates provide additional evidence of magmatism and related mineralization associated with the Eocene extension (Sinclair, 1986).

REFERENCES

Abbott, J.G.
1985: Silver-bearing veins and replacement deposits of the Rancheria district; *in* Yukon Exploration and Geology 1983; Department of Indian Affairs and Northern Development (Canada), Northern Affairs Program, Exploration and Geological Services Division, Whitehorse, p. 34-44.

Gabrielse, H.
1985: Major dextral transcurrent displacements along the Northern Rocky Mountain Trench and related lineaments in north-central British Columbia; Geological Society of America, Bulletin, v. 96, p. 1-14.

Hunt, P. and Roddick, J.C.
1987: A compilation of K-Ar ages, Report 17; *in* Radiogenic Age and Isotopic Studies: Report 1; Geological Survey of Canada, Paper 87-2, p. 143-210.

Sinclair, W.D.
1986: Early Tertiary topaz rhyolites and associated mineral deposits in the northern Canadian Cordillera: products of anorogenic magmatism (abstract); Geological Association of Canada, Program with Abstracts, v. 11, p. 127-128.

GSC 88-38 Muscovite

102±4 Ma

Wt% K=7.530
Rad. Ar=3.063×10^{-5} cc/gm
K-Ar 3768 % Atmos. Ar=10.5

From a granite.
(105 B) Angie silver-lead-zinc occurrence, 6 km northeast of Irvine Lake in the Wolf Lake map area, Yukon; 60°38′N, 131°11′W. Sample SYA95-62 from Hudson Bay Exploration and Development Ltd. drillhole A1 at 134 m, collected and interpreted by W.D. Sinclair.

The sample is from a medium grained, equigranular granite composed of K-feldspar (35%), quartz (30%), albite (30%), and muscovite (5%), with minor amounts of biotite and garnet (⊠1% each). The granite has intruded lower Cambrian schist and marble (Unit 1, Poole et al., 1960), the latter of which is altered to magnetite and diopside skarn containing silver-bearing galena and sphalerite near the contact of the granite (Sinclair et al., 1975). The mid-Cretaceous date represents the age of intrusion and is typical of granitic intrusions in the area such as the Cassiar batholith which outcrops 2 to 3 km to the south.

REFERENCES

Poole, W. H., Roddick, J.A. and Green, L.H.
1960: Geology, Wolf Lake, Yukon Territory; Geological Survey of Canada, Map 10-1960.

Sinclair, W.D., Maloney, J.M. and Craig, D.B.
1975: Mineral Industry Report 1974, Yukon Territory; Department of Indian Affairs and Northern Development (Canada), EGS 1975-9, p. 150.

GSC 88-39 Whole-rock
79±2 Ma

Wt% K=3.140
Rad. Ar=9.823×10^{-6} cc/gm
K-Ar 3707 % Atmos. Ar=8.6

From a biotite hornfels
(105 B) Hot tungsten-molybdenum occurrence, 2.4 km east of the Tootsee River and 0.4 km north of the Yukon-B.C. border; 60°01′07″N, 130°06′56″W. Sample SYA84-137 from Canamax Resources Inc. drill hole TR83-3 at 171.0 m, collected by A.C. Hitchins and interpreted by W.D. Sinclair.

The biotite hornfels represented by the sample is developed in lower Paleozoic argillaceous sedimentary rocks (Unit 4c, Poole et al., 1960). The hornfels is probably associated with a granite intrusion which is represented by a few narrow granitic dykes that cut the hornfels. A stockwork of scheelite- and molybdenite-bearing quartz veins and fractures also cut the hornfels and are likely related to the granitic rocks. The 79±2 Ma date indicates a Late Cretaceous age for the emplacement of the granitic rocks and associated tungsten-molybdenum mineralization. A comparable date of 75±2 Ma was obtained from a hydrothermal alteration zone associated with the Midway silver-lead-zinc deposit, 16 km to the southeast in British Columbia (GSC 88-35, this report). These dates are younger than the mid-Cretaceous age of the Cassiar batholith to the west and are evidence of a separate, Late Cretaceous episode of intrusion and mineralization in the northern Cordillera.

REFERENCE

Poole, W.H., Roddick, J.A. and Green, L.H.
1960: Geology, Wolf Lake, Yukon Territory; Geological Survey of Canada, Map 10-1960.

GSC 88-40 Whole-rock
99±3 Ma

Wt% K=2.710
Rad. Ar=1.072×10^{-5} cc/gm
K-Ar 3719 % Atmos. Ar=6.3

From a biotite hornfels.
(105 C) Mindy tin occurrence in the Thirtymile Range, 54 km north-northeast of Teslin and 2.4 km east-southeast of peak 6550, Yukon; 60°37′30″N, 132°19′41″W. Sample SYA85-90 from Newmont Exploration of Canada Ltd. drill hole 81-5 at 25.5 m, collected and interpreted by W.D. Sinclair.

The Mindy occurrence is a tin-bearing garnet-rich skarn in carbonate rocks of the Mississippian Englishmans Group (D.I.A.N.D., 1982). The biotite hornfels represented by this sample is closely associated with the skarn tin occurrence. The hornfels and mineralized skarn are both likely related to a granitic intrusion although no granitic rocks are exposed in the immediate vicinity of the Mindy occurrence. The closest granitic rocks consist of outcrops of leucocratic granite and pegmatite dykes several kilometres to the west on the Ork claims (D.I.A.N.D., 1983). Larger bodies of Cretaceous granite occur about 6.5 km to the northwest (Mulligan, 1963). The mid-Cretaceous date from the hornfels supports the contention that comparable granitic rocks underlie the Mindy skarn tin occurrence.

REFERENCES

D.I.A.N.D.
1982: Mindy summary; *in* Yukon Exploration and Geology 1981; Department of Indian Affairs and Northern Development (Canada), Northern Affairs Program, Exploration and Geological Services Division, Whitehorse, p. 110.
1983: Ork summary; *in* Yukon Exploration and Geology 1982; Department of Indian Affairs and Northern Development (Canada), Northern Affairs Program, Exploration and Geological Services Division, Whitehorse, p. 107.

Mulligan, R.
1963: Geology, Teslin, Yukon Territory; Geological Survey of Canada, Map 1125A.

GSC 88-41 Biotite
98±2 Ma

Wt% K=6.823
Rad. Ar=2.676×10^{-5} cc/gm
K-Ar 3794 % Atmos. Ar= 9.4

From a crystal tuff.
(105 K/09) NE flank of Peak 2142 m, 9.5 km west of Connally Lake, Yukon, 62°32.15′N, 1232°20.83′W. Sample GGA-83-26C. Collected and interpreted by S. Gordey.

The rock is a densely welded quartz-feldspar-biotite-hornblende crystal tuff of the mid-Cretaceous South Fork Volcanics. The rock is fresh. The age is interpreted as the age of eruption, and is consistent with other age data for the suite.

GSC 88-42 Biotite
96±3 Ma

Wt% K=6.585
Rad. Ar=2.537×10^{-5} cc/gm
K-Ar 3797 % Atmos. Ar=3.6

From a crystal tuff.
(105 K/15) 1.8 km NW of peak 2001 m, along small tributary stream, Yukon. 62°49.10′N, 132°44.63′W. Sample GGA-83-24B. Collected and interpreted by S. Gordey.

The rock is a densely welded quartz-feldspar-biotite-hornblende crystal tuff of the mid-Cretaceous South Fork Volcanics. The age is interpreted as the age of eruption, and is consistent with other age data for the suite. The rock is fresh, although the biotite is slightly corroded.

GSC 88-43 Biotite
108±3 Ma

Wt% K=7.734
Rad. Ar=3.354×10^{-5} cc/gm
K-Ar 3799 % Atmos. Ar=6.3

From a granitic orthogneiss
(115 H/1) S side of Teraktu Creek, Teslin map area, Yukon; 61°01.05′N; 134°29.14′W. Sample VH-DE-397. Collected by V.L. Hansen and interpreted by J.K. Mortensen.

The sample is from a well foliated, poorly lineated muscovite-biotite-quartz-feldspar gneiss of overall granitic composition that occurs within variably mylonitized metasedimentary rocks of the Yukon-Tanana terrane. U-Pb zircon dating by Mortensen (unpublished data) indicates that the granitic protolith of the gneiss is Late Devonian to Early Mississippian in age. The ductile deformation that the rock has experienced is thought to be mainly Late Triassic or Early Jurassic in age (V.L. Hansen, pers. comm., 1988). The mid-Cretaceous K-Ar biotite age reported here probably reflects a younger thermal resetting of the K-Ar system.

DISTRICT OF KEEWATIN
(GSC 88-44 to GSC 88-50)

GSC 88-44 Whole-rock
1360±21

Wt% K=6.75
Rad. Ar=5.326×10^{-4} cc/gm
K-Ar 3255 % Atmos. Ar=0.3

From a highly altered sub-
(66 A/5) porphyritic quartz-plagioclase granite that intrudes ENE-trending Archean(?) polydeformed turbiditic greywacke. The rock consists of quartz+kaolinite+Mg-chlorite+illite. From diamond-drill hole 79-71, Kiggavik uranium deposit (owned by Urangesellschaft Canada Ltd.). Sample collected from drillhole 79-71. 342.5'. Collected and interpreted by A.R. Miller.

Duplicate ages of 1358±20 and 1362±21 Ma for this sample are interpeted as the age of alteration associated with uranium mineralization. A U-Pb age on pitchblende from the deposit is about 1400 Ma (Fuchs and Hilger, 1988). Both K-Ar ages are significantly older than the U-Pb zircon age of about 1900 Ma for this intrusion (Miller and LeCheminant, unpub. data).

REFERENCES

Fuchs, H.D. and Hilger, W.
1988: An unconformity related uranium deposit in the Thelon basin, Northwest Territories, Canada. Talk delivered at the IAEA meeting, Saskatoon.

GSC 88-45 Whole-rock
1563 ±24 Ma

Wt% K=7.26
Rad. Ar=7.017×10^{-4} cc/gm
K-Ar 3254 % Atmos. Ar=0.3

From an altered fine grained clay-
(66 A/5) bearing metagreywacke. The rock contains quartz + chlorite + muscovite + illite. A relict foliation having fine grained muscovite aligned in that fabric indicates that this phase has a metamorphic paragenesis. Sample from diamond-drill core 79-65. 181′, Kiggavik uranium deposit (owned by Urangesellschaft Canada Ltd.). Sampled and interpreted by A.R. Miller.

This age of 1563±24 Ma is interpreted as a composite age derived from relict metamorphic muscovite and illite associated with the hydrothermal alteration associated with mineralization.

GSC 88-46 Whole-rock
1648±24 Ma

Wt% K=8.30
Rad. Ar=8.689×10^{-4} cc/gm
K-Ar 3351 % Atmos. Ar=0.1

From a white to grey clay-altered
(66 A/5) greasy lustre metagreywacke having the assemblage:muscovite +illite+trace montmorillonite+trace chlorite+quartz. A relict metamorphic fabric is present with muscovite aligned in that fabric. Sample from diamond-drill hole 79-53 174′, Kiggavik uranium deposit (owned by Urangesellschaft Canada Ltd.). Sample collected and interpreted by A.R. Miller.

The age of 1648±24 Ma is considered a mixed age derived from older metamorphic muscovite and hydrothermal illite. However this age is significantly older than a similar sample GSC 88-45 dated at 1563±24 Ma.

GSC 88-47 Whole-rock
1386±24 Ma

Wt% K=3.04
Rad. Ar=2.464×10^{-4} cc/gm
K-Ar 3352 % Atmos. Ar=0.6

(66 A/5) From an intensely clay altered metagreywacke. The sample is a chalky, very pale greenish white, greasy lustre and consists of a very fine grained composite of illite+Mg-chlorite (variety clinochlore) with minor quartz. These distinctive physical properties and mineralogy as well as the destruction of the metamorphic foliation indicate this metasediment has been subjected to intense recrystallization and metasomatism. Sample from diamond-drill hole 80-115 553′, Kiggavik uranium deposit (owned by Urangesellschaft Canada Ltd.). Sampled collected and interpreted by A.R. Miller.

The age of 1386±24 Ma dates the time of alteration which is concordant with the about 1400 Ma age for uranium mineralization (Fuchs and Hilger, 1987). It is noteworthy that this age is similar to the age determined from the altered granite that intruded the metagreywacke sequence (See GSC 88-44).

GSC 88-48 Whole-rock
1080±17 Ma

Wt% K=6.89
Rad. Ar=3.96×10^{-4} cc/gm
K-Ar 3353 % Atmos. Ar=1.3

(66 A/5) From an intensely clay altered limonitic porphyry containing thin sooty pitchblende-coffinite veinlets. The porphyry is interpreted based on texture to be related to the granite of sample 79-71 342.5′. This rock consists of very fine grained illite and Mg-chlorite with subordinate quartz. Sample from diamond-drill hole 79-50 192′, Kiggavik uranium deposit (owned by Urangesellschaft Canada Ltd.). Sample collected and interpreted by A.R. Miller.

Duplicate analyses returned ages of 1073 ± 17 and 1087 ± 17 and the average is significantly younger than that of the clay altered granite (GSC No. 88-44 and are interpreted to be related to one of the younger mineralization events, ie. about 1000 Ma) (Fuchs and Hilger, 1988). This younger age is associated with limonite stained rocks. The resetting of illite at about 1100-1000 Ma and the association of limonitic mineralized lithologies may reflect the last significant fluid transfer and mineralization through porous, altered basement.

GSC 88-49 Illite
1266±31 Ma

Wt% K=6.340
Rad. Ar=4.522×10^{-4} cc/gm
K-Ar 3731 % Atmos. Ar=1.8

(66 A/9) From a fluorapatite + illite + hematite/specularite + quartz cemented Thelon conglomerate. It is approximately 10 m above the unconformity. Aggregates of illite intergrown with fluorapatite and hematite/specularite, up to 5 mm in size, are present as irregular knots filling and lining interclast volumes (*see* Miller, 1983, Fig. 63.1). Sample Mill-2-82. Collected and interpreted by A.R. Miller.

The 1266±31 Ma age is a minimum age for diagenesis of the basal sediments in the northeastern Thelon Basin. This age is discordant with the U-Pb and Pb-Pb age of 1685±4 and 1688±5 Ma from coexisting fluorapatite (unpublished data, sample No. 2). This age may be due to renewed fluid migration within the basal Thelon due to faulting in and adjacent to the basin associated with intrusion of Mackenzie diabase dykes dated at 1270 ± 4 Ma (Heaman and LeCheminant, 1988). See GSC 88-50 for comparison and references.

GSC 88-50 Illite
1386±37 Ma

Wt% K=7.190
Rad. Ar=5.828×10^{-4} cc/gm
K-Ar 3724 % Atmos. Ar=0.5

(66 A/9) From a massive banded specularite + illite + fluorapatite vein (see Miller, 1983, Fig. 62.7). It has a maximum width of 3 m and is hosted in the hematite zone of the paleoweathered saprolitic metawacke basement. Vein outcrops approximately 100 m south of the Thelon unconformity and is within 1-2 m of the projected unconformity plane. 82 MYAA 290-1. Collected and interpreted by A.R. Miller.

The 1386±37 Ma age is a minimum for diagenesis in the upper portion of the sub-Thelon paleoweathered basement. This age is discordant with a U-Pb and Pb-Pb ages of 1647 and 1648 Ma derived from coexisting uraniferous fluorapatite (unpublished data, sample No. 1). See GSC 88-49 for comparison.

REFERENCES

Heaman, L.M. and LeCheminant, A.N.
1988: U-Pb baddeleyite ages of the Muskox Intrusion and Mackenzie dyke swarm, N.W.T., Canada. GAC-MAC Program with Abstracts, Vol. 13, p. A53.

Miller, A.R.
1983: A progress report: Uranium-phosphorus association in the Helikian Thelon Formation and sub-Thelon saprolite; *in* Current Research, Part A, Geological Survey of Canada, Paper 83-1A, p. 449-456.

MANITOBA
(GSC 88-51 to GSC 88-72)

GSC 88-51 Biotite
2344±28 Ma

Wt% K=7.975
Rad. Ar=1.491×10^{-3} cc/gm
K-Ar 3748 % Atmos. Ar=0.4

From a granite/granodiorite
(62 I/7) Underground Research Laboratory, Lac du Bonnet Batholith, Manitoba; 50°16′N., 95°51′W. Sample KCA-U1. Collected and interpreted by C. Kamineni

Samples KCA U1, KCA U2 and KCA U3 (GSC 88-51, 52, 53) were collected in a shaft station at 240 m level, Underground Research Laboratory, Lac du Bonnet Batholith, Manitoba. They represent a series of samples approaching towards a fracture zone: Sample U1 located about 25 m from fracture zone; sample U2, 10 m; sample U3 about 1 m from fracture zone. All samples yield Kenoran ages. Note however, sample U3 which was located in the vicinity of fracture zone yields the lowest age; probably due to Ar loss during fracturing.

GSC 88-52 Biotite
2302±26 Ma

Wt% K=7.908
Rad. Ar=1.432×10^{-3} cc/gm
K-Ar 3749 % Atmos. Ar=0.4

From a granite/granodiorite.
(62 I/7) See GSC 88-51 for location and interpretation. Sample KCA-U2. Collected and interpreted by C. Kamineni.

GSC 88-53 Biotite
2316±30 Ma

Wt% K=7.850
Rad. Ar=1.436×10^{-3} cc/gm
K-Ar 3750 % Atmos. Ar=0.3

From a granite/granodiorite.
(62 I/7) See GSC 88-51 for location and interpretation. Sample KCA-U3. Collected and interpreted by C. Kamineni.

GSC 88-54 Biotite
2291±27 Ma

Wt% K=6.855
Rad. Ar=1.231×10^{-3} cc/gm
K-Ar 3751 % Atmos. Ar=0.6

From a granite/granodiorite.
(62 I/7) Whiteshell Nuclear Research Establishment site, Lac du Bonnet Batholith, Manitoba; 50°15′N; 95°50′30″W. Sample WN-1. Collected and interpreted by C. Kamineni.

Samples WN-1 to WN-9 (GSC 88-54, 55, 56, 57, 58, 59, 60, 61, 62) were collected from a deep borehole (about 1000 m), located on the WNRE site, Lac du Bonnet Batholith, Manitoba. The sample depths and ages are as follows:

WN-1	30.5 m	2291±27 Ma
WN-2	121.2 m	2223±32 Ma
WN-3	454.3 m	2209±26 Ma
WN-4	925.8 m	2144±28 Ma
WN-5	275.4 m	2251±48 Ma
WN-6	168.5 m	2193±39 Ma
WN-7	670.9	2087±51 Ma
WN-8	752.2	2176±27 Ma
WN-9	807.6	2080±24 Ma

All ages correspond to late Kenoran event and indicate progressive younging with depths. The latter probably is a manifestation of cooling of the Lac du Bonnet Batholith.

GSC 88-55 Biotite
2223±32 Ma

Wt% K=6.031
Rad. Ar=1.027×10^{-3} cc/gm
K-Ar 3752 % Atmos. Ar=0.4

From a granite/granodiorite.
(62 I/7) See GSC 88-54 for location and interpretation. Sample WN-2. Collected and interpreted by C. Kamineni.

GSC 88-56 Biotite
2209±26 Ma

Wt% K=6.885
Rad. Ar=1.16×10^{-3} cc/gm
K-Ar 3753 % Atmos Ar=0.4

From a granite/granodiorite.
(62 I/7) See GSC 88-54 for location and interpretation. Sample WN-3. Collected and interpreted by C. Kamineni.

GSC 88-57 Biotite
2144±28 Ma

Wt% K=6.559
Rad. Ar=1.05×10^{-3} cc/gm
K-Ar 3754 % Atmos. Ar=0.8

From a granite/granodiorite.
(62 I/7) See GSC 88-54 for location and interpretation. Sample WN-4. Collected and interpreted by C. Kamineni.

GSC 88-58

Biotite
2251±48 Ma

Wt% K=5.977
Rad. Ar=1.041×10^{-3} cc/gm
K-Ar 3770 % Atmos. Ar=0.5

From a granite/granodiorite.
(62 I/7) See GSC 88-54 for location and interpretation. Sample WN-5. Collected and interpreted by C. Kamineni.

GSC 88-59

Biotite
2193×39 Ma

Wt% K=6.025
Rad. Ar=1.002×10^{-3} cc/gm
K-Ar 3771 % Atmos. Ar=0.5

From a granite/granodiorite.
(62 I/7) See GSC 88-54 for location and interpretation. Sample WN-6. Collected and interpreted by C. Kamineni.

GSC 88-60

Biotite
2087×51 Ma

Wt% K=6.743
Rad. Ar=1.031×10^{-3} cc/gm
K-Ar 3772 % Atmos. Ar=0.5

From a granite/granodiorite.
(62 I/7) See GSC 88-54 for location and interpretation. Sample WN-7. Collected and interpreted by C. Kamineni.

GSC 88-61

Biotite
2176±27 Ma

Wt% K=6.845
Rad. Ar=1.123×10^{-3} cc/gm
K-Ar 3773 % Atmos. Ar=0.5

From a granite/granodiorite.
(62 I/7) See GSC 88-54 for location and interpretation. Sample WN-8. Collected and interpreted by C. Kamineni.

GSC 88-62

Biotite
2080±24 Ma

Wt% K=7.366
Rad. Ar=1.119×10^{-3} cc/gm
K-Ar 3774 % Atmos. Ar=0.3

From a granite/granodiorite.
(62 I/7) See GSC 88-54 for location interpretation. Sample WN-9. Collected and interpreted by C. Kamineni.

GSC 88-63

Biotite
2269±39 Ma

Wt% K=7.417
Rad. Ar=1.309×10^{-3} cc/gm
K-Ar 3755 % Atmos. Ar=0.2

From a granodiorite.
(62 I/7) Underground Research Laboratory, Lac du Bonnet Batholith, Manitoba; 50°16'N; 95°51'W. Sample KCA-U-42. Collected and interpreted by C. Kamineni.

The sample represents a late dyke intrusive into Lac du Bonnet Batholith, collected at 240 m level of the shaft station, Underground Research Laboratory. The age (2269±39 Ma) supports the interpretation that the dyke was intruded during the late stages of crystallization of the batholith.

GSC 88-64

Biotite
2278±31 Ma

Wt% K=7.916
Rad. Ar=1.407×10^{-3} cc/gm
K-Ar 3756 % Atmos. Ar=0.4

From a granite/granodiorite.
(62 I/7) Underground Research Laboratory Lease area, Lac du Bonnet Batholith, Manitoba; 50°16'N; 95°51'W. Sample URL-10-12. Collected and interpreted by C. Kamineni.

Samples URL-10-12, URL-4-10, URL-7-45, URL-9-1, URL-12-F, (GSC 88-64, 65, 66, 67, 68) were collected from various boreholes located on the Underground Research Laboratory Lease area. All these samples collected from fracture zones intersected by various borehole. The ages indicate late Kenoran, but all samples yield consistently lower (50 to 100 Ma) than pristine (unfractured) granite. This is probably due to resetting or Ar loss during fracturing.

GSC 88-65

Biotite
2197±41 Ma

Wt% K=7.353
Rad. Ar=1.227×10^{-3} cc/gm
K-Ar 3757 % Atmos. Ar=0.5

From a granite/granodiorite.
(62 I/7) See GSC 88-64 for location and interpretation. Sample URL-4-10. Collected and interpreted by C. Kamineni.

GSC 88-66

Biotite
2197±44 Ma

Wt% K=7.218
Rad. Ar=1.205×10^{-3} cc/gm
K-Ar 3758 % Atmos. Ar=0.4

From a granite/granodiorite.
(62 I/7) See GSC 88-65 for location and interpretation. Sample URL-7-45. Collected and interpreted by C. Kamineni.

GSC 88-67 Biotite

2136±26 Ma

Wt% K=8.039
Rad. Ar=1.278×10^{-3} cc/gm
K-Ar 3759 % Atmos. Ar=0.4

From a granite/granodiorite.
(62 I/7) See GSC 88-65 for location and interpretation. Sample URL-9-1. Collected and interpreted by C. Kaminani.

GSC 88-68 Biotite

2165±34 Ma

Wt% K=8.613
Rad. Ar=1.402×10^{-3} cc/gm
K-Ar 3760 % Atmos. Ar=0.3

From a granite/granodiorite.
(62 I/7) See GSC 88-65 for location and interpretation. Sample URL-12-F. Collected and interpreted by C. Kamineni.

GSC 88-69 Biotite

1719 ± 21 Ma

Wt% K=7.989
Rad. Ar=8.926×10^{-4} cc/gm
K-Ar 3782 % Atmos. Ar=1.1

From an enderbite sill.
(63 N/8) File River; 3 km S of Burntwood Lake, Manitoba; UTM 14, 41400E, 6130900N; Lat/Long=55.318°N/100.412°W. Sample 84-GV-1310. Collected and interpreted by T.M. Gordon.

The rock is a brown weathering, weakly foliated, medium grained rock with minor 2-6 cm, medium-to coarse-grained, plagioclase-hypersthene segregations. Its mineralogical composition is approximately 60% sodic andesine, 20% biotite, 10% quartz, and 10% hypersthene with traces of opaques, zircon and monazite. Hypersthene is locally altered along parting planes to an unidentified mineral, probably serpentine.

The sample is from a 1 km sill of unit 9 of Baldwin et al. (1979) which intrudes metagreywacke and migmatite of the Burntwood Metamorphic Suite. This unit comprises the oldest intrusions recognized in the Kisseynew belt, predating peak metamorphism.

This sample gave a U-Pb zircon age of 1830 +11/−5 Ma, and a U-Pb monazite age of 1806±2 Ma (revision of Gordon et al., 1987).

The K-Ar biotite age is interpreted as the time at which the rock cooled through the 280°C blocking temperature for this isotope system (Parrish and Roddick, 1985) on uplift. This datum, along with GSC 88-70, 71, 72 have been used to constrain a numerical model for post-metamorphic uplift and cooling of the Kisseynew sedimentary gneiss belt (Gordon, in press).

REFERENCES

Baldwin, D.A., Frohlinger, T.G., Kendrick, G., McRitchie, W.D., and Zwanzig, H.W.
1979: Geology of the Nelson House-Pukatawagan Region (Burntwood Project); Manitoba Mineral Resources Division, Geological Maps 78-3-1 to 78-3-22.

Gordon, T.M., Hunt, P.A., Loveridge, W.D., Bailes, A.H., and Syme, E.C.,
1987: U-Pb zircon ages from the Flin Flon and Kisseynew belts, Manitoba: Chronology of Early Proterozoic crust formation; Geological Association of Canada-Mineralogical Association of Canada Joint Annual Meeting Program with Abstracts, v. p. 12, 48.

Gordon, T.M.
in press: Thermal evolution of the Kisseynew sedimentary gneiss belt, Manitoba: Metamorphism at an Early Proterozoic accretionary margin; *in* Daly, J.S., Yardley, B.W.D. and Cliff, R.A. (editors), Evolution of metamorphic belts, Geological Society of London Special Publication, in press.

Parrish, R.R., and Roddick, J.C.
1985. Geochronology and isotope geology for the geologist and explorationist; Geological Association of Canada, Cordilleran Section, Short Course Number 4.

GSC 88-70 Biotite

1705±36 Ma

Wt% K=8.004
Rad. Ar=8.831×10^{-4} cc/gm
K-Ar 3783 % Atmos. Ar=1.0

From a granite.
(63 N/7) Southwest shore of northwest arm of Burntwood Lake, Manitoba; UTM 14, 408400E, 6146000N; Lat/Long=55.453°/100.448°W. Sample 84-GV-1296. Collected and interpreted by T.M. Gordon.

The rock is a light grey to white weathering, heterogeneous, medium-to coarse-grained garnetiferous granite. It has approximately 75% perthitic orthoclase, 15% quartz, 5% biotite, and 5% amoeboid garnet, with minor amounts of zircon, opaques, monazite, and myrmekite. Traces of secondary white mica occur locally.

The sample is from a 1 by 5 km concordant lens in migmatite of the Burntwood River Metamorphic Suite. It is from unit 12 of Baldwin et al. (1979); part of the widespread system of irregular veins, sills, and larger bodies forming the bulk of the anatectic mobilizate in the Burntwood Metamorphic Suite of the Kisseynew sedimentary gneiss belt. It is interpreted as having crystallized at temperatures near the maximum attained in the belt.

This sample has U-Pb zircon age of 1816 +23/12 Ma and a U-Pb monazite age of 1806±2 Ma (revision of Gordon et al., 1987). For references and further interpretation see GSC 88-69.

GSC 88-71 Biotite
1710±25 Ma

Wt% K=8.055
Rad. Ar=8.927×10^{-4} cc/gm
K-Ar 3784 % Atmos. Ar=1.1

From a tonalite.
(63 N/6) East shore of S arm of Highrock Lake, 5 km S of north bend in Churchill River, Manitoba; UTM 14, 408400E, 6171600N; Lat/Long.=55.683°N/100.457°W. Sample 84-GV-1414. Collected and interpreted by T.M. Gordon.

This rock is a light grey weathering, homogeneous to coarsely inequigranular garnetiferous tonalite. It has approximately 80% antiperthitic oligoclase, 10% quartz, 5% biotite, and 5% garnet, with traces of opaques, zircon and monazite. A minor amount of pale green biotite rims some garnet grains.

The sample is from an apophysis of the 30 to 50 km wide tonalite-granodiorite complex southeast of Highrock Lake. These rocks are part of map unit 10 of Baldwin et al. (1979). Crystallization of this material predates the widespread development of granitoid pegmatites and mobilizate in the Burntwood River Metamorphic Suite.

This sample has a U-Pb zircon age of 1841 +35/−15 Ma and a U-Pb monazite age of 1817±5 Ma (revision of Gordon et al., 1987). Field relationships and the zircon data suggest that it may have formed in the early stages of high grade metamorphism in the Kisseynew belt. For references and further interpretation see GSC 88-69.

GSC 88-72 Biotite
1690±29 Ma

Wt% K=7.859
Rad. Ar=8.553×10^{-4} cc/gm
K-Ar 3785 % Atmos. Ar=0.5

From a granodiorite.
(63 N/8) Northeast shore of northwest arm of Burntwood Lake, Manitoba. UTM 14, 407900E 6142300N; 55.420°N/100.455°W. Sample 84-GV-2180. Collected and interpreted by T.M. Gordon.

This rock is a pink weathering, medium grained garnetiferous, porphyritic granodiorite. It comprises approximately 75% perthitic microcline, 15% quartz, 5% oligoclase, 5% biotite, and minor garnet, myrmekite, opaques, zircon, and monazite. Secondary white mica occurs in local patches.

The sample is from an irregular 2 by 10 km thick lens in migmatites of the Burntwood River Metamorphic Suite. It is part of unit 11 of Baldwin et al. (1979). Near the sample locality, this body intrudes sills of unit 9 (GSC 88-69). It is interpreted as having developed at near maximum temperatures in the Kisseynew belt.

The sample has a U-Pb zircon age of 1814 +17/−11 Ma and a U-Pb monazite age of 1804±2 Ma (revision of Gordon et al. 1987). For references and further interpretation see GSC 88-69.

ONTARIO
(GSC 88-73 to GSC 88-79)

GSC 88-73 Biotite
944±14 Ma

Wt% K=7.835
Rad. Ar=3.776×10^{-4} cc/gm
K-Ar 3761 % Atmos. Ar=1.5

From an anorthosite.
(31D) Roadcut on north side of Highway 121, about 5 km east of Minden, Ontario, UTM, 17T, 068500E; 498035N; Sample 85RME-956. For interpretation see Easton and Roddick (this volume).

GSC 88-74 Biotite
898±17 Ma

Wt% K=7.738
Rad. Ar=3.498×10^{-4} cc/gm
K-Ar 3762 % Atmos. Ar=0.9

From a trachyandesite.
(31D) On the east side of Highway 35, about 17.4 km south of Minden, Ontario, UTM, 17T, 067291E; 496250N; Sample 85RME-950. For interpretation see Easton and Roddick (this volume).

GSC 88-75 Whole-rock
902±9 Ma

Wt% K=8.240
Rad. Ar=3.746×10^{-4} cc/gm
K-Ar 3763 % Atmos. Ar=0.2

From a trachyandesite.
(31D) Details as for GSC 88-74. Sample 85-RME-950.

GSC 88-76 Biotite

1061±14 Ma

Wt % K=7.757
Rad. Ar=4.357×10^{-4} cc/gm
K-Ar 3764 % Atmos. Ar=0.9

From a marble breccia.
(31D) Road cut on Highway 35 at Miners Bay, about 13 km south of Minden, Ontario, UTM, 17T, 067600E; 496525N: Sample 85RME-952. For interpretation see Easton and Roddick (this volume).

GSC 88-77 Muscovite

1427±26 Ma

Wt % K=8.940
Rad. Ar=7.559×10^{-4} cc/gm
K-Ar 3721 % Atmos. Ar=0.6

From a granite.
(41 I) Fostung tungsten-molybdenum deposit, 9 km east-southeast of Espanola and 0.8 km northwest of St. Leonard Lake, Ontario; 46°13′52″N, 81°38′52″W. Sample SYA85-95 from Sulpetro Minerals Ltd. drillhole 3115-8 at 479.8 to 480.0 m, collected and interpreted by W.D. Sinclair.

The Fostung tungsten-molybdenum deposit consists of scheelite- and molybdenite-bearing garnet-diopside skarn developed in Espanola Formation limestone (Ginn and Beecham, 1986). The muscovite separate dated is from a muscovite-rich granitic dyke that cuts biotite hornfels associated with the skarn. The dyke locally contains molybdenite and scheelite and is probably related to the skarn mineralization. The date therefore represents the age of formation of the skarn deposit as well as the time of emplacement of the dyke. Other granitic intrusions in the area with comparable ages include the Croker Island Complex (1475±50 Ma; Van Schmus, 1965) and buried plutons on Manitoulin Island (1500±20 Ma; Van Schmus et al., 1975). These ages are correlative with a widespread episode of Proterozoic anorogenic magmatism in North America that occurred 1410 to 1490 Ma ago (Anderson, 1983).

The skarn and hornfels are also cut by 5 to 10 m wide dykes of porphyritic diabase which belong to the "Sudbury Swarm" of Fahrig and Jones (1969). Most of these dykes give dates of about 1250±50 Ma although the range is from 1000 to 1460 Ma (Card, 1978). Recent U-Pb dating indicates an age of 1238±4 Ma (Krogh et al., 1987). The whole-rock K-Ar dates of 1157±32 and 1280±25 Ma (GSC 88-78) and GSC 88-79 (this report) from the biotite hornfels probably reflect resetting of the K-Ar system by the intrusion of these dykes. The muscovite date from the granite dyke apparently was not affected by the diabase dykes because of the higher Ar closure temperature for muscovite relative to biotite and, in particular, K-feldspar (which comprises 30 to 40 % of the hornfels). The muscovite age is supported by preliminary Rb-Sr whole-rock measurements on a suite of samples from the granitic dyke which indicate an age that is in general accord with the muscovite K-Ar date (R.J. Theriault, pers. comm., 1987).

REFERENCES

Anderson, J.L.
1983: Proterozoic anorogenic granite plutonism of North America; *in* Proterozoic Geology: Selected Papers from an International Proterozoic Symposium, ed. L.G. Medaris, Jr., C.W. Byers, D.M. Mickelson and W.C. Shanks; Geological Society of America, Memoir 161, p. 133-154.

Card, K.D.
1978: Geology of the Sudbury-Manitoulin area, districts of Sudbury and Manitoulin; Ontario Geological Survey, Geoscience Report 166, 238 p.

Ginn, R.M. and Beecham, A.W.
1986: The Fostung scheelite deposit, Espanola, Ontario; Canadian Geology Journal of CIM, v. 1, no. 1, p. 46-54.

Fahrig, W.H. and Jones, D.L.
1969: Paleomagnetic evidence of the extent of Mackenzie igneous events; Canadian Journal of Earth Sciences, v. 6, p. 679-688.

Krogh, T.E., Corfu, F., Davis, D.W., Dunning, G.R., Heaman, L.M., Kamo, S.L., Machado, N., Greenough, J.D., and Nakamura, E.
1987: Precise U-Pb isotopic ages of diabase dykes and mafic to ultramafic rocks using trace amounts of baddeleyite and zircon; *in* Mafic Dyke Swarms, ed. H.C. Halls and W.F. Fahrig; Geological Association of Canada, Special Paper 34, p. 147-152.

Van Schmus, R.
1965: The geochronology of the Blind River-Bruce Mines area, Ontario, Canada; Journal of Geology, v. 73, p. 755-780.

Van Schmus, W.R., Card, K.D., and Harrower, K.L.
1975: Geology and ages of buried Precambrian basement rocks, Manitoulin Island, Ontario; Canadian Journal of Earth Sciences, v. 12, p. 1175-1189.

GSC 88-78 Whole-rock

1157±32 Ma

Wt % K=4.260
Rad. Ar=2.685×10^{-4} cc/gm
K-Ar 3722 % Atmos. Ar=0.5

From a biotite hornfels.
(41 I) Fostung tungsten-molybdenum deposit, 9 km east-southeast of Espanola and 0.8 km northwest of St. Leonard Lake, Ontario; 46°13′52″N, 81°38′52″W. Sample SYA85-98 from Sulpetro Minerals Ltd. drillhole 3115-8 at 476.6 m, collected and interpreted by W.D. Sinclair.

The date from the biotite hornfels probably reflects Ar loss related to intrusion of diabase dykes that postdate formation of the hornfels and associated tungsten- and molybdenum-bearing skarn. For further interpretation see GSC 88-77 (this report).

GSC 88-79 Whole-rock
1280±25 Ma

Wt% K=3.090
Rad. Ar=2.238×10^{-4} cc/gm
K-Ar 3723 % Atmos. Ar=0.3

From a biotite hornfels.
(41 I) Fostung tungsten-molybdenum deposit, 9 km east-southeast of Espanola and 0.8 km northwest of St. Leonard Lake, Ontario; 46°13′52″N, 81°38′52″W. Sample SYA85-99 from Sulpetro Minerals Ltd. drillhole 3115-8 at 353.9 m, collected and interpreted by W.D. Sinclair.

The date from the biotite hornfels probably reflects Ar loss related to intrusion of diabase dykes that postdate formation of the hornfels and associated tungsten- and molybdenum-bearing skarn. For further interpretation see GSC 88-77 (this report).

QUEBEC
(GSC 88-80 to GSC 88-97)

GSC 88-80 Biotite
377±9 Ma

Wt% K=7.674
Rad. Ar=1.25×10^{-4} cc/gm
K-Ar 3738 % Atmos. Ar=1.3

From a nepheline syenite.
(22 H/4) McGerrigle plutonic complex, Gaspé, Quebec, UTM 284800E, N5433500N. Sample MG-16. Collected and interpreted by J.B. Whalen.

The McGerrigle plutonic complex contains a diverse suite of gabbros, diorites, quartz monzonites and granites with abundant field evidence for magma-mixing and hydridization (Whalen, 1985, 1986; Whalen and Gariepy, 1986). The K-Ar mineral ages, which overlap in the range 370 to 390 Ma, are interpreted as supporting a magma-mixing model for hybrid rocks of the suite (Whalen and Roddick, 1987).

REFERENCES

Whalen, J.B.
1985: The McGerrigle plutonic complex, Gaspé, Quebec: evidence of magma mixing and hydridization; *in* Current Research, Part A, Geological Survey of Canada, Paper 85-1A, p. 795-800.
1986: Geology of the McGerrigle Mountains plutonic complex, Gaspé, Quebec; 1284, (1:25 000 scale map and marginal notes) Geological Survey of Canada, Open File.

Whalen, J.B. and Gariépy, C.
1986: Petrogenesis of the McGerrigle plutonic complex, Gaspé, Quebec: a preliminary report; *in* Current Research, Part A, Geological Survey of Canada, Paper 86-1A, p. 265-274.

Whalen, J.B. and Roddick, J.C.M.
1987: K-Ar geochronology of the McGerrigle plutonic complex, Gaspésie Peninsula, Quebec; *in* Current Research, Part A. Geological Survey of Canada, Paper 87-1A, p. 375-380, 1987.

GSC 88-81 Biotite
368±5 Ma

Wt% K=5.635
Rad. Ar=8.934×10^{-5} cc/gm
K-Ar 3743 % Atmos. Ar=0.9

From a K-feldspar porphyritic
(22 H/4) granite. McGerrigle plutonic complex, Gaspé, Quebec; UTM 285500E, 5431400N. Sample MG-83. Collected and interpreted by J.B. Whalen. See GSC 88-80 for interpretation and references.

GSC 88-82 Hornblende
389±8 Ma

Wt% K=0.672
Rad. Ar=1.133×10^{-5} cc/gm
K-Ar 3744 % Atmos. Ar= 4.2

From a K-feldspar porphyritic
(22 H/4) granite. McGerrigle plutonic complex, Gaspé, Quebec; UTM. 285599E, 5431400N. Sample MG-83. Collected and interpreted by J.B. Whalen. See GSC 88-80 for interpretation and references.

GSC 88-83 Hornblende
359±12 Ma

Wt% K=0.586
Rad. Ar=9.048×10^{-6} cc/gm
K-Ar 3817 % Atmos. Ar=11.3

From a medium-grained amphibole-
(22 H/4) biotite syenite. McGerrigle plutonic complex, Gaspé, Quebec; UTM 283700E, 543400N. Sample WXMG-8. Collected and interpreted by J.B. Whalen. See GSC 88-80 for interpretation and references.

GSC 88-84 Biotite
378±8 Ma

Wt% K=7.243
Rad. Ar=1.185×10^{-4} cc/gm
K-Ar 3822 % Atmos. Ar=0.5

(22 H/4) From a coarse grained monzodiorite. McGerrigle plutonic complex, Gaspé, Quebec; UTM 285500E, 5432050N. Sample WXMG-23. Collected and interpreted by J.B. Whalen. See GSC 88-80 for interpretation and references.

GSC 88-85 Biotite
391±7 Ma

Wt% K=6.916
Rad. Ar=1.172×10^{-4} cc/gm
K-Ar 3739 % Atmos. Ar=0.6

(22 A/13) From a plagioclase porphyritic granite. McGerrigle plutonic complex, Gaspé, Quebec; UTM 283100E, 5423750N. Sample MG-46. Collected and interpreted by J.B. Whalen. See GSC 88-80 for interpretation and references.

GSC 88-86 Hornblende
392±5 Ma

Wt% K=0.524
Rad. Ar=8.919×10^{-6} cc/gm
K-Ar 3745 % Atmos. Ar=7.8

(22 A/13) From a plagioclase porphyritic granite. McGerrigle plutonic complex, Gaspé, Quebec; UTM 283100E, 5423750N. Sample WXMG-46. Collected and interpreted by J.B. Whalen. See GSC 88-80 for interpretation and references.

GSC 88-87 Biotite
375±7 Ma

Wt% K=7.144
Rad. Ar=1.158×10^{-4} cc/gm
K-Ar 3740 % Atmos. Ar=0.5

(22 A/13) From a quartz-feldspar porphyritic granite. McGerrigle plutonic complex, Gaspé, Quebec; UTM 284500E, 5425850N. Sample MG-51. Collected and interpreted by J.B. Whalen. See GSC 88-80 for interpretation and references.

GSC 88-88 Hornblende
392±17 Ma

Wt% K=0.747
Rad. Ar=1.271×10^{-5} cc/gm
K-Ar 3746 % Atmos. Ar=4.5

(22 A/13) From a quartz-feldspar porphyritic granite. McGerrigle plutonic complex, Gaspé, Quebec; UTM 284500E, 5425850N. Sample WXMG-51. Collected and interpreted by J.B. Whalen. See GSC 88-80 for interpretation and references.

GSC 88-89 Biotite
385±5 Ma

Wt% K=6.172
Rad. Ar=1.029×10^{-4} cc/gm
K-Ar 3741 % Atmos. Ar=1.7

(22 A/13) From a quartz monzonite. McGerrigle plutonic complex, Gaspé, Quebec; UTM 283500E, 5429800N. Sample MG-66. Collected and interpreted by J.B.Whalen. See GSC 88-80 for interpretation and references.

GSC 88-90 Hornblende
395±22 Ma

Wt% K=0.501
Rad. Ar=8.602×10^{-6} cc/gm
K-Ar 3742 % Atmos. Ar=6.1

(22 A/13) From a quartz monzonite. McGerrigle plutonic complex, Gaspé, Quebec; UTM 283500E, 5429800N. Sample MG-66. Collected and interpreted by J.B. Whalen. See GSC 88-88 for interpretation and references.

GSC 88-91 Hornblende
379±6 Ma

Wt% K=0.567
Rad. Ar=9.289×10^{-6} cc/gm
K-Ar 3818 % Atmos. Ar=4.8

(22 A/13) From a medium grained quartz monzonite. McGerrigle plutonic complex, Gaspé, Quebec; UTM 283250E, 5429000N. Sample WXMG-40. Collected and interpreted by J.B. Whalen. See GSC 88-80 for interpretation and references.

GSC 88-92 Hornblende
371±6 Ma

Wt% K=0.672
Rad. Ar=1.076×10^{-5} cc/gm
K-Ar 3819 % Atmos. Ar=3.1

(22 A/13) From a coarse grained amphibole syenite. McGerrigle plutonic complex, Gaspé, Quebec, UTM 284500E, 5429800N. Sample WXMG-44. Collected and interpreted by J.B. Whalen. See GSC 88-80 for interpretation and references.

GSC 88-93 Hornblende
376±11 Ma

Wt% K=0.530
Rad. Ar=8.622×10^{-6} cc/gm
K-Ar 3820 % Atmos. Ar=5.3

(22 A/13) From a medium grained diorite. McGerrigle plutonic complex, Gaspé, Quebec; UTM 284950E, 5425700N. Sample WXMG-53. Collected and interpreted by J.B. Whalen. See GSC 88-80 for interpretation and references.

GSC 88-94 Biotite
375±6 Ma

Wt% K=7.131
Rad. Ar=1.155×10^{-4} cc/gm
K-Ar 3821 % Atmos. Ar=0.5

(22 A/13) From a medium grained diorite. McGerrigle plutonic complex, Gaspé, Quebec; UTM 284950E, 5425700N. Sample WXMG-53. Collected and interpreted by J.B. Whalen. See GSC 88-80 for interpretation and references.

GSC 88-95 Hornblende
375±11 Ma

Wt% K=0.374
Rad. Ar=6.068×10^{-6} cc/gm
K-Ar 3823 % Atmos. Ar=7.4

(22 A/13) From a coarse grained amphibole-biotite quartz monzonite. McGerrigle plutonic complex, Gaspé, Quebec; UTM 281100E. 5431800N. Sample WXMG-63. Collected and interpreted by J.B. Whalen. See GSC 88-80 for interpretation and references.

GSC 88-96 Biotite
375±12 Ma

Wt% K=6.265
Rad. Ar=1.016×10^{-4} cc/gm
K-Ar 3824 % Atmos. Ar=0.7

(22 A/13) From a coarse grained gabbro. McGerrigle plutonic complex, Gaspé, Quebec; UTM. 719350E, 5431700N. Sample WXMG-64. Collected and interpreted by J.B. Whalen. See GSC 88-80 for interpretation and references.

GSC 88-97 Biotite
374±8 Ma

Wt% K=7.847
Rad. Ar=1.269 ± 10^{-4} cc/gm
K-Ar 3825 % Atmos. Ar=0.6

(22 A/13) From a coarse grained diorite. McGerrigle plutonic complex, Gaspé, Quebec; UTM 281600E, 5436600N. Sample WXMG-90. Collected and interpreted by J.B. Whalen. See GSC 88-80 for interpretation and references.

OFFSHORE
(GSC 88-98 to GSC 88-105)

GSC 88-98 Whole-rock
56±1 Ma
Wt% K=2.600
Rad. Ar=5.721×10^{-6} cc/gm
K-Ar 3565 % Atmos. Ar=40.1

offshore From a basal melt horizon. Near continental shelf edge, south-east of Nova Scotia; 42°53′N, 64°13′W. Sample MONTAGNAIS I-94. Collected and interpreted by L.F. Jansa.

For interpretation see the following reference.

REFERENCE

Jansa, L.F. and Pe-Piper, G.
1987: Identification of an underwater extraterrestrial impact crater; Nature, v. 327, no. 6123, p. 612-614.

GSC-88-99 Whole-rock
45±4 Ma

Wt% K=0.029
Rad. Ar=5.242×10^{-8} cc/gm
K-Ar 3778 % Atmos. Ar=94.2

Offshore From a basalt. Ocean Drilling Program Leg 105 Site 647, Labrador Sea; 53°19.867′N, 45°15.717′W. Sample 72R-01; (9-11 cm from section top). Collected by S.P. Srivastava.

Basalt was recovered from 699 to 736 m below the sea floor (mbsf) and the dated samples are from the region of 705 to 736 mbsf. The basalts of the section are generally massive, fine- to medium-grained rocks with stockwork veins near the top of the section and minor serpentinite veins deeper down. The section is possibly a single, thick flow. Seven K-Ar samples were selected from the massive zones, remote from any veins. Petrographically the samples are composed of pyroxene, plagioclase and oxides with minor alteration associated with the oxides and pyroxene grains. The plagioclase, although often fractured, is fresh with very minor sericite developed along the fractures. Because Site 647 is located over marine magnetic anomaly 24, the expected age of the basalt is about 55 to 59 Ma according to Berggren et al. (1985). The oldest sediments above the basalt are of early Eocene age (nanofossil zone NP11) and thus provide a minimum age of 55-56 Ma for the basalt (Srivastava, Arthur, Clement et al., 1987).

The K-Ar ages range from 35 to 71 Ma and are too variable and imprecise to define the age of the basalt. Four of the ages are younger than the lower age limit of 55 Ma from the fossil evidence. The three remaining ages (61 to 71 Ma) are almost within the expected age range of anomaly 24, when the error limits are taken into account.

Electron microprobe analyses carried out on the major phases in two samples (GSC 88-99, 88-105) show that the K-content of the alteration (0.25, 0.29 %K) is ten times the K content of the whole-rocks. The alteration, which perhaps was originally glass is now a smectite or montmorillonite-group clay (by XRD). Mass balance calculations indicate that there is about 3 to 5 % alteration and that the alteration contributes about 45 % of the K in both whole-rock samples. This alteration will have very poor radiogenic argon retention characteristics and is also likely to be the major source of atmospheric argon in the samples. Thus the range of ages can be attributed mainly to this alteration phase. While the older ages are consistent with the expected magnetic anomaly age of about 56 Ma, the ages are not reliable enough to constrain the tectonic evolution of the region.

Additional details are given in Roddick (1988).

REFERENCES

Berggren, W.A., Kent, D.V., and Flynn, J.J.
1985: Paleogene geochronology and chronostratigraphy. *in* Snelling, N.J. (Ed.), Geochronology and the Geologic Time Scale, ed. N.J. Snelling; Geological Society of London, Memoir no. 10, p. 141-195.

Roddick, J.C.
1988: K-Ar Dating of basalts from Site 647, Ocean Drilling Program Leg 105; *in* Srivastava et al., Proc. Ocean Drilling Program (Pt. B), ODP 105.

Srivastava, S.P., Arthur, M., Clement, B., et al.
1987: Introduction; *in* Srivastava, S.P., Arthur, M., Clement, B., et al., Proc., Init. Reports. (Pt A.), ODP v. 105, p. 5-20.

GSC 88-100

Whole-rock
71±11 Ma

K-Ar 3779

Wt % K=0.033
Rad. Ar=9.109×10^{-8} cc/gm
% Atmos. Ar=95.2

Offshore

From a basalt.
See GSC 88-99 for location and interpretation. Sample 72R -03; 9-10.

GSC 88-101

Whole-rock
35±12 Ma

K-Ar 3781

Wt % K=0.032
Rad. Ar=4.366×10^{-8} cc/gm
% Atmos. Ar=92.8

Offshore

From a basalt.
See GSC 88-99 for location and interpretation. Sample 72R -04; 10-11.

GSC 88-102

Whole-rock
39±4 Ma

K-Ar 3776

Wt % K=0.050
Rad. Ar=7.58×10^{-8} cc/gm
% Atmos. Ar=95.0

Offshore

From a basalt.
See GSC 88-99 for location and interpretation. Sample 72R -02; 25-32.

GSC 88-103

Whole-rock
61±12 Ma

K-Ar 3780

Wt % K=0.049
Rad. Ar=1.177×10^{-7} cc/gm
% Atmos. Ar=98.0

Offshore

From a basalt.
See GSC 88-99 for location and interpretation. Sample 72R -02; 32-35.

GSC 88-104

Whole-rock
47±7 Ma

K-Ar 3775

Wt % K=0.050
Rad. Ar=9.222×10^{-8} cc/gm
% Atmos. Ar=96.5

Offshore

From a basalt.

See GSC 88-99 for location and interpretation. Sample 75R -04; 49-52.

GSC 88-105

Whole-rock
67±13 Ma

K-Ar 3777

Wt % K=0.024
Rad. Ar=6.259×10^{-8} cc/gm
% Atmos. Ar=97.8

Offshore

From a basalt.
See GSC 88-99 for location and interpretation. Sample 73R -04; 99-101.

APPENDIX

The numbers listed below refer to the individual sample determination numbers, e.g. (GSC) 62-189, published in the Geological Survey of Canada age reports listed below:

	Determinations		Determinations
GSC Paper 60-17, Report 1	59-1 to 59-98	GSC Paper 71-2, Report 10	70-1 to 70-156
GSC Paper 61-17, Report 2	60-1 to 60-152	GSC Paper 73-2, Report 11	72-1 to 72-163
GSC Paper 62-17, Report 3	61-1 to 61-204	GSC Paper 74-2, Report 12	73-1 to 73-198
GSC Paper 63-17, Report 4	62-1 to 62-190	GSC Paper 77-2, Report 13	76-1 to 76-248
GSC Paper 64-17, Report 5	63-1 to 63-184	GSC Paper 79-2, Report 14	78-1 to 78-230
GSC Paper 65-17, Report 6	64-1 to 64-165	GSC Paper 81-2, Report 15	80-1 to 80-208
GSC Paper 66-17, Report 7	65-1 to 65-153	GSC Paper 82-2, Report 16	81-1 to 81-226
GSC Paper 67-2A, Report 8	66-1 to 66-176	GSC Paper 87-2, Report 17	87-1 to 87-245
GSC Paper 69-2A, Report 9	67-1 to 67-146	GSC Paper 88-2, Report 18	88-1 to 88-105

GSC Age Determinations Listed by N.T.S. Co-ordinates

1-M	62-189, 190; 63-136, 137; 66-170, 171; 70-145, 146, 147, 152
1-N	65-150; 70-156
2-C	70-155
2-D	59-94, 95, 96, 97, 98; 60-151, 152; 63-182; 65-142, 143; 66-172; 70-153, 154
2-E	62-187, 188; 63-168, 169, 170, 171, 183, 184; 64-159; 65-144, 145, 146, 147, 148, 149; 67-144; 70-151; 78-229, 230
2-F	70-148; 80-206
2-L	72-158, 159
2-M	66-173; 73-192, 193, 194
3-D	63-161
10-N	72-163
11-D	70-122, 123
11-E	66-156, 157, 158; 70-124, 125; 78-209; 87-14
11-F	62-168, 169; 78-211; 80-200; 87-14
11-J	78-212
11-K	66-159, 160, 161; 78-210; 80-199
11-L	65-133, 134, 135; 66-163; 70-128, 129, 130; 72-124, 125, 126; 76-231, 232, 233, 234, 235, 236, 237, 238, 239
11-N	78-206, 207, 208; 81-206, 207
11-O	61-202; 63-162; 65-138, 139, 140, 141; 66-168
11-P	67-143
12-A	67-142; 70-120, 121; 72-160, 161; 73-197, 198; 81-212, 213, 214, 215, 216, 217
12-B	60-147; 61-199; 62-186; 63-166, 167; 81-218, 219
12-E	65-129; 66-153; 70-102, 103, 104, 105; 72-95
12-H	60-148; 61-203, 204; 70-143, 144, 149
12-I	60-149; 61-200, 201; 64-158; 66-169; 70-150; 72-153, 154, 155, 156, 157; 73-195, 196
12-L	60-133, 134, 143
12-M	78-202, 203, 204, 205
12-O	60-135
12-P	73-191
13-C	66-167; 67-138
13-D	60-132
13-E	64-160; 70-133; 80-201
13-F	60-145; 67-136, 137
13-H	60-146; 67-141
13-I	70-138, 142; 72-140, 150
13-J	70-134, 135, 136, 137; 72-139; 78-228; 87-1, 2, 3, 4, 5
13-K	60-144; 61-196; 62-183, 184, 185; 63-178, 179; 72-141, 142, 143; 73-168, 169; 76-241, 242, 244, 247, 248; 81-208, 209, 211
13-L	61-197; 62-177; 63-148, 163, 177; 64-157; 65-151; 73-163, 164, 167; 76-240, 245
13-M	63-174; 64-162; 70-131, 132; 73-174; 76-243
13-M/3	87-19
13-M/6	87-6
13-M/11	87-7
13-M/14	87-8
13-N	62-178; 63-172; 73-176, 177, 178, 179, 183, 184; 76-246; 81-210
13-N/6	87-9
13-N/9	87-10
13-O	62-179, 180, 181, 182; 67-133, 134, 135; 70-140, 141; 72-144, 145, 146, 147, 148, 149, 151, 152; 73-180, 181, 185, 186, 187, 188, 189, 190
13-0/13	87-11
14-C	72-138; 73-182
14-D	60-143; 63-175; 65-122, 152; 73-166
14-D/3	87-12
14-E	61-195; 62-172; 63-181; 64-164; 65-153; 66-166; 72-134; 73-165, 172
14-F	62-171; 63-180; 64-163; 72-135, 136, 137
14-L	63-173, 176; 64-165; 67-130, 131, 132, 140; 73-171, 175; 78-213, 214, 215, 216, 217, 218, 219, 220, 221, 222, 223, 224, 225, 226, 227
14-M	67-129; 72-133; 73-170, 173
15-M	76-174, 175
20-I	72-162
20-P	61-194; 62-167
21-A	59-93; 62-163, 164, 165, 166; 65-132; 66-155
21-B	61-193; 62-161, 162
21-E	59-89, 90, 91; 60-117, 118; 64-132; 66-142; 72-103, 104, 105
21-G	60-136; 62-159; 63-155; 66-154; 67-128; 70-108, 109, 110; 72-111, 112, 113, 114, 115, 116, 117, 118, 119, 120, 121, 122, 123; 80-198; 87-15, 16, 17

OTHER PUBLICATIONS CONTAINING GEOCHRONOLOGICAL DATA GENERATED BY THE GEOCHRONOLOGY SECTION OF THE GEOLOGICAL SURVEY OF CANADA

Baldwin, D.A, Syme, E.C., Zwanzig, H.V., Gordon, T.M., Hunt, P.A., and Stevens, R.D.

1987: U-Pb zircon ages from the Lynn Lake and Rusty Lake metavolcanic belts, Manitoba: two ages of Proterozoic magmatism; Canadian Journal of Earth Sciences, v. 24, p. 1053-1063.
A rhyolite flow from the mafic to felsic Lynn Lake metavolcanic belt has yielded a U-Pb age of 1910 +15/−10 Ma. Tonalite and quartz diorite from two composite plutons emplaced into the volcanic rocks subsequent to isoclinal folding have yielded ages of 1876 +8/−6 Ma and 1876 +8/−7 Ma. A rhyolite from the dominantly felsic Rusty Lake metavolcanic belt has yielded an indistinguishable age of 1878 +/−3 Ma indicating that this belt, as well as the La Ronge belt, are younger than the Lynn Lake Belt.

Barr, M.B., Raeside, R.R., and van Breemen, O.

1987: Grenvillian basement in the northern Cape Breton Highlands, Nova Scotia; Canadian Journal of Earth Sciences, v. 24, p. 992-997.
U-Pb zircon data from the Lowland Brook syenite of the Blair River Complex indicate a metamorphic age of 1040 +10/−40 Ma and an igneous age of 1100-1500 Ma. A correlation is made between the distinctive rock assemblage of the Blair River Complex and the Grenvillian rocks of western Newfoundland.

Parrish, R.R., Carr, S.D., and Parkinson, D.L.

1988: Eocene extensional tectonics and geochronology of the southern Omineca belt, British Columbia and Washington; Tectonics, v. 7, p. 181-212.
48 U-Pb zircon and monazite, 10 Rb-Sr and 5 K-Ar analyses from Valhalla, southern Monashee and Okanagan complexes in British Columbia are Eocene (47-58 Ma) and document Eocene plutonism and deformation.

Parrish, R.R.

1987: An improved micro-capsule for zircon dissolution in U-Pb geochronology; Chemical Geology (Isotope Geoscience section), v. 66, p. 99-102.
A new design of dissolution capsule is described which offers advantages over conventional crucibles. These are in routine use in the Geochronology laboratory.

Parrish, R.R., and Krogh, T.E.

1987: Synthesis and purification of ^{205}Pb for U-Pb geochronology; Chemical Geology (Isotope Geoscience section), v. 66, p. 103-110.
The recent synthesis of ^{205}Pb is described in detail. This material is essential to precise U-Pb geochronology, and has been distributed to about 50 laboratories worldwide in an effort to raise technology levels in this specialized field.

Roddick, J.C.

1987: Generalized numerical error analysis with applications to geochronology and thermodynamics; Geochimica et Cosmochimica Acta, v. 51, p. 2129-2135.
A general numerical error propagation procedure is developed to calculate the error in a quantity derived from measurements which are subject to errors. It can be applied to quite complex analytical problems where correlation among the measurement errors and among the final errors in results are present. Some of the assumptions involved in error propagation can also be checked numerically. Formulation as computer subroutines permits the analysis to be added to existing programs. Examples from the fields of geochronology and thermodynamics are used to highlight the advantages and the flexibility of the method.

Roddick, J.C., Loveridge, W.D., and Parrish, R.R.

1987: Precise U/Pb dating of zircon at the sub-nanogram Pb level; Chemical Geology (Isotope Geoscience Section), v. 66, p. 111-121
An improved method of measuring radiogenic Pb isotopic compositions with a Finnigan-MAT 261 multi-collector mass spectrometer equipped with a secondary electron multiplier (SEM) is described. The SEM is calibrated relative to the Faraday cups. Pb isotopic ratios are determined by the simultaneous collection of the radiogenic Pb isotopes (and ^{205}Pb, added for Pb concentration) in the Faraday cups and the small ^{204}Pb peak in the SEM. Precise ratios are determined on zircon Pb samples in 10 minutes, allowing the routine analyses of smaller quantities of Pb in zircon than was previously possible. Uranium concentrations are determined by simultaneous measurement with three Faraday cups collecting the U isotopes 233, 235 and 238. Zircon preparation and dissolution procedures have been modified to take advantage of the improved analytical technique. With the present Pb blank levels (10 to 50 pg), precision on the radiogenic ^{207}Pb/^{206}Pb is better than 0.1 % (1) for samples of 1. ng or larger.

van Breemen, O. and Davidson, A.

1988: Northeast extension of Proterozoic terranes of mid-continental North America; Geological Society of America, Bulletin, v. 100, p. 630-638.

From the Killarney complex adjacent to the Grenville Front, Georgian Bay, U-Pb ages of 1742 ± 1.4 Ma and 1732 +7/−6 Ma have been obtained respectively from granite and porphyry. A crosscutting pegmatite postdating deformation has yielded an age of 1400 ± 50 Ma. The Bell Lake granite, adjacent to the complex, has yielded an age of 1471 ± 3 Ma. Prevalence of similar U-Pb zircon ages obtained from metaplutonic rocks southeast of the Grenville Front prompts the suggestion that mid-continental Proterozoic rocks form the bulk of the crust in the Central Gneiss Belt.

Whalen, J.B. and Bevier, M.L.

1987: Field, geochemical, and isotopic studies of granitoid rocks in New Brunswick, *in* Twelfth Annual Review of Activities, ed. S.A. Abbott; New Brunswick Department of Natural Resources and Energy, Information Circular 87-2, p. 150-155.

Preliminary U-Pb zircon ages are reported for the following plutons: Fox Ridge (452 +15/−1 Ma), Meridian Brook (464 +43/−10 Ma), Mullin Stream Lake (458 +16/−1 Ma), Serpentine River (455 +12/−9 Ma), South Renous (448 +17/−16), Trousers Lake orthogneiss (434 +29/−6 Ma), and Mount Elizabeth alkali granite (414 +11/−1 Ma). These indicate two major plutonic episodes in the Miramichi terrane - Middle to Late Ordovician and Silurian.

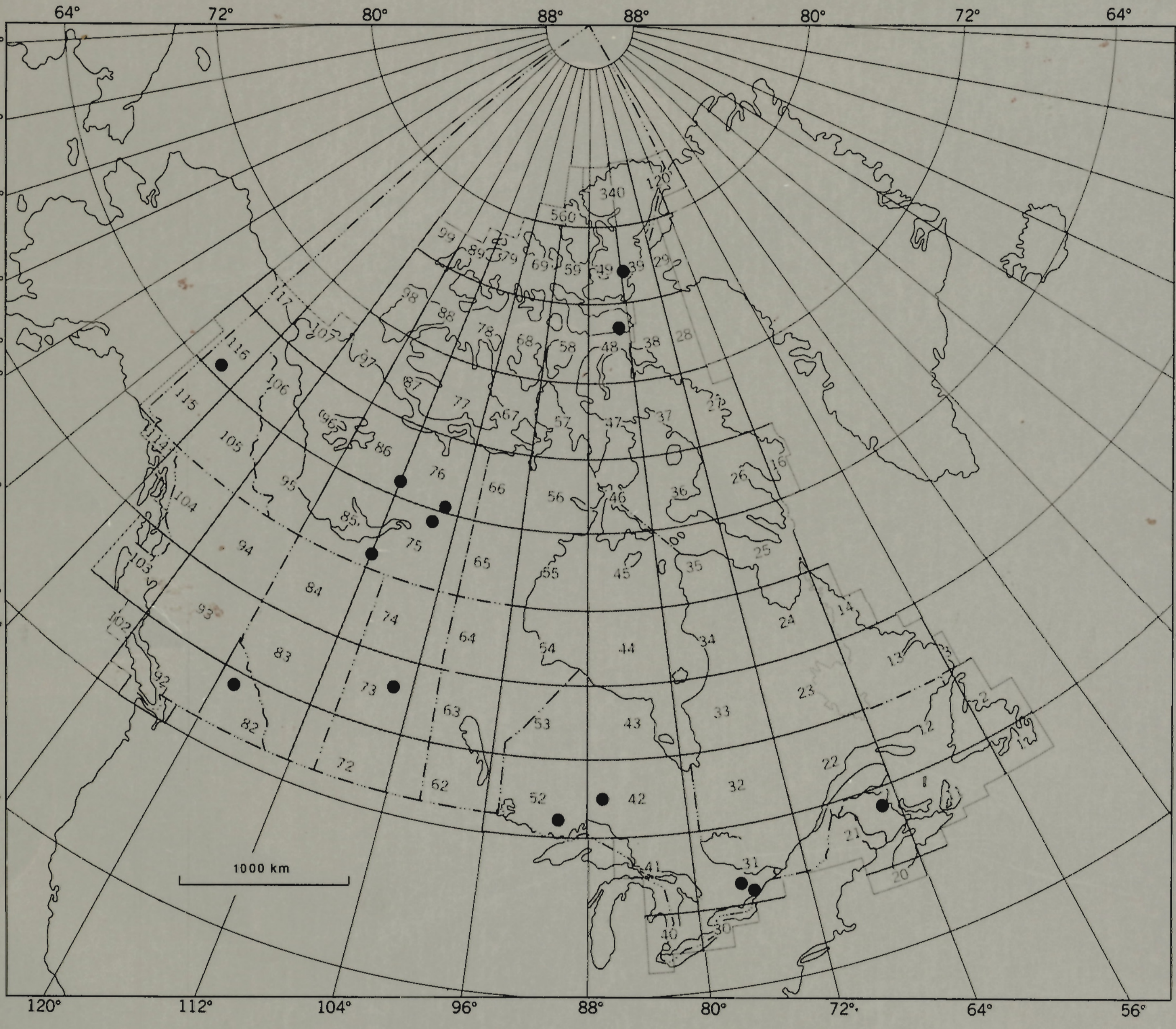

Energy, Mines and Resources Canada

Énergie, Mines et Ressources Canada